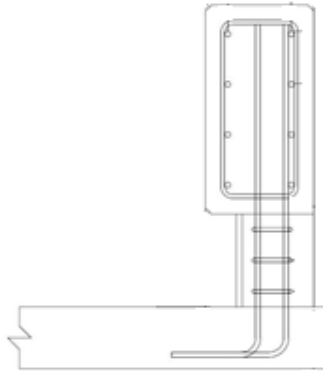


*Research Project TPF-5(193) Supplement #151*

# **DEVELOPMENT OF A MASH TEST LEVEL 4 OPEN CONCRETE BRIDGE RAIL**



Submitted by

Jacob A. DeLone, M.S.C.E.  
Former Graduate Research Assistant

Ronald K. Faller, Ph. D., P.E.  
Research Professor and MwRSF Director

Jennifer D. Rasmussen, Ph.D., P.E.  
Former Research Associate Professor

Scott K. Rosenbaugh, M.S.C.E.  
Research Engineer

Robert W. Bielenberg, M.S.M.E.  
Research Engineer

## **MIDWEST ROADSIDE SAFETY FACILITY**

Nebraska Transportation Center  
University of Nebraska-Lincoln

### **Main Office**

Prem S. Paul Research Center at Whittier School  
Room 130, 2200 Vine Street  
Lincoln, Nebraska 68583-0853  
(402) 472-0965

### **Outdoor Test Site**

4630 N.W. 36<sup>th</sup> Street  
Lincoln, Nebraska 68524

Submitted to

**IOWA DEPARTMENT OF TRANSPORTATION  
KANSAS DEPARTMENT OF TRANSPORTATION  
NEBRASKA DEPARTMENT OF TRANSPORTATION  
SOUTH DAKOTA DEPARTMENT OF TRANSPORTATION  
VIRGINIA DEPARTMENT OF TRANSPORTATION**

MwRSF Research Report No. TRP-03-406a-23

November 30, 2023

## TECHNICAL REPORT DOCUMENTATION PAGE

<b>1. Report No.</b> TRP-03-406a-23	<b>2. Government Accession No.</b>	<b>3. Recipient's Catalog No.</b>	
<b>4. Title and Subtitle</b> Development of a MASH Test Level 4 Open Concrete Bridge Rail		<b>5. Report Date</b> November 30, 2023	
		<b>6. Performing Organization Code</b>	
<b>7. Author(s)</b> DeLone, J.A., Faller, R.K., Rasmussen, J.D., Rosenbaugh, S.K., and Bielenberg, R.W.		<b>8. Performing Organization Report No.</b> TRP-03-406a-23	
<b>9. Performing Organization Name and Address</b> Midwest Roadside Safety Facility (MwRSF) Nebraska Transportation Center University of Nebraska-Lincoln  Main Office: Prem S. Paul Research Center at Whittier School Room 130, 2200 Vine Street Lincoln, Nebraska 68583-0853		<b>10. Work Unit No.</b>	
		<b>11. Contract</b> TPF-5(193) Supplement #151	
<b>12. Sponsoring Agency Name and Address</b> Iowa Department of Transportation: 800 Lincoln Way, Ames, IA 50010 Kansas Department of Transportation: 700 S.W. Harrison Street, Topeka, KS, 66603 Nebraska Department of Transportation: 1500 Nebraska Pkwy, Lincoln, NE 68502 South Dakota Department of Transportation: 700 E. Broadway Ave, Pierre, SD 57501 Virginia Department of Transportation: 1401 E. Broad St., Richmond, VA 23219		<b>13. Type of Report and Period Covered</b> Final Report: 2019–2023	
		<b>14. Sponsoring Agency Code</b>	
<b>15. Supplementary Notes</b> Prepared in cooperation with U.S. Department of Transportation, Federal Highway Administration			
<b>16. Abstract</b> An open concrete bridge rail was developed according to safety performance guidelines in the American Association of State Highway Transportation Officials (AASHTO) <i>Manual for Assessing Safety Hardware</i> (MASH) for Test Level 4 (TL-4). Systems designed and developed under previous safety guidance were reviewed, and their geometry and crash testing performance were used to establish the geometry of the new bridge rail. Yield-Line Theory and the AASHTO Inelastic Post and Beam design methods were modified and utilized to determine the capacity of the new open concrete bridge rail. Both 36-in. and 39-in. tall variants of the new open concrete bridge rail were configured. Both variants incorporated a 27-in. tall by 14-in. wide rail, supported by 36-in. long x 10 in. wide posts in the interior region, and 72-in. long posts in the end region. Posts in both regions were separated by a 72-in. long gap. Posts in the 36-in. tall variant were 9 in. tall, and posts in the 39-in. tall variant were 12 in. tall. Three bridge deck reinforcement configurations were developed to provide different reinforcement patterns that were compatible with the new bridge rail. Three full-scale crash tests were recommended to be conducted under MASH test designation nos. 4-10, 4-11, and 4-12 to evaluate the safety performance of the new open concrete bridge rail.			
<b>17. Key Words</b> Highway Safety, Roadside Appurtenances, MASH 2016, Open Concrete Bridge Rail, Roadside Safety, Bridge Deck, Design, Analysis, Inelastic Analysis		<b>18. Distribution Statement</b> No restrictions. This document is available through the National Technical Information Service. 5285 Port Royal Road Springfield, VA 22161	
<b>19. Security Classification (of this report)</b> Unclassified	<b>20. Security Classification (of this page)</b> Unclassified	<b>21. No. of Pages</b> 150	<b>22. Price</b>

Form DOT F 1700.7 (8-72)

Reproduction of completed page authorized

## DISCLAIMER STATEMENT

This report was completed with funding from the Federal Highway Administration, U.S. Department of Transportation and the Iowa, Kansas, Nebraska, South Dakota, and Virginia Departments of Transportation under TPF -5(193) Supplement #151. The contents of this report reflect the views and opinions of the authors who are responsible for the facts and the accuracy of the data presented herein. The contents do not necessarily reflect the official views or policies of the University of Nebraska-Lincoln, state highway departments participating in the Midwest Pooled Fund Program, nor the Federal Highway Administration, U.S. Department of Transportation. This report does not constitute a standard, specification, or regulation. Trade or manufacturers' names, which may appear in this report, are cited only because they are considered essential to the objectives of the report. The United States (U.S.) government and the State of Nebraska do not endorse products or manufacturers.

## ACKNOWLEDGEMENTS

The authors wish to acknowledge several sources that made a contribution to this project: (1) the Iowa Department of Transportation, Kansas Department of Transportation, Nebraska Department of Transportation, South Dakota Department of Transportation, and Virginia Department of Transportation, for sponsoring this project; and (2) MwRSF personnel. Acknowledgement is also given to the following individuals who contributed to the completion of this research project.

### **Midwest Roadside Safety Facility**

J.C. Holloway, M.S.C.E., Research Engineer & Assistant  
Director –Physical Testing Division  
K.A. Lechtenberg, M.S.M.E., Research Engineer  
C.S. Stolle, Ph.D., Research Assistant Professor  
J.S. Steelman, Ph.D., P.E., Associate Professor  
M. Asadollahi Pajouh, Ph.D., P.E., Research Assistant  
Professor  
B.J. Perry, M.E.M.E., Research Associate Engineer  
A.T. Russell, B.S.B.A., Testing and Maintenance Technician II  
E.W. Krier, B.S., Former Engineering Testing Technician II  
D.S. Charroin, Engineering Testing Technician II  
R.M. Novak, Engineering Testing Technician II  
S.M. Tighe, Engineering Testing Technician I  
T.C. Donahoo, Engineering Testing Technician I  
J.T. Jones, Engineering Testing Technician I  
C. Charroin, Former Temporary Engineering Construction  
Testing Technician I  
T. Shapland, Former Temporary Engineering Construction  
Testing Technician I  
E.L. Urbank, B.A., Research Communication Specialist  
Z.Z. Jabr, Engineering Technician  
Undergraduate and Graduate Research Assistants

### **Iowa Department of Transportation**

Chris Poole, P.E., Roadside Safety Engineer  
Daniel Harness, P.E., Transportation Engineer Specialist  
Stuart Nielsen, P.E., Transportation Engineer Administrator,  
Design

### **Kansas Department of Transportation**

Ron Seitz, P.E., Director of Design  
Scott King, P.E., Road Design Bureau Chief  
Brian Kierath Jr., Engineering Associate III, Bureau of Road  
Design

### **Nebraska Department of Transportation**

Phil TenHulzen, P.E., Design Standards Engineer  
Jim Knott, P.E., Construction Engineer  
Mick Syslo, P.E., State Roadway Design Engineer  
Brandon Varilek, P.E., Materials and Research Engineer &  
Division Head  
Mark Fischer, P.E., PMP, Research Program Manager  
Lieska Halsey, Research Project Manager  
Angela Andersen, Research Coordinator  
David T. Hansen, Internal Research Coordinator  
Jodi Gibson, Former Research Coordinator

### **South Dakota Department of Transportation**

Thad Bauer, Research Program Manager  
Randy Brown, P.E., Standards Engineer  
Steve Johnson, P.E., Chief Bridge Engineer

### **Virginia Department of Transportation**

Charles Patterson, P.E., Standards/Special Design Section  
Manager  
Andrew Zickler, P.E., Complex Bridge Design and ABC  
Support Program Manager

## TABLE OF CONTENTS

DISCLAIMER STATEMENT .....	ii
ACKNOWLEDGEMENTS .....	ii
LIST OF FIGURES .....	v
LIST OF TABLES .....	ix
1 INTRODUCTION .....	1
1.1 Background.....	1
1.2 Problem Statement.....	6
1.3 Objective.....	7
1.4 Scope.....	7
2 LITERATURE REVIEW .....	8
2.1 Overview.....	8
2.2 Vertical Openings and Post Setbacks .....	8
2.3 Head Ejection.....	11
2.4 Impact Loads .....	12
2.5 MASH TL-4 Barrier Heights.....	14
2.6 Open Concrete Bridge Rails .....	15
2.6.1 TxDOT T224 Bridge Rail.....	17
2.6.2 NDOR’s TL-5 Aesthetic Open Concrete Bridge Rail .....	19
2.6.3 Nebraska Open Concrete Rail.....	21
2.6.4 Nebraska Open Concrete Rail on an Inverted Tee Bridge Deck .....	24
2.6.5 TxDOT T202 and T203 (T202 MOD).....	26
2.6.6 Aesthetic Precast Concrete Bridge Rail.....	29
2.6.7 TxDOT T223 .....	29
2.6.8 California Type 85 .....	31
2.6.9 Kansas Corral Rail .....	31
2.7 Steel Bridge Rails .....	32
2.7.1 California ST-70SM.....	35
2.7.2 Massachusetts Type S3 .....	38
2.7.3 Illinois-Ohio Steel Bridge Rail .....	41
2.8 Other Systems .....	44
2.8.1 Minnesota Noise Wall.....	47
2.8.2 Restore Barrier .....	51
2.8.3 NDOT Standardized Approach Guardrail Transition End Buttress .....	53
2.8.4 NDOT 34-in. Approach Guardrail Transition .....	56
3 DESIGN CRITERIA .....	58
3.1 Barrier Height .....	58
3.2 Impact Loads .....	58
3.3 System Geometry.....	58
3.4 Sponsor Survey .....	66
3.4.1 Preferred Preliminary Configurations.....	66

3.4.2 Post Shape .....	69
3.4.3 Rear Post Offset from Edge of Bridge Deck .....	70
3.4.4 Bridge Rail Footprint .....	70
3.4.5 Expansion Gap Locations and Use of Dowels.....	71
3.4.6 Overhang Width, Thickness, and Additional Thickness .....	72
3.4.7 Preferred Reinforcement.....	73
3.5 Summary.....	73
4 DESIGN METHODOLOGY.....	75
4.1 Overview.....	75
4.2 Yield-Line Theory .....	75
4.3 AASHTO Post and Beam Method (Inelastic Method) .....	77
4.4 AASHTO Post and Beam Method (Inelastic Method) Limitations.....	80
4.5 Effective Load Application Heights .....	82
4.6 Yield-Line Theory and AASHTO Post and Beam Method Comparisons.....	82
4.7 Modified AASHTO Post and Beam Method (Modified Inelastic Method) .....	83
4.8 Barrier Punching Shear.....	87
4.9 Deck Design.....	87
5 CURRENT KANSAS CORRAL RAIL .....	95
5.1 Overview.....	95
5.2 27-in. Tall Kansas Corral Rail Without Curb.....	95
5.3 32-in. Tall Kansas Corral Rail Without Curb.....	99
5.4 Summary.....	103
6 BARRIER DESIGN.....	104
6.1 Overview.....	104
6.2 Initial Configurations.....	104
6.2.1 Initial Configuration 1.....	105
6.2.2 Initial Configuration 2.....	106
6.3 Final Design.....	107
6.4 36-in. Tall Configuration .....	109
6.5 Comparison to Similar Systems.....	110
6.6 Summary.....	113
7 DECK DESIGN .....	114
7.1 Design Loads and Minimum Steel Required.....	114
7.2 Bridge Deck Overhang Configurations .....	116
7.2.1 Option 1 .....	117
7.2.2 Option 2 .....	119
7.2.3 Option 3 .....	121
7.3 Summary.....	123
8 SUMMARY, CONCLUSIONS, AND RECOMMENDATIONS.....	124
8.1 Summary and Conclusions .....	124
8.2 Recommendations.....	125
9 REFERENCES .....	146

## LIST OF FIGURES

Figure 1. Rectangular Open Concrete Rail Posts [1].....	1
Figure 2. Tapered Trapezoidal Open Concrete Rail Posts with a Lower Curb [2].....	1
Figure 3. Concrete Barrier with Head Ejection Setback Region [3].....	2
Figure 4. 27-in. Tall Kansas Corral Rail Details .....	3
Figure 5. 32-in. Tall Kansas Corral Rail Details [7].....	3
Figure 6. 32-in. Tall Kansas Corral Rail, Pretest [7] .....	4
Figure 7. 32-in. Tall Kansas Corral Rail Damage [7].....	4
Figure 8. 32-in. Tall Kansas Corral Rail Damage [7].....	5
Figure 9. 27-in. Tall Corral Rail with a 6-in. Tall Curb Details .....	5
Figure 10. 32-in. Tall Corral Rail with a 6-in. Tall Curb Details .....	6
Figure 11. Snag Potential Based on Ratio of Vertical Clear Opening and Post Setback [14].....	9
Figure 12. Snag Potential Based on Ratio of Contact Width to Height and Post Setback [14].....	9
Figure 13. NCHRP Report 350 and MASH Small Car Snag Potential for Open Concrete Bridge Rails [15].....	10
Figure 14. NCHRP Report 350 and MASH Pickup Truck Snag Potential for Open Concrete Bridge Rails [15].....	11
Figure 15. Head Ejection Envelope [3].....	12
Figure 16. Open Concrete Bridge Rail General Dimensions Cross Section.....	15
Figure 17. Open Concrete Bridge Rail General Dimensions Elevation .....	15
Figure 18. TxDOT T224 System Photograph [2] .....	17
Figure 19. TxDOT T224 Bridge Rail Drawing [2].....	18
Figure 20. Lateral Extent of 1100C Vehicle Tire Marks on the T224 Bridge Rail [2] .....	18
Figure 21. Lateral Extent of 2270P Vehicle Tire Marks on the T224 Bridge Rail [2].....	19
Figure 22. NDOR TL-5 Aesthetic Rail System Photograph [21].....	20
Figure 23. NDOR TL-5 Aesthetic Rail Drawing [21] .....	20
Figure 24. NDOR TL-5 Aesthetic Rail Damage [21].....	21
Figure 25. Nebraska Open Concrete Rail System Photograph [22] .....	22
Figure 26. Nebraska Open Concrete Rail Drawing [22].....	22
Figure 27. Lateral Extent of the 5,399-lb Pickup Truck on the Nebraska Open Concrete Rail [22] .....	23
Figure 28. Lateral Extent of the 5,394-lb Pickup Truck on the Nebraska Open Concrete Rail [22] .....	23
Figure 29. Nebraska Open Concrete Rail on an IT Bridge Deck System Photograph [1] .....	24
Figure 30. Nebraska Open Concrete Rail on an IT Bridge Deck System Drawing [1].....	25
Figure 31. Lateral Extent of the 2000P Vehicle on the Nebraska Open Concrete Rail on an IT Bridge Deck [1].....	25
Figure 32. T203 Bridge Rail 27-in. Configuration System Photograph [23] .....	26
Figure 33. T203 Bridge Rail 30-in. Configuration System Photograph [23] .....	27
Figure 34. T203 Bridge Rail Drawing [23] .....	27
Figure 35. Lateral Extent of the 2000P Vehicle on the 27-in. Tall T203 Barrier [23] .....	28
Figure 36. Lateral Extent of the 2000P Vehicle on the 30-in. Tall T203 Barrier [23] .....	28
Figure 37. Precast Fence Concept [24].....	29
Figure 38. TxDOT T223 Bridge Rail System Photograph [25].....	30
Figure 39. TxDOT T223 Bridge Rail Drawing [25].....	30
Figure 40. California Type 85 Bridge Rail [12] .....	31

Figure 41. 32-in. Tall Kansas Corral Rail Details [7].....32

Figure 42. Steel Bridge Rail General Dimensions, Cross Section.....33

Figure 43. Steel Bridge Rail General Dimensions, Plan View .....33

Figure 44. California ST-70SM Bridge Rail System Photograph [27].....35

Figure 45. California ST 70 Bridge Rail Drawing [27].....36

Figure 46. Lateral Extent of the 1100C Vehicle on the ST-70SM Bridge Rail [27] .....37

Figure 47. Lateral Extent of the 2270P Vehicle on the ST-70SM Bridge Rail [27].....37

Figure 48. Massachusetts Type S3 Bridge Rail System Photograph [28] .....38

Figure 49. Massachusetts Type S3 Bridge Rail Drawing [28] .....39

Figure 50. Lateral Extent of the 820C Vehicle on the Massachusetts Type S3 Bridge Rail  
[28].....39

Figure 51. Lateral Extent of 2000P Vehicle on the Massachusetts Type S3 Bridge Rail [28].....40

Figure 52. Lateral Extent of the 8000S Vehicle on the Massachusetts Type S3 Bridge Rail  
[28].....40

Figure 53. 36-in. Tall, Illinois-Ohio steel Bridge Rail System Photograph [29-32] .....41

Figure 54. 39-in. Tall, Illinois-Ohio Steel Bridge Rail System Photograph [29-32].....42

Figure 55. 36-in. Tall Illinois-Ohio Steel Bridge Rail Drawing [29-32] .....42

Figure 56. 39-in. Tall Illinois-Ohio Steel Bridge Rail Drawing [29-32].....43

Figure 57. Lateral Extent of the 1100C Vehicle on the 39-in. Tall Illinois-Ohio Steel Bridge  
Rail [29-32].....43

Figure 58. Lateral Extent of the 2270P Vehicle on the 36-in. Tall Illinois-Ohio Steel Bridge  
Rail [29-32].....44

Figure 59. Other System General Dimensions, Cross Section .....45

Figure 60. Other System General Dimensions, Plan View.....45

Figure 61. Minnesota Noise Wall Test Nos. MNNW-1 and MNNW-2 System Photograph  
[33].....47

Figure 62. Minnesota Noise Wall Test No. MNNW-3 System Photograph [33] .....48

Figure 63. Test Nos. MNNW-1 and MNNW-2 Drawing [33] .....48

Figure 64. Test No. MNNW-3 Drawing [33] .....49

Figure 65. Lateral Extent of the 2270P Vehicle in Test No. MNNW-1 on the Minnesota  
Noise Wall [33].....49

Figure 66. Lateral Extent of the 1100C Vehicle in. Test No. MNNW-2 on the Minnesota  
Noise Wall [33].....50

Figure 67. Lateral Extent of the 2270P Vehicle in. Test No. MNNW-3 on the Minnesota  
Noise Wall [33].....50

Figure 68. Restore Barrier System Photograph [34].....51

Figure 69. Restore Barrier Drawing [34].....52

Figure 70. Lateral Extent of the 1100C Vehicle on the Restore Barrier [34].....52

Figure 71. Standardized AGT Buttress, Test No. AGTB-1, System Photograph [35] .....53

Figure 72. Standardized AGT Buttress, Test No. AGTB-1, System Drawing [35] .....54

Figure 73. Standardized AGT Buttress, Test No. AGTB-2, System Photograph [35] .....54

Figure 74. Standardized AGT Buttress, Test No. AGTB-2, System Drawing [35] .....54

Figure 75. Lateral Extent of the 2270P Vehicle on the Standardized AGT Buttress, Test No.  
AGTB-1 [35].....55

Figure 76. Lateral Extent of the Second 2270P Vehicle on the Standardized AGT Buttress,  
Test No. AGTB-2 [35].....55

Figure 77. 34-in. Tall Approach Guardrail Transition System Photograph [36].....56

Figure 78. 34-in. Thrie Beam to End Buttress Connection Drawing [36] .....57

Figure 79. Lateral Extent of the 1100C Vehicle on the 34-in. Tall AGT [36] .....57

Figure 80. Lateral Extent of the 2270P Vehicle on the 34-in. Tall AGT [36].....57

Figure 81. Post Setback Measurements .....59

Figure 82. Estimated Lateral Extent vs. Vertical Opening, Small Car Tests.....61

Figure 83. Estimated Lateral Extent vs. Post Setback, Small Car Tests.....61

Figure 84. Estimated Lateral Extent vs. Vertical Opening for Pickup Truck Tests .....64

Figure 85. Estimated Lateral Extent vs. Post Setback for Pickup Truck Tests .....64

Figure 86. Preliminary Option 1 .....67

Figure 87. Preliminary Option 2 .....67

Figure 88. Preliminary Option 3 .....68

Figure 89. Preliminary Option 4 .....68

Figure 90. Preliminary Option 5 .....69

Figure 91. Rectangular and Tapered Posts .....69

Figure 92. Post Offset from Edge of Bridge Deck – (a) No Offset and (b) 2-in. Offset .....70

Figure 93. Bridge Rail Footprint (a) Rear of System Flush with Edge of Deck and Offset  
from Edge of Deck (b) .....71

Figure 94. Expansion Gap Locations.....72

Figure 95. Overhang Width, Thickness, and Additional Thickness .....73

Figure 96. Preliminary Open Concrete Bridge Rail and Deck Configuration .....73

Figure 97. Preliminary Open Concrete Bridge Rail and Deck Cross Section .....74

Figure 98. Preliminary System Post Lengths.....74

Figure 99. Yield Line of a Concrete Post and Beam System [26].....76

Figure 100. AASHTO Post and Beam Method Failure Mechanisms for Bridge Rail Interior  
Sections [14] .....79

Figure 101. AASHTO Inelastic Method End Section Failure Mechanisms .....80

Figure 102. Modified AASHTO Post and Beam Method Failure Mechanism for Bridge  
Rail Interior Sections (Example of Two-Span Failure) .....81

Figure 103. Modified AASHTO Post and Beam Method Failure Mechanism for Bridge  
Rail End Sections .....82

Figure 104. Open Concrete Bridge Rail Failure Mechanism [39].....84

Figure 105. 45-Degree Load Distribution for Steel Post-and-Beam Bridge Rails [14].....89

Figure 106. 30-Degree Load Distribution for Closed Concrete Parapets [19-20].....90

Figure 107. 30-Degree Load Distribution for End Posts of Open Concrete Bridge Rails.....91

Figure 108. 30-Degree Load Distribution for Interior Posts of Open Concrete Bridge Rails .....92

Figure 109. Deck Design Sections.....92

Figure 110. ¼ Width of Flange Design Section for Steel Girders [40] .....93

Figure 111. ½ Flange Width or 15-in. Wide Design Section for Prestressed Concrete  
Girders [41] .....94

Figure 112. Rear of Post to Edge of Girder and Centerline of Girder .....94

Figure 113. 27-in. Tall Kansas Corral Rail Without Curb.....95

Figure 114. 32-in. Tall Kansas Corral Rail Without Curb [7] .....99

Figure 115. New MASH TL-4 Open Concrete Rail-Initial Configuration.....104

Figure 116. Initial Configuration 1, Reinforcement Details .....105

Figure 117. Initial Configuration 1, Elevation View .....105

Figure 118. Initial Configuration 2, Reinforcement Details .....106

Figure 119. Initial Configuration 2, Elevation View .....106



Figure 120. New Open Concrete Bridge Rail Interior Section, Cross Section.....	108
Figure 121. New Open Concrete Bridge Rail End Section, Cross Section .....	108
Figure 122. New Open Concrete Bridge Rail End and Interior Section, Elevation View .....	108
Figure 123. 36-in. Open Concrete Bridge Rail Interior Section, Cross Section.....	109
Figure 124. 36-in. Open Concrete Bridge Rail End Section, Cross Section .....	110
Figure 125. 36-in. Open Concrete Bridge Rail End and Interior Section, Elevation View .....	110
Figure 126. Design Section Lengths at Interior Posts.....	114
Figure 127. End Post Design Section Lengths.....	115
Figure 128. Option 1, Interior Post Deck Reinforcement, Plan and Elevation Views .....	118
Figure 129. Option 1, End Post to Interior Post Transition Deck Reinforcement, Plan and Elevation Views .....	118
Figure 130. Option 1, Bridge Deck Overhang Cross Section.....	119
Figure 131. Option 2, Interior Post Deck Reinforcement, Plan and Elevation Views .....	120
Figure 132. Option 2, End Post to Interior Post Transition Deck Reinforcement, Plan and Elevation Views .....	121
Figure 133. Option 2, Bridge Deck Overhang Cross Section.....	121
Figure 134. Option 3, Interior Post Deck Reinforcement, Plan and Elevation Views .....	122
Figure 135. Option 3, End Post to Interior Post Transition Deck Reinforcement, Plan and Elevation Views .....	123
Figure 136. Option 3, Bridge Deck Overhang Cross Section.....	123
Figure 137. Open Concrete Bridge Rail Overall View.....	127
Figure 138. Open Concrete Bridge Rail System Profile View .....	128
Figure 139. Open Concrete Bridge Rail Deck and Grade Beam Assembly, Interior Section .....	129
Figure 140. Open Concrete Bridge Rail Post Nos. 1 and 2 .....	130
Figure 141. Open Concrete Bridge Rail Interior Post Details .....	131
Figure 142. Open Concrete Bridge Rail Interior Post and Downstream End Section Assembly.....	132
Figure 143. Open Concrete Bridge Rail Assembly .....	133
Figure 144. Open Concrete Bridge Rail Bridge Deck Assembly .....	134
Figure 145. Open Concrete Bridge Rail Upstream End Section and First Interior Post Bridge Deck Assembly .....	135
Figure 146. Open Concrete Bridge Rail Upstream End Section and First Interior Post Bridge Deck Assembly .....	136
Figure 147. Open Concrete Bridge Interior Post on Bridge Deck and Tarmac Assembly.....	137
Figure 148. Open Concrete Bridge Rail Bridge Deck Assembly Details.....	138
Figure 149. Open Concrete Bridge Rail Deck Detail .....	139
Figure 150. Open Concrete Bridge Rail Deck Detail .....	140
Figure 151. Open Concrete Bridge Rail Grade Beam Detail.....	141
Figure 152. Open Concrete Bridge Rail System Rebar .....	142
Figure 153. Open Concrete Bridge Rail System Rebar .....	143
Figure 154. Open Concrete Bridge Rail System Rebar .....	144
Figure 155. Open Concrete Bridge Rail Bill of Materials .....	145

## LIST OF TABLES

Table 1. MASH TL-4 Test Matrix for Longitudinal Barriers [8] .....	6
Table 2. <i>AASHTO LRFD Bridge Design Specifications</i> Design Forces for Traffic Railings [14].....	13
Table 3. Summary of Resultant Impact Loads for MASH TL-4 SUT [17].....	14
Table 4. Recommended Design Impact Loads for MASH TL-4 Traffic Barriers [17] .....	14
Table 5. Open Concrete Bridge Rail Design Details .....	16
Table 6. Steel Bridge Rail Design Details .....	34
Table 7. Other Systems Design Details .....	46
Table 8. Testing Criteria and Test Vehicles for Passenger Vehicles .....	59
Table 9. System Geometry and Estimated Lateral Extent for Small Car Crash Tests.....	60
Table 10. System Geometry and Estimated Lateral Extent for Pickup Truck Crash Tests .....	63
Table 11. Recommended Vertical Openings and Post Setbacks .....	66
Table 12. Preliminary Configuration Details.....	66
Table 13. Design Cases, Loads, and Limit States [14,17] .....	88
Table 14. <i>AASHTO LRFD Bridge Design Specifications</i> Load Modification Factors [14] .....	88
Table 15. <i>AASHTO LRFD Bridge Design Specifications</i> Multiple Presence Factors [14] .....	89
Table 16. <i>AASHTO LRFD Bridge Design Specifications</i> Dynamic Load Allowance Factors [14].....	89
Table 17. 27-in. and 32-in. Corral Rail, Capacities and Failure Mechanisms .....	103
Table 18. Similar Concrete Bridge Rail System Comparisons.....	112
Table 19. Interior and End Section Tensile and Moment Loads .....	116
Table 20. Area of Steel Requirements .....	116
Table 21. New Open Concrete Bridge Rail Capacities and Failure Mechanisms .....	125

## 1 INTRODUCTION

### 1.1 Background

To prevent errant motorists traversing bridge structures from leaving the roadway, bridge rails are installed along the edges of the bridge deck. Concrete bridge rails are typically closed parapets with a vertical, single-sloped, or safety-shaped face as well as open post and beam systems, also known as open concrete rails. Open concrete rails typically consist of rectangular posts, as shown in Figure 1 [1], or tapered trapezoidal posts, as shown in Figure 2 [2], with vertical-faced rails on top. When impacting post-and-beam systems, vehicle components, such as wheels and bumpers, have the potential to extend beneath the rail and contact a post, potentially resulting in snagging. Significant snagging can result in excessive occupant compartment deformation or occupant deceleration. Open concrete rails can also be designed with a lower curb, as shown in Figure 2, which may mitigate the potential for vehicle components to extend under the rail [2]. Systems without curbs allow for easier snow removal and water drainage directly away from the bridge deck. Some taller bridge rails may incorporate an offset region at the top of the rail to decrease the potential for an occupant's head to contact the barrier, as shown in Figure 3 [3].



Figure 1. Rectangular Open Concrete Rail Posts [1]



Figure 2. Tapered Trapezoidal Open Concrete Rail Posts with a Lower Curb [2]



Figure 3. Concrete Barrier with Head Ejection Setback Region [3]

Two variations of the Kansas Corral Rail, as shown in Figures 4 and 5, have been tested under NCHRP Report 230 and the American Association of State Highway and Transportation Officials (AASHTO) Guide Specifications for Bridge Railings (GSBR) Performance Level 2 (PL-2) conditions [4-5]. In 1987, the Southwest Research Institute (SwRI) successfully conducted crash test nos. MKS-1 and MKS-2 on the 27-in. tall Kansas Corral Rail shown in Figure 4 under NCHRP Report 230 conditions using test designation no. 10 with a 4,690-lb 4500S car and test designation no. 12 with a 1,971-lb 1800S car [6]. Both crash tests were successful, and both vehicles were redirected without causing significant damage to the bridge rail. In 1991, MwRSF conducted crash test no. KSCR-1 on the 32-in. tall Kansas Corral Rail shown in Figures 5 and 6 under AASHTO GSBR PL-2 conditions with a 18,040 lb single-unit truck (SUT) [7]. The rail successfully contained the SUT but sustained considerable damage, as shown in Figures 7 and 8.

The Kansas Corral Rail, or a variation of it, is currently used in Kansas, Nebraska, Iowa, Virginia, and South Dakota. These variants include 27-in. and 32-in. tall configurations, both of which may incorporate a 6-in. tall curb, as shown in Figures 9 and 10.

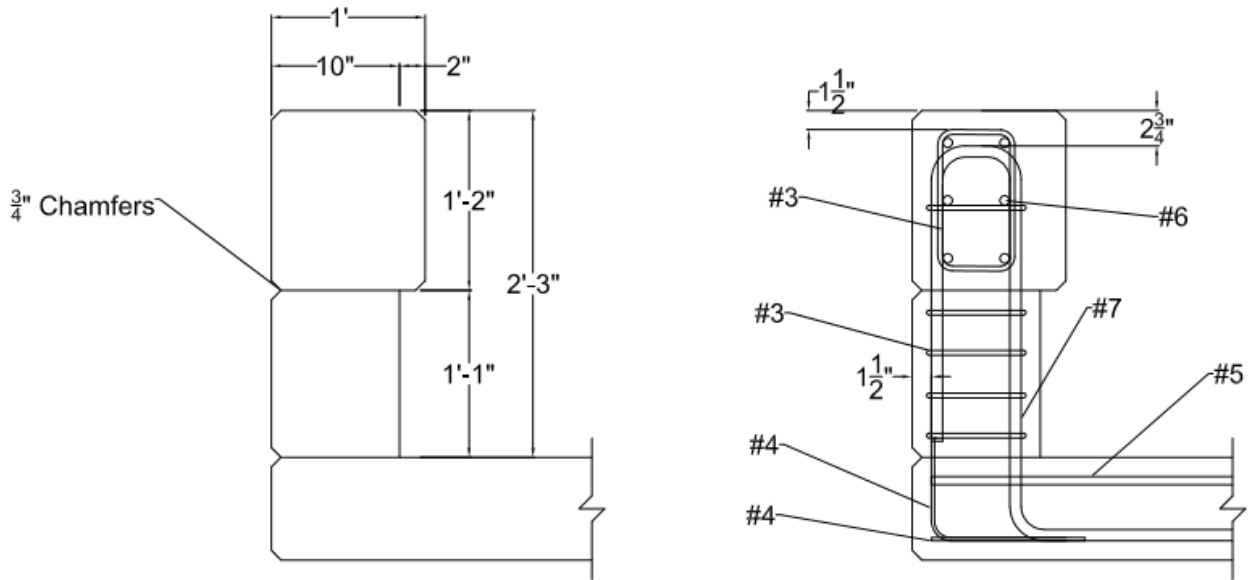


Figure 4. 27-in. Tall Kansas Corral Rail Details

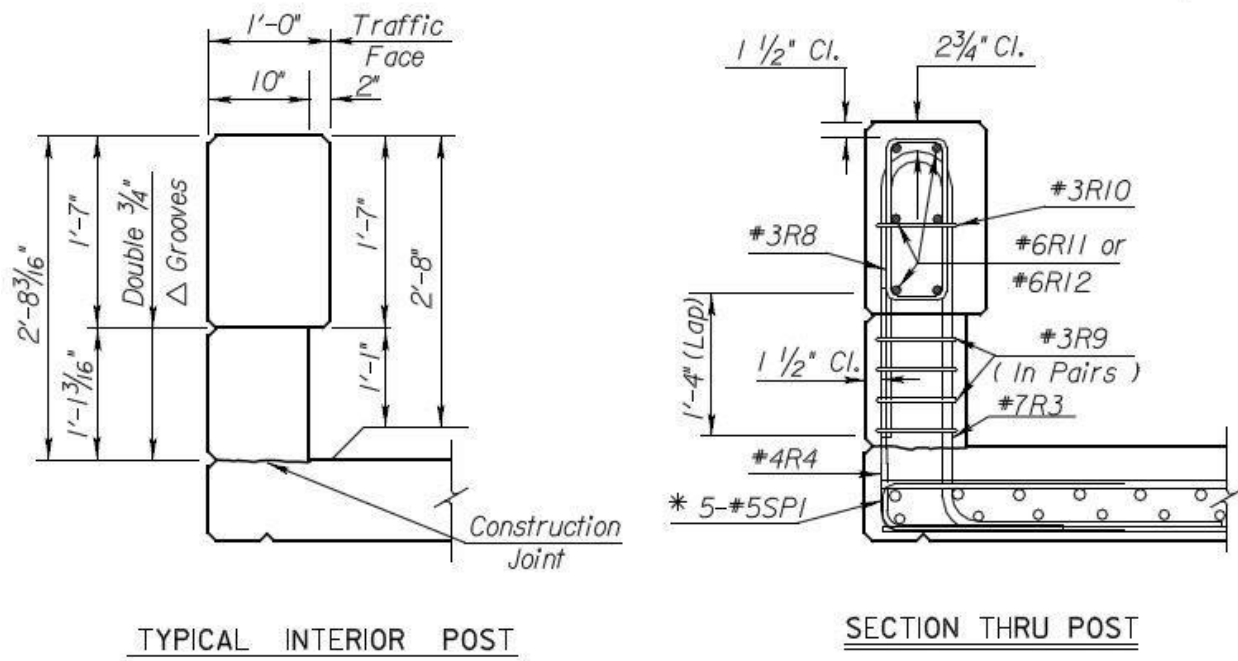


Figure 5. 32-in. Tall Kansas Corral Rail Details [7]



Figure 6. 32-in. Tall Kansas Corral Rail, Pretest [7]

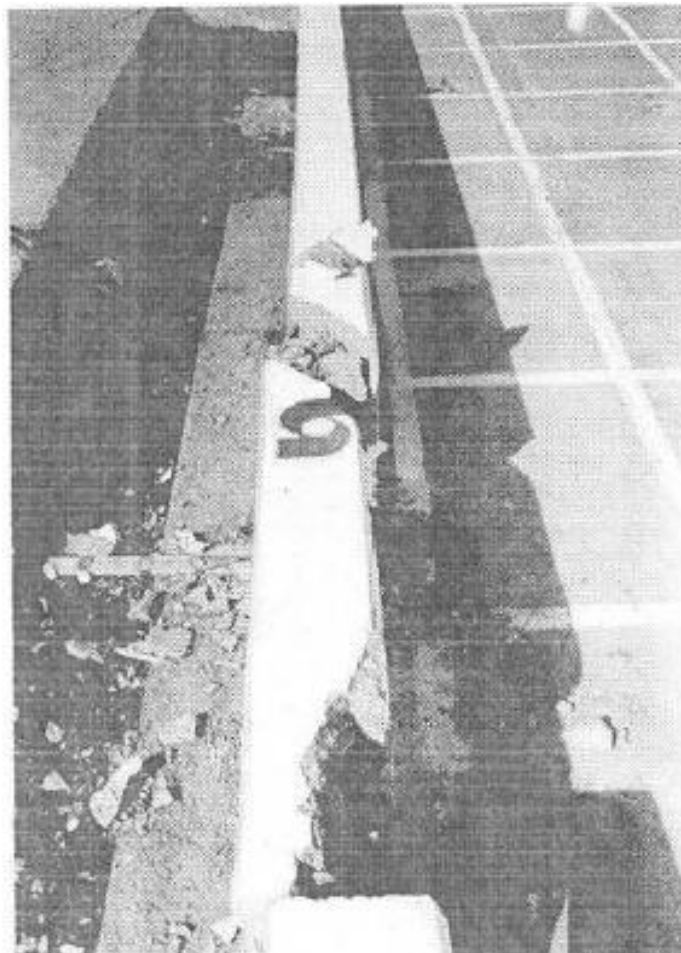


Figure 7. 32-in. Tall Kansas Corral Rail Damage [7]

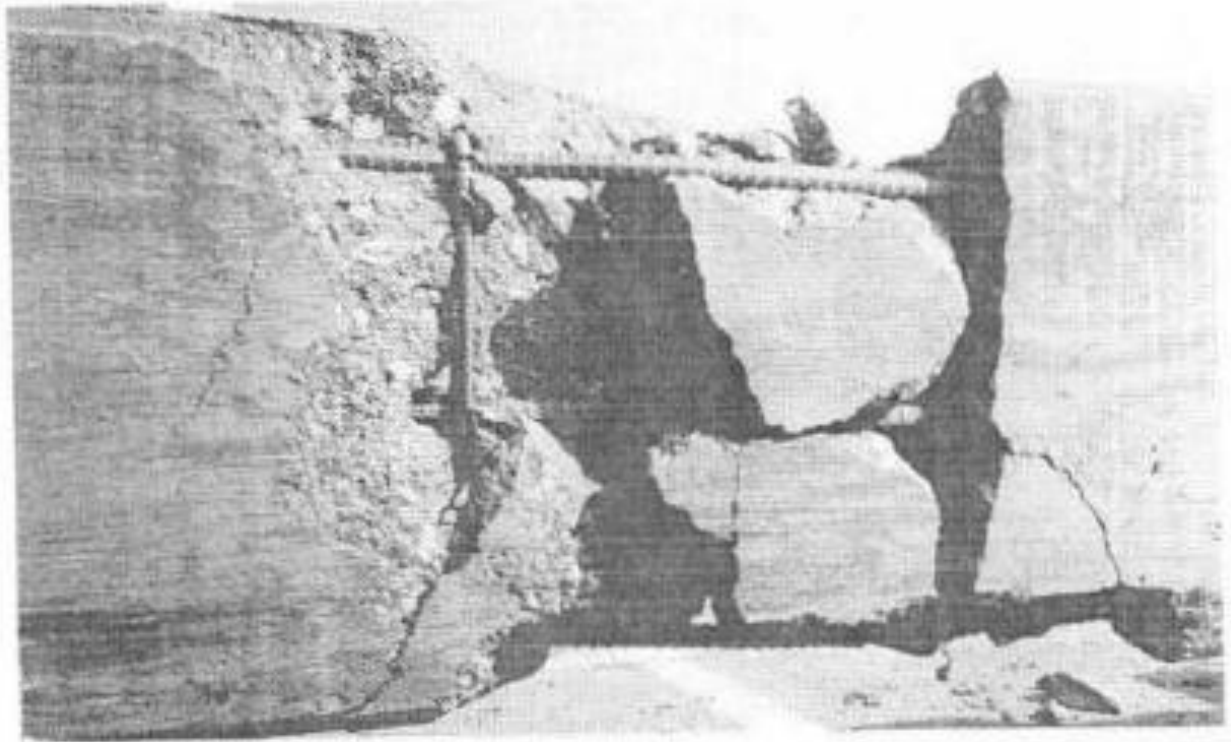


Figure 8. 32-in. Tall Kansas Corral Rail Damage [7]

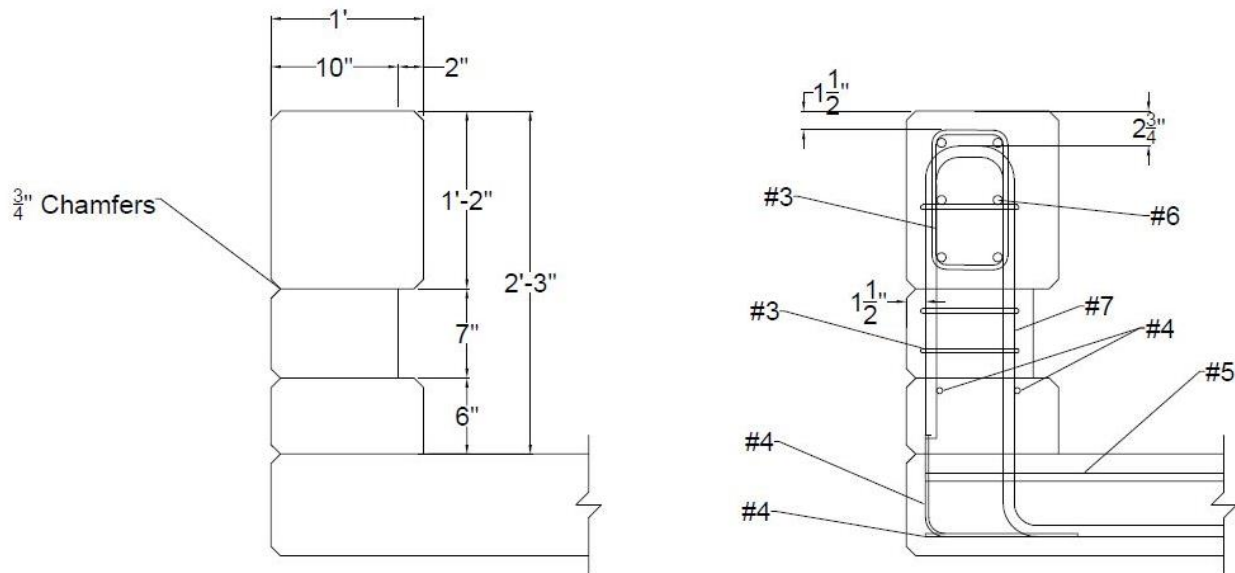


Figure 9. 27-in. Tall Corral Rail with a 6-in. Tall Curb Details

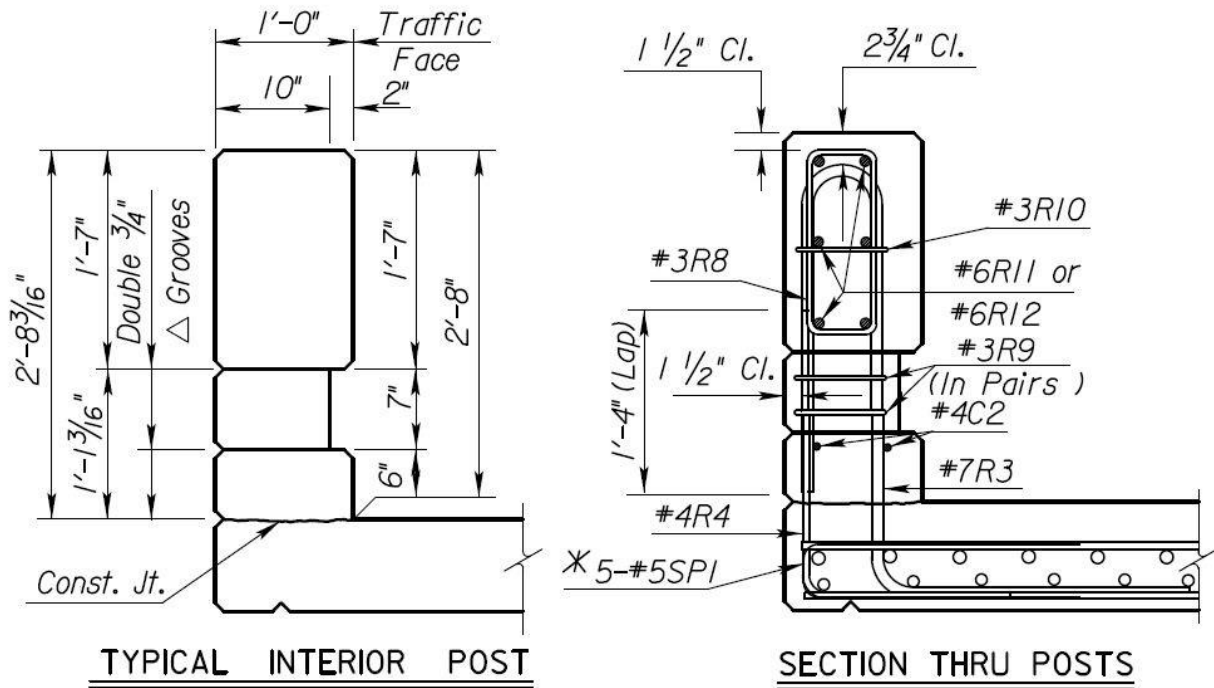


Figure 10. 32-in. Tall Corral Rail with a 6-in. Tall Curb Details

### 1.2 Problem Statement

The *Manual for Assessing Safety Hardware* (MASH) [8] is the current guideline for crash-testing roadside safety hardware, and includes many changes from the prior guidance in NCHRP Report 350 [9]. Required test matrices are specified for each category of roadside device, which includes test vehicle, impact speed, impact angle, and critical impact point. The safety performance evaluation criteria used to evaluate each test consists of structural adequacy, occupant risk, and vehicle trajectory. MASH includes updated test vehicles and impact conditions for longitudinal barriers. Historically, rigid concrete bridge rails satisfying Test Level 4 (TL-4) criteria under NCHRP Report 350 were 32 in. tall. However, with the adoption of MASH and an increase in both mass and impact speed for the SUT, MASH TL-4 tests on 32-in. tall safety-shaped barriers have resulted in SUTs rolling over the barrier [10-11]. As such, bridge rails taller than 32 in. are now required to meet the MASH TL-4 criteria. Additionally, vehicle mass has increased for small cars, pickup trucks, and SUTs; impact angle has increased for the small car; and impact speed for the SUT has increased. The MASH TL-4 test matrix is shown in Table 1.

Table 1. MASH TL-4 Test Matrix for Longitudinal Barriers [8]

Test No.	Vehicle Designation	Vehicle Mass lb	Speed mph	Impact Angle deg.
4-10	1100C	2,420	62	25
4-11	2270P	5,000	62	25
4-12	10000S	22,000	56	15



Currently, no open concrete bridge rails similar to the Kansas Corral Rail have been developed and crash tested under MASH TL-4 impact conditions. Open concrete rails that have been tested under MASH conditions include: the Texas Department of Transportation (TxDOT) T224, a MASH TL-5 open concrete rail developed and tested by the Texas A&M Transportation Institute (TTI) which included a 9-in. tall curb [2]; the California Department of Transportation (Caltrans) Type 85, a MASH TL-4 open concrete rail developed and tested by Caltrans which included a 12-in. tall curb [12]; and the TxDOT T223, a MASH TL-3 open concrete rail developed and tested by TTI [13].

Additionally, many existing open concrete bridge rails would not meet the minimum height requirements for a MASH TL-4 barrier with future roadway overlays. Increasing a concrete bridge rail's height may lead to better containment of SUTs, but it can also lead to an increase in head slap incidents for occupants in passenger vehicles. Past research regarding the geometry of rigid concrete barriers has also indicated that certain barrier shapes, such as safety shapes, increase the propensity for vehicle climb, instability, and rollover [10-11]. Thus, an optimized geometric shape that considers vehicle stability and pavement overlays is desired for new TL-4 bridge rails. If desired, occupant head ejection may be considered.

### **1.3 Objective**

The objective of this research effort was to develop an optimized MASH TL-4 open concrete bridge rail utilizing the geometry of the original Kansas Corral Rail as the starting point for the design. The railing was designed for strength, vehicle stability, reduced snagging risk, and to minimize installation costs while accommodating up to a 3-in. thick future pavement overlay. The load transfer into the deck was designed to minimize the potential for damage to the bridge deck. Details were developed for both interior and end regions of the bridge rail. In a future research effort, full-scale crash testing will be conducted to evaluate the new bridge rail shape, strength, load transfer to the deck, and the zone of intrusion (ZOI) for the new bridge rail.

### **1.4 Scope**

Development of the TL-4 open concrete rail comprised several tasks. Task 1 consisted of reviewing previously crash-tested open concrete rails and steel post and beam rails. The geometric details and crash test results for each rail were reviewed to establish safe bridge rail dimensions. Bridge rail dimensions, such as the vertical opening and post setback, were selected to maximize aesthetics while mitigating the potential for vehicle snag on the bridge rail posts. Sponsor input on current and desired rail characteristics guided the design process. Rail characteristics included deck thickness, overhang width, reinforcement sizes, rail width, post length, post spacing, vertical opening, and post setback. Task 2 consisted of a structural analysis of the current Kansas Corral Rail, design of several bridge rail configurations, and design of the bridge deck overhang. Several bridge rail and overhang configurations were proposed to the sponsors, and their feedback was used to select the final rail and deck configurations. Task 3 consisted of providing recommendations for future full-scale crash testing.

## 2 LITERATURE REVIEW

### 2.1 Overview

A literature review was conducted to gather information on the performance of open concrete bridge rails, current and historical design criteria, and design impact loads. Systems that are similar to open concrete bridge rails were also studied, including steel post and beam bridge rails, concrete end buttresses, and other longitudinal barriers that incorporate rails supported by posts. Open concrete bridge rails, steel post and beam bridge rails, and other relevant systems tested under AASHTO GSB, NCHRP Report 230, NCHRP Report 350, or MASH criteria were reviewed [4, 5, 8, 9]. Although the objective of the project was to design a MASH TL-4 open concrete bridge rail, other systems with discrete posts supporting an elevated rail have a structure similar to open concrete rails in which vehicle elements could extend under a rail and snag on the posts, which was critical to the new rail design. Review of current and historical design criteria was necessary to predict how systems evaluated under previous testing standards would perform under the current MASH testing standards. Systems tested to NCHRP Report 350 and MASH TL-3 through TL-5 conditions were included in this review. The impact conditions for MASH test designation nos. 3-10, 4-10, and 5-10 with the small car and MASH test designation nos. 3-11, 4-11, and 5-11 with the pickup truck are the same at MASH TL-3 through TL-5. NCHRP Report 350 and MASH impact conditions are similar, but test vehicle weights, small car impact angle, and SUT impact speed have all increased in MASH.

### 2.2 Vertical Openings and Post Setbacks

The tendency for vehicles' structural components to extend beneath the rails of post and beam systems creates a risk of vehicles' structural components snagging on posts, which can lead to excessive vehicle crush, vehicle instability, and elevated occupant ridedown accelerations (ORAs) and occupant impact velocities (OIVs). Numerous studies and design standards were reviewed to determine the influence of vertical opening and post setback on vehicle snagging and the amount of snagging that is detrimental to test results.

*AASHTO Load and Resistance Factor Design (LRFD) Bridge Design Specification* discusses the snag potential for various bridge designs [14]. The data were obtained from previous NCHRP Report 230 crash tests and were used to determine the geometric parameters that posed a threat of snagging. Snag potential graphs with post setback distance versus vertical clear opening and post setback distance versus to the ratio of rail contact width to height were developed, showing which combinations have low and high potential for vehicle snagging. Recommendations were provided on whether a configuration would be acceptable, as shown in Figures 11 and 12. As vertical openings increase, post setbacks should also increase to mitigate the potential for snagging, as shown in Figure 11. Post setback criteria can also be determined by comparing the post setback distance versus the ratio of rail contact width to height, as shown in Figure 12. The ratio of rail contact width to height is defined as the summation of the surface area of the front face of the bridge rail divided by the overall height of the system.

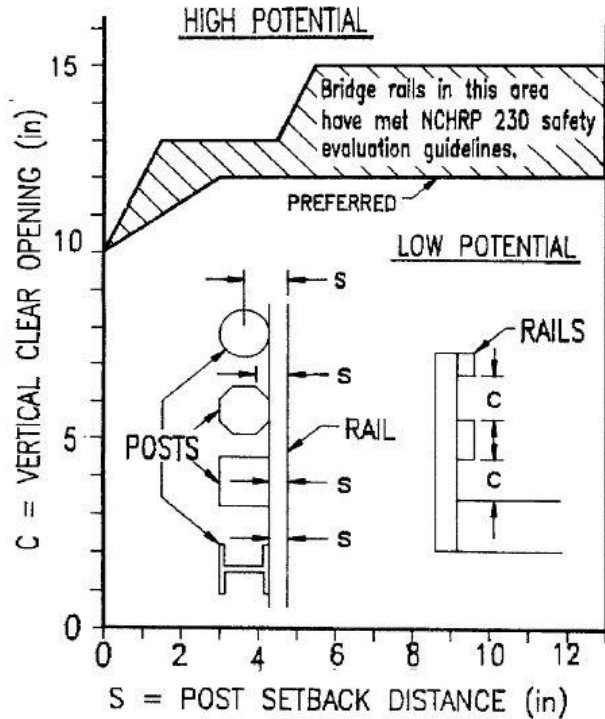


Figure 11. Snag Potential Based on Ratio of Vertical Clear Opening and Post Setback [14]

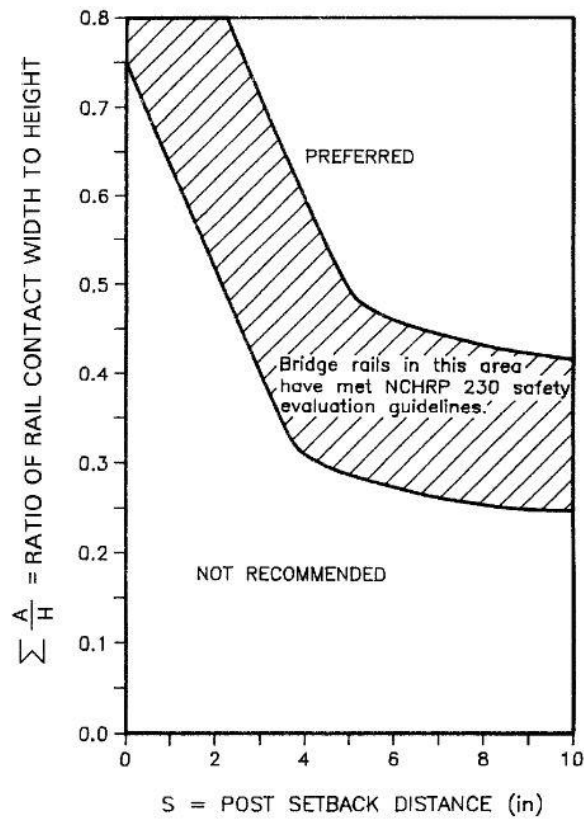


Figure 12. Snag Potential Based on Ratio of Contact Width to Height and Post Setback [14]

In NCHRP Project 20-07, the research team evaluated the equivalency between NCHRP Report 350 and MASH test levels, as the changes from NCHRP Report 350 to MASH resulted in increased impact severity [15]. Increased impact severity could correspond to an increased risk of vehicle snagging, as higher impact velocities and higher speeds may cause vehicles to extend farther underneath rail elements. The research effort studied closed concrete parapets, metal bridge rails, open concrete bridge rails, combination concrete and metal bridge rails, combination traffic and pedestrian rails, wood rails, noise walls, and retrofit rails. Crash tests conducted on open concrete bridge rails were plotted on the snag potential graphs, as shown in Figures 13 and 14. The one failed test was conducted under MASH TL-3 criteria on the TxDOT T202, a 27-in. tall open concrete bridge rail, and the failure was not due to snagging, as the vehicle rolled over due to insufficient rail height [16]. Due to the lack of tests, further testing was recommended in order to update the geometric relationships that are currently shown in the *AASHTO LRFD Bridge Design Specifications*.

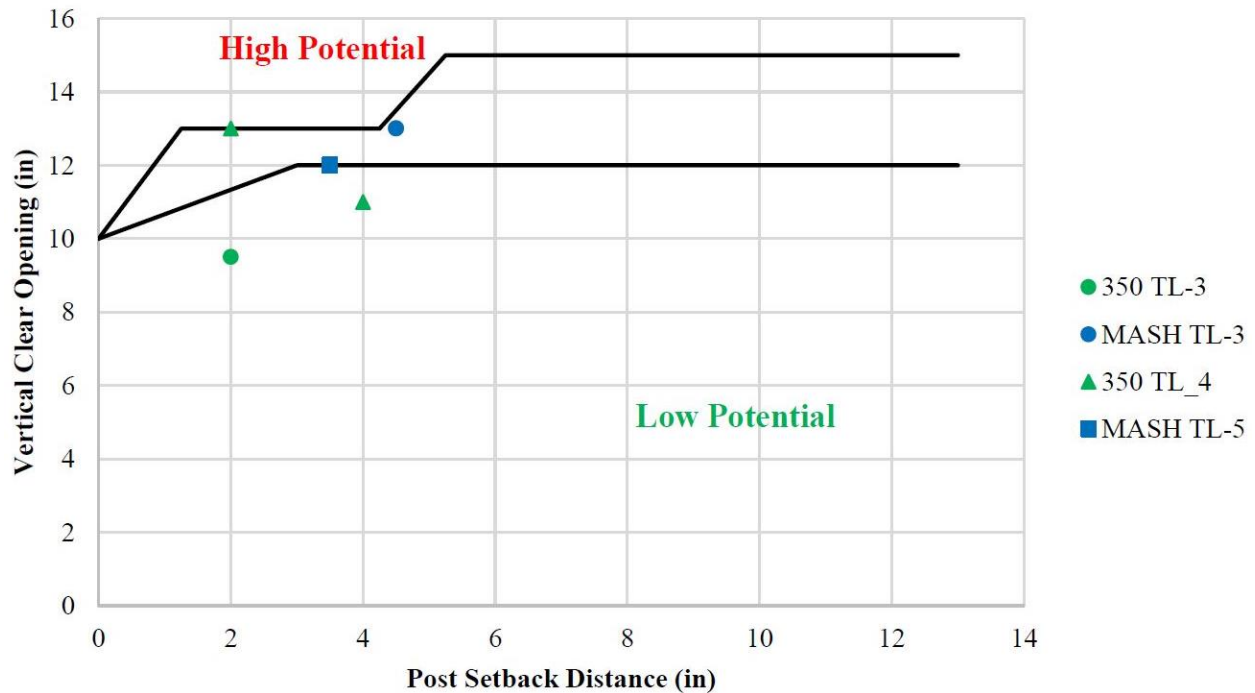


Figure 13. NCHRP Report 350 and MASH Small Car Snag Potential for Open Concrete Bridge Rails [15]

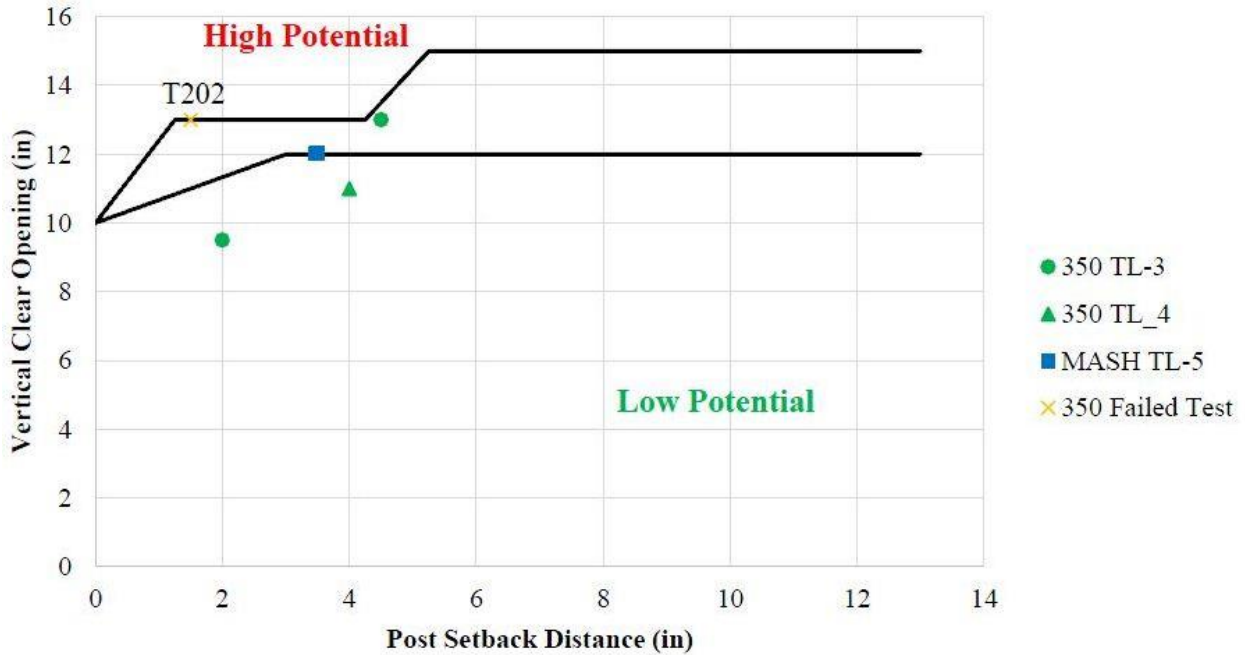


Figure 14. NCHRP Report 350 and MASH Pickup Truck Snag Potential for Open Concrete Bridge Rails [15]

### 2.3 Head Ejection

During impact events with vertical-face barriers, the occupant’s head may leave the occupant compartment through the window, known as head ejection. If the occupant’s head contacts an adjacent barrier, serious occupant harm could occur. Thus, a head ejection envelope was recommended [3]. The occupant head ejection envelope was developed by MwRSF researchers in 2007 by studying high-speed video of small car and pickup truck crash tests, as shown in Figure 15. The envelope was drawn relative to the front face of the barrier and determines how far the top of the barrier must be set back for an occupant’s head to not contact the barrier. This setback distance is based on the overall barrier height. Due to the geometry of open concrete bridge rails, passenger vehicle impacts with bridge rails can also result in occupant head ejection, and the setback region can reduce the risk of occupant head-slap. Modern vehicle side-curtain airbags, which were not accounted for in the original study, may also reduce the number of head ejections that could occur in a crash impact event, but the changes have not been quantified yet.

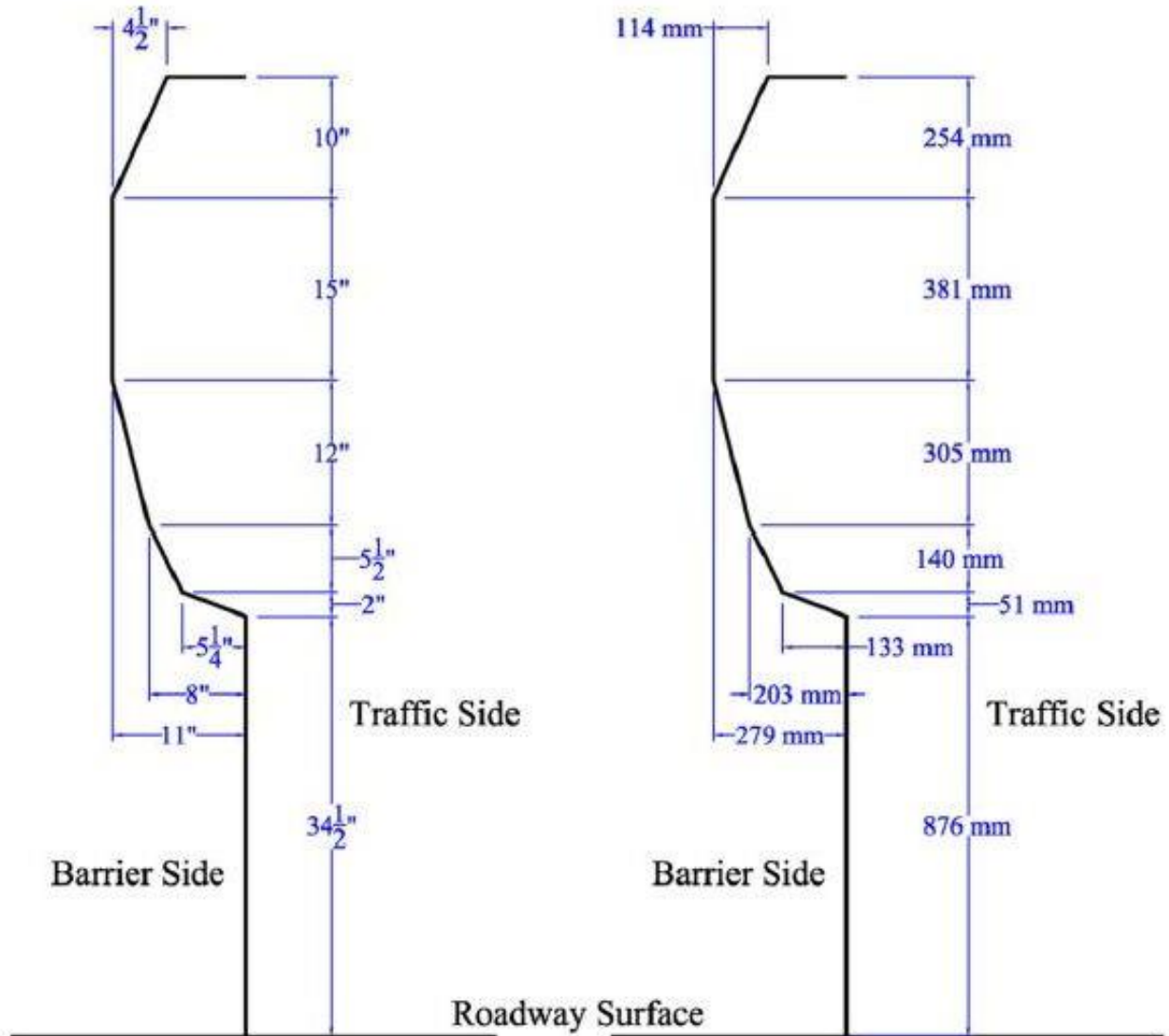


Figure 15. Head Ejection Envelope [3]

## 2.4 Impact Loads

Various design impact loads have been utilized to design open concrete bridges, and historical design impact loads were reviewed to determine what loads the new open concrete bridge rail had to be designed to resist. Design loads for traffic railings are published in *AASHTO LRFD Bridge Design Specifications*, as shown in Table 2 [14]. TL-4 conditions specify pickup truck transverse and longitudinal design loads to be 54 kips and 18 kips respectively, applied at a height of 24 in., and a vertical load of 18 kips applied over 18 ft. Transverse and longitudinal design loads for the SUT were 54 kips and 18 kips respectively, applied at a height of 32 in., and a vertical load of 18 kips applied over 18 ft. These impact loads were developed from the NCHRP Report 350 crash testing effort and have not been updated to reflect MASH impact conditions.

Table 2. AASHTO LRFD Bridge Design Specifications Design Forces for Traffic Railings [14]

Design Forces and Designation	Railing Test Levels					
	TL-1	TL-2	TL-3	TL-4	TL-5	TL-6
$F_t$ Transverse (kips)	13.5	27	54	54	124	175
$F_L$ Longitudinal (kips)	4.5	9	18	18	41	58
$F_v$ Vertical (kips)	4.5	4.5	4.5	18	80	80
$L_t$ and $L_L$ (ft)	4	4	4	3.5	8	8
$L_v$ (ft)	18	18	18	18	40	40
$H_e$ (min) (in.)	18	20	24	32	42	56
Minimum $H$ Height of rail (in.)	27	27	27	32	42	90

Where:

$F_t$  = Transverse force applied perpendicular to the barrier

$F_L$  = Longitudinal force applied by friction along the barrier's direction

$F_v$  = Vertical force applied downward on the top of the barrier

$L_T$  = Length of transverse distributed design load

$L_L$  = Length of longitudinal distributed design load

$L_v$  = Length of vertical distributed design load

$H_e$  = Effective height of vehicle rollover force

$H$  = Minimum height of rail

In NCHRP Project 22-20(2), recommended guidelines were developed for designing MASH TL-3 through TL-5 roadside barrier foundation systems placed on mechanically stabilized earth (MSE) retaining walls [17]. Through this effort, finite element analyses with LS-DYNA were conducted to estimate MASH TL-4 impact loads of a 10000S vehicle on barriers at different heights. As barrier height increases, transverse and longitudinal forces increase and vertical forces decrease due to the reduced amount of vehicle roll, as shown in Table 3. Recommended design loads based on LS-DYNA results are shown in Table 4, which are divided into two categories: TL-4-1 for barriers 36 in. and shorter and TL-4-2 for barriers taller than 36 in. TL-4-1 impact conditions correspond to 70-kip transverse and 22-kip longitudinal loads applied at an effective height of 25 in. distributed over 4 ft, and a 38-kip vertical load distributed over 18 ft. TL-4-2 impact conditions correspond to 80-kip transverse and 27-kip longitudinal loads applied at an effective height of 30 in. distributed over 5 ft, and a 33-kip vertical load distributed over 18 ft.

Table 3. Summary of Resultant Impact Loads for MASH TL-4 SUT [17]

Design Forces and Designations	Barrier Height			
	36 in.	39 in.	42 in.	90 in.
F <sub>t</sub> Transverse (kips)	67.2	72.3	79.1	93.3
F <sub>L</sub> Longitudinal (kips)	21.6	23.6	26.8	27.5
F <sub>v</sub> Vertical (kips)	37.8	32.7	22	N/A
L <sub>L</sub> and L <sub>t</sub> (ft)	4	5	5	14
H <sub>e</sub> (in.)	25.1	28.7	30.2	45.5

N/A = Not Applicable

Table 4. Recommended Design Impact Loads for MASH TL-4 Traffic Barriers [17]

Design Forces and Designations	TL-4-1	TL-4-2
Rail Height, H (in.)	36	>36
F <sub>t</sub> Transverse (kips)	70	80
F <sub>L</sub> Longitudinal (kips)	22	27
F <sub>v</sub> Vertical (kips)	38	33
L <sub>L</sub> and L <sub>t</sub> (ft)	4	5
L <sub>v</sub> (ft)	18	18
H <sub>e</sub> (in.)	25	30

## 2.5 MASH TL-4 Barrier Heights

The minimum barrier height for each test level has varied based upon the impact conditions. Under NCHRP Report 350 conditions, full-scale crash tests demonstrated that a 32-in. tall barrier could successfully redirect an SUT impacting at TL-4 conditions. However, in 2006, MwRSF conducted an unsuccessful crash test under MASH conditions on a 32-in. tall barrier in which the SUT rolled over the barrier [10]. Additionally, TTI conducted another unsuccessful crash test of an SUT impacting a 32-in. tall barrier, also resulting in rollover [11]. Thus, selection of a new minimum required bridge rail height was required for design of the new open concrete bridge rail. In 2011, TTI conducted a full-scale crash test on a 36-in. tall barrier which successfully redirected the MASH SUT [18]. In 2018, MwRSF conducted another full-scale crash test on a 36-in. tall barrier which successfully redirected the MASH SUT [19-20], thus 36 in. has been established as the minimum height necessary to contain a SUT.



## 2.6 Open Concrete Bridge Rails

Data from full-scale crash tests of open concrete bridge rails were reviewed to determine whether testing was successful, whether the vehicle snagged on the barrier, and if the system geometry contributed to an unsuccessful crash test. Relevant system geometry, depicted in in Figures 16 and 17, included overall system height, overall system width, vertical opening, curb height, post setback, post taper, post length, and gap length. The collected data is summarized in Table 5. Relevant system geometry was defined based on its influence on snag potential and was collected to guide future recommendations for the new open concrete bridge rail. Open concrete bridge rails were selected for study based on their geometric similarity to the Kansas Corral Rail and the ability to determine the potential for vehicle snagging. The systems are described in the subsequent sections of this report.

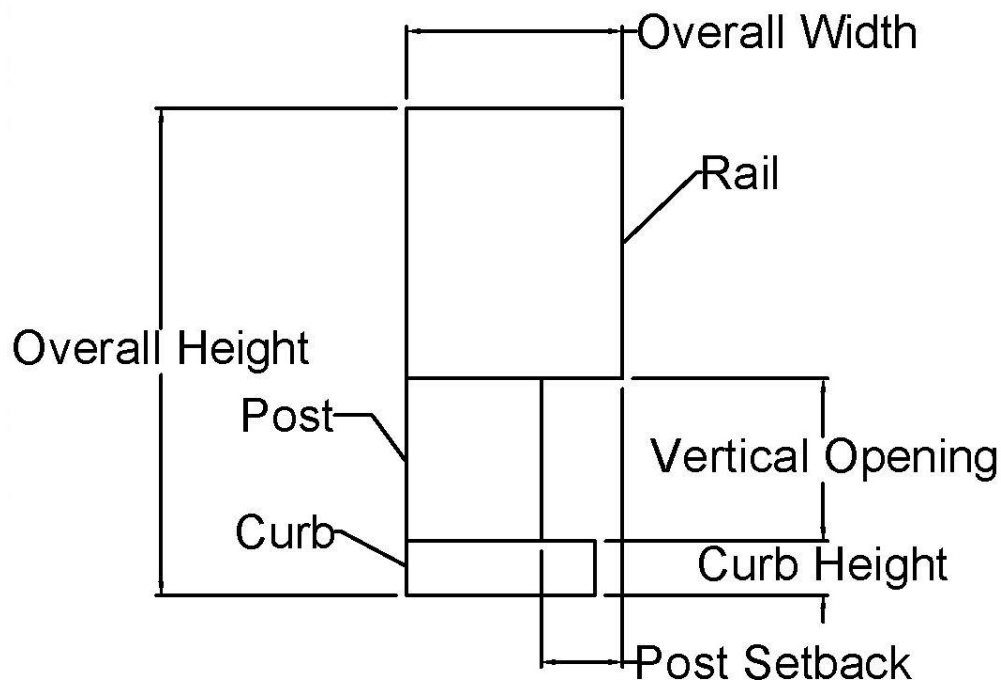


Figure 16. Open Concrete Bridge Rail General Dimensions Cross Section

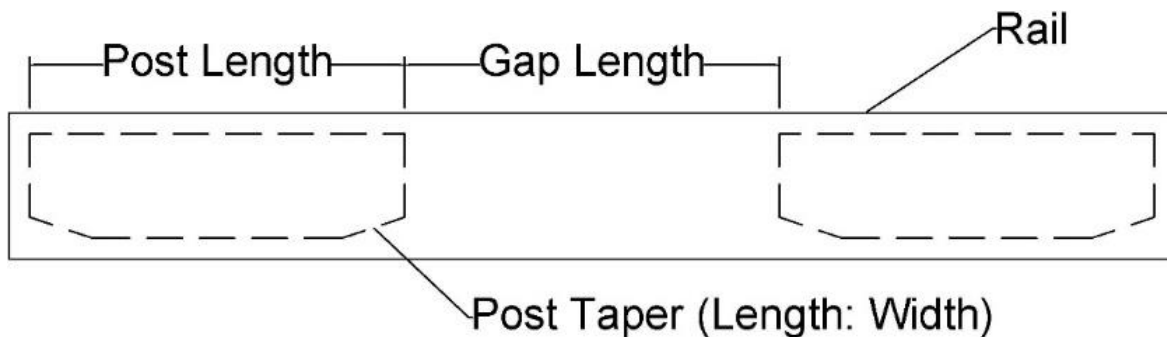


Figure 17. Open Concrete Bridge Rail General Dimensions Elevation

Table 5. Open Concrete Bridge Rail Design Details

System Name	Test Criteria	Test Level	Overall Height in. (mm)	Overall Width in. (mm)	Vertical Opening in. (mm)	Curb Height in. (mm)	Post Setback in. (mm)	Post Taper	Post Length in. (mm)	Gap Length in. (mm)
TxDOT T224 [2]	MASH	TL-5	42 (1,067)	16½ (419)	12 (305)	9 (229)	0 (0)	2:1	60 (1,524)	120 (3,048)
NDOR Aesthetic Open Concrete Rail [21]	NCHRP Report 350	TL-5	42 (1,067)	14 (356)	12 (305)	N/A	2 (51)	3:1	30 (762)	72 (1,829)
NE Open Concrete Rail [22]	AASHTO GSB	PL-2	29 (737)	14 (356)	13 (330)	N/A	2 (51)	N/A	24 (610)	60 (1,524)
NE Open Concrete Rail on Inverted Tee Bridge Deck [1]	NCHRP Report 350	TL-4	29 (737)	14 (356)	13 (330)	N/A	2 (51)	N/A	24 (610)	60 (1,524)
TxDOT T203 [23]	NCHRP Report 350	TL-3	30 (762)	13½ (343)	13 (330)	N/A	4½ (114)	N/A	60 (1,524)	60 (1,524)
NDOR Aesthetic Precast Open Concrete Rail [24]	MASH	TL-4	36½ (927)	19 (483)	10⅝ (270)	N/A	4 (102)	N/A	24 (610)	72 (1,829)
TxDOT T223 [25]	NCHRP Report 350	TL-3	32 (813)	19 (483)	13 (330)	N/A	4 (102)	N/A	48 (1,219)	72 (1,829)
CA Type 85 [12]	MASH	TL-4	42 (1,067)	22 (559)	12 (305)	12 (305)	8 (203)	N/A	18 (457)	102 (2,591)
KS Corral Rail [6]	NCHRP Report 230	TL-4	27 (686)	14 (356)	13 (330)	N/A	2 (51)	N/A	36 (914)	84 (2,134)
KS Corral Rail [7]	AASHTO GSB	PL-2	32 (813)	14 (356)	13 (330)	N/A	2 (51)	N/A	36 (914)	84 (2,134)

N/A – Not Applicable

### 2.6.1 TxDOT T224 Bridge Rail

The TxDOT T224 bridge rail was a MASH TL-5 open concrete bridge rail system developed and tested by TTI in 2015 [2]. The overall height of the bridge rail was 42 in., and the system consisted of a 21-in. tall by 16½-in. wide rail supported by 12-in. tall posts atop a 9-in. tall curb, as shown in Figures 18 and 19. The overall width of the system was 16½ in. The post faces were flush with the face of the rail and curb and were tapered at a 2:1 rate to produce a setback of 7 in. at the upstream and downstream edges of the posts. The posts were 8 in. wide by 60 in. long and were separated by a 120-in. long gap. The TxDOT T224 bridge rail was successfully tested with 1100C and 2270P vehicles in test nos. 490025-2-2 and 49005-2-3, respectively, as well as a 79,300-lb 36000V tractor trailer in test no. 490025-2-1, all of which met all safety evaluation criteria according to MASH TL-5.

Through reviewing videos and photographs, it was determined that the tire of the 1100C vehicle extended between the rail and curb, contacted the tapered portion of a post, and was estimated to extend laterally approximately 3½ in. from the face of the post, as shown in Figure 20. The tire of the 2270P vehicle extended between the rail and curb, contacted the post, and was estimated to extend laterally approximately 7 in. from the face of the post, as shown in Figure 21. However, both passenger vehicle tests were successful according to MASH TL-5 criteria.



Figure 18. TxDOT T224 System Photograph [2]





Figure 21. Lateral Extent of 2270P Vehicle Tire Marks on the T224 Bridge Rail [2]

### **2.6.2 NDOR's TL-5 Aesthetic Open Concrete Bridge Rail**

The Nebraska Department of Roads (NDOR) Aesthetic Open Concrete Bridge rail was a NCHRP Report 350 TL-5 open concrete bridge rail system developed and tested by MwRSF in 2005 [21]. The overall height of the bridge rail was 42 in. with a 12-in. vertical opening, as shown in Figures 22 and 23. The rail was 30 in. tall by 14 in. wide with a 4½-in. tall by 7¾-in. wide setback region at the top to account for potential head ejection. The front face of the rail incorporated two longitudinal asperities protruding 1½ in. from the front face of the rail. Post faces were set back 2 in. from the face of the rail and were 10½ in. wide by 30 in. long and separated by a 72-in. long gap. The NDOR TL-5 Aesthetic Open Concrete Bridge Rail was successfully tested under NCHRP Report 350 TL-5 conditions with a 78,975-lb tractor trailer in test no. ACBR-1. Videos and photographs were reviewed, and as seen in Figure 24, contact marks were not apparent on the upstream post faces,



Figure 22. NDOR TL-5 Aesthetic Rail System Photograph [21]

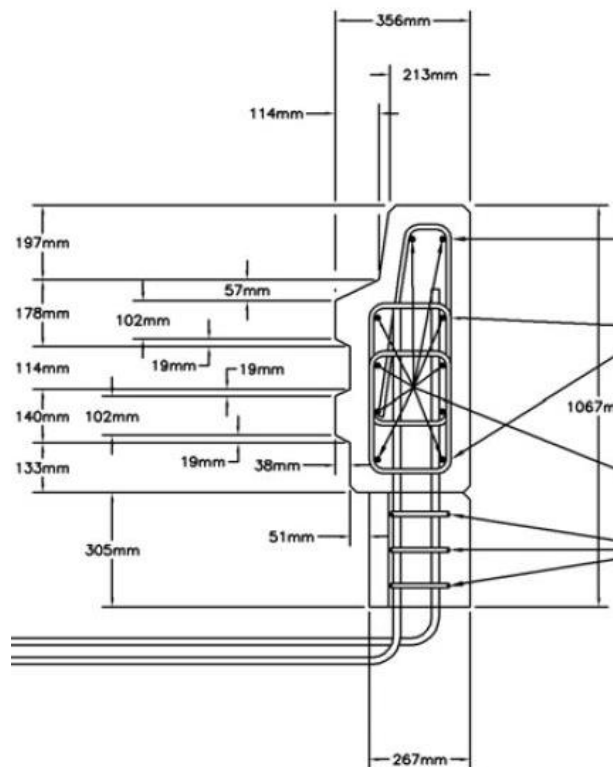


Figure 23. NDOR TL-5 Aesthetic Rail Drawing [21]



Figure 24. NDOR TL-5 Aesthetic Rail Damage [21]

### **2.6.3 Nebraska Open Concrete Rail**

The Nebraska Open Concrete Rail was an AASHTO GSBP PL-2 open concrete bridge rail developed and tested by MwRSF in 1996 [22]. The overall height of the bridge rail was 29 in. with a 13-in. vertical opening, and a 14-in. wide by 16-in. tall rail, as shown in Figures 25 and 26. Posts were 11 in. wide by 24 in. long and were separated by a 60-in. gap in the interior region. End posts at the expansion gap location were 11 in. wide by 36 in. long. Post faces were set back 2 in. from the face of the rail.

Four successful crash tests were conducted under AASHTO GSBP PL-2 conditions. Test nos. NEOCR-3 and NEOCR-4 were conducted with 18,000-lb SUTs and test nos. NEOCR-5 and NEOCR-6 were conducted with 5,394-lb and 5,399-lb pickup trucks, respectively. Although the SUT impacted the barrier near the expansion gap resulting in rail damage, the performance was considered satisfactory according to AASHTO GSBP performance criteria. A review of photographs of test no. NEOCR-5 showed that the tire of the 5,399-lb pickup truck extended beneath the rail, contacted a post, and was estimated to extend laterally 1 in. from the face of the rail, as shown in Figure 27. A review of photographs of test no. NEOCR-6 found that the tire of the 5,394-lb pickup truck extended beneath the rail, contacted a post, and was estimated to extend laterally 3 in. from the face of the rail, as shown in Figure 28. However, all passenger vehicle tests were successful according to AASHTO GSBP PL-2 criteria.



Figure 25. Nebraska Open Concrete Rail System Photograph [22]

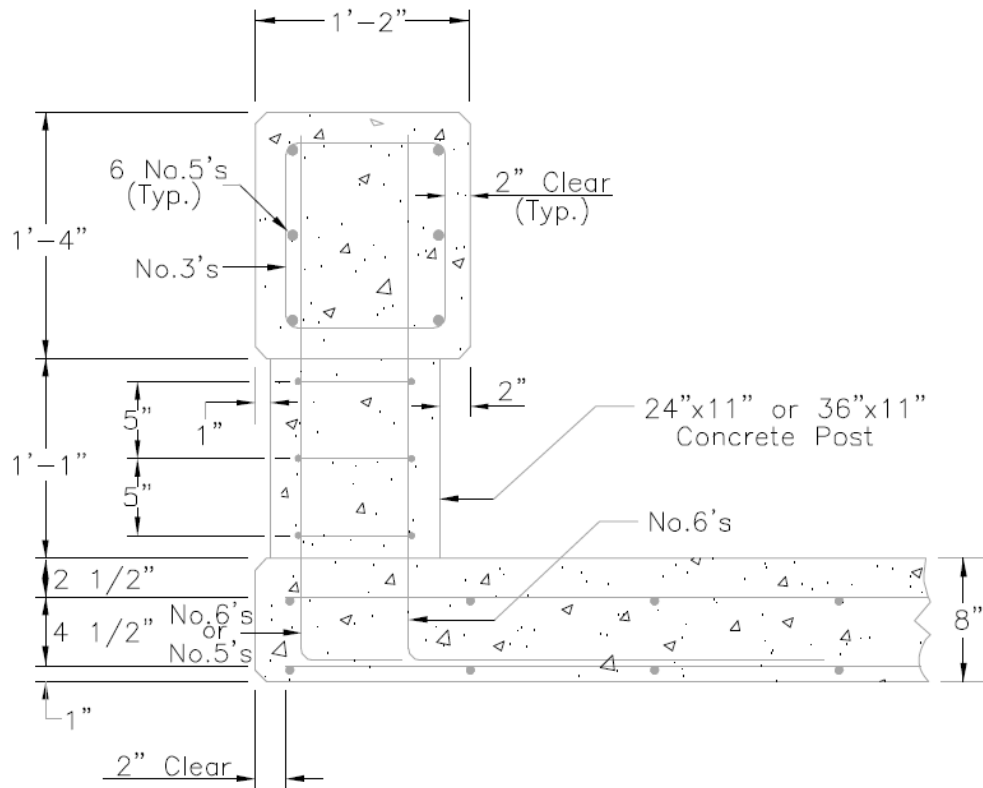


Figure 26. Nebraska Open Concrete Rail Drawing [22]





Figure 27. Lateral Extent of the 5,399-lb Pickup Truck on the Nebraska Open Concrete Rail [22]



Figure 28. Lateral Extent of the 5,394-lb Pickup Truck on the Nebraska Open Concrete Rail [22]

### 2.6.4 Nebraska Open Concrete Rail on an Inverted Tee Bridge Deck

The Nebraska Open Concrete Rail on an Inverted Tee (IT) Bridge deck was the same as the original Nebraska Open Concrete Rail but was installed on a simulated inverted tee bridge deck and tested under NCHRP Report 350 standards [1]. No expansion gaps were included in this system, as shown in Figures 29 and 30. Test no. NIT-1, conducted with a 4,400-lb 2000P pickup truck, was successfully conducted to NCHRP Report 350 TL-3 standards. A review of photographs showed that the tire of the 2000P vehicle extended beneath the rail, contacted a post, and was estimated to extend laterally approximately 4½ in. from the face of the rail, as shown in Figure 31. However, the passenger vehicle test was successful according to NCHRP Report 350 criteria.



Figure 29. Nebraska Open Concrete Rail on an IT Bridge Deck System Photograph [1]

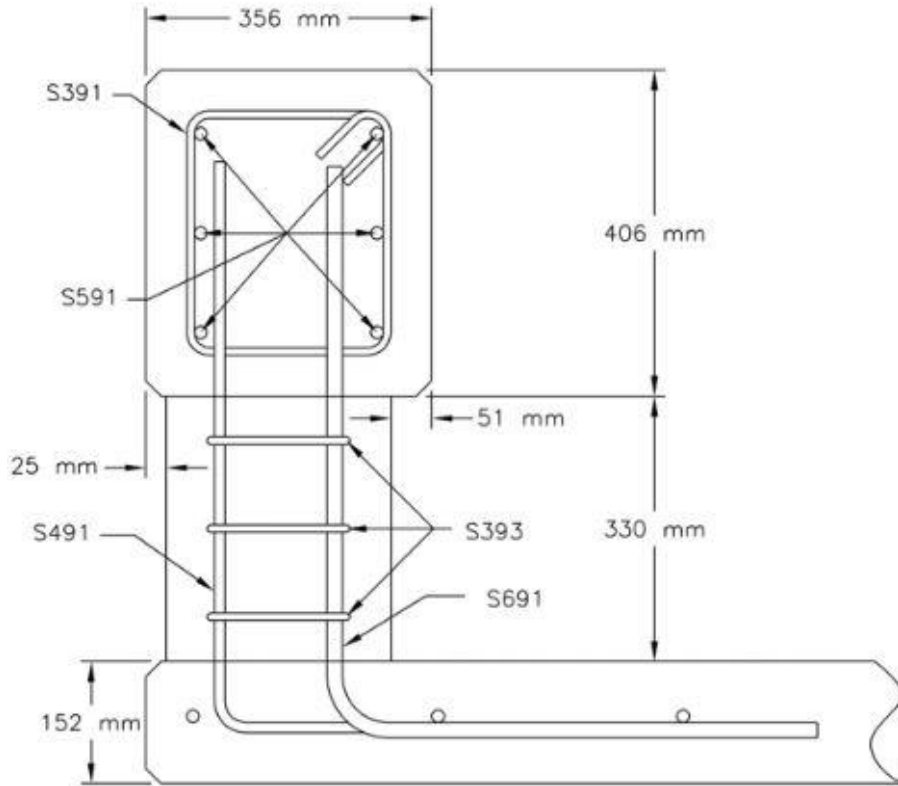


Figure 30. Nebraska Open Concrete Rail on an IT Bridge Deck System Drawing [1]



Figure 31. Lateral Extent of the 2000P Vehicle on the Nebraska Open Concrete Rail on an IT Bridge Deck [1]

### 2.6.5 TxDOT T202 and T203 (T202 MOD)

The TxDOT T203 was a NCHRP Report 350 TL-3 open concrete bridge rail developed and tested by TTI [23]. The bridge rail was tested at overall heights of 27 in. and 30 in., with the addition of a 3-in. tall steel rail mounted on top, as shown in Figures 32 through 34. In both configurations, the concrete rail was 13½ in. wide by 14 in. tall. Posts were 13 in. tall by 7½ in. wide by 60 in. long and were separated by a 60-in. long gap. Post faces were set back 4½ in. from the face of the rail. The TxDOT T203 was based off the TxDOT T202 bridge rail, which was identical to the TxDOT T203 bridge rail, with the exception that its post faces were set back 1½ in. from the face of the rail. The TxDOT T202 was successfully crash tested under NCHRP Report 230 conditions [16], and unsuccessfully crash tested under NCHRP Report 350 conditions [26]. NCHRP Report 350 test designation no. 3-10 was unsuccessful due to excessive occupant compartment deformation, which was believed to have occurred due to vehicle interaction with the posts. Thus, post setback was increased to 4½ in., resulting in a successful crash test under test designation no. 3-11. Pictures of the crash tests conducted on the TxDOT T202 bridge rail did not clearly display lateral extent or vehicle interaction with posts.

Two crash tests with a 4,400-lb 2000P pickup truck vehicle were conducted: one on the 27-in. tall variation and one on the 30-in. tall variation. Test no. 441382-1, conducted on the 27-in. tall variation, resulted in the pickup rolling over due to insufficient rail height and was a failed test according to NCHRP Report 350 criteria. Analysis of photographs determined there was no contact between the wheel of the vehicle and posts, as shown in Figure 35. The absence of contact with the posts was likely due to the insufficient rail height. In test no. 441382-2, the addition of a 3-in. steel rail resulted in a successful crash test of the 2000P vehicle according to NCHRP Report 350 criteria. By reviewing photographs, it was determined the tire of the vehicle extended laterally approximately 6½ in. and contacted the upstream and front faces of the post, as shown in Figure 36.



Figure 32. T203 Bridge Rail 27-in. Configuration System Photograph [23]



Figure 33. T203 Bridge Rail 30-in. Configuration System Photograph [23]

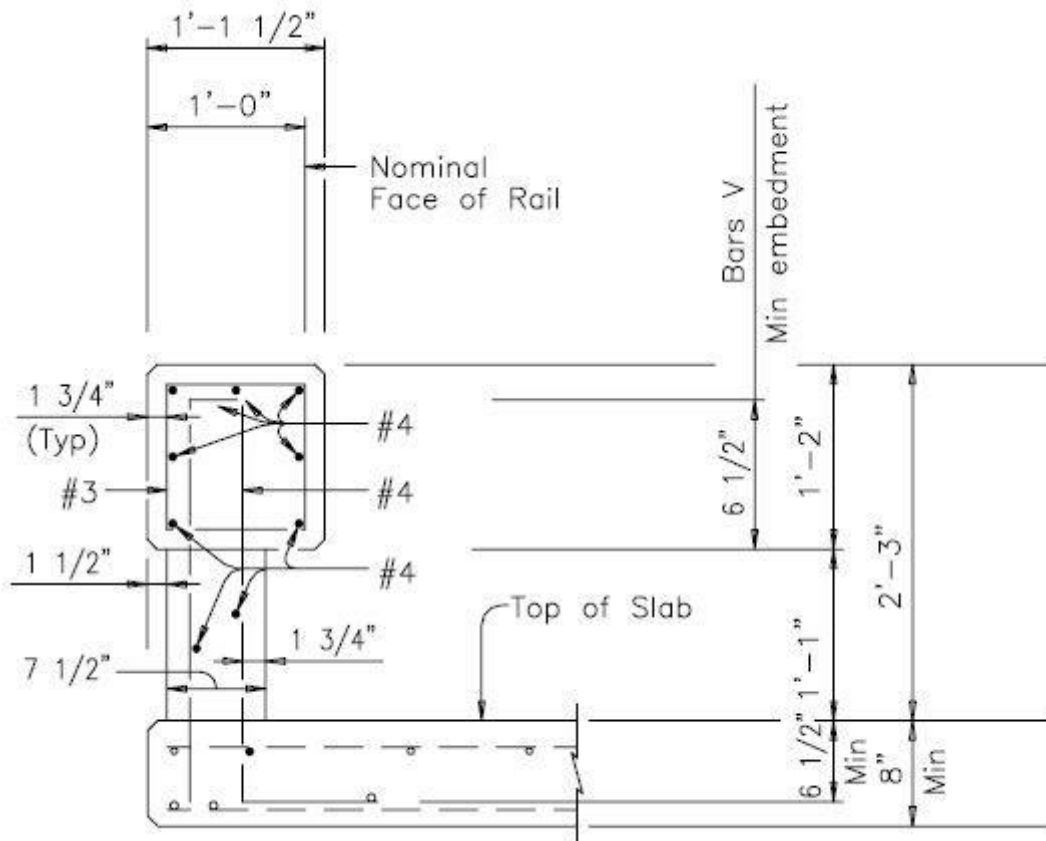


Figure 34. T203 Bridge Rail Drawing [23]



Figure 35. Lateral Extent of the 2000P Vehicle on the 27-in. Tall T203 Barrier [23]



Figure 36. Lateral Extent of the 2000P Vehicle on the 30-in. Tall T203 Barrier [23]

### 2.6.6 Aesthetic Precast Concrete Bridge Rail

An aesthetic MASH TL-4 precast concrete bridge rail was developed by MwRSF in 2012 [24]. Multiple concepts were developed based off provisions for open and closed rail options, constructability, weight limitations, segment length, design impact loads, connection of the barrier segments, and connection to the bridge deck. The fence option shown in Figure 37 was the preferred option, as the rail-to-rail and post-to deck joints were believed to decrease impact loading and damage to the bridge deck. The fence option was 36½ in. tall, consisted of two rail elements vertically spaced at 5¾ in., and was supported by 24-in. long by 11-in. wide posts separated by a 72-in. gap. Post faces were set back 4 in. from the face of the rail.

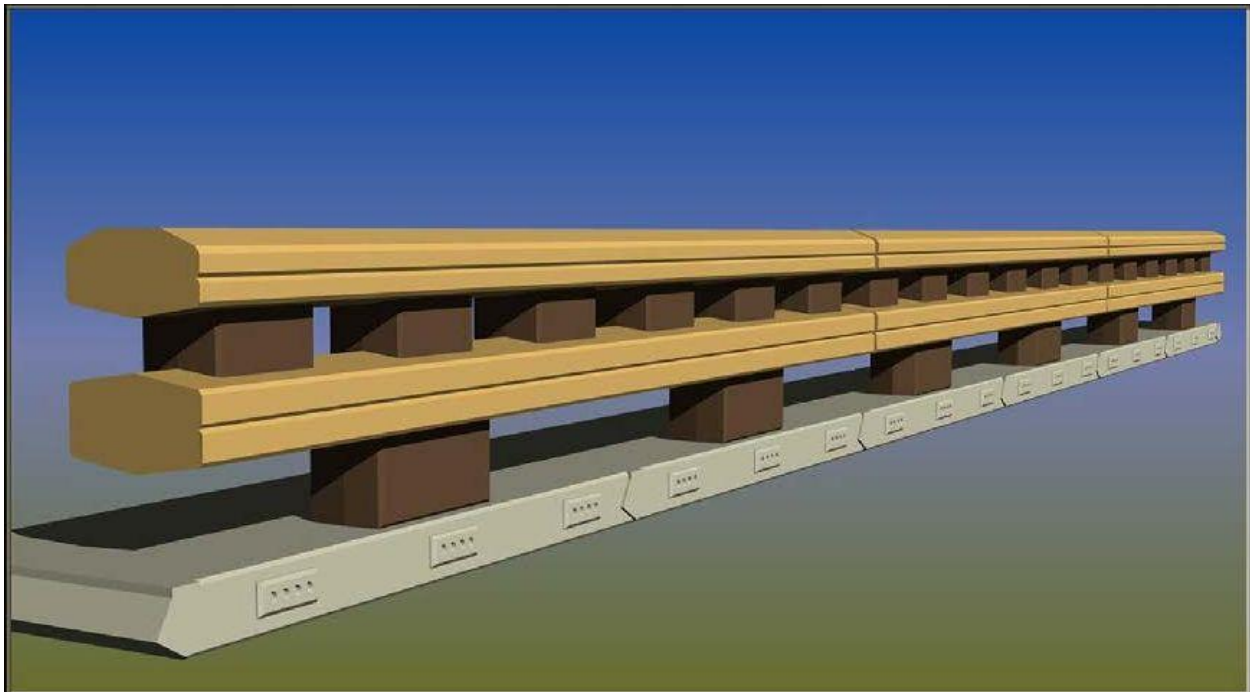


Figure 37. Precast Fence Concept [24]

### 2.6.7 TxDOT T223

The TxDOT T223 bridge rail was a NCHRP Report 350 TL-3 open concrete bridge rail developed and tested by TTI in 2009 [25]. The overall height of the bridge rail was 32 in. with a 13-in. tall vertical opening, as shown in Figures 38 and 39. The system consisted of a 19-in. tall by 15½-in. wide rail atop 48-in. long by 9½-in. wide posts. Posts were separated by a 72-in. long gap, and post faces were set back 4-in. from the front face of the rail. The TxDOT T223 was not full-scale crash tested, but five dynamic bogie tests were conducted, resulting in rail and deck cracking at various impact locations. Although no full-scale crash tests were conducted, the system geometry was similar to the new MASH TL-4 open concrete bridge rail, and its geometry, reinforcement details, and weight were included in comparisons of similar bridge rails.



Figure 38. TxDOT T223 Bridge Rail System Photograph [25]

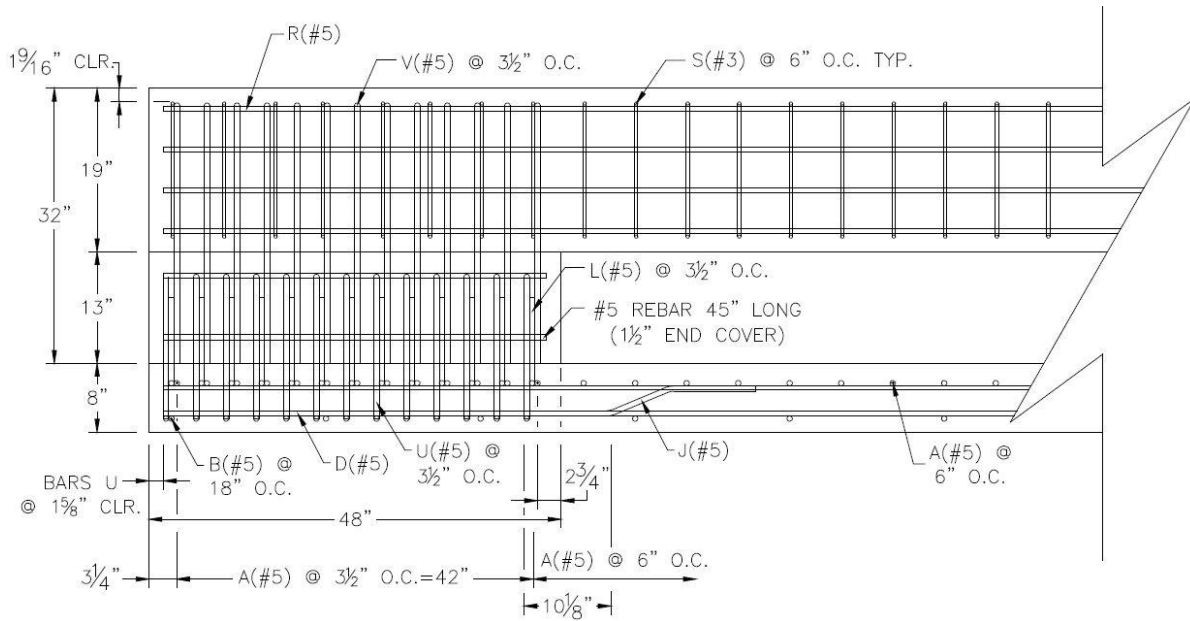


Figure 39. TxDOT T223 Bridge Rail Drawing [25]



### 2.6.8 California Type 85

The California Type 85 Bridge Rail was a MASH TL-4 open concrete bridge rail developed and tested by Caltrans in 2019 [12]. The overall height of the bridge rail was 42 in. with a 12-in. tall curb, 12-in. tall vertical opening, and 6-in. tall steel rail atop the concrete rail elements, as shown in Figure 40. The system consisted of a 12-in. tall by 15-in. wide rail atop 15-in. wide by 18-in. long posts separated by a 102-in. long gap. Three full-scale crash tests were conducted on the bridge rail with 1100C, 2270P, and 10000S vehicles. All crash tests were successful according to MASH TL-4 criteria, but the lateral extent was unable to be determined from the provided photographs.

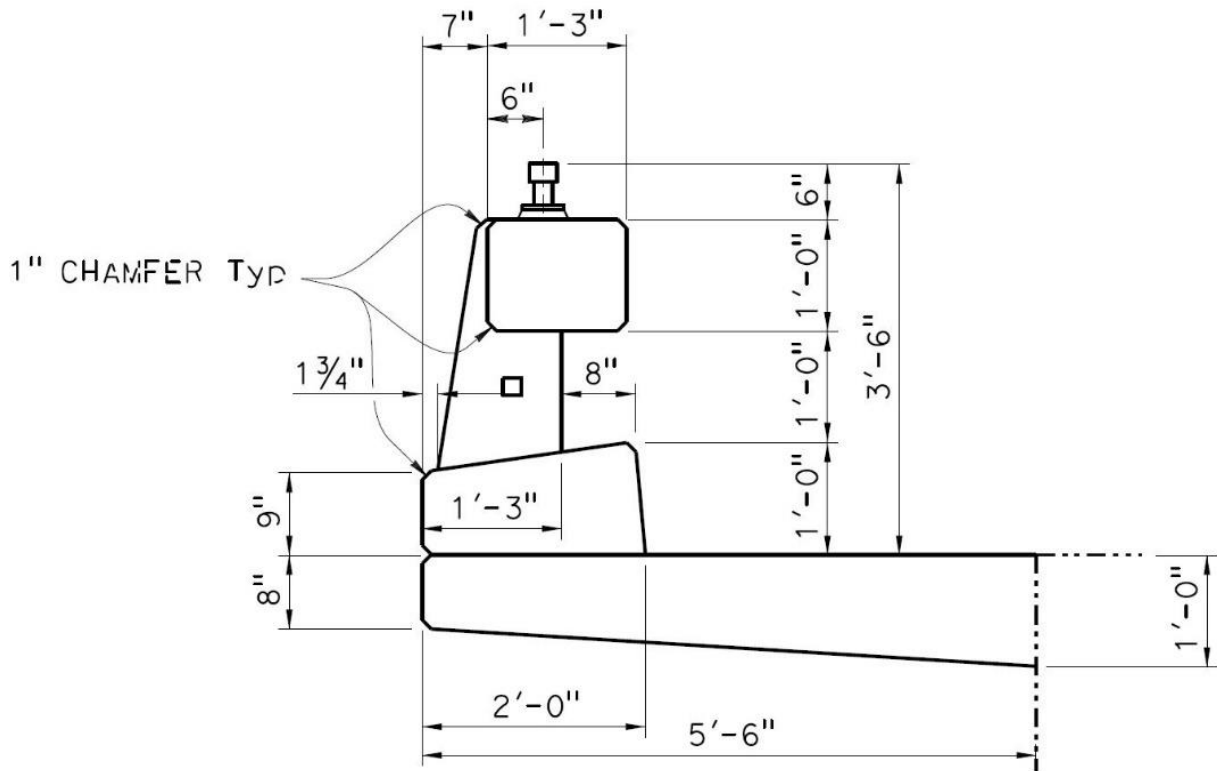


Figure 40. California Type 85 Bridge Rail [12]

### 2.6.9 Kansas Corral Rail

The Kansas Corral Rail was an open concrete bridge rail tested under NCRHP Report No. 230 by SwRI in 1987 [6], and under AASHTO PL-2 conditions by MwRSF in 1991 [7]. The overall height of the bridge rail was 32 in. with a 13-in. tall vertical opening, as shown in Figure 41. The system consisted of a 19-in. tall by 14-in. wide rail atop 12-in. wide by 36-in. long posts. Posts were separated by an 84-in. long gap, and the front faces of the posts were offset 2 in. from the front face of the rail. Test nos. MKS-1 and MKS-2 were successfully conducted under NCHRP Report 230 conditions with 1,971-lb and 4,690-lb vehicles, but lateral extent could not be determined from provided photographs. In test no. KSCR-1, which was successfully conducted under AASHTO GSBP PL-2 conditions with an SUT, lateral extent was also unable to be determined.

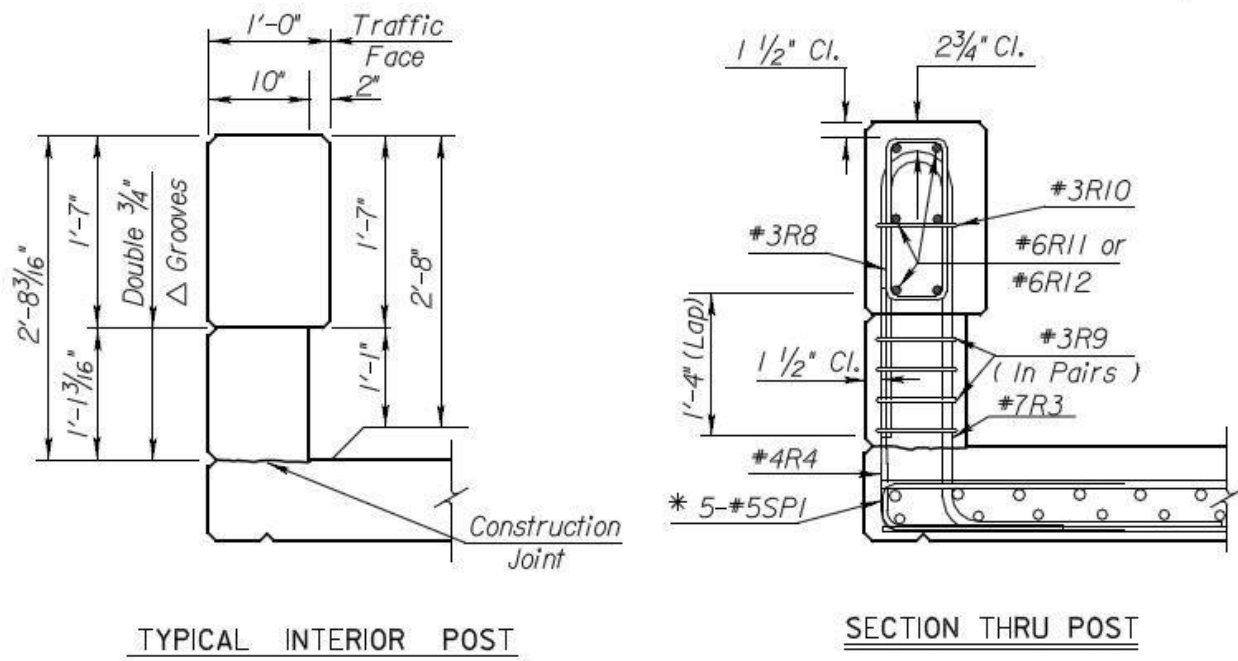


Figure 41. 32-in. Tall Kansas Corral Rail Details [7]

### 2.7 Steel Bridge Rails

Steel bridge rails, which have similar post and beam construction as open concrete bridge rails, were reviewed as they could also result in vehicle snagging on posts. The steel rails were reviewed to determine whether full-scale crash testing was successful, whether the vehicle snagged on the barrier, and if the system geometry contributed to an unsuccessful crash test. Relevant system geometry was collected, as shown in Figures 42 and 43. This information included overall system height, overall system width, vertical opening, curb height, post setback, post taper, post length, and gap length, as shown in Table 6. Relevant system geometry was defined based on its influence on snag potential and was collected to guide future recommendations for the new open concrete bridge rail. Steel bridge rails studied were selected based on the ability to determine the potential for vehicle snagging. Although steel systems typically undergo more deformation than concrete systems, these systems were still relevant to determining how rail geometry influences snag potential and are described in the subsequent sections of this report.

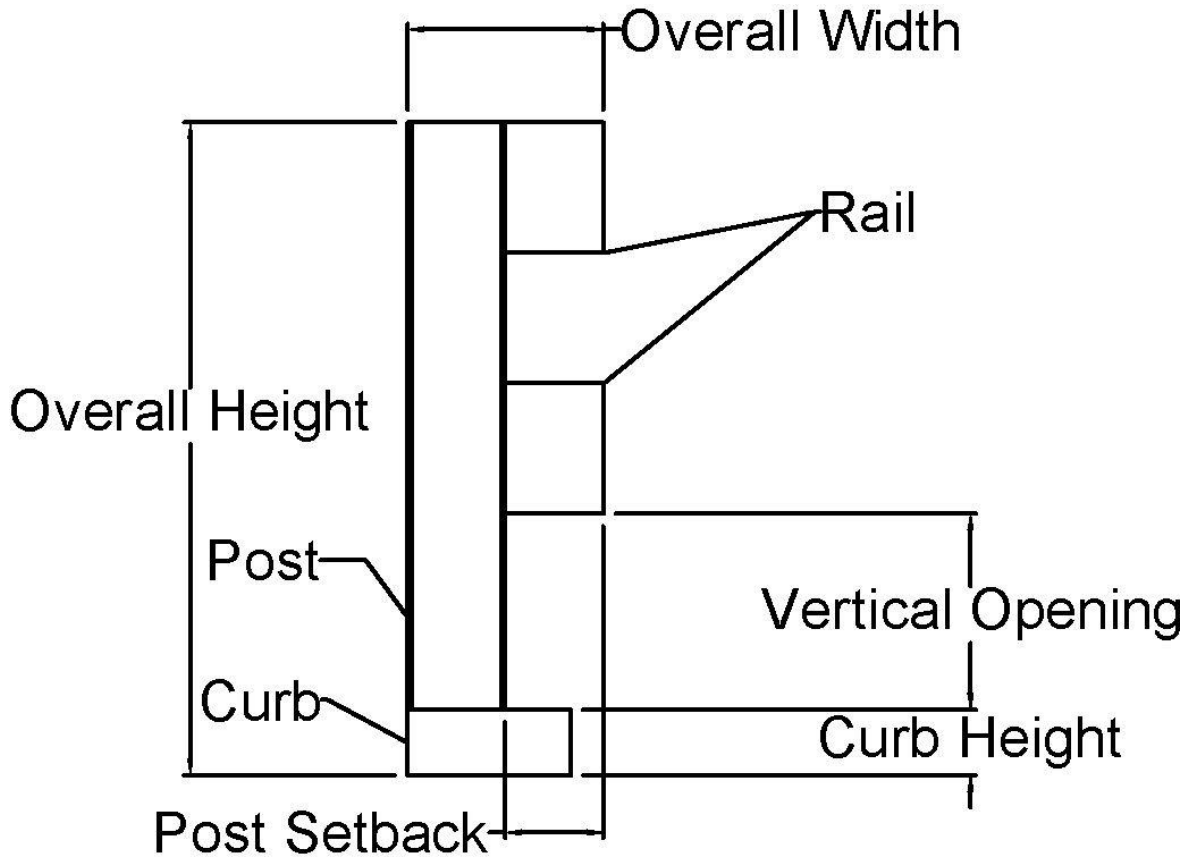


Figure 42. Steel Bridge Rail General Dimensions, Cross Section

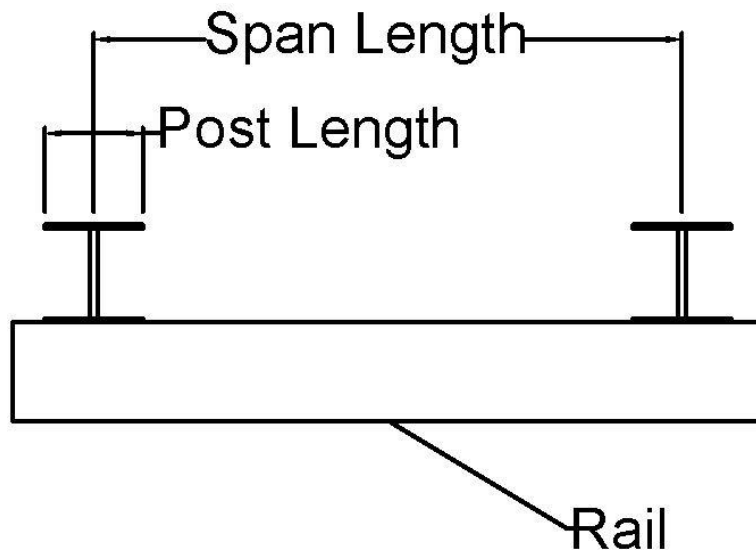


Figure 43. Steel Bridge Rail General Dimensions, Plan View

Table 6. Steel Bridge Rail Design Details

System Name	Test Criteria	Test Level	Overall Height in. (mm)	Overall Width in. (mm)	Vertical Opening in. (mm)	Curb Height in. (mm)	Post Setback in. (mm)	Post Taper	Post Length in. (mm)	Span Length in. (mm)
California ST-70SM [27]	MASH	TL-4	42 (1,067)	18 (457)	8 (203)	9 (229)	6 (152)	N/A	8 (203)	120 (3,048)
Massachusetts Type S3 [28]	MASH	TL-4	42 (1,067)	14½ (368)	12½ (318)	N/A	5 (127)	N/A	6 (152)	72 (1,829)
IL-OH Steel BR [29-32]	MASH	TL-4	36 (914)	13 (330)	9 (229)	N/A	6 (152)	N/A	6 (152)	60 (1,524)
IL-OH Steel BR [29-32]	MASH	TL-4	39 (991)	13 (330)	12 (305)	N/A	6 (152)	N/A	6 (152)	60 (1,524)

N/A = Not Applicable

### 2.7.1 California ST-70SM

The California ST-70SM bridge rail was a side-mounted, steel post and beam bridge rail tested under MASH TL-4 conditions by Caltrans in 2017 [27]. The overall height of the bridge rail was 42 in. and incorporated an 8-in. vertical opening, as shown in Figures 44 and 45. The bridge rail consisted of four tube splice (TS) rails supported by side-mounted steel posts. The top and bottom rails were ASTM A500 TS8x3x $\frac{5}{16}$ , and the middle two rail elements were ASTM A36 TS8x4x $\frac{5}{16}$ . The four rails were vertically spaced at 9 $\frac{1}{2}$  in., 11 in., and 10 $\frac{1}{2}$  in. on center. All rails were attached to the front of the posts with two  $\frac{3}{4}$ -in. diameter stud bolts. Posts were spaced at 120 in. on center and consisted of two ASTM A36  $\frac{3}{4}$ -in. thick by 60-in. long plates spaced at 8 in. on center. Post faces were set back 6 in. from the face of the rail, with the lower portion of the post having a smaller offset. Test nos. 110MASH3P15-01, 110MASH3P15-02, and 110MASH3P15-03 were conducted under MASH TL-4 conditions with the 1100C, 2270P, and 10000S vehicles, respectively. All crash tests were successful according to MASH TL-4 criteria, and a review of photographs determined that no vehicle components laterally extended beneath or between rail elements, as shown in Figures 46 and 47.



Figure 44. California ST-70SM Bridge Rail System Photograph [27]

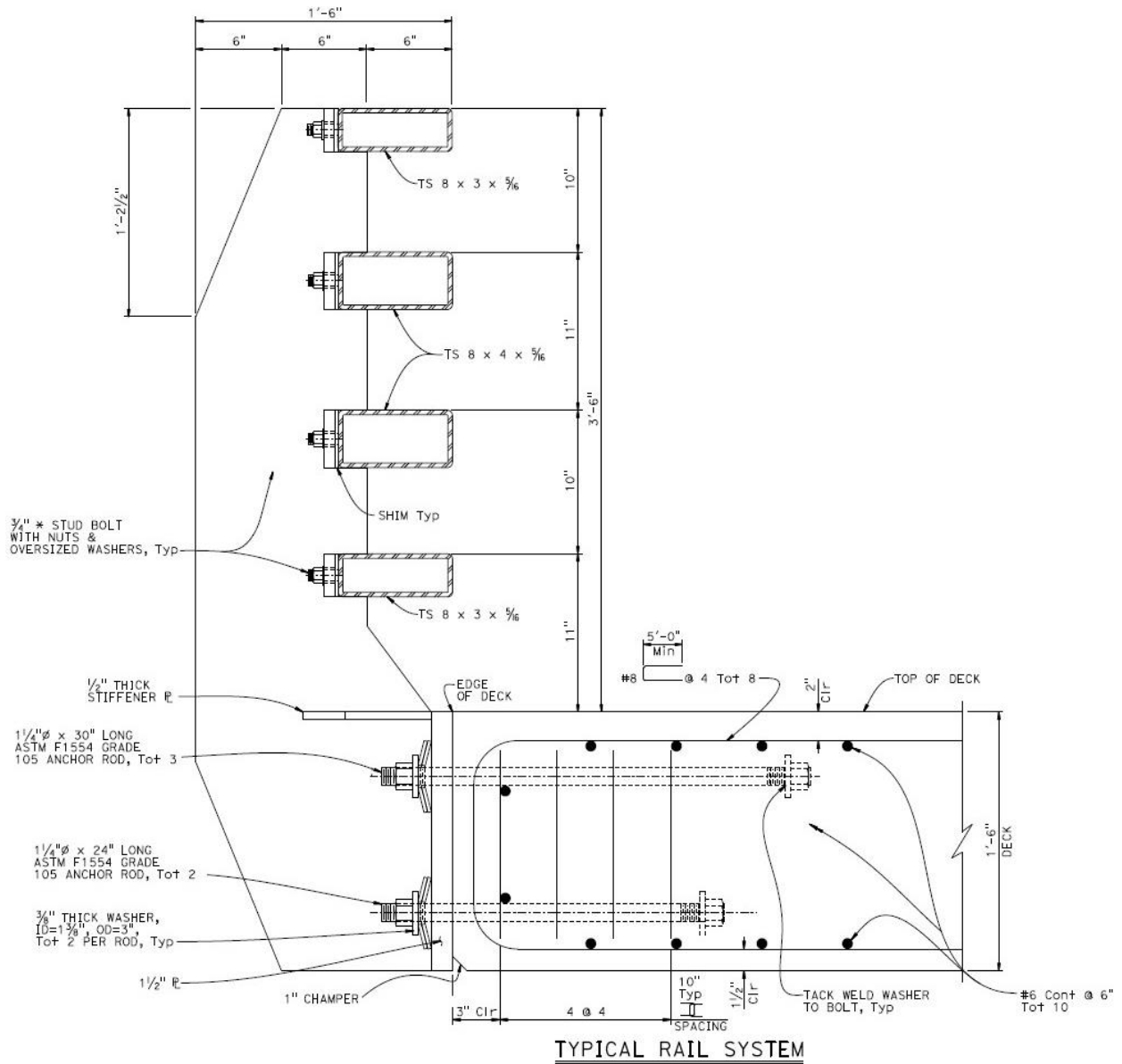


Figure 45. California ST 70 Bridge Rail Drawing [27]



Figure 46. Lateral Extent of the 1100C Vehicle on the ST-70SM Bridge Rail [27]



Figure 47. Lateral Extent of the 2270P Vehicle on the ST-70SM Bridge Rail [27]

### 2.7.2 Massachusetts Type S3

The Massachusetts Type S3 bridge rail was a deck-mounted, steel post and beam bridge rail tested under NCHRP Report 350 TL-4 criteria in 1999 by TTI [28]. Full-scale crash tests were conducted on variants of the bridge rail with and without an 8-in. tall curb. Variants without the 8-in. tall curb did not incorporate a vertical opening large enough for vehicle elements to extend beneath the rail; therefore, those full-scale crash tests were not included in the literature review. The overall height of the bridge rail was 40 in. with a 12½-in. vertical opening, as shown in Figures 48 and 49. The bridge rail consisted of three HSS steel rails mounted to W6x25 steel posts spaced at 79½ in. on center. Posts were welded to 1¼-in. thick baseplates, which were bolted to the bridge deck. Post faces were set back 5 in. from the face of the rails. The lower and middle rails were HSS5x5x¼ and the top rail was HSS5x4x¼. The three rails were vertically spaced at 13 in. and 11½ in. on center. Steel picket elements were welded to the rear of the HSS rail elements. The system was successfully tested under NCHRP Report 350 TL-4 conditions with an 820C small car, 2000P pickup truck, and an 8000S SUT in test nos. 404251-1, 404251-2, and 404251-3. The 820C test system is shown in Figure 50, the 2000P test system in Figure 51, and the 8000S system in Figure 52.

Photographs showed that the tires of the 820C and 8000S vehicles did not contact the posts, but the right-front tire of the 2000P vehicle extended beneath the rail, extended laterally approximately 5 in. from the face of the post, and contacted the vertical picket elements on the rear side of the rail. However, all tests were successful according to NCHRP Report 350 TL-4 criteria.



Figure 48. Massachusetts Type S3 Bridge Rail System Photograph [28]







Figure 51. Lateral Extent of 2000P Vehicle on the Massachusetts Type S3 Bridge Rail [28]



Figure 52. Lateral Extent of the 8000S Vehicle on the Massachusetts Type S3 Bridge Rail [28]

### 2.7.3 Illinois-Ohio Steel Bridge Rail

The Illinois-Ohio steel bridge rail was a side-mounted, steel post and beam system developed under MASH TL-4 criteria by MwRSF in 2019 [29-32]. The bridge rail consisted of ASTM A500 W6x15 steel posts mounted to the side of the bridge deck and three HSS rail elements, as shown in Figures 53 through 56. The lower and middle rail elements were both HSS8x6x¼, and the top rail was a HSS12x4x¼. Posts were spaced at 96 in. on center. Post faces were set back 6 in. from the face of the rail. The bridge rail was tested at overall heights of 36 in. and 39 in. The 1100C vehicle was tested at the 39-in. height, as this height corresponded to a 12-in. tall vertical opening and maximized snag potential. The 2270P and 10000S vehicles were tested at the 36-in. height, corresponding to a 9-in. tall vertical opening, as this height corresponded to an increased likelihood of rollover.

Test nos. STBR-2, STBR-3, and STBR-4 were conducted according to MASH TL-4 criteria with the 1100C, 2270P, and 10000S vehicles, respectively, and all three tests were successful. A review of videos and photographs found that the 1100C vehicle tire extended under the lower rail, left the surface of the bridge deck, contacted the upstream and front faces of the post, and extended laterally approximately 9¼ in. from the face of the post, as shown in Figure 57. It was determined that structural components of the 2270P vehicle did not extend laterally beneath the rail enough to contact any posts, as the only contact mark was left by the plastic bumper cover, as shown in Figure 58.



Figure 53. 36-in. Tall, Illinois-Ohio steel Bridge Rail System Photograph [29-32]



Figure 54. 39-in. Tall, Illinois-Ohio Steel Bridge Rail System Photograph [29-32]

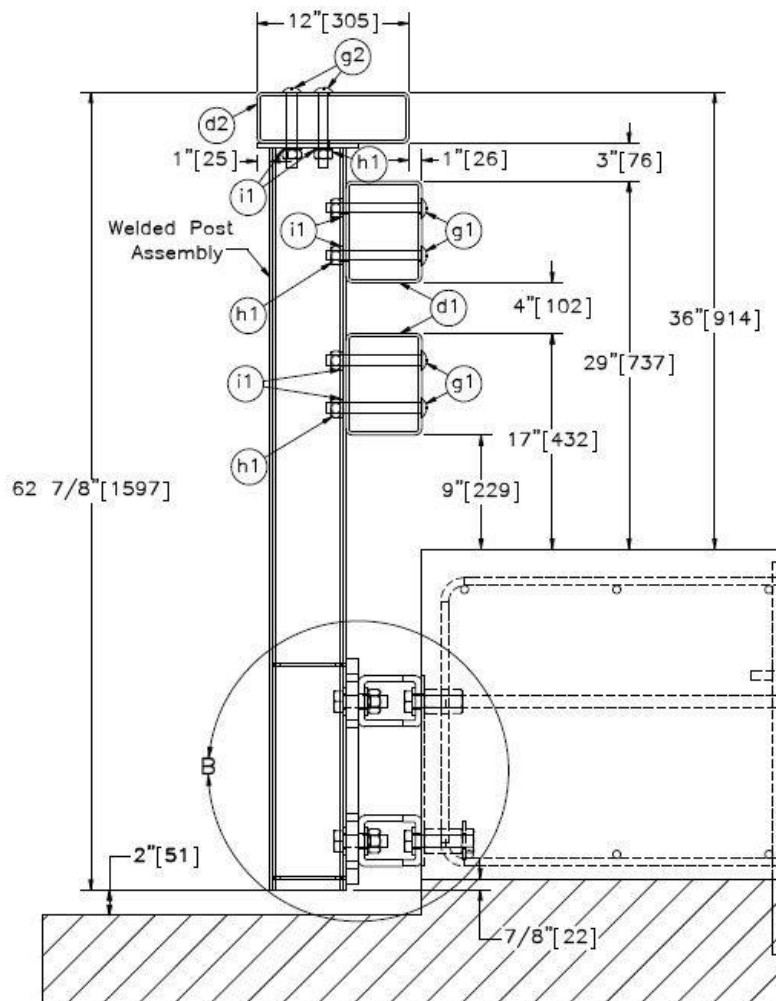


Figure 55. 36-in. Tall Illinois-Ohio Steel Bridge Rail Drawing [29-32]

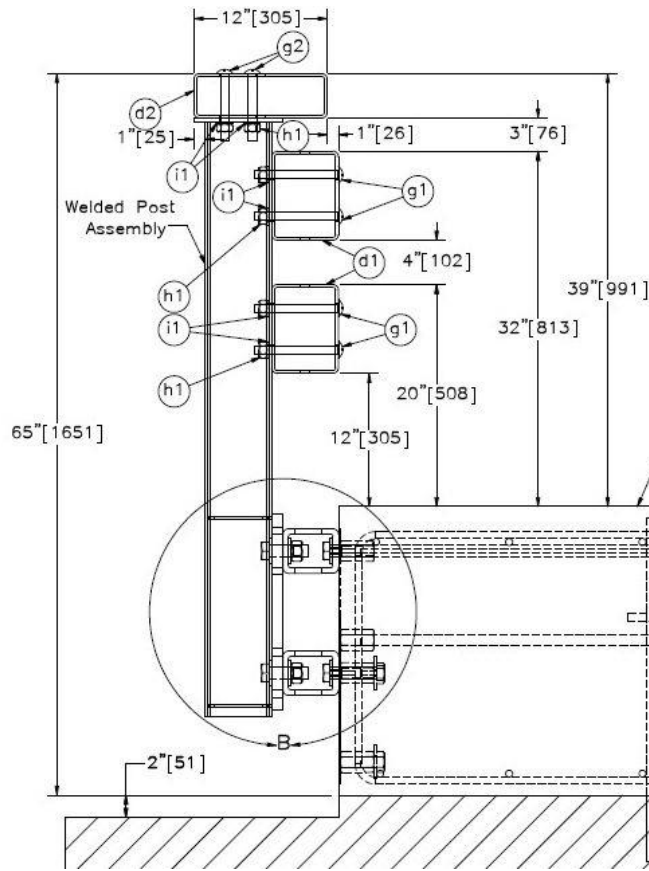


Figure 56. 39-in. Tall Illinois-Ohio Steel Bridge Rail Drawing [29-32]



Figure 57. Lateral Extent of the 1100C Vehicle on the 39-in. Tall Illinois-Ohio Steel Bridge Rail [29-32]



Figure 58. Lateral Extent of the 2270P Vehicle on the 36-in. Tall Illinois-Ohio Steel Bridge Rail [29-32]

## 2.8 Other Systems

Other systems with post and beam construction or with a rigid barrier exposed to potential vehicle snag were also reviewed to determine whether full-scale crash testing was successful, whether the vehicle snagged on the barrier, and if the system geometry contributed to a test failure. Relevant system geometry was collected, shown in Figures 59 and 60. This information included overall system height, overall system width, vertical opening, curb height, post setback, post taper, post length, and gap length, as shown in Table 7. Relevant system geometry was defined based on its influence on snag potential and was collected to guide future recommendations for the new open concrete bridge rail. Other systems studied were selected based on the ability to determine the potential for vehicle snagging, or if their geometry was similar to that of the Kansas Corral Rail. Although some of these systems have the potential to undergo more deformation than concrete systems, they were still relevant to determining how rail geometry influences snag potential.

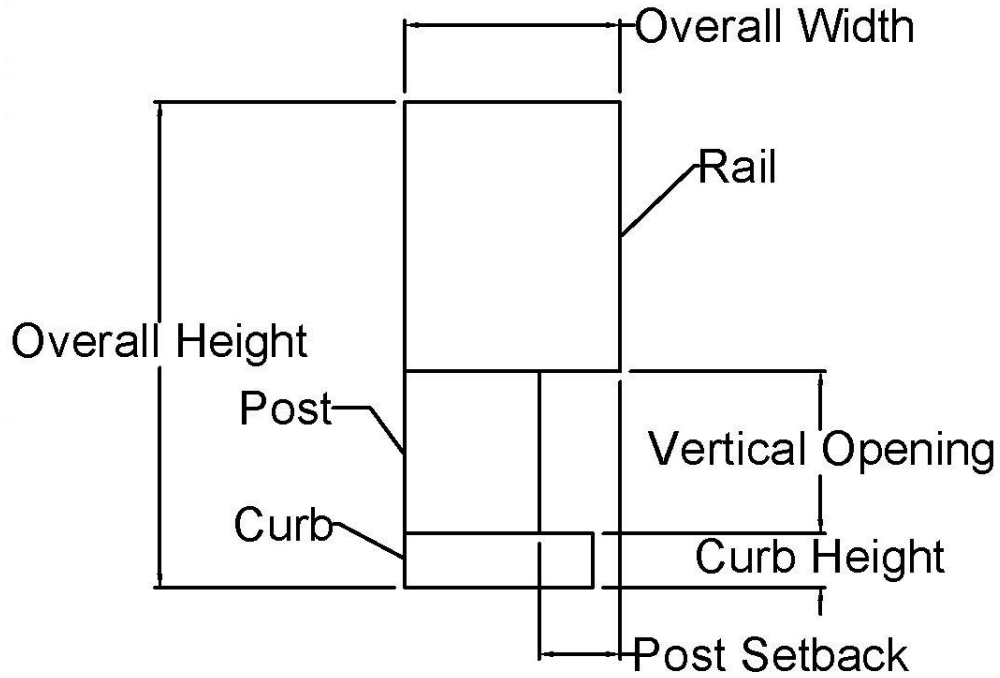


Figure 59. Other System General Dimensions, Cross Section

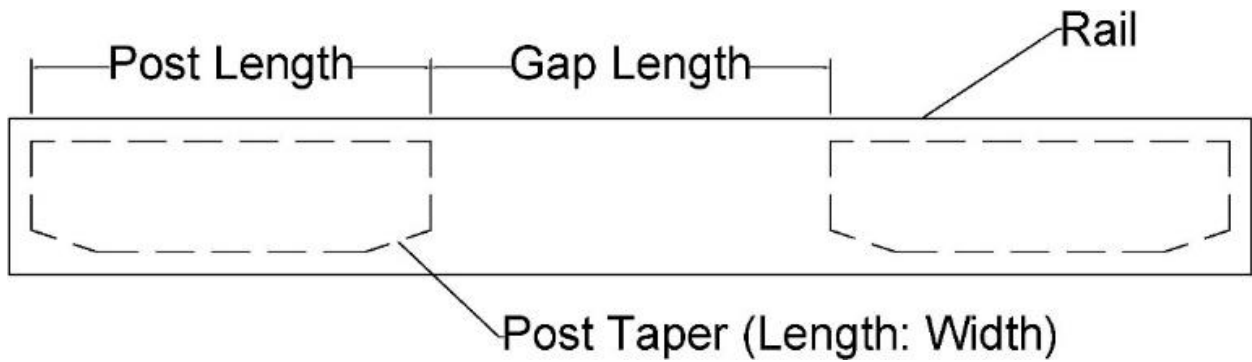


Figure 60. Other System General Dimensions, Plan View

Table 7. Other Systems Design Details

System Name	Test Criteria	Test Level	Overall Height in. (mm)	Overall Width in. (mm)	Vertical Opening in. (mm)	Curb Height in. (mm)	Post Setback <sup>1</sup> in. (mm)	Post Taper	Post Length in. (mm)	Span Length in. (mm)
MN Noise Wall [33]	MASH	TL-3	30 (762)	10 <sup>3</sup> / <sub>4</sub> (273)	16 <sup>1</sup> / <sub>2</sub> (419)	N/A	16 <sup>3</sup> / <sub>4</sub> (425)	N/A	12 (305)	96 (2,438)
MN Noise Wall [33]	MASH	TL-3	30 (762)	10 <sup>3</sup> / <sub>4</sub> (273)	16 <sup>1</sup> / <sub>2</sub> (419)	N/A	12 <sup>3</sup> / <sub>4</sub> (324)	N/A	12 (305)	96 (2,438)
Restore Barrier [34]	MASH	TL-4	38 <sup>5</sup> / <sub>8</sub> (981)	21 <sup>1</sup> / <sub>2</sub> (546)	11 <sup>5</sup> / <sub>8</sub> (295)	N/A	5 <sup>1</sup> / <sub>2</sub> (140)	N/A	10 (254)	30 (762), 60 (1,524)
Standardized AGT [35]	MASH	TL-3	31 (787)	12 (305)	11 (279)	N/A	3 <sup>1</sup> / <sub>4</sub> (83)	4 <sup>1</sup> / <sub>2</sub> :1	NA	N/A
34-in. AGT [36]	MASH	TL-3	34 (864)	12 (305)	14 (356)	N/A	3 <sup>1</sup> / <sub>4</sub> (83)	4 <sup>1</sup> / <sub>2</sub> :1	NA	N/A

<sup>1</sup> Post setback distances for the standardized AGT and 34-in. (864-mm) AGT refer to buttress setbacks.

N/A – Not Applicable



### 2.8.1 Minnesota Noise Wall

The Minnesota Noise Wall was a wood plank noise wall with precast concrete posts and a glue-laminated timber rubrail developed under MASH TL-3 standards by MwRSF in 2019 [33]. The system was tested in configurations with the rubrail offset from the wooden noise wall by the precast posts and with the wooden noise wall directly behind the timber rubrail, as shown in Figures 61 through 64. These setbacks were 16¾ in. from the face of the rail to the face of the posts, and 12¾ in. from the face of the rail to the face of the wall. The rubrail had an overall height of 30 in., a vertical opening of 16½ in., and was 10¾ in. wide by 13½ in. tall. The rubrail was connected to the precast posts by ¾-in. diameter bolts. Three successful crash tests according to MASH TL-3 criteria were run: one with the 1100C vehicle and a post setback of 16¾ in., and two with the 2270P vehicle with a wall setback of 12¾ in. and post setback of 16¾ in.

Test no. MNNW-1 consisted of the 2270P vehicle impacting the Minnesota Noise Wall in the configuration with the 16¾-in. post setback. Through reviewing videos and photographs, it was determined that the right-front tire of the 2270P vehicle extended beneath the rail, did not contact a post or the wall of the system, detached from the vehicle as it was redirected, and laterally extended approximately 20¾ in. from the face of the rail. Test no. MNNW-2 consisted of the 1100C vehicle impacting the Minnesota Noise Wall in the configuration with the 16¾ in. post setback. Through reviewing videos and photographs, it was determined the right-front tire of the 1100C vehicle extended beneath the rail, did not contact a post or the wall of the system, and laterally extended approximately 16¾ in. from the face of the rail. Test no. MNNW-3 consisted of the 2270P vehicle impacting the Minnesota Noise Wall in the configuration with the 12¾-in. wall setback. Through reviewing videos and photographs, it was determined the right-front tire of the 2270P vehicle extended beneath the rail, contacted the wooden noise wall, and laterally extended 12¾ in. from the face of the rail. All passenger vehicle tests were successful according to MASH TL-3 criteria, and system damage is shown in Figures 65 through 67.



Figure 61. Minnesota Noise Wall Test Nos. MNNW-1 and MNNW-2 System Photograph [33]



Figure 62. Minnesota Noise Wall Test No. MNNW-3 System Photograph [33]

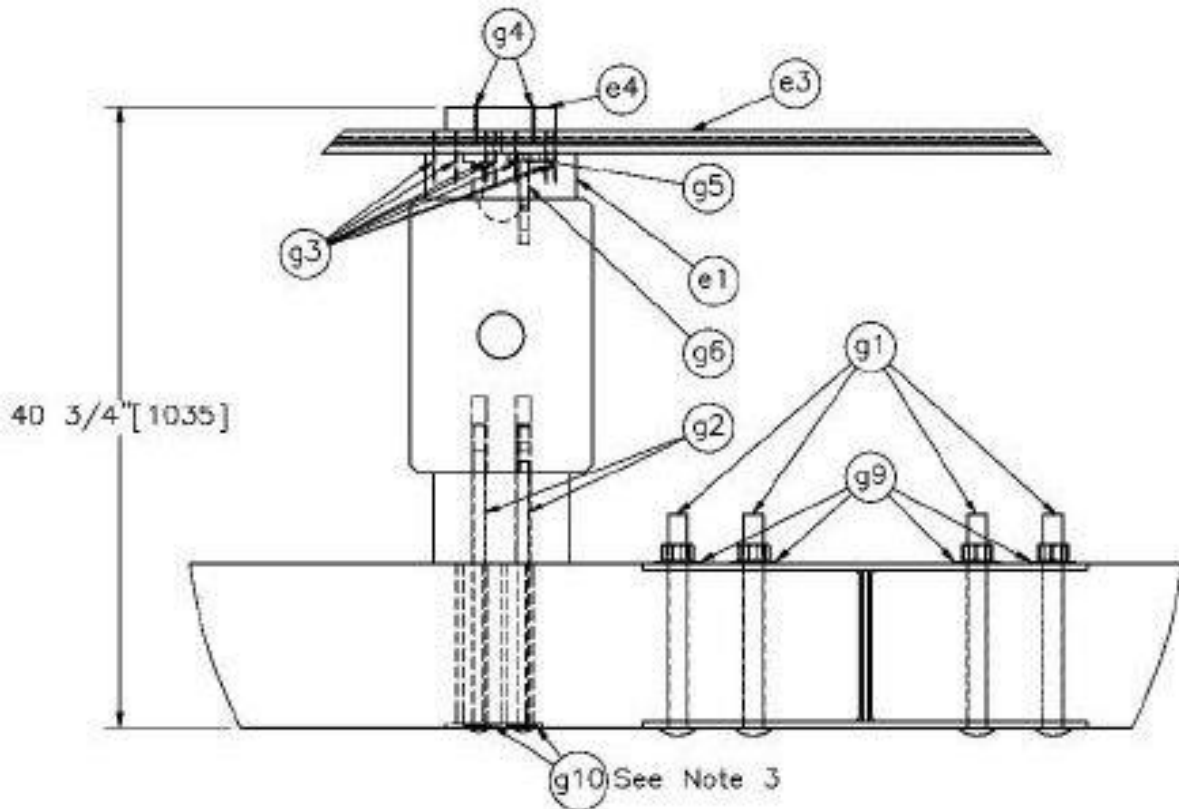


Figure 63. Test Nos. MNNW-1 and MNNW-2 Drawing [33]

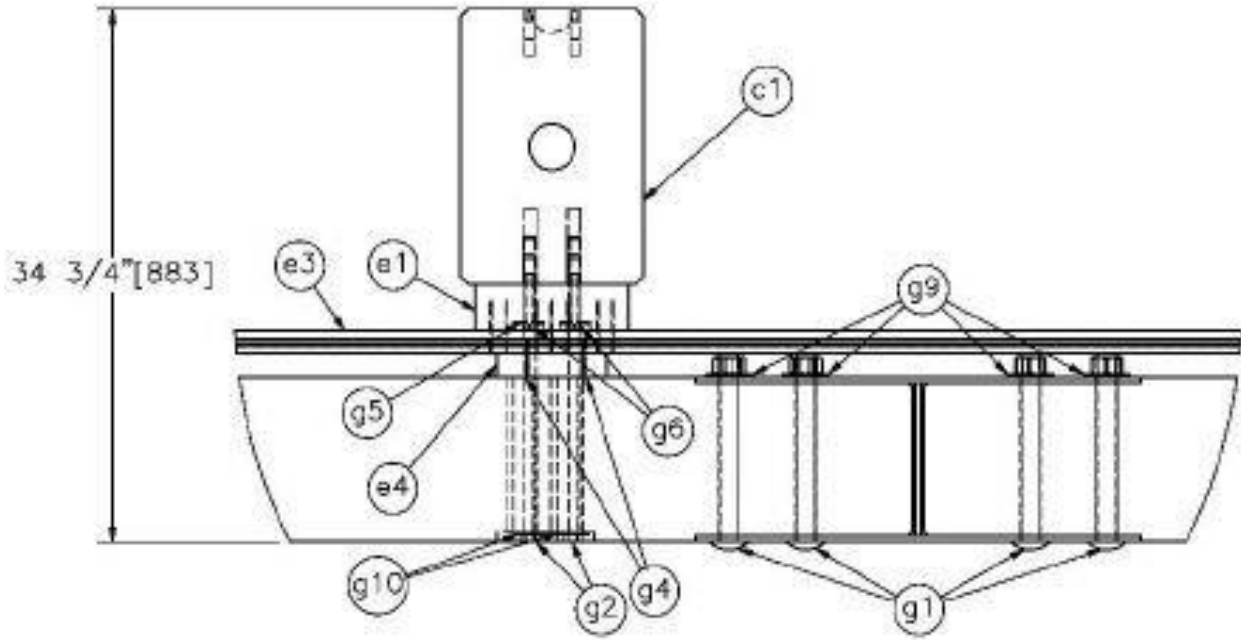


Figure 64. Test No. MNNW-3 Drawing [33]



Figure 65. Lateral Extent of the 2270P Vehicle in Test No. MNNW-1 on the Minnesota Noise Wall [33]



Figure 66. Lateral Extent of the 1100C Vehicle in. Test No. MNNW-2 on the Minnesota Noise Wall [33]



Figure 67. Lateral Extent of the 2270P Vehicle in. Test No. MNNW-3 on the Minnesota Noise Wall [33]

## 2.8.2 Restore Barrier

The Restore Barrier was a concrete barrier supported by rubber posts and steel skids developed by MwRSF in 2015 and tested under MASH TL-4 conditions [34]. The system had a 38<sup>5</sup>/<sub>8</sub> in. overall height and consisted of twelve 19-ft 11<sup>1</sup>/<sub>2</sub>-in. long by 18<sup>1</sup>/<sub>2</sub>-in. tall by 21<sup>1</sup>/<sub>2</sub>-in. wide concrete beams with an 8<sup>1</sup>/<sub>2</sub>-in. steel rail mounted to the top of the concrete barrier. Concrete beams were supported by 11<sup>5</sup>/<sub>8</sub>-in. tall rubber posts and metal skids, as shown in Figures 68 and 69. The rubber posts were spaced at 60 in., and metal skids spaced at 120 in. Rubber posts and metal skids were both 12 in. long and set back 5<sup>1</sup>/<sub>2</sub> in. from the face of the rail.

The Restore Barrier was successfully tested under MASH TL-4 conditions with 1100C, 2270P, and 1000S vehicles in test nos. SFH-1 through SFH-3. By reviewing videos and photographs, it was determined the tire of the 1100C vehicle extended underneath the rail, contacted a rubber post, and laterally extended approximately 9 in. from the original position of the front face of the rail, as shown in Figure 70. The tire of the 2270P vehicle extended underneath the rail, contacted a rubber post, and laterally extended 5 in. from the original position of the front face of the rail.



Figure 68. Restore Barrier System Photograph [34]

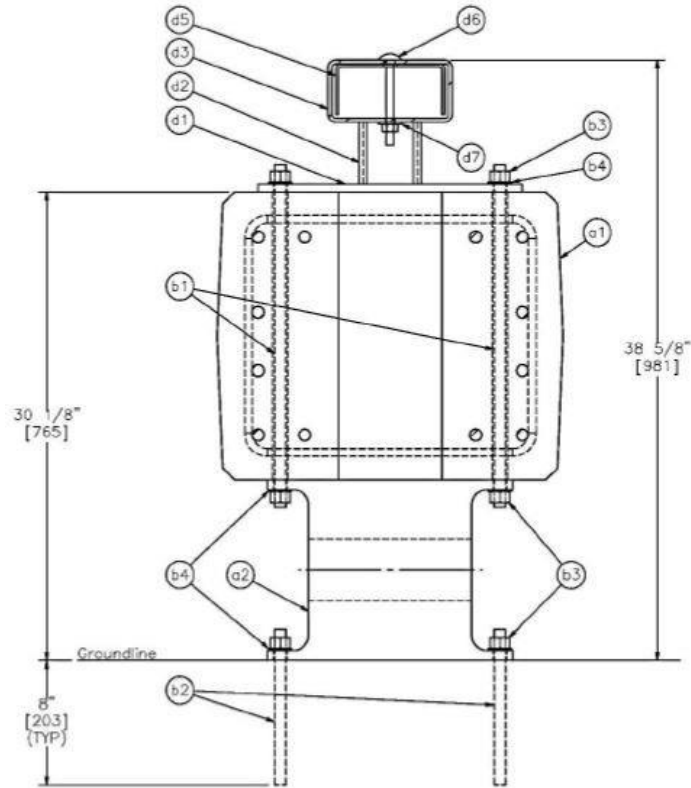


Figure 69. Restore Barrier Drawing [34]



Figure 70. Lateral Extent of the 1100C Vehicle on the Restore Barrier [34]

### 2.8.3 NDOT Standardized Approach Guardrail Transition End Buttress

The Nebraska Department of Transportation (NDOT) Standardized Approach Guardrail Transition End Buttress was a thrie beam to concrete end buttress transition developed by MwRSF under MASH TL-3 conditions [35]. Although not a bridge rail, its geometry was relevant to the literature review, as the vertical opening underneath the thrie beam allowed for vehicle components to extend underneath it and potentially snag on the upstream face of the end buttress. Two variants of the end buttress were tested. In both variants, the thrie beam height was 31 in. with an 11-in. vertical opening beneath the rail. The end buttress was 32 in. tall at its upstream end and transitioned to a 36-in. overall height at a 6:1 taper rate, as shown in Figures 71 through 74. Both variants incorporated an 18-in. tall by 4-in. long by 3-in. wide tapered region behind the thrie beam. An 11-in. tall by 4-in. wide by 12-in. long tapered region was incorporated beneath the thrie beam of the first variant, and an 11-in. tall by 4½-in. wide by 12-in. long tapered region was incorporated beneath the thrie beam in the second variant. Buttress faces were set back ¾ in. from the face of the thrie beam, and the end of the tapered region was set back 7¼ in. from the face of the thrie beam in the first variant and 7¾ in. from the face of the thrie beam in the second variant. System photographs and drawings are shown in Figures 71 through 74.

Crash tests with the 2270P vehicle were run on both variants of the end buttress. Through reviewing videos and photographs of test no. AGTB-1, conducted on the variant incorporating the 11-in. tall by 4-in. wide by 12-in. long tapered region, it was determined that the left-front tire of the 2270P vehicle extended beneath the thrie beam, contacted the upstream face of the concrete end buttress, and laterally extended 9¼ in. from the face of the thrie beam, as shown in Figure 75. The vehicle's left-front floor pan deformed 3⅜ in., causing the accelerometer to move during impact and resulting in a longitudinal ORA of 30.03 g's, which exceeded the MASH limit of 20.49 g's and resulted in an unsuccessful test. It is unknown if the interaction of the 2270P vehicle's tire with the end buttress led to the test failure. Test no. AGTB-2, conducted on the variant incorporating the 11-in. tall by 4½-in. wide by 12-in. long tapered region with the 2270P vehicle, was successful under MASH TL-3 conditions. Through reviewing videos and photographs of the second full-scale test, it was determined that the right-front tire of the 2270P vehicle extended beneath the thrie beam, contacted the upstream face of the concrete end buttress, and laterally extended approximately 10 in., as shown in Figure 76.



Figure 71. Standardized AGT Buttress, Test No. AGTB-1, System Photograph [35]

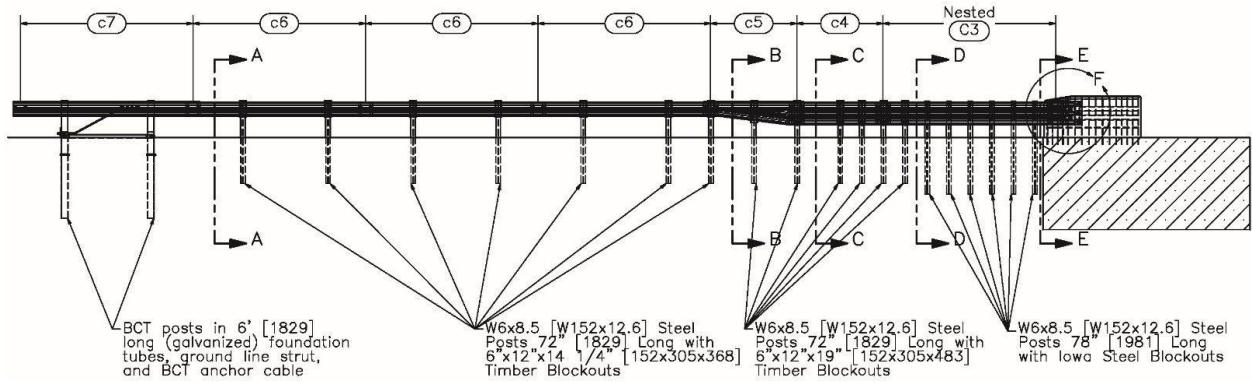


Figure 72. Standardized AGT Buttress, Test No. AGTB-1, System Drawing [35]



Figure 73. Standardized AGT Buttress, Test No. AGTB-2, System Photograph [35]

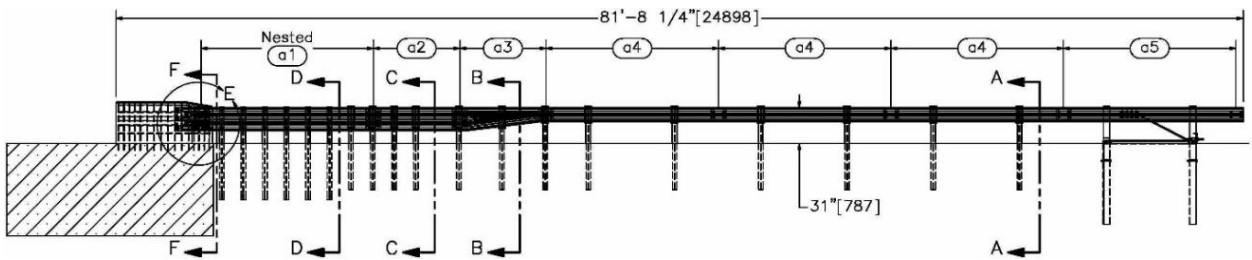


Figure 74. Standardized AGT Buttress, Test No. AGTB-2, System Drawing [35]





Figure 75. Lateral Extent of the 2270P Vehicle on the Standardized AGT Buttress, Test No. AGTB-1 [35]



Figure 76. Lateral Extent of the Second 2270P Vehicle on the Standardized AGT Buttress, Test No. AGTB-2 [35]

### 2.8.4 NDOT 34-in. Approach Guardrail Transition

The NDOT 34-in. Approach Guardrail Transition was a thrie beam to concrete end buttress transition developed by MwRSF under MASH TL-3 conditions [36]. Although not a bridge rail, its geometry was relevant to the literature review, as the vertical opening underneath the thrie beam allowed for vehicle components to extend underneath it and potentially snag on the upstream face of the end buttress. The nested thrie beam was 34 in. in height with a 14-in. vertical opening, as shown in Figures 77 and 78. The end buttress was 35 in. tall at its upstream end and transitioned to a 39-in. overall height at a 6:1 taper rate. The end buttress incorporated an 18-in. tall by 4-in. long by 3-in. wide tapered region behind the thrie beam. The larger vertical opening increased the likelihood and severity of wheel snagging on the upstream face of the end buttress, so a 17-in. tall tapered region measuring 4½ in. wide by 18 in. long was incorporated into the design. Buttress faces were set back ¾ in. from the face of the thrie beam, and an additional 7¾ in. from the face of the thrie beam to the end of the taper.

The approach guardrail transition was successfully tested under MASH TL-3 conditions with 1100C and 2270P vehicles in test nos. 34AGT-1 and 34AGT-2, respectively. Through reviewing videos and photographs, it was determined that the tire of the 1100C vehicle extended beneath the thrie beam and laterally extended approximately 14¼ in. from the face of the thrie beam, overlapping the entirety of the upstream face of the concrete end buttress and leaving significant contact marks, as shown in Figure 79. The tire of the 2270P vehicle extended beneath the thrie beam and laterally extended approximately 13¾ in. from the face of the post, overlapping majority of the upstream face of the concrete end buttress, as shown in Figure 80. However, both passenger vehicle tests were successful according to MASH TL-3 criteria.



Figure 77. 34-in. Tall Approach Guardrail Transition System Photograph [36]

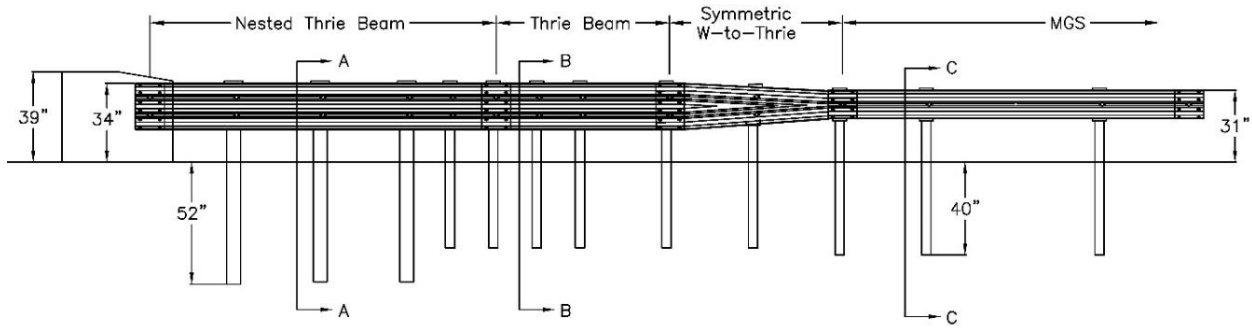


Figure 78. 34-in. Thrie Beam to End Buttress Connection Drawing [36]



Figure 79. Lateral Extent of the 1100C Vehicle on the 34-in. Tall AGT [36]



Figure 80. Lateral Extent of the 2270P Vehicle on the 34-in. Tall AGT [36]

## **3 DESIGN CRITERIA**

### **3.1 Barrier Height**

A minimum bridge rail height of 36 in. was established based on the previous MASH TL-4 SUT full-scale crash tests conducted by TTI [11] and MwRSF [19-20]. Additionally, it was desired for the newly developed bridge rail to meet the 36-in. minimum barrier height both with and without a 3-in. thick pavement overlay. Therefore, two barrier configurations were targeted: one with an overall height of 36 in. and one with a 39-in. overall height. The more critical of the two configurations was to be evaluated.

### **3.2 Impact Loads**

Lateral and vertical impact loads for the new MASH 2016 TL-4 open concrete bridge rail were selected based on the impact load study conducted by TTI in NCHRP Project 22-20(2) [17]. TL-4 design loads were estimated for both 36-in. and 39-in. tall barriers using finite element simulations conducted with LS-DYNA. Recommended design loads for a 36-in. tall barrier were a lateral load of 67.2 kips applied at a height of 25.1 in. distributed over 4 ft and a vertical load of 37.8 kips distributed over 18 ft. Recommended design loads for a 39-in. tall barrier were a lateral load of 72.3 kips applied at a height of 28.7 in. and a vertical load of 32.7 kips distributed over 18 ft. Based on studies of various barrier heights, Bligh et al. recommended using a lateral load of 80 kips applied at 30 in. and a vertical load of 33 kips distributed over 18 ft. Thus, it was recommended that the minimum lateral capacity of the new MASH TL-4 open concrete bridge rail fall between 72.3 kips and 80 kips applied at a height of 30 in. with the vertical design load at 33 kips applied over 18 ft.

### **3.3 System Geometry**

When impacting post-and-beam systems, vehicle components, such as wheels (tires and rims) and bumpers, have the potential to extend beneath the rail and contact a post, resulting in snagging. Significant snagging can result in excessive occupant compartment deformations or occupant decelerations. Minimizing the clear vertical openings beneath the rail and maximizing post setback away from the front face of the rail was critical to ensure that vehicle components would experience minimal snag on the posts beneath the rail. However, maximizing the vertical opening and post setback was necessary for enhanced drainage, aesthetics, and minimizing the width of the system. Thus, the vertical opening and post setback were optimized by implementing vertical openings as tall as possible while minimizing snag potential by studying previous full-scale crash tests.

The lateral extent of vehicle components beneath the rail was estimated during the literature review to guide the recommendations of acceptable vertical openings and post setbacks for the new open concrete bridge rail. The lateral extent was obtained from documentation in reports, measurements from videos, or by reviewing and estimating from post-test photographs. In most of the full-scale crash tests that were studied, the lateral extent of vehicle components was measured by estimating the lateral extent of contact marks on the upstream faces of the posts or other bridge rail components. For full-scale crash tests where the vehicle did not contact a post or another bridge rail component, video analysis was used to measure how far laterally beneath the rail the vehicle

extended. Full-scale crash tests that were conducted under the AASHTO GSB, NCHRP Report 230, NCHRP Report 350, and MASH evaluation criteria were studied. The analyzed vehicle tests included small cars and pickup trucks, with test designations shown in Table 8. The geometry of SUTs and tractor trailers does not allow for their components to extend beneath the rails as far as was observed for smaller vehicles; thus, they were not evaluated in the determination of lateral extent.

Table 8. Testing Criteria and Test Vehicles for Passenger Vehicles

Test Specification	Test Vehicle Designations	
	Small Car Designation	Pickup Truck Designation
NCHRP Report 230 [4]	1800S	2250S and 4500S
AASHTO GSB [5]	1,800-lb Small Automobile	5,400-lb Pickup Truck
NCHRP Report 350 [9]	820C	2000P
MASH [8]	1100C	2270P

The estimated lateral extent of small cars and pickup trucks was plotted against both vertical openings and post setbacks. SUTs and tractor trailers were excluded from this analysis, as their larger size resulted in a reduced potential for snagging and for their components to extend laterally underneath the rail. Post setbacks were measured from the front face of the rail to the front face of the post and from the front face of the rail to the end of the taper, as shown in Figure 81. Some systems incorporated tapered elements that increased lateral setback from the face of the rail, and for such systems estimated lateral extent was measured relative to both points.

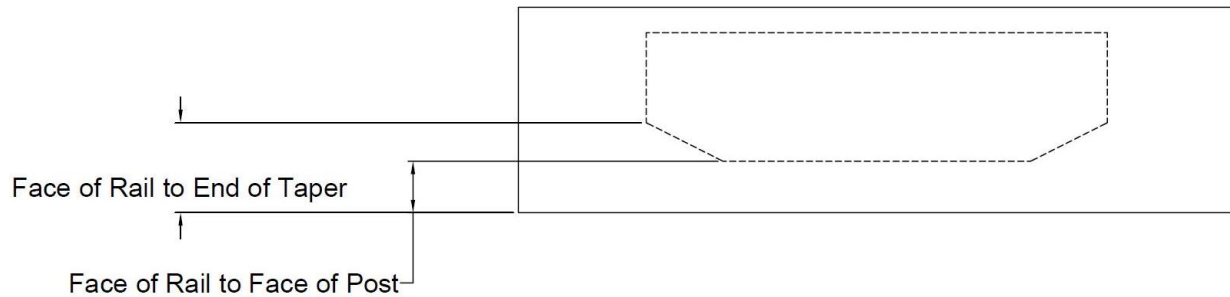


Figure 81. Post Setback Measurements

A total of seven small car tests from the literature review where lateral extent could be measured were studied. Six of these tests were conducted under MASH test conditions with the 1100C vehicle and one test was conducted under NCHRP Report 350 conditions with the 820C vehicle, as shown in Table 9. Lateral extent could not be determined from crash tests conducted on the Kansas Corral Rail. Comparison of the system’s vertical openings to the estimated vehicle lateral extent, shown in Figure 82, displayed an approximately linear trend as increases in vertical openings tended to result in increased lateral extent. Multiple crash tests on bridge rails incorporating 8-in. vertical openings displayed no observed vehicle lateral extent, while all bridge rails that incorporated 11-in. or taller vertical openings displayed 9 in. or more of lateral extent,

except for the TxDOT T224 Bridge Rail, which incorporated a 9-in. tall curb at its base. The comparison of post setbacks to the estimated vehicle lateral extent, as shown in Figure 83, did not display a clear trend, and post setback was determined not to be an effective indicator of how far vehicles laterally extended beneath rail elements. All small car tests were successful, although significant lateral extent was recorded on systems with taller vertical openings.

Table 9. System Geometry and Estimated Lateral Extent for Small Car Crash Tests

System Name	Testing Standard	Test Vehicle	Vertical Opening in.	Post Setback <sup>1</sup> in.	Taper in. Rate =	Lateral Extent in.
34-in. Tall AGT [36]	MASH	1100C	14	3¼	4½ Rate = 4:1	14¼
CA ST-70 Steel Bridge Rail [27]	MASH	1100C	8	6	N/A	0
IL-OH Steel Bridge Rail [29-32]	MASH	1100C	9	6	N/A	9¼
MA Type S3 Bridge Rail [28]	NCHRP Report 350	820C	12½	5	N/A	0
MN Noise Wall [33]	MASH	1100C	16½	16¾	N/A	16¾
Restore Barrier [34]	MASH	1100C	11⅝	5½	N/A	9
TxDOT T224 Bridge Rail [2]	MASH	1100C	12	0	7 Rate = 2:1	3½

<sup>1</sup> Post setback distance for the 34-in. Tall AGT refers to buttress setback.  
N/A – Not applicable, as posts were not tapered.

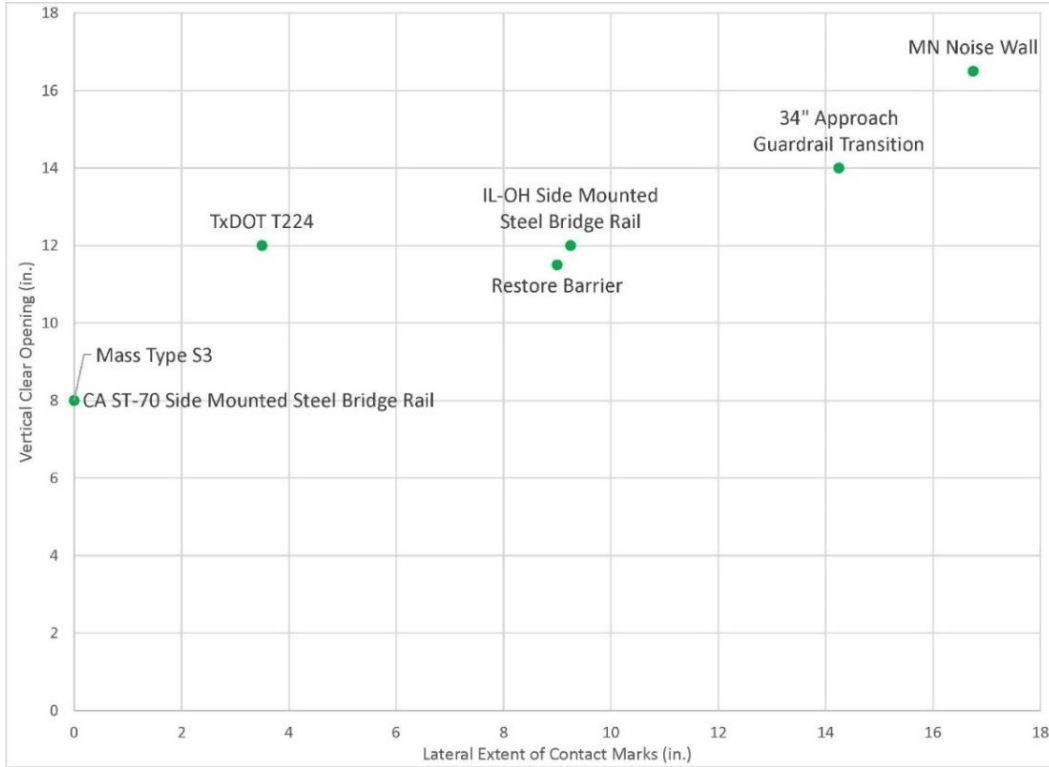


Figure 82. Estimated Lateral Extent vs. Vertical Opening, Small Car Tests

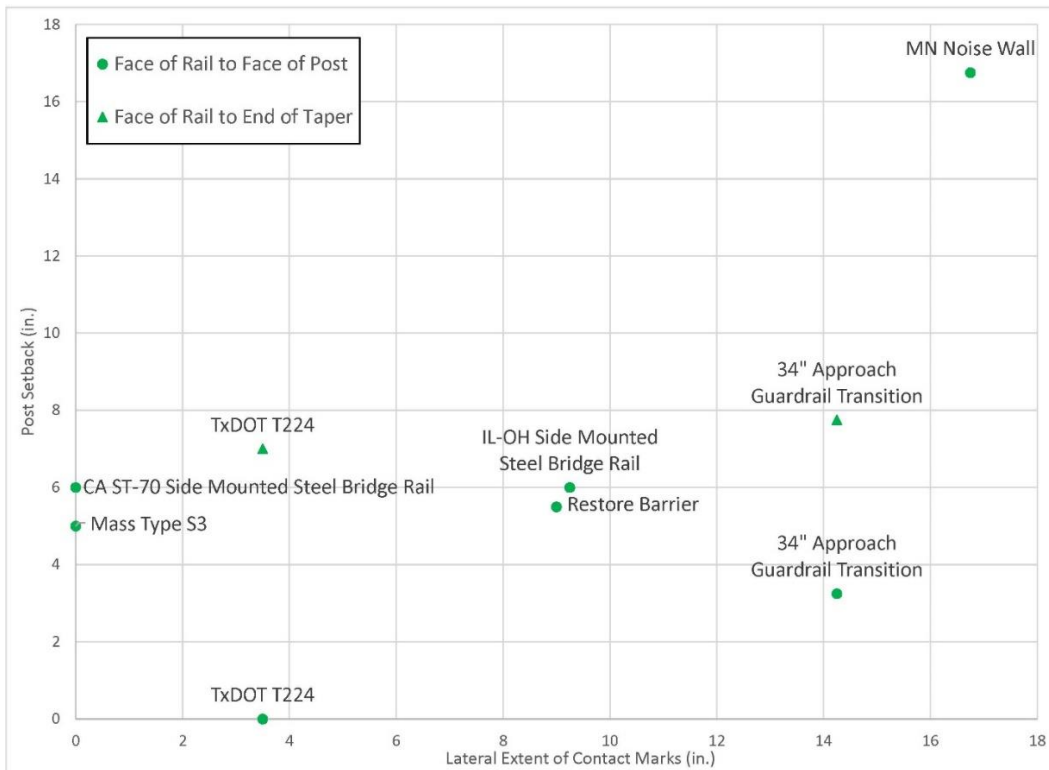


Figure 83. Estimated Lateral Extent vs. Post Setback, Small Car Tests

A total of fourteen pickup truck tests from the literature review where lateral extent could be measured were studied. Eight tests were conducted under MASH conditions, four tests were conducted under NCHRP Report 350 conditions, and two tests were conducted under AASHTO GSBP conditions, as shown in Table 10. Comparisons of vertical openings to estimated lateral extent, as well as post setbacks compared to estimated lateral extent, did not display clear trends, as shown in Figures 84 and 85. Although there were no apparent trends with pickup truck data, systems with 8-in. to 9-in. tall vertical openings had no estimated lateral extent, and vertical openings 14 in. tall or greater had the largest estimated lateral extent. All but two tests were successful.

The first unsuccessful test was test no. 441382-1, conducted on the 27-in. tall TxDOT T203 bridge rail, which failed due to insufficient rail height, while the second unsuccessful test was test no. AGTB-1, conducted on the first standardized end buttress, which failed due to excessive ORA. It is unknown whether the end buttress geometry led to a test failure. The full-scale crash test on the 27-in. tall TxDOT T203 bridge rail failed due to insufficient system height, causing the vehicle to roll over and was not due to snagging as the 2000P vehicle also did not contact the upstream face of the posts. The first full-scale crash test of the standardized approach guardrail transition buttress, test no. AGTB-1, failed due to ORA exceeding the MASH allowable limit. This result was potentially inaccurate due to the floor pan of the vehicle deforming during impact, causing movement of the accelerometer. Although movement of the accelerometer may have contributed to the test failure, the vehicle interaction with the end buttress could have also contributed. In the second full-scale crash test, test no. AGTB-2, an additional ½-in. setback was added to the lower taper of the buttress, resulting in a 4½-in. setback from the face of the buttress to the end of the taper. The slope of the lower taper was reduced from 3:1 to 4:1, and its height was increased from 11 in. to 14 in. The setback of the upper taper was also reduced from 4 in. to 3 in. This full-scale crash test was successful, though there was still significant vehicle lateral extent and contact with the upstream face of the buttress.



Table 10. System Geometry and Estimated Lateral Extend for Pickup Truck Crash Tests

System Name	Testing Standard	Test Vehicle	Vertical Opening in.	Post Setback <sup>1</sup> in.	Taper in. Rate =	Lateral Extent in.
34-in. Tall AGT [36]	MASH	2270P	14	3¼	4½ Rate = 4:1	13¾
Standardized End Buttress 1 [35]	MASH	2270P	11	3¼	4 Rate = 3:1	9¼
Standardized End Buttress 2 [35]	MASH	2270P	11	3¼	4½ Rate = 4:1	10
CA ST-70 Steel Bridge Rail [27]	MASH	2270P	8	6	N/A	0
IL-OH Steel Bridge Rail [29-32]	MASH	2270P	9	6	N/A	0)
MA Type S3 [28]	NCHRP Report 350	2000P	8	6	N/A	5
MN Noise Wall 1 [33]	MASH	2270P	16½	16¾	N/A	20½
MN Noise Wall 2 [33]	MASH	2270P	16½	12¾	N/A	12¾
NE Open Rail 1 [22]	AASHTO GSB	Pickup	13	2	N/A	1
NE Open Rail 2 [22]	AASHTO GSB	Pickup	13	2	N/A	3
NE Open Rail on IT Bridge [1]	NCHRP Report 350	2000P	13	2	N/A	4½
27 in. Tall TxDOT T203 Bridge Rail [23]	NCHRP Report 350	2000P	13	4½	N/A	0
30 in. Tall TxDOT T203 Bridge Rail [23]	NCHRP Report 350	2270P	13	4½	N/A	6½
TxDOT T224 Bridge Rail [2]	MASH	2270P	12	0	7 Rate = 2:1	7

<sup>1</sup> Post setback distances for the standardized AGT and 34-in. AGT refer to buttress setbacks.  
N/A – Not applicable, as posts were not tapered.

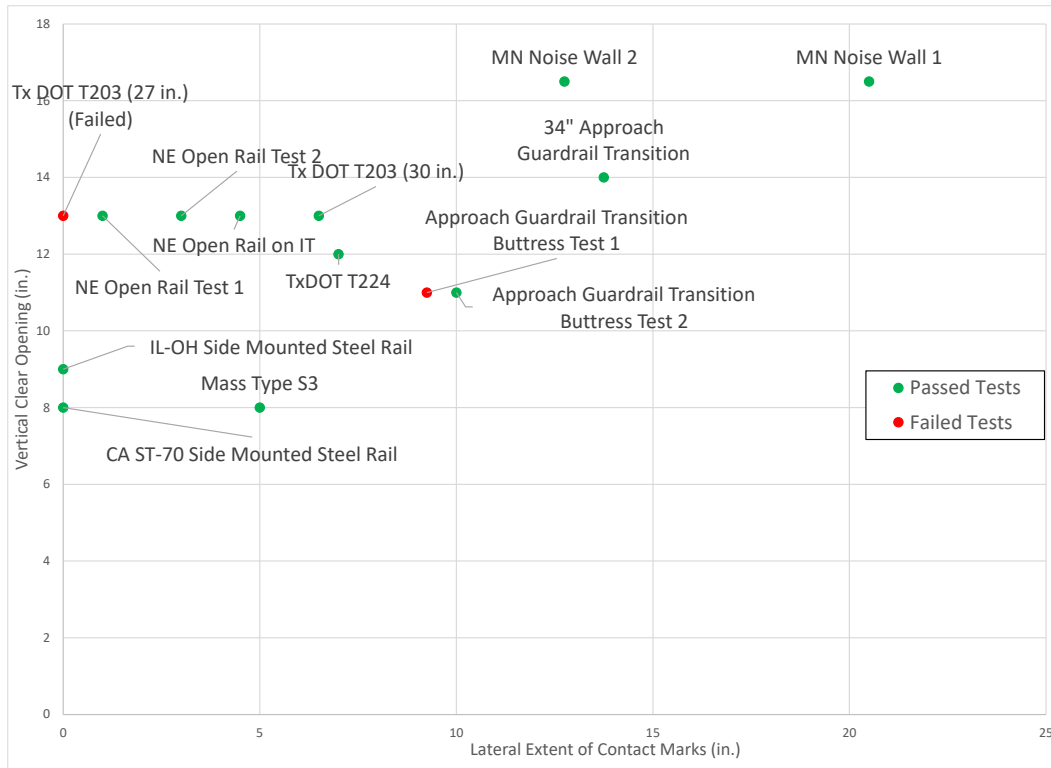


Figure 84. Estimated Lateral Extent vs. Vertical Opening for Pickup Truck Tests

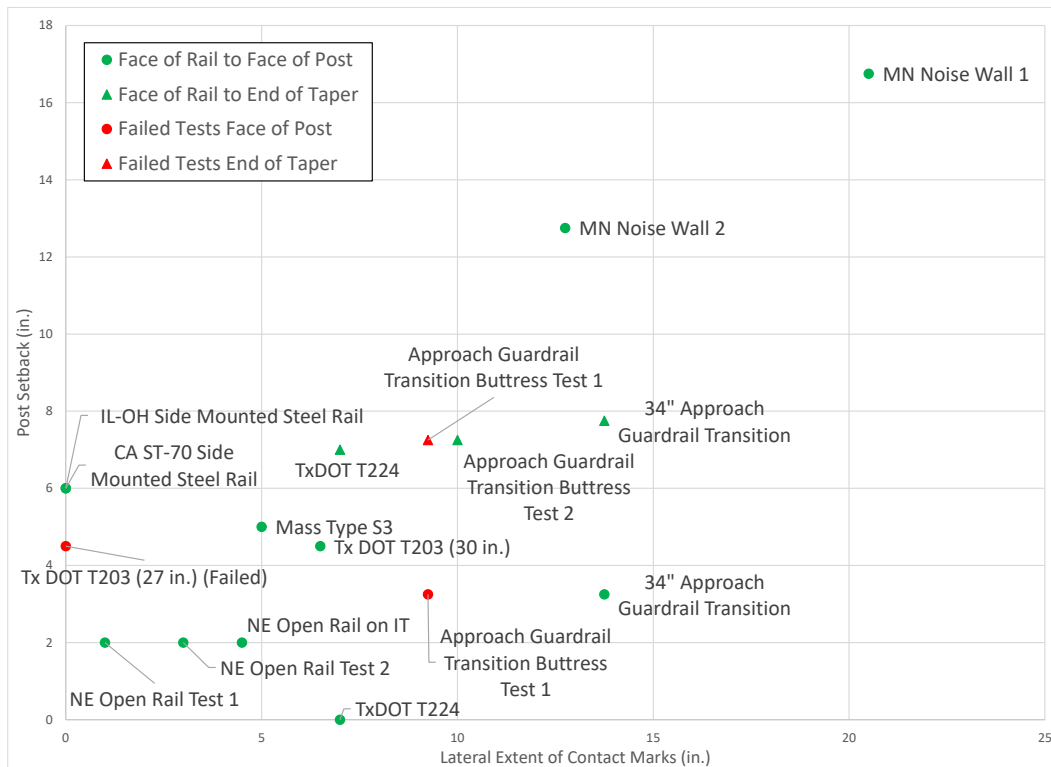


Figure 85. Estimated Lateral Extent vs. Post Setback for Pickup Truck Tests

Although vehicle snagging on posts was not commonly observed to contribute to unsuccessful crash tests, it was desired to mitigate the potential for vehicle extension underneath the rail, as multiple MASH tests have shown over 12 in. of lateral extent on systems with 14-in. or taller vertical openings. Full-scale crash tests on the Minnesota Noise Wall, which incorporated a 16½-in. vertical opening, displayed the greatest lateral extent for both small cars and pickup trucks. Currently, the noise wall crash tests are the only known MASH tests conducted on vertical openings greater than 14 in. Due to the lack of data on rigid barriers with vertical openings greater than 14 in., the vertical opening was desired to be limited to 14 in. Vertical openings were shown to have a greater influence on lateral extent of contact, with the relationship being most apparent for small car crash tests. In small car crash tests, the lateral extent of contact increased approximately linearly as vertical openings increased in height, allowing for more of the vehicle to extend underneath the rail with increased vertical openings.

Because vehicle extension underneath the rail appeared to be most dependent on the vertical opening, acceptable post setbacks were determined for vertical openings based on prior crash tests and the researchers' judgement, as shown in Table 11. To mitigate snag potential, recommended post setbacks were required to increase along with vertical opening height. Recommended post setbacks reflected a minimum value at which post faces needed to be setback from the face of the rail to mitigate snag potential, and the posts could be set back farther from the face of the rail to further mitigate snag.

Table 11. Recommended Vertical Openings and Post Setbacks

Vertical Opening in.	Minimum Post Setback in.
8	0
9	2
10	4
11	4
12	4
13	5
14	6

### 3.4 Sponsor Survey

Sponsors were surveyed regarding their preferences for various bridge rail and bridge deck overhang details. Responses were used to establish desired system geometry and optimize variable parameters throughout the design process.

#### 3.4.1 Preferred Preliminary Configurations

Five preliminary configurations were proposed based on sponsor feedback and recommended vertical openings and post setbacks, as shown in Table 12 and Figures 86 through 90. Although all configurations may pass MASH safety performance criteria, the options are listed in order of their safety with option 1 being the safest. The majority of sponsors did not prefer options 1 or 5 with 9-in. and 14-in. tall vertical openings, instead tending to prefer options 2 through 4 with 12-in. and 13-in. tall vertical openings. MwRSF recommended utilizing a 12-in. tall vertical opening with a 4-in. post setback to mitigate the potential for wheel snag.

Table 12. Preliminary Configuration Details

Option	Vertical Opening in.	Post Setback in.	Taper		System width in.	Concrete Weight lb/ft
			Width in.	Rate (Longitudinal: Lateral)		
1	9	2	0	None	11	364
2	12	4	2	4:1	13	391
3	12	4	0	None	13	393
4	13	5	2	4:1	14	407
5	14	6	2	4:1	15	421

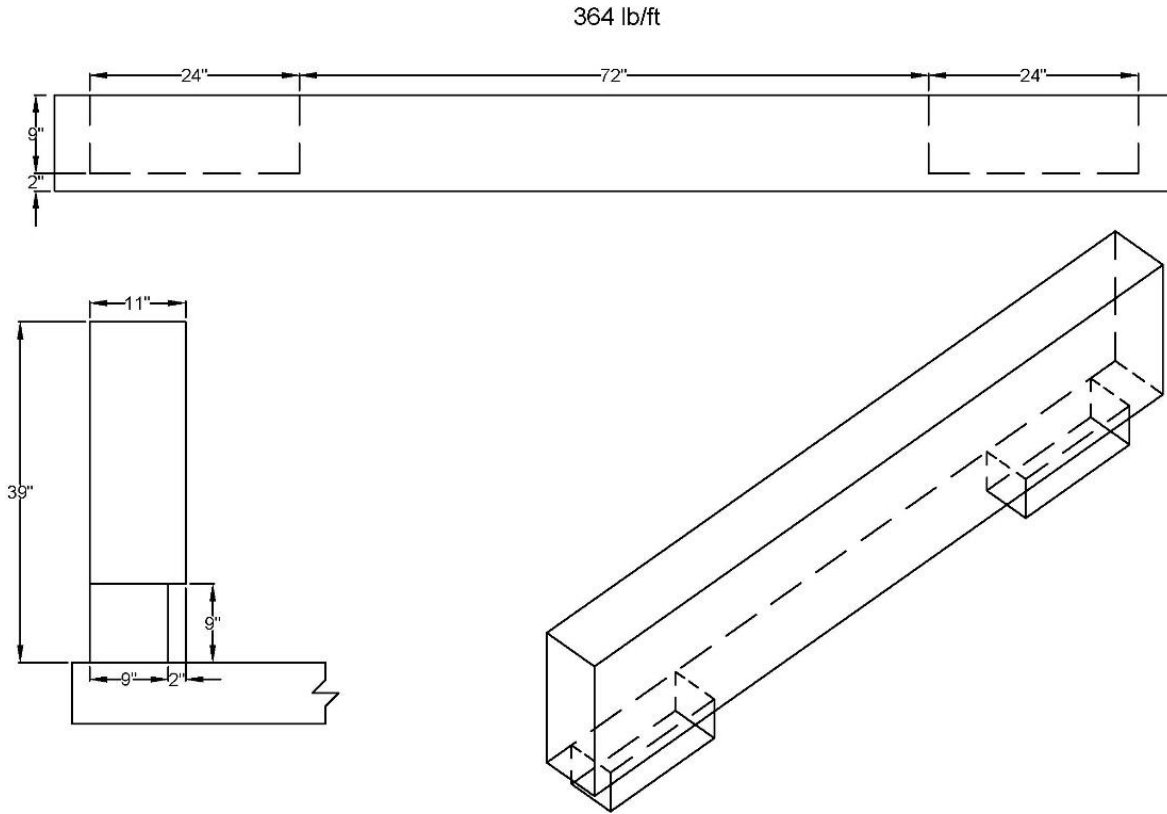


Figure 86. Preliminary Option 1

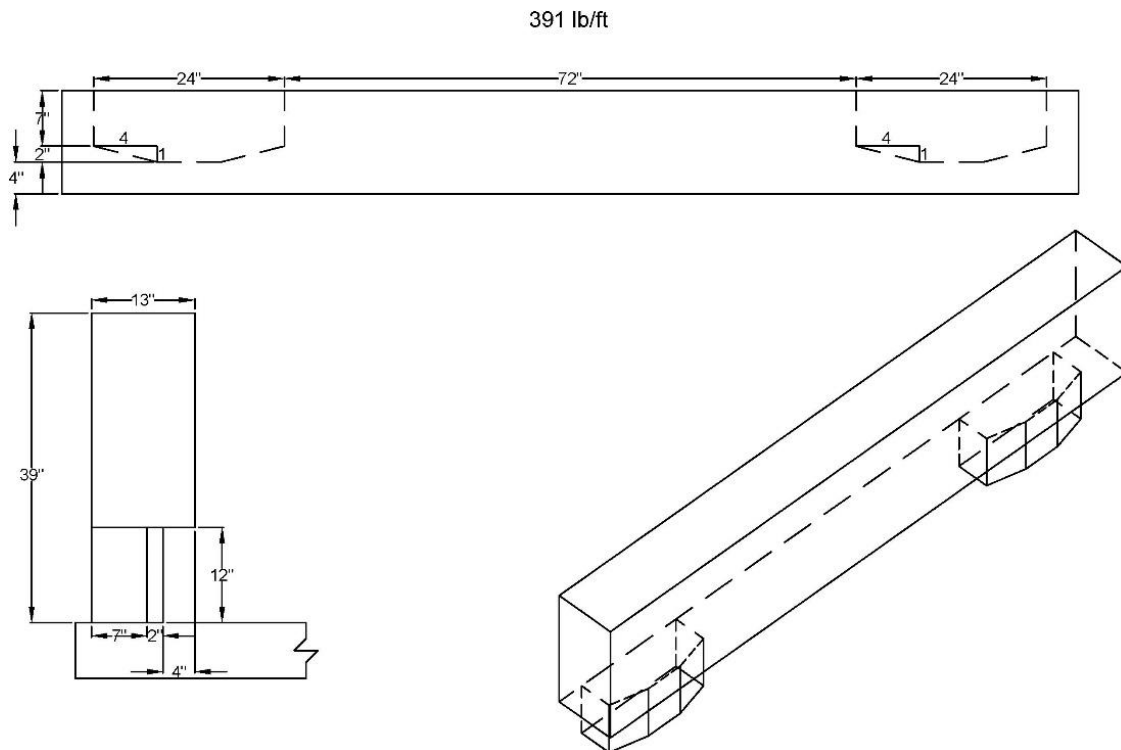


Figure 87. Preliminary Option 2

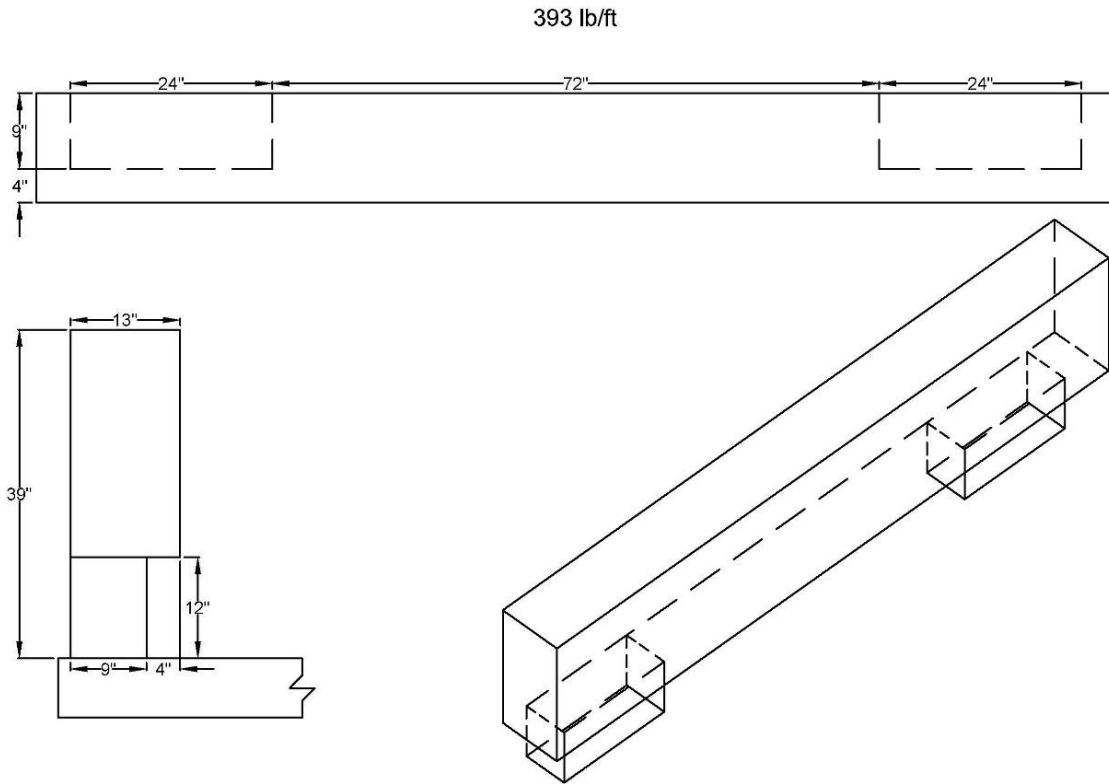


Figure 88. Preliminary Option 3

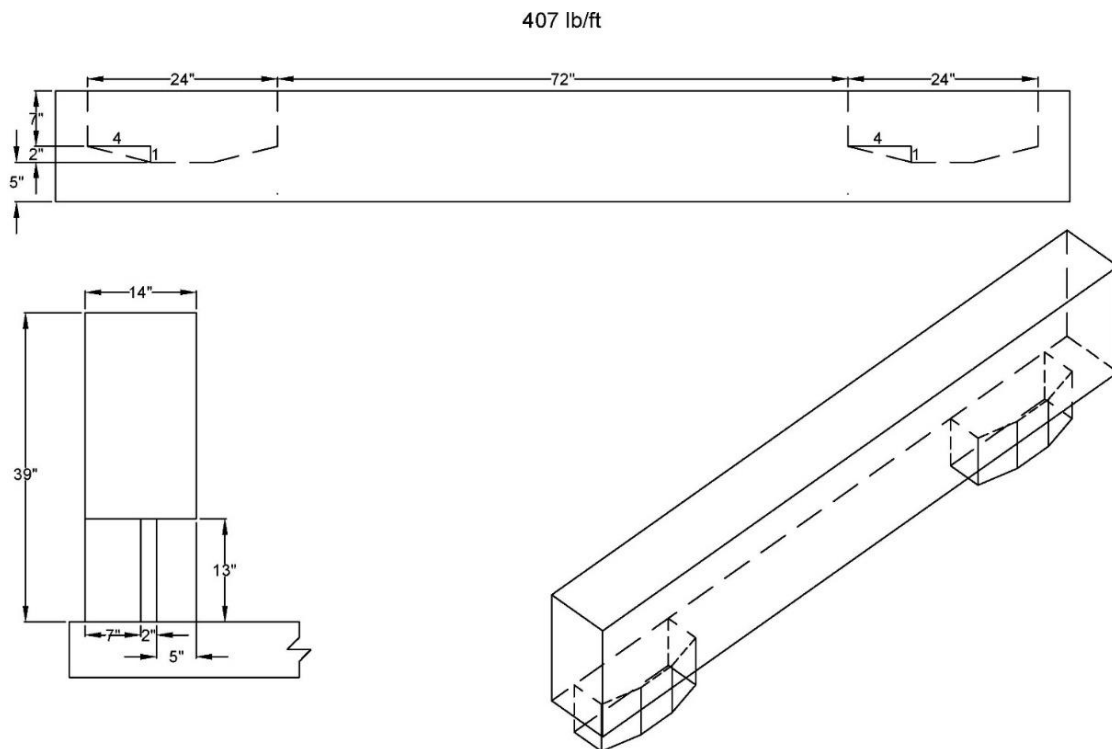


Figure 89. Preliminary Option 4

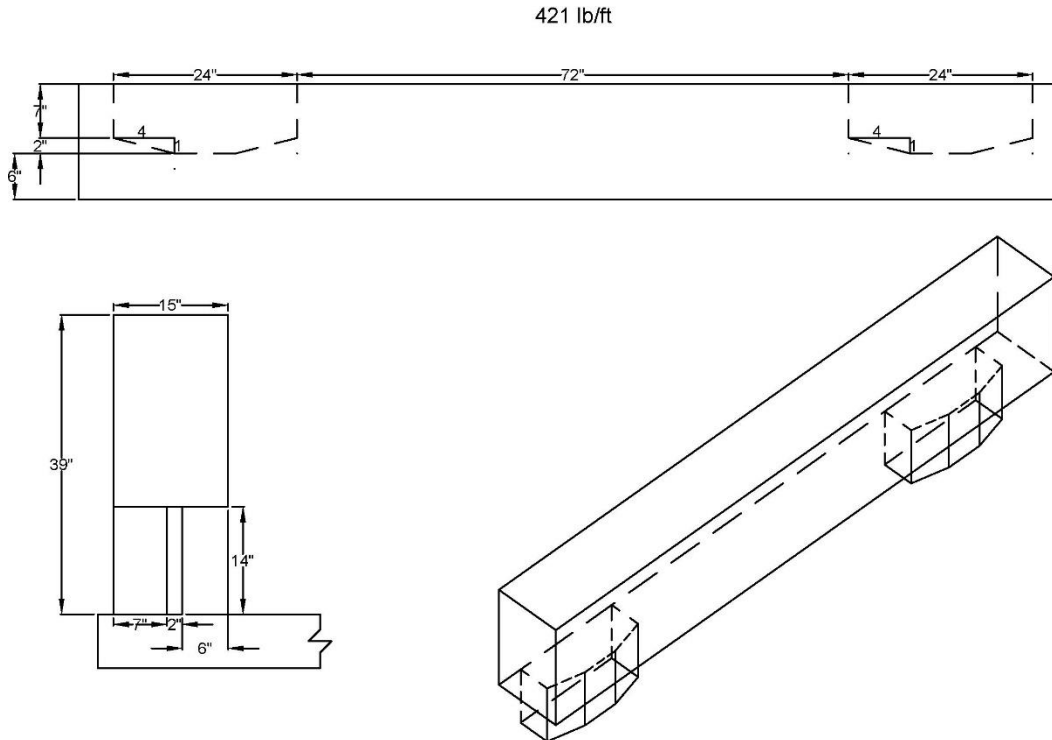


Figure 90. Preliminary Option 5

### 3.4.2 Post Shape

Tapered posts have been implemented on previous bridge rail and end buttress systems to mitigate vehicle snag. However, rectangular-shaped posts have also been used in many prior open concrete bridge rails, and tapered posts similar to those shown in Figure 91 could be implemented to further reduce the potential for snag on the new open concrete bridge rail. While all sponsors found tapered posts to be acceptable, rectangular posts were preferred. MwRSF recommended designing and evaluating the new railing with rectangular posts as they were more critical for snag potential. Successful MASH crash testing of the railing with rectangular posts would provide end users the option to include tapered posts if they desired further snag mitigation or preferred them for aesthetics. However, post size or reinforcement may need to be adjusted for tapered posts to provide equivalent strength.

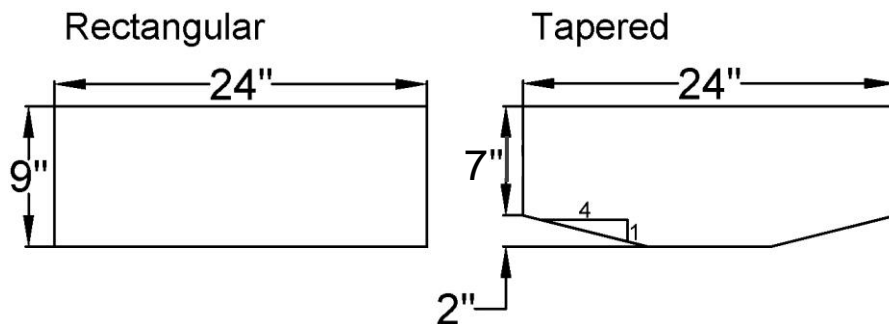


Figure 91. Rectangular and Tapered Posts

### 3.4.3 Rear Post Offset from Edge of Bridge Deck

Previous bridge rail systems and some states' current practices include offsetting bridge rail posts away from the edge of the bridge deck overhang, as shown in Figure 92. This offset aids constructability and provides additional space in the overhang for development of reinforcement. A rear post with no offset and a rear post with a 2-in. offset were explored. The project sponsors selected a 2-in. offset to aid with construction of the bridge rail anchorage in the deck. Note that the rear face of the rail does not have to be flush with the rear face of the posts and can extend to the edge of the bridge deck.

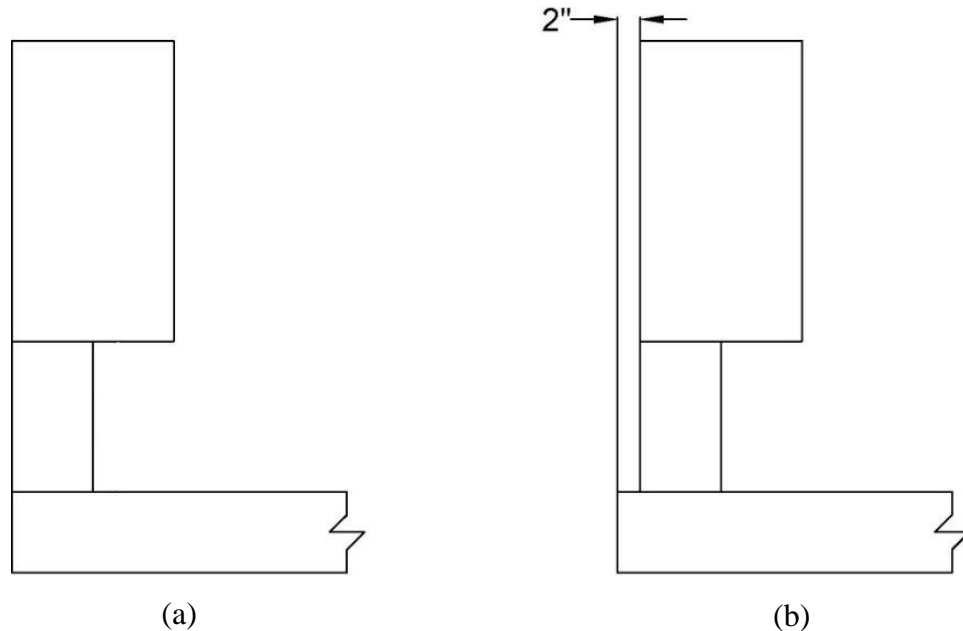


Figure 92. Post Offset from Edge of Bridge Deck – (a) No Offset and (b) 2-in. Offset

### 3.4.4 Bridge Rail Footprint

Bridge rail footprint is defined as the total lateral distance from the edge of the bridge deck to the face of the system, as shown in Figure 93. Selection of the bridge rail footprint was important because sponsors expressed the desire for the footprint of the new open concrete bridge rail to fit within the footprints of the single-slope concrete rails currently in use, and smaller footprints require additional reinforcement compared to larger footprints. Footprints between 11 in. and 18 in. were evaluated, and the project sponsors preferred a 16-in. footprint to optimize the system width for strength and post setback distance.



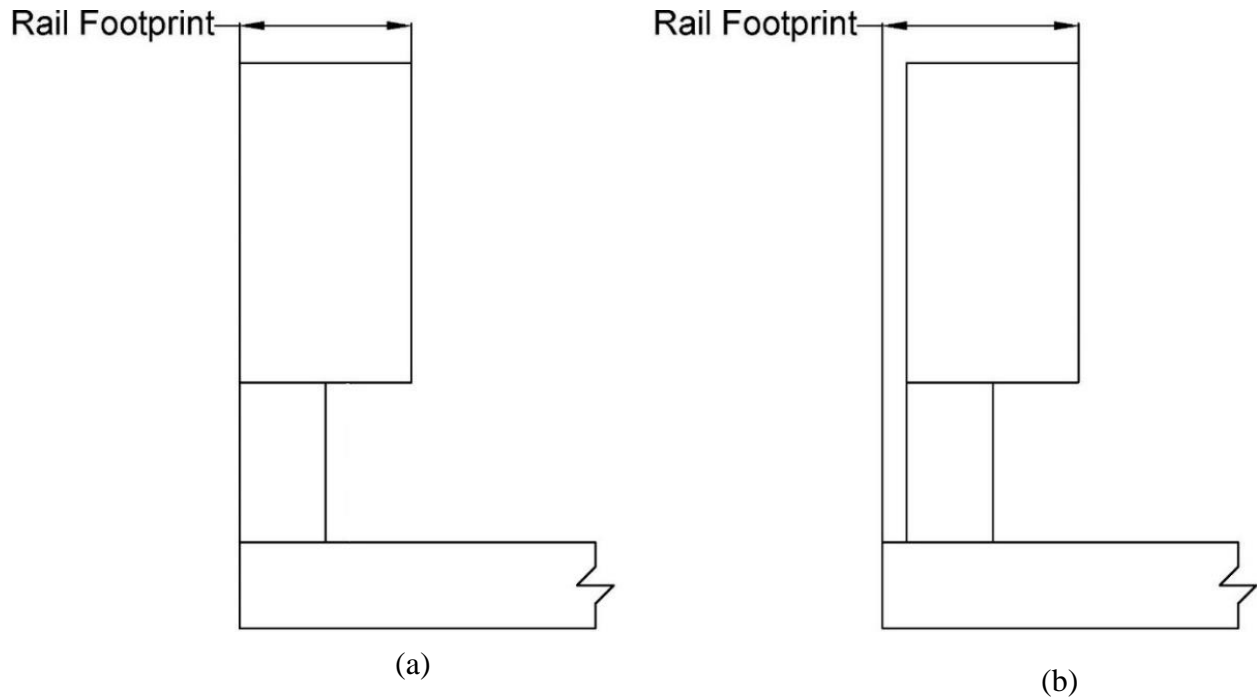


Figure 93. Bridge Rail Footprint (a) Rear of System Flush with Edge of Deck and Offset from Edge of Deck (b)

### 3.4.5 Expansion Gap Locations and Use of Dowels

Previous bridge rails have incorporated expansion gaps in the rail or post as well as partial expansion gaps in the post, as shown in Figure 94. These three options, as well as the use of dowels in the expansion gap to provide transfer of shear loads between bridge rail segments, have been incorporated in existing bridge rails. Majority of the project sponsors preferred Option 1, as shown in Figure 94, as it was the strongest of the three options, the easiest to construct, and did not require dowels. Thus, Option 1 was implemented into the railing design at expansion joints. It was also recommended that the expansion gap not exceed 4 in. wide unless hardware was incorporated to shield the gap and prevent vehicle snag.

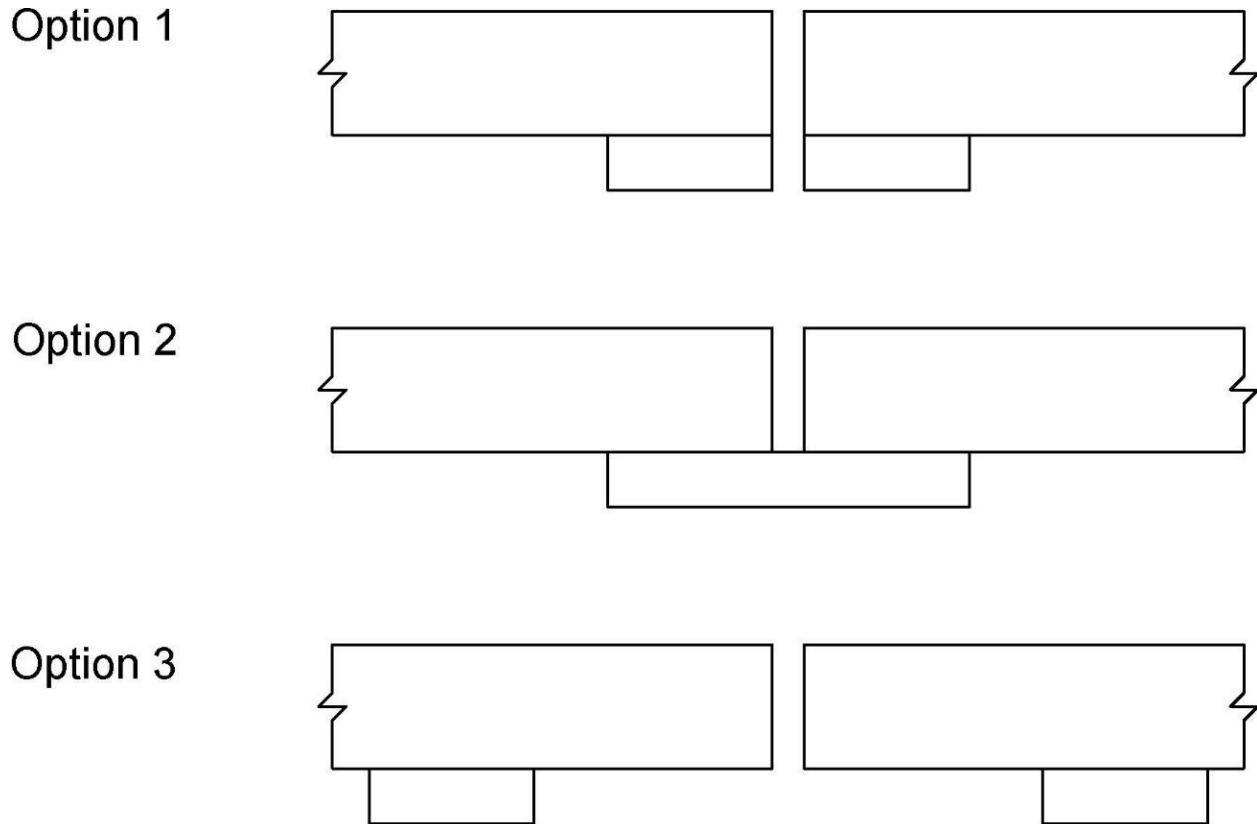


Figure 94. Expansion Gap Locations

### 3.4.6 Overhang Width, Thickness, and Additional Thickness

A survey was sent to the project sponsors to help gain an understanding of current deck overhang configurations and to select a critical configuration for full-scale crash testing. Questions were focused on deck thickness and overhang width, as shown in Figure 95. Sponsors indicated an acceptable range of deck thicknesses between 7½ in. and 9 in., with 7½ in. and 8 in. being the two most preferred options. An 8-in. thick bridge deck design was recommended, as an 8-in. thick bridge deck was previously crash tested successfully with a continuous concrete parapet, and loading is expected to increase in the posts of the new open concrete bridge rail [19-20]. Additionally, the 8-in. thick bridge deck corresponded to the critical thickness for evaluating deck damage and would allow for sponsors to increase the deck thickness if full-scale crash testing is successful. There was not a desire to vary the thickness of the bridge deck throughout its width.

Preferred overhang widths ranged between 36 in. and 60 in. with a 48-in. wide overhang being the most desired. A 60-in. wide overhang was recommended for design and full-scale crash testing as an overhang of this width has been successfully crash tested with a continuous concrete parapet [19-20]. Additionally, designing and testing the widest overhang would impart the highest loads to the deck and, if testing was successful, the same deck design could be used on any shorter overhang width.



Figure 95. Overhang Width, Thickness, and Additional Thickness

### 3.4.7 Preferred Reinforcement

The survey also included questions concerning preferred sizes and configurations of steel reinforcement. No. 5 and No. 6 size rebar were preferred for longitudinal rail and vertical post reinforcement, and No. 4 bars were preferred for rail and post stirrup reinforcement. Clear cover, minimum bar spacings, bend radii requirements, and other code requirements were also considered for selection of steel reinforcement.

### 3.5 Summary

Preliminary bridge rail configurations were developed based on barrier height requirements, recommended vertical openings and post setbacks, and sponsor feedback. Additional criteria not established in the literature review that were determined by sponsor feedback included desired post shape, the offset of the bridge rail from the edge of the bridge deck, the footprint of the bridge rail, expansion gap locations, overhang dimensions, and preferred reinforcement sizes. The preliminary rail configuration shown in Figures 96 through 98 consisted of 12-in. tall, by 10-in. wide by 24-in. long posts separated by 72-in. gaps in the interior section, and 12-in. tall, by 10-in. wide by 36-in. long posts separated by 72-in. gaps in the end section. The rail was 16 in. wide by 27 in. tall, resulting in a 4-in. wide post setback and 2-in. wide extension over the rear face of the posts.

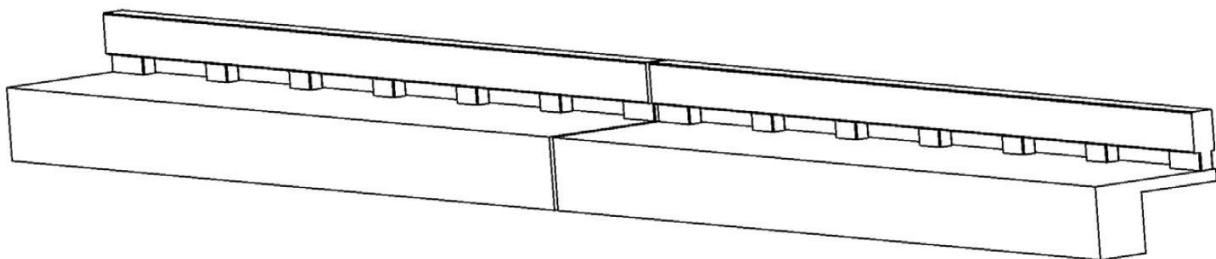


Figure 96. Preliminary Open Concrete Bridge Rail and Deck Configuration

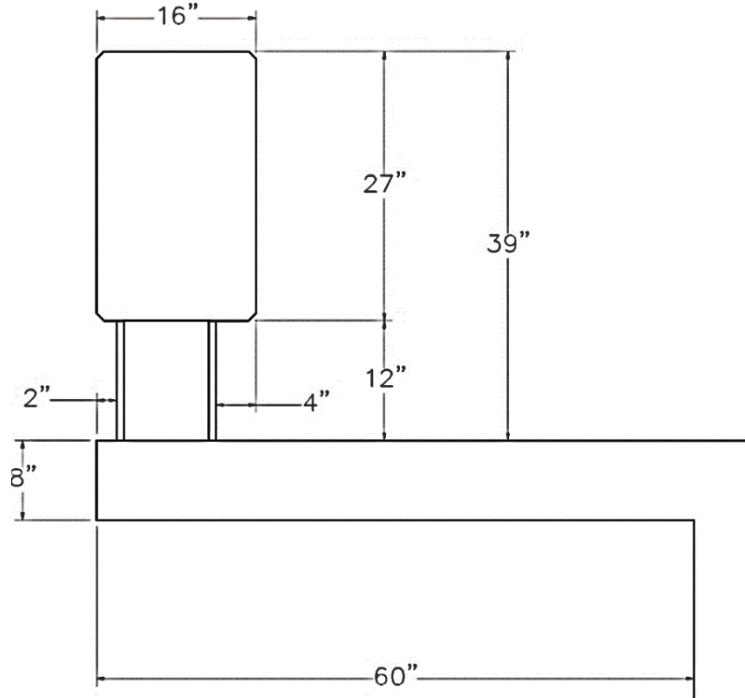


Figure 97. Preliminary Open Concrete Bridge Rail and Deck Cross Section

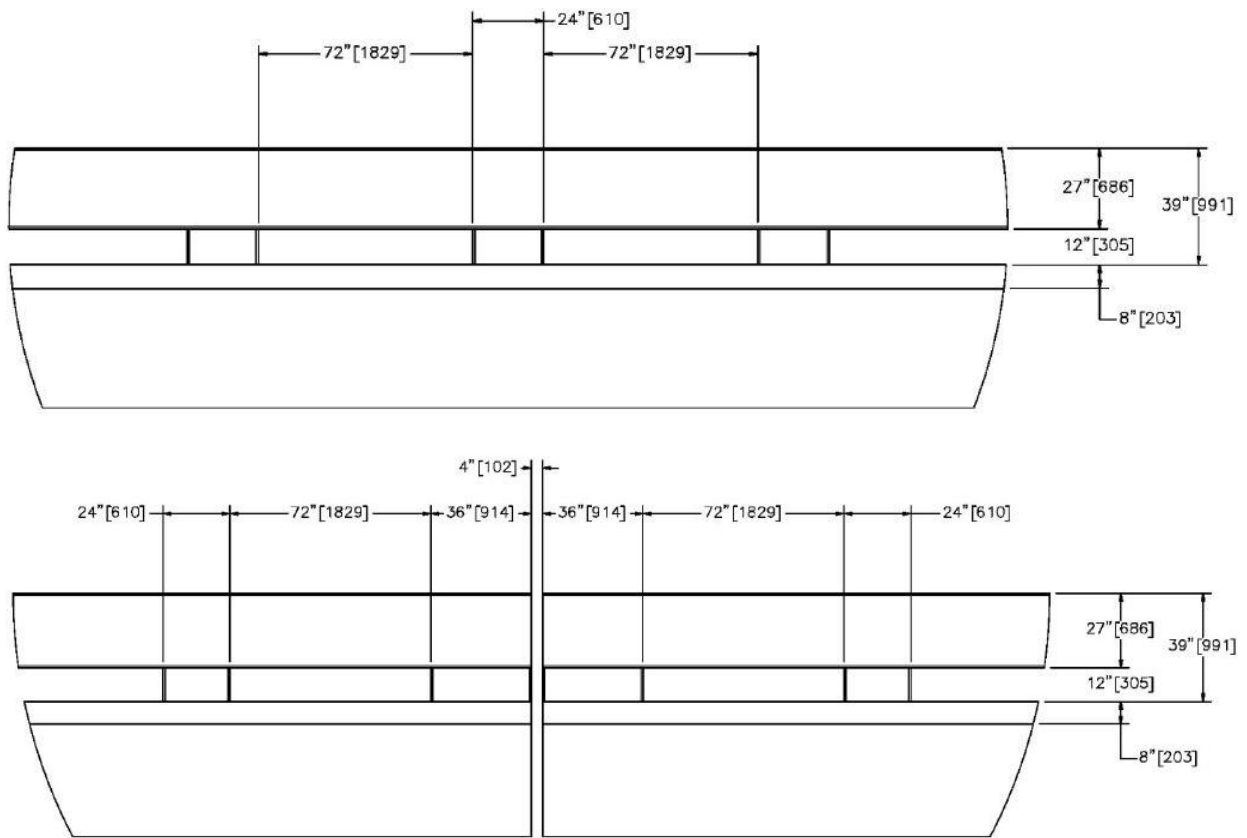


Figure 98. Preliminary System Post Lengths

## 4 DESIGN METHODOLOGY

### 4.1 Overview

Historically, multiple design methods have been utilized to design open concrete rails. These methods include Yield-Line Theory [37] as well as the AASHTO Post and Beam Method [14]. These methods utilize the capacities of the posts and rail along with their geometry to determine the capacity of the bridge rail. Design of the MASH TL-4 open concrete bridge rail was conducted by investigating both methods and determining which method was best suited for the design.

### 4.2 Yield-Line Theory

Yield-Line Theory is an energy balance approach that utilizes an assumed failure shape and plastic bending strengths to determine the capacity of a structure. Yield-Line analyses are most often utilized to design and analyze slabs. To conduct the Yield-Line analysis, a plastic failure mechanism and location of maximum deflection is assumed. Moments acting about the yield lines can then be used to balance external work acting on the slab/railing and internal energy absorbed, and this relationship can then be used to determine the load required to cause failure. Additionally, moments acting about the yield lines are utilized to determine the length of the failure mechanism.

Hirsch adapted Yield-Line Theory to concrete barriers and developed equations that relate barrier geometry and component strength that can be utilized to predict overall barrier capacity [26]. The external work caused by the applied load and deflection of the system is equated to the internal energy absorbed by the rail and posts. Moments in the rail,  $M_b$ , are assumed to develop along yield lines that form in either the rail, or in the rail and post, as well as at the mid span of the rail. Moments in the posts,  $M_c$ , are assumed to develop about the base of the posts. The applied load is assumed to be a distributed load acting over length,  $l$ , applied at the top height of the barrier,  $H$ , and applied at the mid-span between two posts. For open concrete bridge rails, the assumed failure mechanism consists of the beam failing at mid-span between two posts and diagonal yield lines developing through the two posts and extending into the beam, as shown in Figure 99.

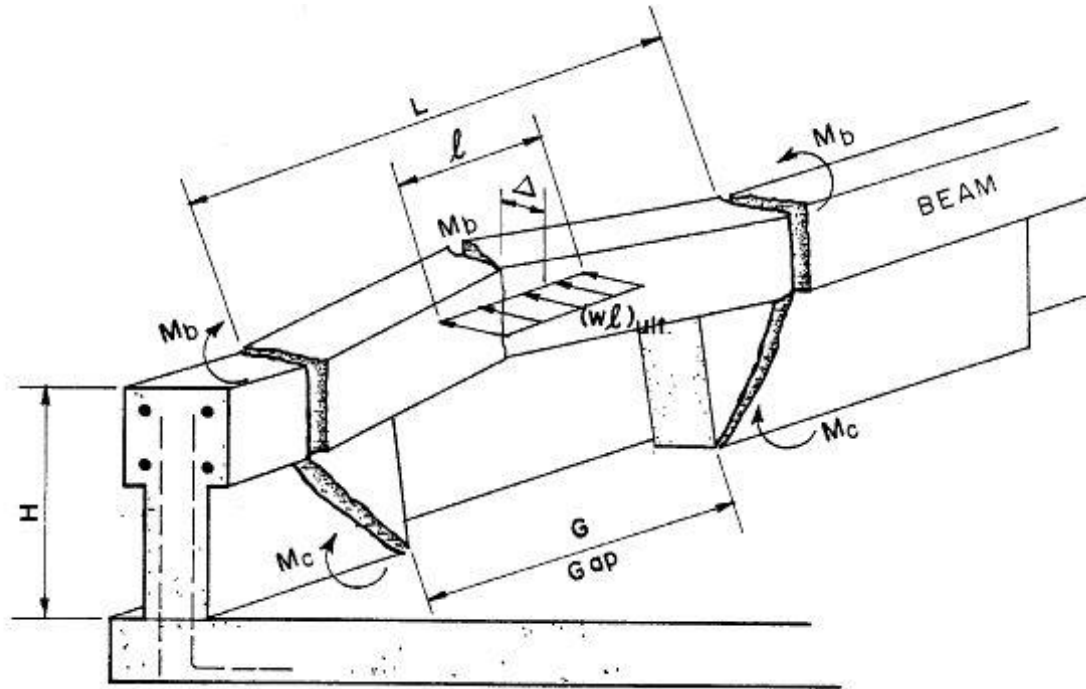


Figure 99. Yield Line of a Concrete Post and Beam System [26]

The ultimate capacity of the barrier,  $wu$ , is a function of the bending strength of the posts, bending strength of the beam, length of the distributed impact load, and post spacing. The ultimate strength,  $wu$ , consists of two separate terms: beam bending strength and post bending strength. The equation for  $wu$  is given by:

$$wu = \frac{8M_b}{(L - \frac{l}{2})} + \frac{M_c L(L - G)}{H(L - \frac{l}{2})} \quad (1)$$

Where:

$l$  = Length of distributed impact load

$wu$  = Total ultimate distributed load capacity of wall

$H$  = Height of wall

$L$  = Critical length of wall failure, as defined in Equation 2

$M_b$  = Ultimate moment capacity of beam at top of wall

$M_c$  = Ultimate moment capacity of posts per unit length of post, and

$G$  = Length of gap or wall opening.

$$L = \frac{l}{2} + \sqrt{\left(\frac{l}{2}\right)^2 + \frac{8HM_b}{M_c} - \frac{Gl}{2}} \quad (2)$$

Yield-Line Theory for open concrete bridge rails relies on several assumptions that must be followed for the use of the equation to be valid. As the ratio of  $\frac{M_b}{M_c}$  increases, so does the critical length of wall failure,  $L$ . As this length increases, it is possible that the failure mechanism extends across multiple spans and involves multiple posts. The yield line equations become invalid in this scenario, as the assumed failure mechanism has yield lines occurring in two posts and the beam in between them. The derived equations assume that  $L$  must be greater than  $G$ , as the post strength term in  $wu$  becomes negative in the case that  $L$  is less than  $G$ , implying that the strength of the bridge rail is reduced in this scenario. Although not specified, this negative result is invalid and should not be included in strength calculations; thus, the post strength term should be capped at a lower bound of zero. This assumption implies that when the critical length of failure is contained entirely within the beam, the strength of the posts does not contribute to the overall strength of the system.

Equations 1 and 2 do not evaluate failure mechanisms that extend into multiple spans and do not provide the ability to evaluate impacts occurring at a post location. The inability to evaluate failure mechanisms that extend into multiple posts is not conservative, as failure mechanisms that extend into multiple spans can potentially have lower capacities than scenarios in which the failure mechanism is contained in a single span. As the critical length of failure increases, it can potentially extend past the length of the posts and into the adjacent bridge rail spans. In this case, the assumed failure mechanism requires the strength of posts adjacent to these spans be included in the calculation of system capacity, which the provided equations do not allow. Additionally, scenarios exist where load application occurs at a post location and not at the mid span of rail elements, which must also take multiple railing spans and multiple posts into account. The current yield line method also assumes load application occurs at the top of the barrier. Thus, the estimated barrier strength may be calculated at a different height than the design load application height. Yield-Line Theory has been adapted for end sections of closed concrete parapets, but not for open concrete bridge rails. Similar equations could be developed for open concrete bridge rails, which do not consider the moment of the wall.

### **4.3 AASHTO Post and Beam Method (Inelastic Method)**

Found in Chapter 13 of the *AASHTO LRFD Bridge Design Specifications*, the AASHTO Post and Beam Method involves the use of the inelastic resistance of beams and posts contributing to plastic hinges that develop in the bridge rail in order to determine the capacities of post and beam bridge rail systems [14]. The ability to evaluate failure mechanisms that extend into multiple posts is conservative, as failure mechanisms that extend into multiple spans can potentially have lower capacities than scenarios in which the failure mechanism is contained in a single span. This differs from Yield-Line Theory in that a predicted length of failure is not calculated. Rather, multiple failure mechanisms of multiple lengths are compared to determine the lowest capacity mechanism. Derivation of the AASHTO Post and Beam Method was completed by equating the external work acting on the system to the internal energy absorbed by the system from load application. External work is calculated as the load acting on the bridge rail system multiplied by the distance the bridge rail deflects laterally. The applied load is assumed to act at the geometric center of all rail elements,  $\bar{Y}$ . The internal energy of the bridge rail is defined as the internal energy absorbed by the beam elements as well as the internal energy absorbed by all posts within the failure mechanism. The internal energy of the beams is defined as  $M_p\theta$ , where  $\theta$  is the angle of

rotation of the beams. The internal energy of the posts is defined as  $P_p \Sigma \Delta$ , where  $\Sigma \Delta$  represents the total displacement of all the posts. Each deflected post within the failure mechanism has its own  $\Delta$  term. The value of  $\Delta$  for each deflected post is calculated by determining the ratio of the post deflection to the overall bridge rail deflection, and  $\Sigma \Delta$  is determined by summation of the individual post values. The pattern the post strength modification factor follows for the increasing amount of railing spans is accounted for by considering load application at midspan of a beam and load application at the center of a post, thus resulting in the  $(N - 1)(N + 1)$  and  $N^2$  terms in the aforementioned capacity equations.

The resistive capacity of the barrier is a function of post strength,  $P_p$ , beam strength,  $M_p$ , span length,  $L$ , length of the applied load,  $L_t$ , and the number of failing spans,  $N$ , as shown in Figure 100. The resistive capacity of the bridge rail,  $R$ , is defined by Equations 3 and 4 when the mechanism develops across an odd or even number of spans [14], respectively:

$$R = \frac{16M_p + (N - 1)(N + 1)P_p L}{2NL - L_t} \quad (3)$$

$$R = \frac{16M_p + N^2 P_p L}{2NL - L_t} \quad (4)$$

Where:

$M_p$  = Yield line, or inelastic resistance of the beams contributing to a plastic hinge

$M_{post}$  = Plastic moment resistance of a single post

$N$  = Number of spans

$P_p$  = Shear force on a single post corresponding to  $M_{post}$  applied at a height  $\bar{Y}$  above the bridge deck

$L$  = Center to center post spacing, and

$L_t$  = Transverse length of distributed vehicle impact loads.



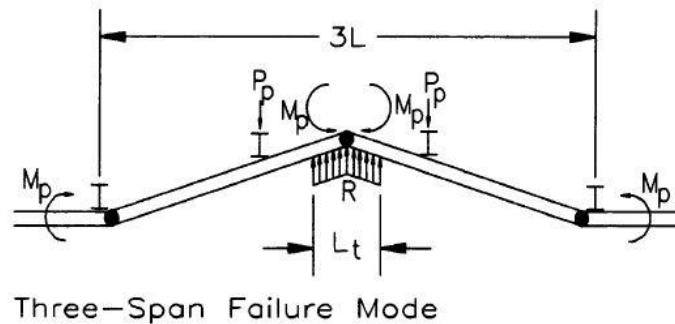
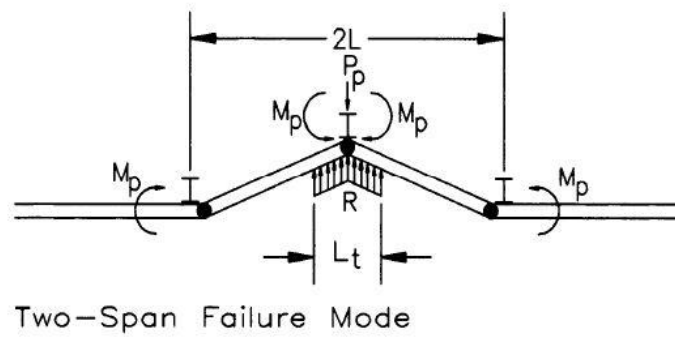
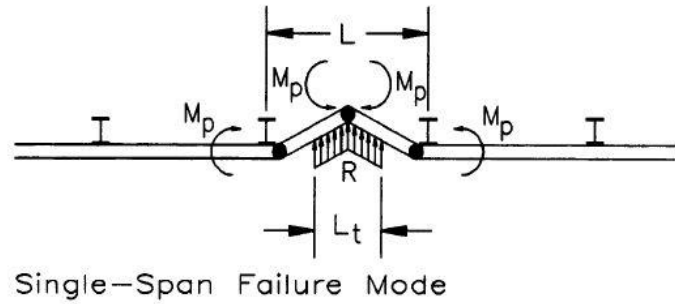


Figure 100. AASHTO Post and Beam Method Failure Mechanisms for Bridge Rail Interior Sections [14]

When  $N = 1$  for the case of an odd number of failing spans, the post strength term of the equation becomes zero, as no posts are within the failure mechanism and are not contributing to the strength of the bridge rail. As the value of  $N$  increases, a controlling capacity and failure mechanism can be determined, and successive iterations will determine what number of failing spans corresponds to the lowest value of  $R$ , which represents the failure mechanism and controlling capacity of the bridge rail.

The AASHTO Post and Beam Method can also be utilized to evaluate bridge rail end sections [14]. Bridge rail end sections occur when there is a discontinuity within the bridge rail, typically at the beginning or end of a bridge or expansion joints. Bridge rail end sections differ from interior sections in that the failure of the end post must occur, resulting in a different failure mechanism. The assumed failure mechanism of bridge rail end sections shown in Figure 101

assumes that the impact load is applied at the edge of the end post and extends inward toward the rest of the interior posts. The resistive capacity,  $R$ , of bridge rail end sections is defined by Equation 5, using the same variables as for the interior section.

$$R = \frac{2M_p + 2P_p L(\sum_{i=1}^N i)}{2NL - L_t} \quad (5)$$

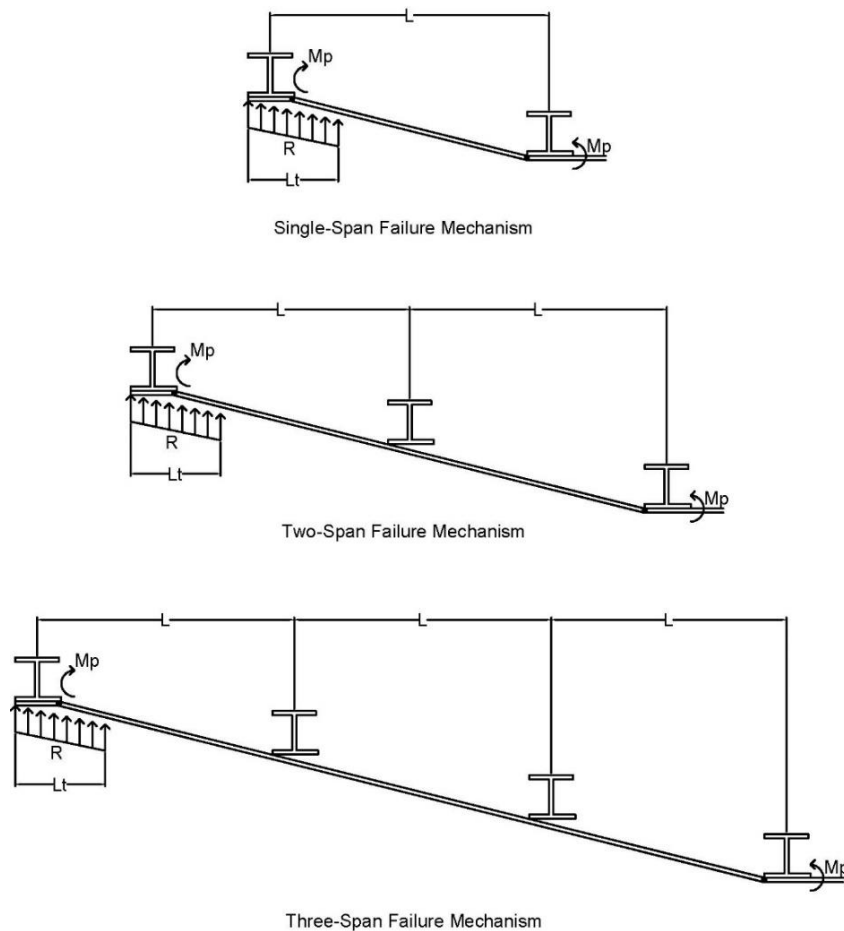


Figure 101. AASHTO Inelastic Method End Section Failure Mechanisms

#### 4.4 AASHTO Post and Beam Method (Inelastic Method) Limitations

Open concrete bridge rails have several key differences compared to steel post and beam bridge rails, including geometry, material behavior, and failure mechanisms. Additionally, the original equations assume load application and bridge rail lateral resistance,  $R$ , occurs at a height of  $\bar{Y}$ . The construction of open concrete bridge rails differs from that of steel post and beam bridge rails in several ways. Open concrete bridge rails often consist of a single, large concrete beam cast atop concrete posts, whereas steel post and beam bridge rails often consist of multiple steel beam elements that are either welded or bolted to the faces and tops of steel posts. Additionally, the length of typical open concrete bridge rail posts is much longer than the length of steel post and beam bridge rail posts, which can also result in the length of the failure mechanism varying for

open concrete bridge rails. This difference in geometry means that it is unlikely that concrete beams will be able to rotate about the center of concrete posts (the strongest section within the bridge rail), and that failure mechanisms may develop in the beam at the edge of the concrete posts rather than at the centerline of the posts as was the case for steel post and beam bridge rails, shown in Figures 102 and 103. When the length of  $L_t$  exceeds or equals the length of  $2NL$ , the result given by the AASHTO Post and Beam equations becomes invalid, as this results in a negative or undefined value for the capacity of the bridge rail. In this case, failure mechanisms that produce an invalid result should not be considered, or the designer must select a value of  $L_t$  such that the equations produce a valid result.

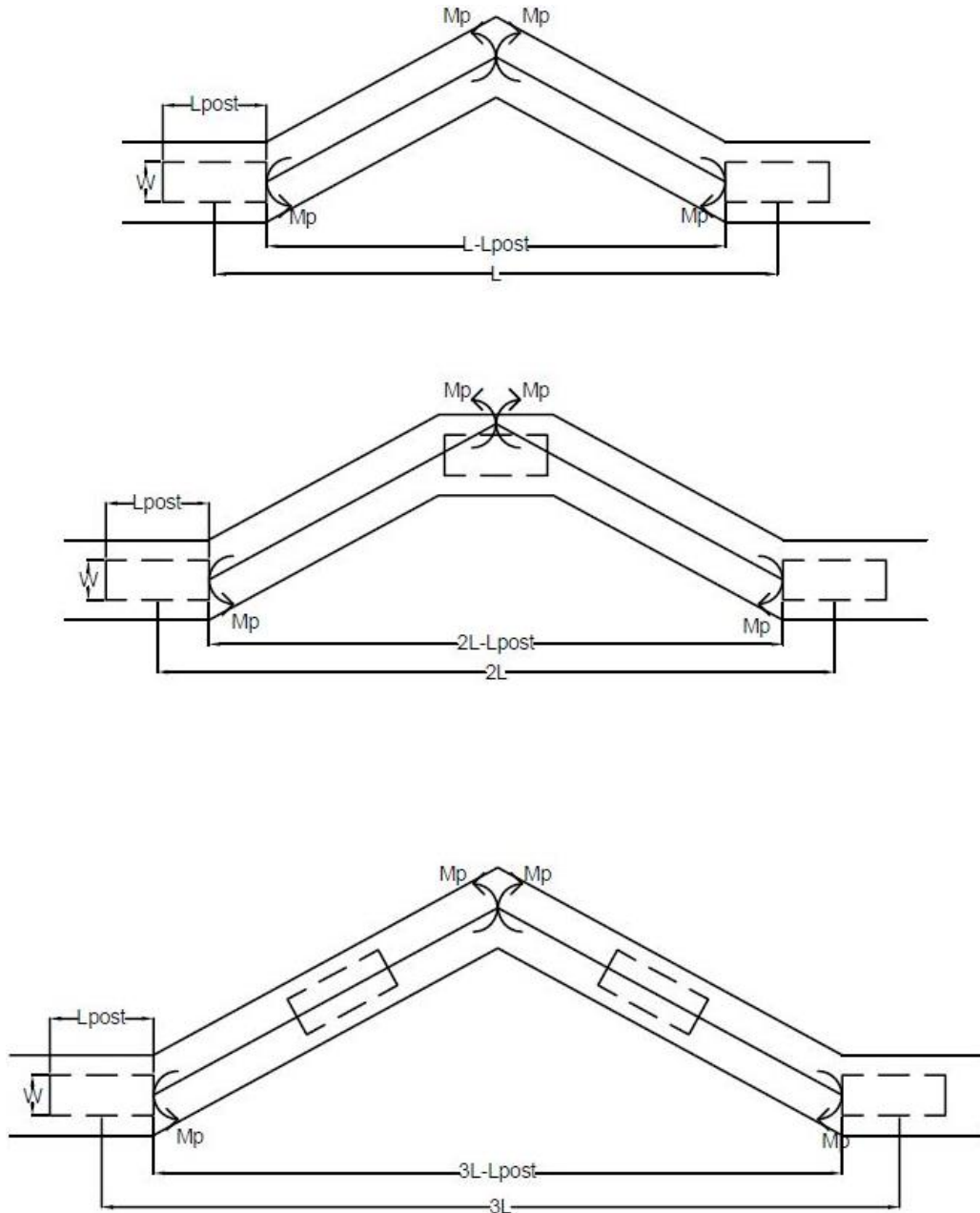


Figure 102. Modified AASHTO Post and Beam Method Failure Mechanism for Bridge Rail Interior Sections (Example of Two-Span Failure)

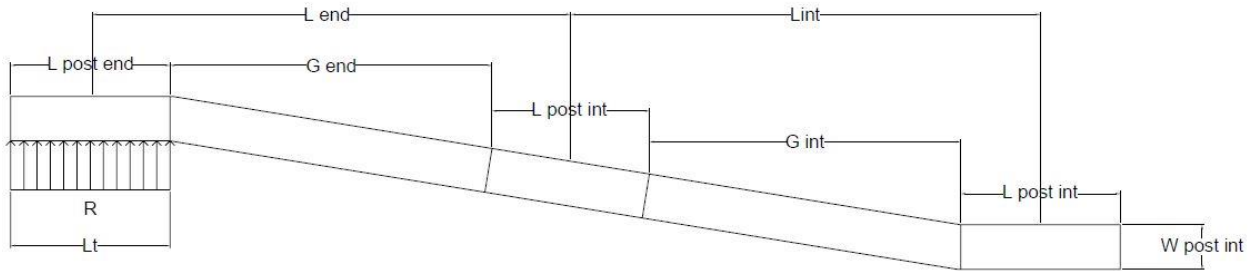


Figure 103. Modified AASHTO Post and Beam Method Failure Mechanism for Bridge Rail End Sections

#### 4.5 Effective Load Application Heights

Load application heights vary for different design scenarios. The effective load application height is a function of both the vehicle geometry and barrier height. In their current states, Yield-Line Theory and the AASHTO Post and Beam Method do not allow for bridge rail capacities to be calculated based at the effective load application height. NCHRP Project 22-20(2) provided updated recommendations of effective load application heights for TL-3 through TL-5 barriers and recommends MASH TL-4 effective load application heights of 25 in. for barriers less than 39 in. tall, and 30 in. for barriers 39 in. or taller [17].

Although effective load application heights have been proposed by various design guides and research efforts, Yield-Line Theory as well as the AASHTO Post and Beam Method assume load application height to be fixed at the top of the barrier,  $H$ , and at centroid height of the beams,  $\bar{Y}$ , respectively. Changing the effective load application height can significantly change the capacity of the bridge rail. If  $H_e$  is greater than  $H$  or  $\bar{Y}$ , then the overall strength of the barrier would decrease. Conversely,  $H_e$  values less than  $H$  or  $\bar{Y}$  would result in increased barrier strength. The inclusion of  $H_e$  in strength calculations would allow for a more accurate determination of bridge rail capacity. In both the Yield Line and AASHTO Post and Beam Methods, the barrier resistance could be calculated to be at the effective height by assuming that the deflection of the system that occurs at  $H_e$  is linearly proportional to the deflection at the original load application height. For Yield-Line Theory, this is defined by the ratio between  $H_e$  and the height of the barrier. For the AASHTO Post and Beam Method, this is defined by ratio between  $H_e$  and  $\bar{Y}$ .

#### 4.6 Yield-Line Theory and AASHTO Post and Beam Method Comparisons

Yield-Line Theory and the AASHTO Post and Beam Method both utilize the strengths of bridge rail posts and beams as well as their geometry to determine the resistive capacity of open concrete bridge rails. In both methods, the ratio of the beam capacity to post capacity determines the length of the failure mechanism.

For Yield-Line Theory, the length of failure,  $L$ , and the ultimate strength of the barrier are calculated by Equations 1 and 2 as previously described. As the ratio of  $\frac{M_b}{M_c}$  increases, so does the critical length of failure. For the AASHTO Post and Beam Method, the capacity of the bridge rail for an odd and even number of spans is defined by Equations 3 and 4, respectively, as previously

described. As the ratio of  $\frac{M_p}{M_{post}}$  increases, behavior similar to the yield line method is observed. Example calculations for various post-to-beam strength ratios can be found in a thesis written by DeLone [38].

Because various load application heights have been proposed, designers may wish to consider the effect of the different load application heights with both Yield-Line Theory and the AASHTO Post and Beam Method. The effective load application heights that were proposed in NCHRP Project 22-20(2) were a function of both barrier height and the vehicle geometry at the various test levels. However, as originally derived, Yield-Line Theory and the AASHTO Post and Beam Method do not allow for bridge rail capacities to be calculated at the effective load application height. To incorporate the effective load application height into the design methods, the ratio of the system deflection at the load application height to the system deflection at the effective height must be taken into consideration. This ratio can then be multiplied by the calculated barrier capacity, resulting in the system capacity at the effective load application height. For Yield-Line Theory, load application was originally at the top of the barrier and the capacity being scaled by  $\left(\frac{H}{H_e}\right)$ , as shown in Equation 6. For the AASHTO Post and Beam Method, load application was originally at  $\bar{Y}$  and the capacity is scaled by  $\left(\frac{\bar{Y}}{H_e}\right)$ , as shown in Equations 7 and 8. Note, the railing capacity at the effective load height should be greater than or equal to the design load.

$$wu = \left( \frac{8M_b}{(L - \frac{l}{2})} + \frac{M_c L(L - G)}{H(L - \frac{l}{2})} \right) \left( \frac{H}{H_e} \right) \quad (6)$$

$$R = \frac{16M_p + (N-1)(N+1)P_p L}{2NL - L_t} \left( \frac{\bar{Y}}{H_e} \right) \text{ if number of failing spans, } N, \text{ is odd} \quad (7)$$

$$R = \frac{16M_p + N^2 P_p L}{2NL - L_t} \left( \frac{\bar{Y}}{H_e} \right) \text{ if number of failing spans, } N, \text{ is even} \quad (8)$$

Example cases show that scaling the bridge rail capacity by  $\left(\frac{H}{H_e}\right)$  when utilizing Yield-Line Theory will always increase the calculated capacity, and therefore, it is a less conservative method. When utilizing the AASHTO Post and Beam Method, scaling the bridge rail capacity by  $\left(\frac{\bar{Y}}{H_e}\right)$  increases calculated capacity for cases in which  $\bar{Y}$  is greater than  $H_e$  (less conservative), and reduces calculated capacities for cases in which  $\bar{Y}$  is less than  $H_e$ , (more conservative). Example calculations using Equations 6, 7, and 8 can be found in a thesis written by DeLone [38].

#### 4.7 Modified AASHTO Post and Beam Method (Modified Inelastic Method)

Due to the large post and beam dimensions commonly utilized with open concrete rails, a modified analysis method may more accurately reflect the failure mechanisms that occur in open concrete rails. Although significant damage has not occurred in many open concrete rail crash

tests, test no. KSCR-1 experienced failure that occurred primarily in the beam adjacent to posts, as shown previously in Figure 7. Static load and bogie testing on open concrete rails conducted by TTI has also shown failure mechanisms developing adjacent to posts, as shown in Figure 104 [39]. Additionally, failure over multiple bridge rail spans occurred in test no. ACBR-1, as shown previously in Figure 22. Many previous open concrete rails may have been significantly overdesigned, which is why minimal damage occurred. Yield-Line Theory is limited to a single failure span and becomes invalid for  $L > G + 2L_{post}$ , limiting applicability, especially when the beam capacity becomes much greater than the post capacity. Additionally, Yield-Line Theory does not allow for load application at a post location as the AASHTO Post and Beam Method does, further limiting the applicable scenarios. With the AASHTO Post and Beam Method, it is unlikely that concrete beams will be able to rotate about the center of concrete posts and that failure mechanisms may develop in the beam at the edge of the concrete posts and in the posts at the post-to-deck interface.



Figure 104. Open Concrete Bridge Rail Failure Mechanism [39]

After considering the limitations of Yield-Line Theory and the AASHTO Post and Beam Method, the AASHTO Post and Beam Method was further modified for the design of open concrete bridge rails. Modifications to the method included the option to scale the capacity based on  $H_e$ , the inclusion of plastic hinges forming at the edges of posts (rather than at the centerline of posts), and the inclusion of variable post lengths and gap lengths when designing bridge rail end sections. Modifications to the equations were made by utilizing the principles of work and energy and balancing the external work applied to the bridge rail with the internal energy absorbed by the bridge rail. Full derivations are shown in a thesis written by DeLone [38]. The new failure mechanisms for interior sections and end sections are shown in Figures 102 and 103. For the interior section, the failure mechanism is assumed to develop at the edges of the posts and at the location of maximum deflection. For an odd number of failing spans, plastic hinges form at the location of maximum deflection, and for an even number of failing spans, plastic hinges were assumed to form at the center of the post. Although it is unknown where these hinges may form, the assumption that failure would occur at the center of the posts for an even number of failing spans was more conservative than assuming hinges formed at the edges of the posts.

To allow the designer to scale the capacity of the system based on the effective applied load height, the deflection of the system,  $\Delta$ , was multiplied by the ratio of  $\frac{\bar{Y}}{H_e}$  when calculating the external work acting on the system. To account for the new failure assumption of hinges forming in the beam at the edges of the posts instead of at midspan of the posts, half of  $L_{post}$  was subtracted from each side of the failure length,  $NL$ , resulting in the subtraction of one post length when calculating the angle of rotation of the bridge rail. This change is consistent with the assumption that plastic hinges will not form in the beam at the middle of the posts, as was assumed previously, and that the failure mechanism of the beam will occur at the edges of the posts. This change was not applied at the center post location for an even number of spans. Instead, the original assumption of a plastic hinge forming in the beam at the center of the post was utilized because the formation of two closely spaced plastic hinges on each side of the center post was considered unlikely.

The newly derived equation differs from the original equations in that the inclusion of the post length does not result in the previous distinct equations for even and odd spans. Rather there is only one equation with a unique post displacement factor,  $PF$ , for every  $N$ . Recall that the original AASHTO Post and Beam Method utilized one equation for an odd value of  $N$  and one for an even value of  $N$ . When these equations were originally developed, a pattern was observed for increasing values of  $N$  that showed there was a different factor multiplied by  $P_p$  for odd and even spans, resulting in the unique terms in either equation. When deriving the modified equations, the implementation of  $PF$  was used in favor of determining unique terms for odd and even spans. Similar to the original AASHTO Post and Beam Method, the  $\left(\frac{\bar{Y}}{H_e}\right)$  factor should not be included in calculations for single span failure mechanisms. The capacity,  $R$ , with the Modified AASHTO Post and Beam Method is calculated as:

$$R = \left( \frac{16M_p + 2P_p(PF)(NL - L_{post})}{2(NL - L_{post}) - L_t} \right) \left( \frac{\bar{Y}}{H_e} \right) \quad (9)$$

Where:

- $M_p$  = Yield line, or inelastic resistance of the rails contributing to a plastic hinge
- $M_{post}$  = Plastic moment resistance of a single post
- $N$  = Number of spans
- $P_p$  = Shear force on a single post corresponding to  $M_{post}$  applied at a height  $\bar{Y}$  above the bridge deck
- $L$  = Post spacing
- $L_t$  = Transverse length of distributed vehicle impact loads
- $L_{post}$  = Post length
- $H_e$  = Effective height, and
- $PF$  = Post displacement factor.

Post displacement factors will vary based on the number of spans in the failure pattern as well as the specific geometry of the concrete bridge rail. Because the plastic hinges in the beam were moved from center-of-post locations to the edge of the posts, both the post spacing and the post length will play a part in calculating post displacements. Thus, the old post displacement factors may no longer apply and designers will have to calculate them based on their specific railing geometry.

For bridge rail end sections, a similar approach was taken, except the option to include variable span lengths and post lengths was taken into consideration. End sections of open concrete bridge rails may implement greater post lengths to achieve higher strengths than interior section posts due to the loss of strength resulting from the railing discontinuity. End post geometry can be modified by altering either the end post length or the end section span length. The Modified AASHTO Post and Beam Method equations for bridge rail end sections allows the designer to account for modified bridge rail geometry in the end section, an option not available with the original equations. Failure of the beam was assumed to occur at the edge of an interior post. The deflection of the system  $\Delta$  was multiplied by the ratio of  $\frac{\bar{Y}}{H_e}$  when calculating the internal energy absorbed by the system, allowing the internal energy absorbed by the bridge rail system to be scaled based on variable load application heights. Unlike the AASHTO Post and Beam Method for bridge rail interior sections, all end section failure mechanisms involve the failure of a post and the  $\left(\frac{\bar{Y}}{H_e}\right)$  factor is always applicable. However, as was discussed for the interior section calculations, the designer may wish to exclude the  $\left(\frac{\bar{Y}}{H_e}\right)$  factor due to its effect on conservatism. The newly derived equation for a single-span failure of the bridge rail end section scaled based on variable load application heights is given by Equation 10 for a single-span failure and Equation 11 for any failure mechanism involving multiple spans.

$$R = \left( \frac{2(G_e + \frac{L_e}{2})P_{p,end} + 2M_p}{2(G_e + L_e) - L_t} \right) \left( \frac{\bar{Y}}{H_e} \right) \quad (10)$$

$$R = \left( \frac{2P_{p,end}((N-1)L_i + G_e + \frac{L_e}{2}) + 2(P_{p,int}(\sum_{i=1}^{N-1} iL_i - \frac{(N-1)}{2}W_i)) + 2M_p}{2(N-1)L_i + 2G_e + 2L_e - L_t} \right) \left( \frac{\bar{Y}}{H_e} \right) \quad (11)$$

Where:

$M_p$  = Yield line, or inelastic resistance of the rails contributing to a plastic hinge

$M_{post}$  = Plastic moment resistance of a single post

$N$  = Number of spans

$P_{p,end}$  = Shear force on the end post corresponding to  $M_{post}$  applied at a height  $\bar{Y}$  above the bridge deck



- $P_{p,int}$  = Shear force on the end post corresponding to  $M_{post}$  applied at a height  $\bar{Y}$  above the bridge deck
- $L$  = Center to center post spacing
- $L_t$  = Transverse length of distributed vehicle impact loads
- $L_e$  = Exterior post length
- $L_i$  = Interior post length
- $H_e$  = Effective height, and
- $G_e$  = End post gap length.

#### 4.8 Barrier Punching Shear

Although not contained in the *AASHTO LRFD Bridge Design Specifications*, punching shear failure of the rail, where a block of concrete fails along a critical perimeter in the impact region for both interior and end sections, can occur as well, and can be conservatively estimated as:

$$V_c = 2\lambda\sqrt{f'_c}b_o d \quad (12)$$

Where:

$\lambda$  = Lightweight concrete factor

$f'_c$  = Concrete compressive strength, psi

$b_o$  = Critical punching shear perimeter, in.

$d$  = average depth of barrier across the punching shear region, in.

#### 4.9 Deck Design

The *AASHTO LRFD Bridge Design Specifications* provide three design cases for bridge decks, as shown in Table 13 [14]. Utilizing the recommended loads in NCHRP Project 22-20(2), the design loads for these cases can be updated to be more reflective of MASH TL-4 conditions [17]. The updated design cases, load types, and limit states are shown in Table 13.

Table 13. Design Cases, Loads, and Limit States [14,17]

Design Case	Load Type	<i>AASHTO LRFD Bridge Design Specifications</i> Loads [14]	NCHRP 22-20(2) Loads [17]	Limit State
1	Horizontal Impact Load	54 kips over 3.5 ft	72.3 to 80 kips over 4 to 5 ft <sup>1</sup>	Extreme Event II
2	Vertical Impact Load	18 kips over 18 ft	33 kips over 18 ft	Extreme Event II
3	Live Load	1 kip/ft @ 1 ft from face of barrier	-	Strength I

<sup>1</sup>Horizontal load distribution length is defined as 4 ft for bridge rails shorter than 39 in., and 5 ft for bridge rails 39 in. or taller.

*AASHTO LRFD Bridge Design Specifications* also states that the horizontal impact load in design case 1 can be taken as the horizontal load required to cause the barrier to overturn. For the new open concrete bridge rail, this load was specified as the lateral force required to cause failure of a post,  $P_p$ . The 1-kip/ft live load in design case 3 is based on one 25-kip axle of the design tandem being uniformly distributed over 25 ft, and is applicable provided the deck overhang cantilever is 6 ft or less in length from the centerline of the exterior girder [40-41]. For all three design cases, the dead weight of the deck, a future 3-in. thick roadway overlay, and the bridge rail were considered in addition to the applied loads shown in Table 13. *AASHTO LRFD Bridge Design Specifications* specifies that the factors shown in Table 14 can be applied to the impact and dead loads for the Strength I and Extreme Event limit states [14]. Dead load modification factors have a range for which the designer can select the value, to either decrease or increase the magnitude of the dead loads. When investigating the effect of the live load in design case 3, the designer may also wish to consider the multiple presence factors and dynamic load allowance factors presented in the *AASHTO LRFD Bridge Design Specifications*, and shown in Tables 15 and 16 [14]. Dynamic load allowance factors represent a percent increase in applied load based off the dynamic interaction between the bridge and moving vehicles. For the design of the new open concrete bridge rail, multiple presence factors and dynamic load allowance factors were not considered.

Table 14. *AASHTO LRFD Bridge Design Specifications* Load Modification Factors [14]

Limit State	Component Dead Load, $\gamma_s$	Wearing Surface Dead Load, $\gamma_s$	Impact Load	Live Load
Strength I	0.9-1.25	0.65-1.5	1.75	1.75
Extreme Event II	0.9-1.25	0.65-1.5	0.5	0.5

Table 15. AASHTO LRFD Bridge Design Specifications Multiple Presence Factors [14]

Number of Loaded Lanes	Multiple Presence Factor, m
1	1.2
2	1.0
3	0.85
>3	0.65

Table 16. AASHTO LRFD Bridge Design Specifications Dynamic Load Allowance Factors [14]

Limit State	Dynamic Load Allowance, IM
Deck Joints: All Limit States	75%
All other Components: Fatigue and Fracture Limit State	15%
All other Components: All other Limit States	33%

For all the design cases, it is recommended that the deck be analyzed at two design sections. The first design section is located at the face of the post, and the second is located at the exterior support girder/beam. Various design methods assume this distance to vary slightly, as different methods assume different distances relative to the location of the exterior girder. For closed concrete parapets, AASHTO LRFD Bridge Design Specifications states that for design case 1, the bridge deck overhang should provide a flexural resistance greater than the cantilever capacity of the parapet, and that tensile loads can be determined based on the critical length of wall failure calculated with Yield-Line Theory. Design sections in the overhang and their locations are not discussed. For steel post and beam bridge rails, AASHTO LRFD Bridge Design Specifications assumes that tensile force forces imparted on steel post-and-beam bridge rails distribute at a 45-degree angle from the back of the post, as shown in Figure 105.

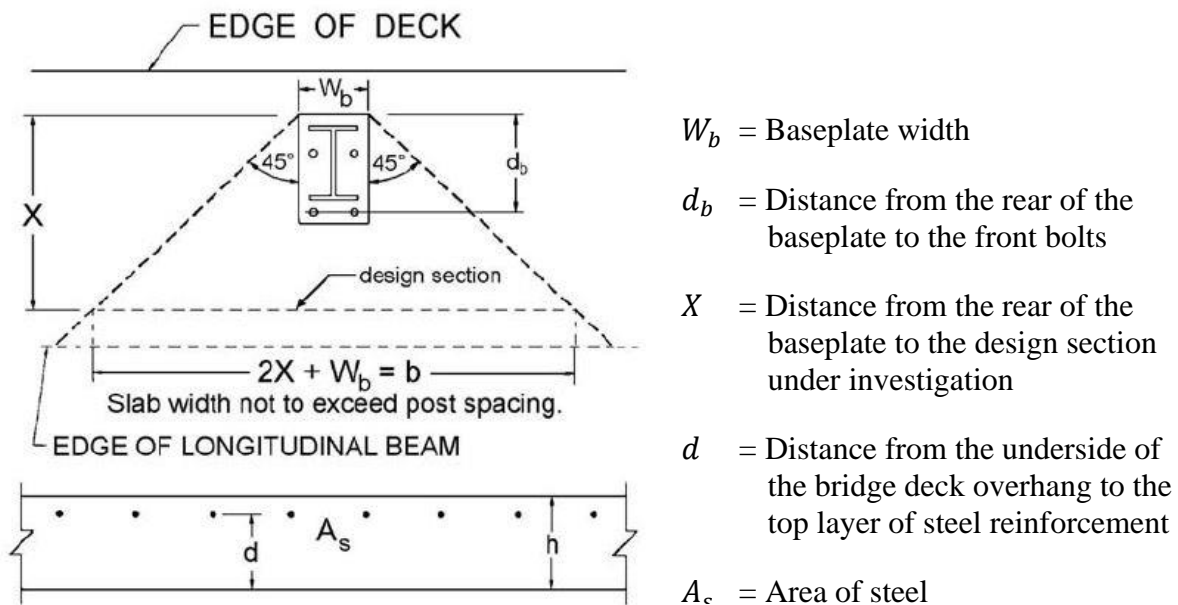
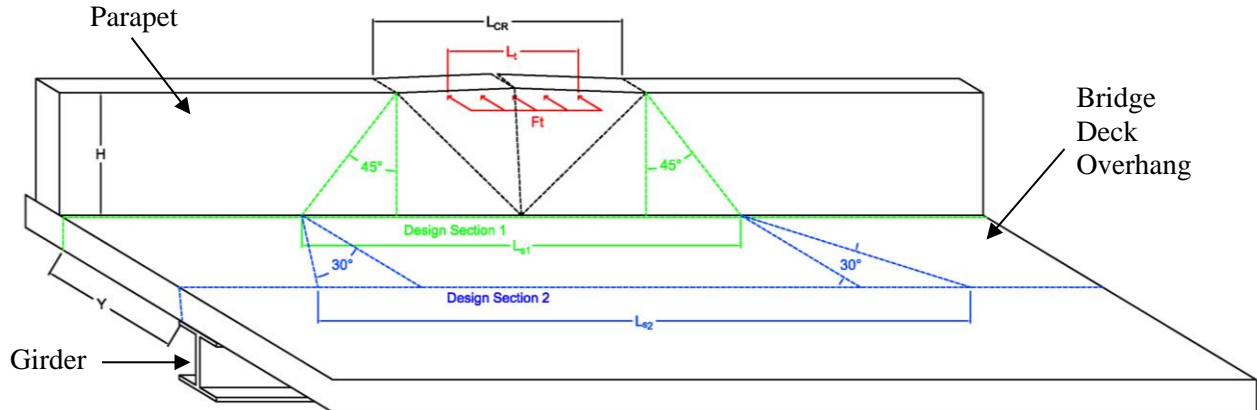


Figure 105. 45-Degree Load Distribution for Steel Post-and-Beam Bridge Rails [14]

Additionally, research conducted by Frosch and Morel on closed concrete parapets has shown that forces can distribute into the deck at approximately 30 degrees [19-20, 42]. This scenario assumes that impact loads are distributed longitudinally over a length,  $L_t$ , with a yield line forming on the face of the parapet over a critical length,  $L_{cr}$ , which is the same as  $L$  in the yield line method. The load is then vertically distributed down the face of the parapet at a 45-degree angle before being distributed into the deck at a 30-degree angle, as shown in Figure 106.



Where:

- $L_{cr}$  = Critical length of failure
- $L_t$  = Length of distributed impact load
- $L_{s1}$  = Length of design section 1
- $L_{s2}$  = Length of design section 2
- $H$  = Height of concrete parapet, and
- $Y$  = Overhang width.

Figure 106. 30-Degree Load Distribution for Closed Concrete Parapets [19-20]

Rosenbaugh et al. proposed evaluating the loads acting in two design sections [19-20]. Design section 1 is located at the face of the post and design section 2 is located at a distance  $X$  measured from the back of the post to a section adjacent to the exterior girder. For interior posts, the design section lengths,  $L_{s1}$  and  $L_{s2}$ , are calculated as:

$$L_{s1\_int} = L_{post} + 2W_{post} \tan(\theta) \quad (13)$$

$$L_{s2\_int} = L_{post} + 2X \tan(\theta) \quad (14)$$

Where:

$L_{post}$  = Length of the post, in.

- $W_{post}$  = Width of the post, in.  
 $X$  = Distance to the design section adjacent to the girder, in., and  
 $\theta$  = Load distribution angle, degrees.

For end posts, the discontinuity in the bridge deck does not allow for load transfer, thus, loads become concentrated along this edge and do not distribute at a 30-degree angle, as shown in Figure 107. Design sections 1 and 2 are located at the same distances as they were for the interior post, but  $L_{s1}$  and  $L_{s2}$  are now calculated as:

$$L_{s1\_end} = L_{post} + W_{post} \tan(\theta) \quad (15)$$

$$L_{s2\_end} = L_{post} + X \tan(\theta) \quad (16)$$

Evaluating loads acting in sections at the face of the bridge rail and at a location adjacent to the girder allows for scenarios in which the tensile load is highly concentrated at the face of the post, as well as scenarios in which there is a large moment acting about the section adjacent to the girder. For the new open concrete bridge rail, a 30-degree load distribution was recommended in lieu of the 45-degree load distribution. The steeper angle concentrates tensile load over a smaller distance, which will produce a more conservative design and will help prevent damage to the deck. The load is distributed into the beam over a distance  $L_t$ , up to a value equal to the capacity of an individual post,  $P_p$ . Loads then distribute into the deck from the rear face of the post at an angle of 30 degrees, as shown in Figure 108.

Design sections were assumed to be at the face of the post and at the edge of the girder, as shown in Figures 108 and 109. The distance  $X$  can be calculated in multiple ways depending on the designer's preference.

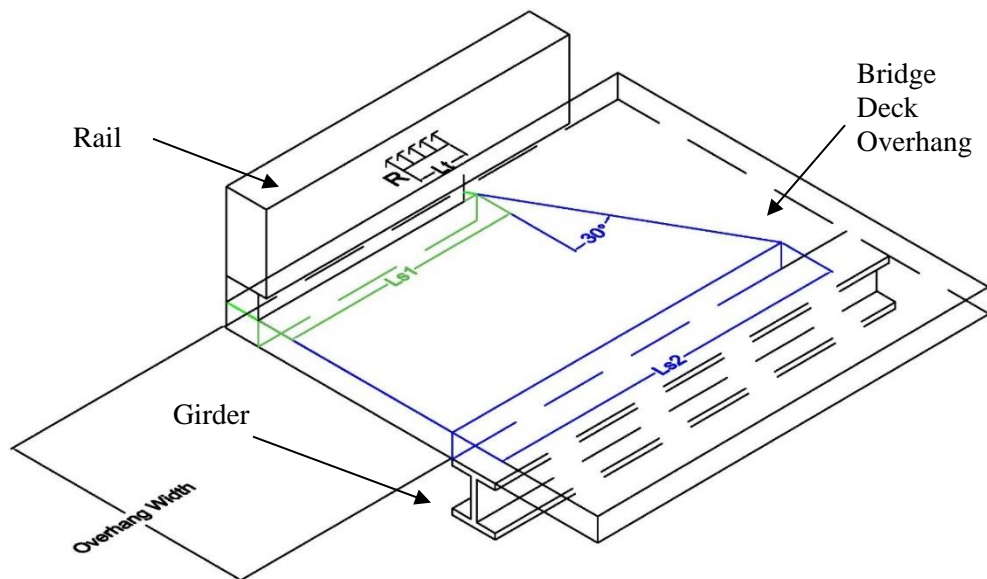
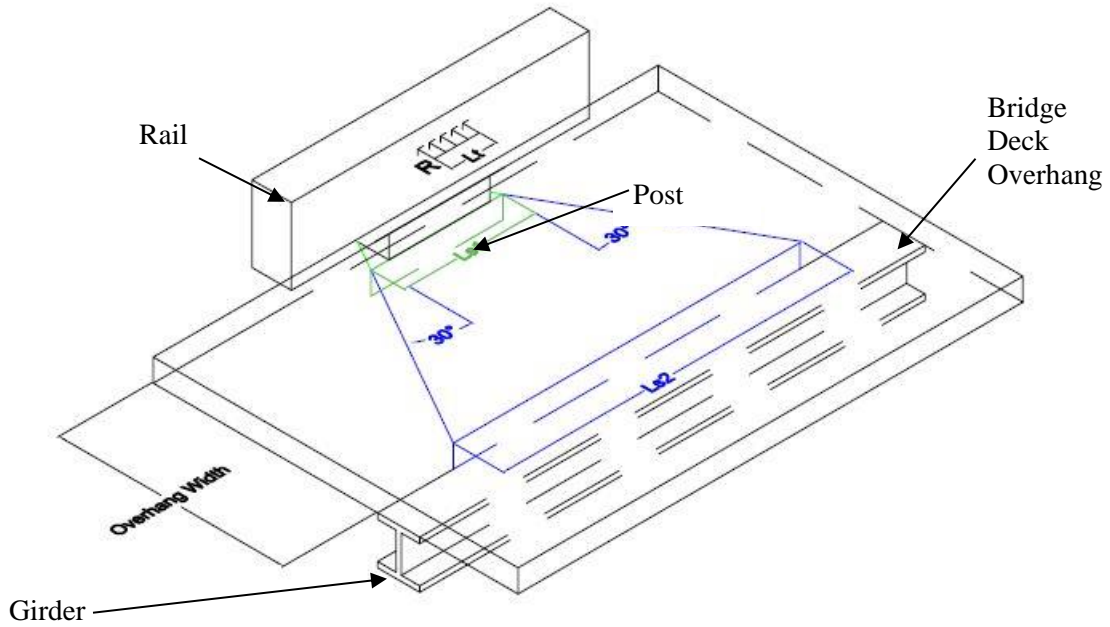


Figure 107. 30-Degree Load Distribution for End Posts of Open Concrete Bridge Rails



Where:

$L_{s1}$  = Length of design section 1

$L_{s2}$  = Length of design section 2

$R$  = Distributed impact load

$L_t$  = Length of distributed impact load

Figure 108. 30-Degree Load Distribution for Interior Posts of Open Concrete Bridge Rails

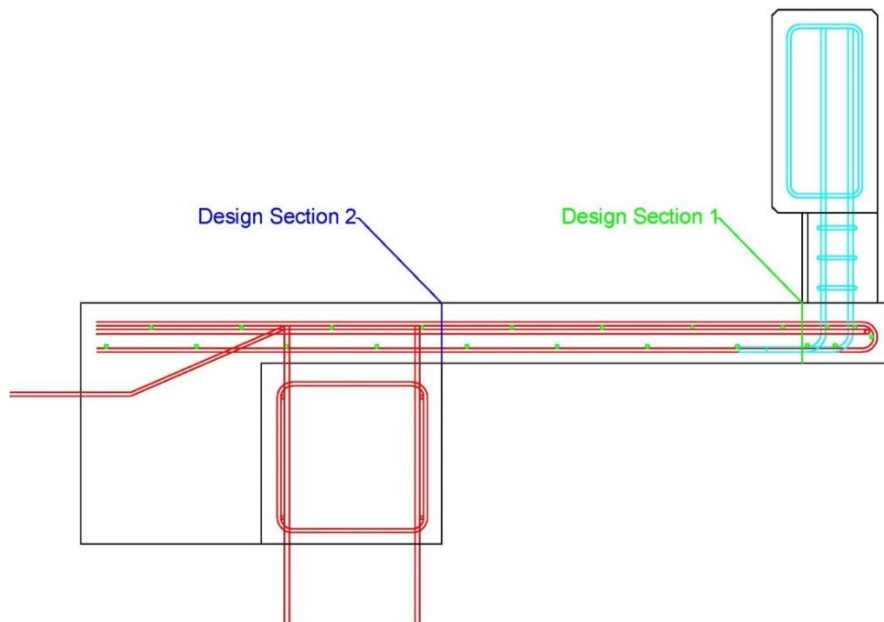


Figure 109. Deck Design Sections

The location of design section 2 is to be determined by the designer, and examples of how to determine this distance are shown in the National Highway Institute (NHI) *Load and Resistance Factor Design (LRFD) for Highway Bridge Superstructures Reference Manual* as well as NHI *LRFD for Highway Bridge Superstructures Design Examples* [40-41]. Design sections were measured from the rear face of the parapet to  $\frac{1}{4}$  of the flange width for steel girders, and to the lesser of  $\frac{1}{3}$  of the flange width or 15 in. for prestressed concrete girders, as shown in Figures 110 and 111. The location of design section 2 was selected to be at the edge of the girder in the 60-in. overhang to be used for full-scale crash testing, as shown in Figure 112. Selecting the location of the design section to be at the edge of the girder would be more critical than at  $\frac{1}{3}$  or  $\frac{1}{4}$  of the flange for the full-scale crash testing effort. The location of design section 2 may vary between transportation agencies.

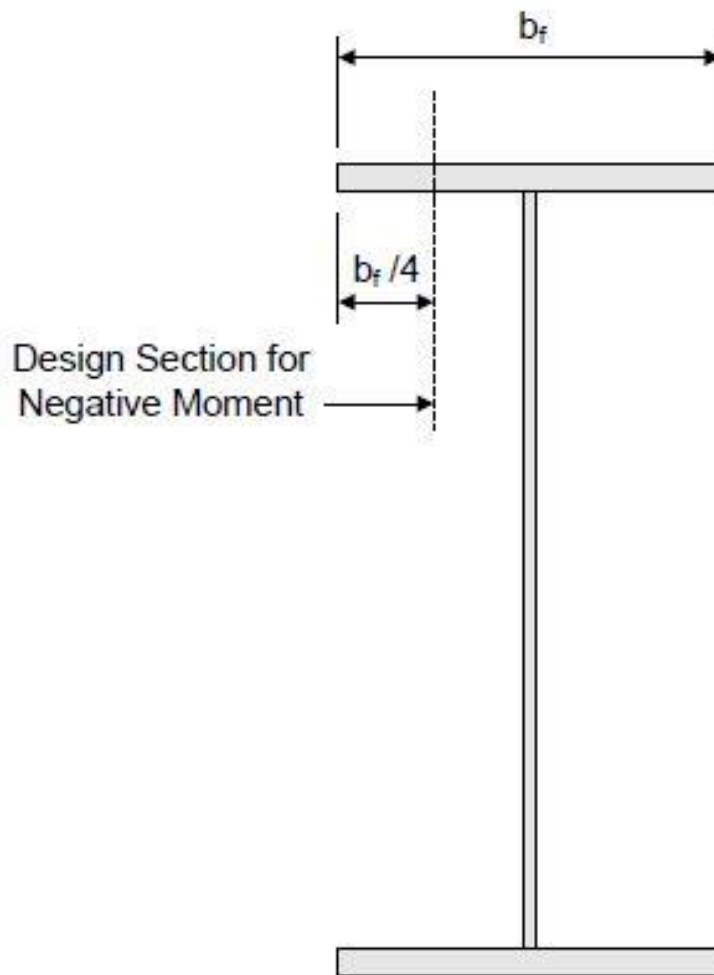


Figure 110.  $\frac{1}{4}$  Width of Flange Design Section for Steel Girders [40]

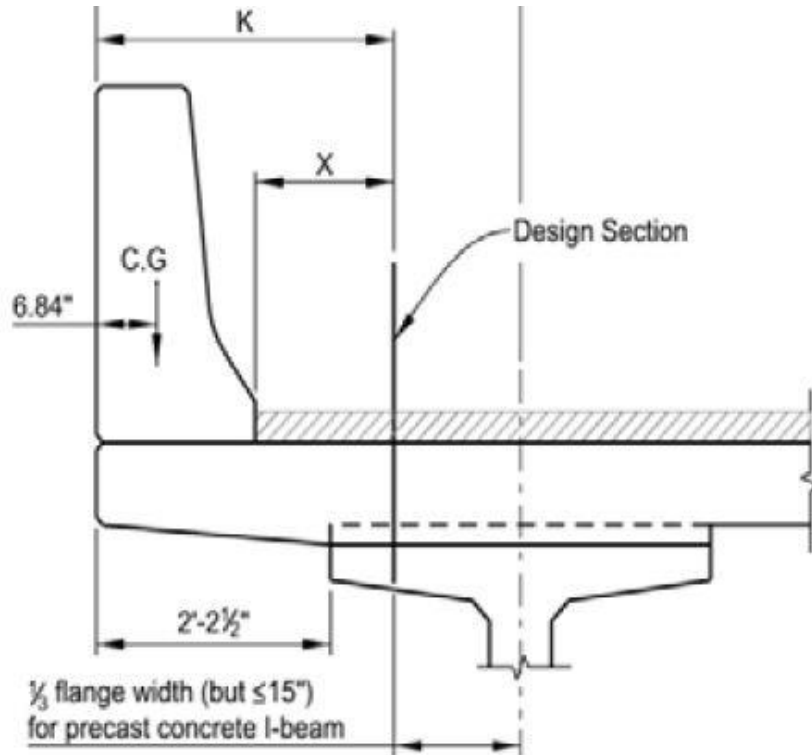


Figure 111. 1/3 Flange Width or 15-in. Wide Design Section for Prestressed Concrete Girders [41]

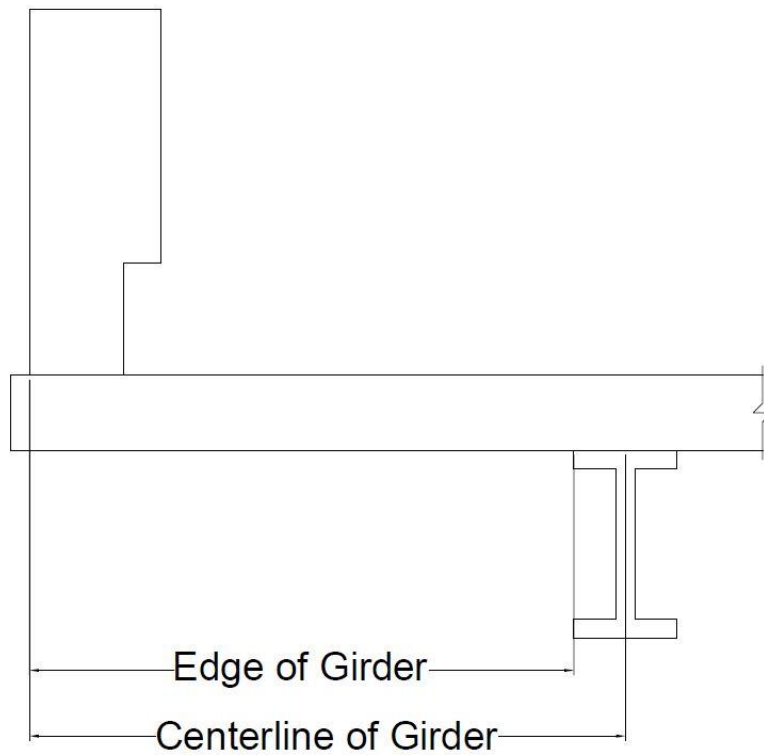


Figure 112. Rear of Post to Edge of Girder and Centerline of Girder



## 5 CURRENT KANSAS CORRAL RAIL

### 5.1 Overview

Prior to designing the new TL-4 open concrete rail, the capacity of the current Kansas Corral Rail was analyzed with Yield-Line Theory, the AASHTO Post and Beam Method, and the Modified AASHTO Post and Beam Method. Results from the analysis methods were compared to determine which method to use with the design of the new open concrete bridge rail. Variants of the Kansas Corral Rail without a lower curb were included in this analysis.

### 5.2 27-in. Tall Kansas Corral Rail Without Curb

The 27-in. tall Kansas Corral Rail consisted of a 14-in. tall by 14-in. wide beam supported by 13-in. tall by 10-in. wide by 36-in. long posts, as shown in Figure 113. Posts were separated by an 84-in. long gap, and the front faces of the posts were offset 2 in. from the front face of the rail. Beam longitudinal reinforcement consisted of six No. 6 bars, three each on the front and rear faces of the beam, spaced at 5½ in. on center. Beam shear reinforcement consisted of No. 3 bars longitudinally spaced at 4¼ in. on center in the region supported by the posts and spaced at 15 in. on center in the unsupported region. Vertical post reinforcement consisted of 16 No. 7 bars, eight on each face, spaced at 4¼ in. on center. Post shear reinforcement consisted of four No. 3 bars vertically spaced at 3 in. on center. Additionally, partial expansion gaps passing through the rail were incorporated at the midspan of post locations. The capacity of the bridge rail was determined according to NCHRP Report 350 TL-3 conditions. The length of the distributed impact load was selected to be 48 in. based on guidance from *AASHTO LRFD Bridge Design Specifications* [14]. The effective load application height was selected to be 24 in. based on guidance provided in NCHRP Report No. 22-20(2) [17].

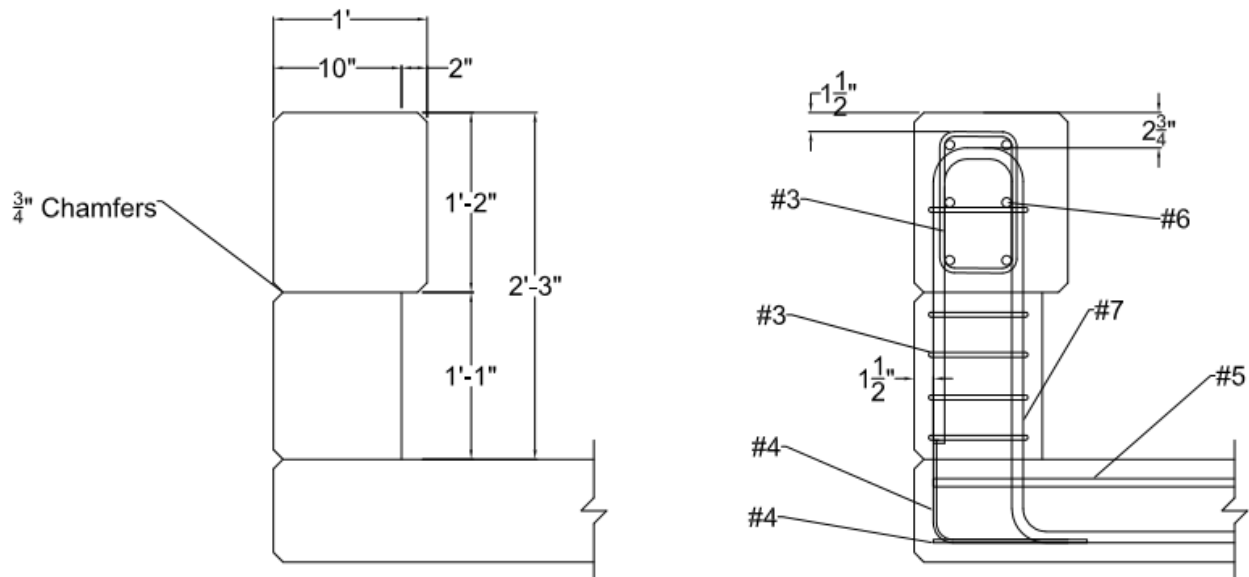


Figure 113. 27-in. Tall Kansas Corral Rail Without Curb

### Yield-Line Theory Strength Calculations for 27-in. Corral Rail

Evaluating the 27-in. tall Kansas Corral Rail without a curb by the yield line method, the critical length of failure,  $L$ , calculated from Equation 2 is:

$$L = \frac{l}{2} + \sqrt{\left(\frac{l}{2}\right)^2 + \frac{8H\phi M_b}{\phi M_c} - \frac{Gl}{2}}$$

Where:

$$l = 48 \text{ in. [14]}$$

$$H = 27 \text{ in.}$$

$$\phi M_b = 60.0 \text{ kip-ft}$$

$$\phi M_c = 49.8 \text{ kip-ft/ft}$$

$$G = 84 \text{ in.}$$

$$\phi = 0.9$$

$$L = \frac{48/12}{2} + \sqrt{\left(\frac{48/12}{2}\right)^2 + \frac{8(27)(60)}{(49.8)} - \frac{(84*48)/144}{2}} = 5.4 \text{ ft} = 65.0 \text{ in.}$$

With  $L < G$ , the post strength term is excluded from barrier strength calculations, and the capacity of the bridge rail  $wu$ , calculated from Equation 1 at a 27-in. height is:

$$wu = \frac{8\phi M_b}{(L-\frac{l}{2})} + \frac{\phi M_c L(L-G)}{H(L-\frac{l}{2})} = \frac{8(60*12)}{(63.4-\frac{48}{2})} + 0 = 140.4 \text{ kips}$$

If the barrier resistance is modified by  $\left(\frac{H}{H_e}\right)$ , where  $H_e = 24 \text{ in.}$ , the resistance of the barrier  $wu = 157.9 \text{ kips.}$

### AASHTO Post and Beam Method Calculations for 27-in. Corral Rail

Evaluating the 27-in. tall Kansas Corral Rail without a curb by the AASHTO Post and Beam Method, the capacity of the bridge rail,  $R$ , calculated at a 20-in. height is:

$$R = \frac{16\phi M_P + (N-1)(N+1)P_P L}{2NL - L_t} \text{ for odd } N, \quad R = \frac{16\phi M_P + N^2 P_P L}{2NL - L_t} \text{ for even } N$$

Where:

$$\phi M_P = 60.0 \text{ kip-ft}$$

$$\phi M_{post} = 149.5 \text{ kip-ft}$$

$$\bar{Y} = 20 \text{ in. (508 mm)}$$

$$P_P = \frac{\phi M_{post}}{\bar{Y}} = \frac{149.5}{20/12} = 89.7 \text{ kip}$$

$$L = 120 \text{ in.}$$

$$L_t = 48 \text{ in.}$$

$$\phi = 0.9.$$

$$\text{For } N=1, \quad R = \frac{16(60*12) + (1-1)(1+1)(89.7*120)}{2(1*120) - 48} = 60.0 \text{ kips}$$

$$\text{For } N=2, \quad R = \frac{16(60*12) + 2^2(89.7*120)}{2(2*120) - 48} = 126.3 \text{ kips}$$

$$\text{For } N=3, \quad R = \frac{16(60*12) + (3-1)(3+1)(89.7*120)}{2(3*120) - 48} = 145.3 \text{ kips}$$

If the barrier resistance is modified by  $\left(\frac{\bar{Y}}{H_e}\right)$ , where  $H_e = 24 \text{ in.}$ :

$$\text{For } N=1, \quad R = 60.0 \text{ kips,}$$

$$\text{For } N=2, \quad R = 105.3 \text{ kips}$$

$$\text{For } N=3, \quad R = 121.1 \text{ kips}$$

The capacity with and without the effective height consideration was determined to be 60.0 kips, with a single-span failure mechanism, as capacities continue to increase for increasing values of  $N$ . Because the critical length of failure did not exceed the span length, and a single-span failure mechanism was determined from the AASHTO Post and Beam Method, bridge rail capacity was determined to be unaffected by discontinuities in the rail at the partial expansion gap location.

### Modified AASHTO Post and Beam Method Calculations for 27-in. Corral Rail

Evaluating the 27-in. tall Kansas Corral Rail without a curb by the Modified AASHTO Post and Beam Method, the bridge rail capacity,  $R$ , calculated at a 24-in. height is:

$$R = \left( \frac{16\phi M_P + 2P_P(PF)(NL - L_{post})}{2(NL - L_{post}) - L_t} \right) \left( \frac{\bar{Y}}{H_e} \right)$$

Where:

$$M\phi_p = 60.0 \text{ kip-ft}$$

$$\phi M_{post} = 149.5 \text{ kip-ft}$$

$$\bar{Y} = 20 \text{ in.}$$

$$P_p = \frac{\phi M_{post}}{\bar{Y}} = \frac{149.5}{20/12} = 89.7 \text{ kip}$$

$$L = 120 \text{ in.}$$

$$L_t = 48 \text{ in. [14]}$$

$$L_{post} = 36 \text{ in.}$$

$$H_e = 24 \text{ in. [17]}$$

For  $N=1$ , and  $PF=0$ ,

$$R = \left( \frac{16\phi M_P + 2P_P(PF)(NL - L_{post})}{2(NL - L_{post}) - L_t} \right) = \left( \frac{16(60 \cdot 12) + 2(89.7)(0)(1(120) - 36)}{2((1 \cdot 120) - 36) - 48} \right)$$

$$= 96 \text{ kips}$$

For  $N=2$ , and  $PF=1$ ,

$$R = \left( \frac{16\phi M_P + 2P_P(PF)(NL - L_{post})}{2(NL - L_{post}) - L_t} \right) \left( \frac{\bar{Y}}{H_e} \right) = \left( \frac{16(60 \cdot 12) + 2(89.7)(1)(2(120) - 36)}{2((2 \cdot 120) - 36) - 48} \right) \left( \frac{20}{24} \right)$$

$$= 111.4 \text{ kips}$$

For  $N=3$  and  $PF=1.333$ ,

$$R = \left( \frac{16\phi M_P + 2P_P(PF)(NL - L_{post})}{2(NL - L_{post}) - L_t} \right) \left( \frac{\bar{Y}}{H_e} \right) = \left( \frac{16(60 \cdot 12) + 2(89.7)(3)(1.333(120) - 36)}{2((3 \cdot 120) - 36) - 48} \right) \left( \frac{20}{24} \right)$$

$$= 123.6 \text{ kips}$$

Because the capacity of the bridge rail continued to increase for increasing values of  $N$ , the capacity was determined to be 96 kips, with a single-span failure mechanism.

These analyses showed that critical length of failure did not exceed the span length, and both the original and Modified AASHTO Post and Beam method determined a single-span failure mechanism. Therefore, the bridge rail was determined to be unaffected by discontinuities in the rail at the partial expansion gap location.

### 5.3 32-in. Tall Kansas Corral Rail Without Curb

The 32-in. tall Kansas Corral Rail consisted of a 19-in. tall by 14-in. wide rail supported by 13-in. tall by 10-in. wide by 36-in. long posts, as shown in Figure 114. Posts were separated by an 84-in. long gap, and the front faces of the posts were offset 2 in. from the front face of the rail. Additionally, partial expansion gaps passing through the rail were incorporated at the midspan of post locations. Longitudinal rail reinforcement consisted of six No. 6 bars, three on the front and rear faces of the bridge rail, spaced at 8 in. on center. Rail shear reinforcement consisted of No. 3 bars longitudinally spaced at 4¼ in. on center in the region supported by the posts and spaced at 15 in. on center in the unsupported region. Vertical post reinforcement consisted of eight No. 7 bars spaced at 4¼ in. on center. Post shear reinforcement consisted of four No. 3 bars vertically spaced at 3 in. on center. The capacity of the bridge rail was determined according to NCHRP Report 350 TL-4 conditions. The length of the distributed impact load was selected to be 42 in. long based off guidance from the *AASHTO LRFD Bridge Design Specifications* [14]. The effective load application height was selected to be 25 in. based off guidance provided in NCHRP Report No. 22-20(2) [17].

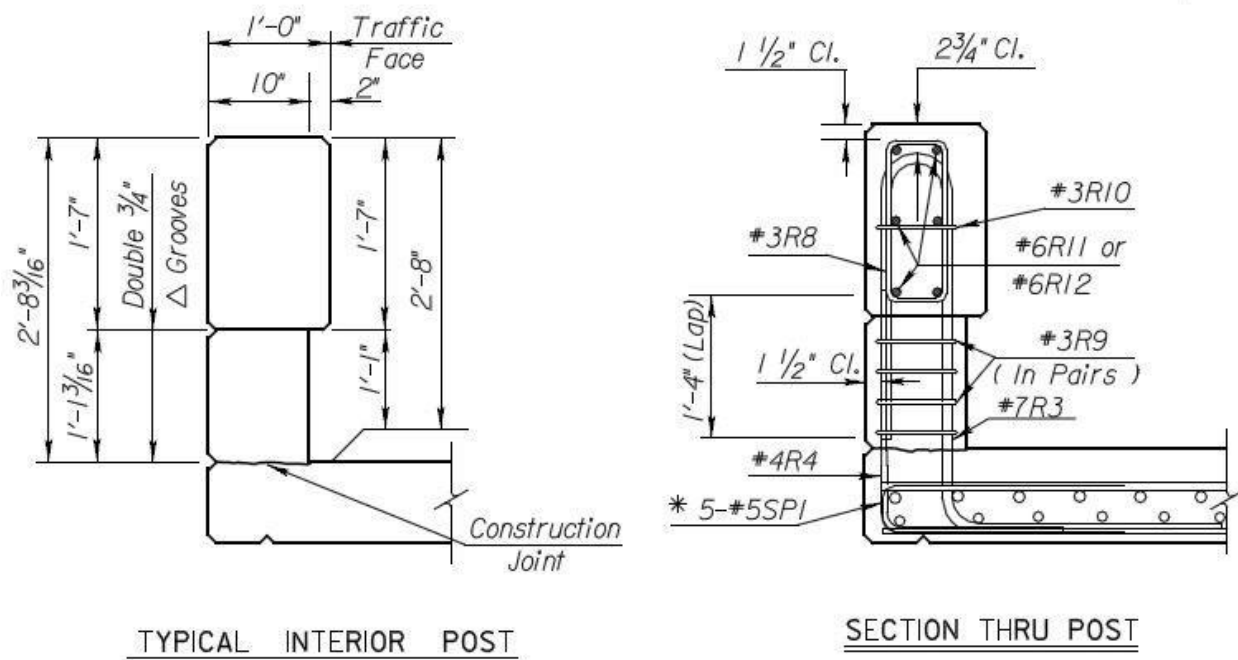


Figure 114. 32-in. Tall Kansas Corral Rail Without Curb [7]

### Yield-Line Theory Strength Calculations for 32-in. Corral Rail

Evaluating the 32-in. tall Kansas Corral Rail without a curb by the yield line method, the critical length of failure,  $L$ , calculated from Equation 2 is:

$$L = \frac{l}{2} + \sqrt{\left(\frac{l}{2}\right)^2 + \frac{8H\phi M_b}{\phi M_c} - \frac{Gl}{2}}$$

Where:

$$l = 42 \text{ in.}$$

$$H = 32 \text{ in.}$$

$$\phi M_b = 68.2 \text{ kip-ft}$$

$$\phi M_c = 49.8 \text{ kip-ft/ft}$$

$$G = 84 \text{ in.}$$

$$L = \frac{42/12}{2} + \sqrt{\left(\frac{42/12}{2}\right)^2 + \frac{8(32)(68.2)}{(49.8)} - \frac{(84*42)/144}{2}} = 6.2 \text{ ft} = 74.7 \text{ in.}$$

With  $L < G$ , the post strength term is excluded from barrier strength calculations, and the capacity of the bridge rail  $wu$ , calculated from Equation 1 at a 32-in. height is:

$$wu = \frac{8\phi M_b}{(L-\frac{l}{2})} + \frac{\phi M_c L(L-G)}{H(L-\frac{l}{2})} = \frac{8(68.2*12)}{(76.6-\frac{42}{2})} + 0 = 124.5 \text{ kips}$$

If the barrier resistance is modified by  $\left(\frac{H}{H_e}\right)$ , where  $H_e = 30$  in., the resistance of the barrier  $wu$  becomes 132.8 kips.

### AASHTO Post and Beam Method Calculations for 32-in. Corral Rail

Evaluating the 27-in. tall Kansas Corral Rail without a curb by the AASHTO Post and Beam Method, the capacity of the bridge rail,  $R$ , calculated at a 22½-in. height is:

$$R = \frac{16\phi M_p + (N-1)(N+1)P_p L}{2NL - L_t} \text{ for odd } N, \quad R = \frac{16\phi M_p + N^2 P_p L}{2NL - L_t} \text{ for even } N$$

Where:

$$\phi M_p = 68.2 \text{ kip-ft}$$

$$\phi M_{post} = 149.5 \text{ kip-ft}$$

$$\bar{Y} = 22\frac{1}{2} \text{ in.}$$

$$P_p = \frac{\phi M_{post}}{\bar{Y}} = \frac{149.5}{22.5/12} = 79.7 \text{ kip}$$

$$L = 120 \text{ in.}$$

$$L_t = 42 \text{ in. [14]}$$

$$\text{For } N=1, R = \frac{16(68.2*12) + (1-1)(1+1)(79.7*120)}{2(1*120) - 42} = 68.2 \text{ kips}$$

$$\text{For } N=2, R = \frac{16(68.2*12) + 2^2(79.7*120)}{2(2*120) - 42} = 118.9 \text{ kips}$$

$$\text{For } N=3, R = \frac{16(68.2*12) + (3-1)(3+1)(79.7*120)}{2(3*120) - 42} = 133.4 \text{ kip}$$

If the barrier resistance is modified by  $\left(\frac{\bar{Y}}{H_e}\right)$ , where  $H_e = 30$  in.

$$\text{For } N=1, R = 68.2 \text{ kips}$$

$$\text{For } N=2, R = 101.1 \text{ kips}$$

$$\text{For } N=3, R = 113.4 \text{ kips}$$

The capacity with and without the effective height consideration was determined to be 68.2 kips, with a single-span failure mechanism, as capacities continue to increase for increasing values of  $N$ .

### Modified AASHTO Post and Beam Method Calculations for 32-in. Corral Rail

Evaluating the 27-in. tall Kansas Corral Rail without a curb by the Modified AASHTO Post and Beam Method, the bridge rail capacity,  $R$ , calculated at a 25-in. height is:

$$R = \left( \frac{16\phi M_p + 2P_p(PF)(NL - L_{post})}{2(NL - L_{post}) - L_t} \right) \left( \frac{\bar{Y}}{H_e} \right)$$

Where:

$$M_p = 68.2 \text{ kip-ft}$$

$$M_{post} = 149.5 \text{ kip-ft}$$

$$\bar{Y} = 22\frac{1}{2} \text{ in.}$$

$$P_p = \frac{\phi M_{post}}{\bar{Y}} = \frac{149.5}{22.5/12} = 79.7 \text{ kip}$$

$$L = 120 \text{ in.}$$

$$L_t = 42 \text{ in. [14]}$$

$$L_{post} = 36 \text{ in.}$$

$$H_e = 25 \text{ in. [17]}$$

For  $N = 1$  and  $PF = 0$ :

$$R = \left( \frac{16M_p + 2P_p(PF)(NL - L_{post})}{2(NL - L_{post}) - L_t} \right) = \left( \frac{16(68.2 \cdot 12) + 2(79.7)(0)(1(120) - 36)}{2((1 \cdot 120) - 36) - 42} \right)$$

$$= 109.1 \text{ kips}$$

For  $N = 2$  and  $PF = 1$ :

$$R = \left( \frac{16M_p + 2P_p(PF)(NL - L_{post})}{2(NL - L_{post}) - L_t} \right) \left( \frac{\bar{Y}}{H_e} \right) = \left( \frac{16(68.2 \cdot 12) + 2(79.7)(1)(2(120) - 36)}{2((2 \cdot 120) - 36) - 42} \right) \left( \frac{22.5}{25} \right)$$

$$= 112.2 \text{ kips}$$

For  $N = 3$  and  $PF = 1.333$ :

$$R = \left( \frac{16M_p + 2P_p(PF)(NL - L_{post})}{2(NL - L_{post}) - L_t} \right) \left( \frac{\bar{Y}}{H_e} \right) = \left( \frac{16(68.2 \cdot 12) + 2(79.7)(3)(1.333(120) - 36)}{2((3 \cdot 120) - 36) - 42} \right) \left( \frac{22.5}{25} \right)$$

$$= 121.7 \text{ kips}$$

Because the capacity of the bridge rail continued to increase for increasing values of  $N$ , the capacity was determined to be 109.1 kips, with a single-span failure mechanism.



These analyses showed that critical length of failure did not exceed the span length, and both the original and Modified AASHTO Post and Beam method determined a single-span failure mechanism. Therefore, the bridge rail was determined to be unaffected by discontinuities in the rail at the partial expansion gap location.

### 5.4 Summary

Lateral structural capacities of the 27-in. and 32-in. tall corral rails are shown in Table 17. The 32-in. tall corral rail was stronger than the 27-in. tall variant by all five evaluation methods. The AASHTO Post and Beam Method resulted in the lowest capacities, but the subtraction of the post length from strength calculations in the Modified AASHTO Post and Beam Method resulted in increased capacity. The effective load height resistance scaling applied to Yield-Line Theory calculations resulted in increased capacities for both corral rail variants. The effective load height resistance scaling applied to the AASHTO Post and Beam Method resulted in decreased capacities for both corral rail variants for failure mechanisms of two or more spans. The Modified AASHTO Post and Beam Method is believed to provide the most accurate determination of the capacity of the bridge rail due to the assumption that the failure mechanism develops adjacent to the posts. The Modified AASHTO Post and Beam Method also allows for analysis of scenarios involving multiple failing spans, as well as load application at a post, unlike Yield-Line Theory. Additionally, use of the Modified AASHTO Post and Beam Method is more conservative than the use of Yield-Line Theory in cases where the critical length of failure determined from Yield-Line Theory is shorter than the span length minus the post length. Therefore, the Modified AASHTO Post and Beam Method was the preferred method.

Table 17. 27-in. and 32-in. Corral Rail, Capacities and Failure Mechanisms

Design Methodology	27-in. Kansas Corral Rail			32-in. Kansas Corral Rail		
	Capacity kips	Number of Failing Spans	Length of Failure in.	Capacity kips	Number of Failing Spans	Length of Failure in.
Yield-Line Theory	140.4	N/A	65.0	124.5	N/A	74.7
Yield Line-Theory at $H_e$	154.9	N/A	65.0	132.8	N/A	74.7
AASHTO Post and Beam Method	60	1	N/A	68.2	1	N/A
AASHTO Post and Beam Method at $H_e$	60	1	N/A	68.2	1	N/A
Modified AASHTO Post and Beam Method	96	1	N//A	109.1	1	N//A

N/A – Not Applicable

## 6 BARRIER DESIGN

### 6.1 Overview

The design criteria discussed in Chapter 3, which were based on sponsor feedback, were utilized to design the new MASH TL-4 open concrete bridge rail. The design criteria used throughout the barrier design process included a 4-in. post setback, 12-in. tall vertical opening, a 2-in. offset from the rear of the posts to the edge of the bridge deck, a 16-in. wide footprint, No. 5 and No. 6 rebar for longitudinal beam reinforcement and vertical post reinforcement, and No. 4 rebar for post and beam stirrups. From these criteria, several designs were explored with varying post lengths, gap lengths, and reinforcement configurations. The Modified AASHTO Post and Beam Method was utilized to determine the capacity of the designs, as assumptions with this method align with damage seen in full-scale crash tests, and that capacity is calculated at the effective load application height. The validity of this method will be explored further after future full-scale crash testing efforts. Variants measuring 36 in. and 39 in. tall were designed, and the 39-in. tall system was determined to be the critical configuration for full-scale crash testing. The 36-in. tall variant was designed to resist a 72.3-kip load applied at an effective height of 25 in. above the surface of the bridge deck, and the 39-in. tall variant was designed to resist a 72.3-kip load applied at an effective height of 30 in. above the surface of the bridge deck. When calculating moment capacities of rail and post elements, a strength reduction factor of 0.9 was applied throughout the design process.

### 6.2 Initial Configurations

The initial configuration consisted of a 39-in. tall bridge rail with a 12-in. tall vertical opening and 4-in. post setback. The system incorporated a 27-in. tall by 16-in. wide rail on 10-in. wide posts, as shown in Figure 115. The post was offset 2 in. from the edge of the bridge deck, and the rail extended 2 in. over the rear side of the posts to increase rail bending strength. The overall system width was 16 in. Reinforcement consisted of longitudinal and vertical No. 5 and No. 6 rebar in the rail and post, and No. 4 stirrups in the rail and post.

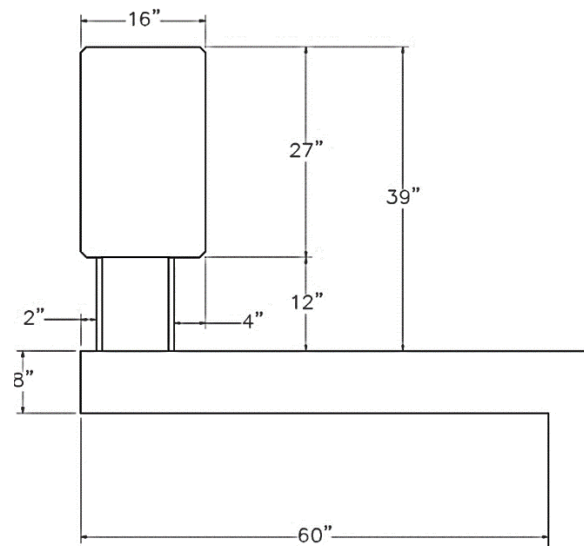


Figure 115. New MASH TL-4 Open Concrete Rail-Initial Configuration

### 6.2.1 Initial Configuration 1

From the initial geometry, two options were designed and proposed to the project sponsors. The first option consisted of a 27-in. tall by 16-in. wide rail atop 12-in. tall by 10-in. wide by 24-in. long posts spaced at 96 in. on center, as shown in Figures 116 and 117. Post reinforcement consisted of ten No. 5 rebars, 5 each on the front and back faces, longitudinally spaced at  $4\frac{5}{16}$  in. Rail reinforcement consisted of ten No. 6 rebars, 5 each on the front and back faces, vertically spaced at  $5\frac{1}{16}$  in. Shear reinforcement consisted of four No. 4 stirrups vertically spaced at 3 in. in the post, and No. 4 stirrups spaced at 12 in. throughout the rail. Shear reinforcement spacings were preliminarily selected to be similar to previous open concrete bridge rail designs. The rail moment capacity was 127.0 kip-ft, and the post moment capacity was 51.3 kip-ft. Rail shear capacity was calculated to be 120.6 kips for a single span length, and post shear capacity was calculated to be 101.0 kips. Utilization of the Modified AASHTO Post and Beam Method determined the total capacity of the bridge rail to be 75.2 kips with a 3-span failure mechanism, exceeding the design load of 72.3 kips. Full calculations are provided in a thesis written by DeLone [38].

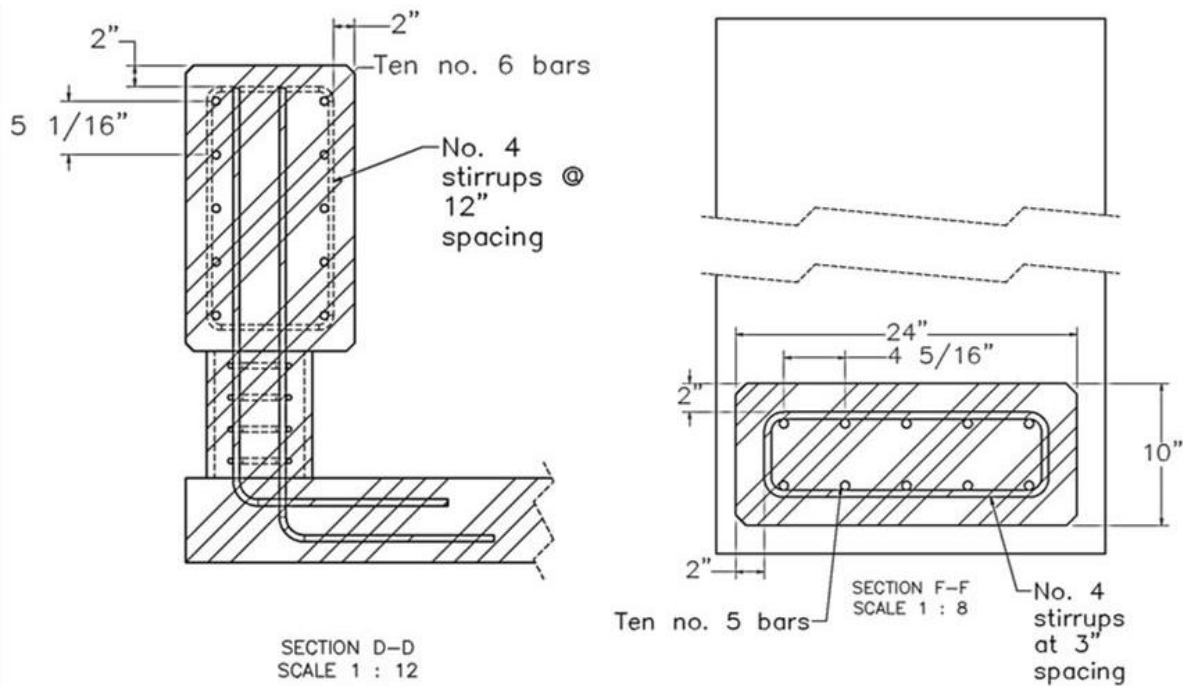


Figure 116. Initial Configuration 1, Reinforcement Details

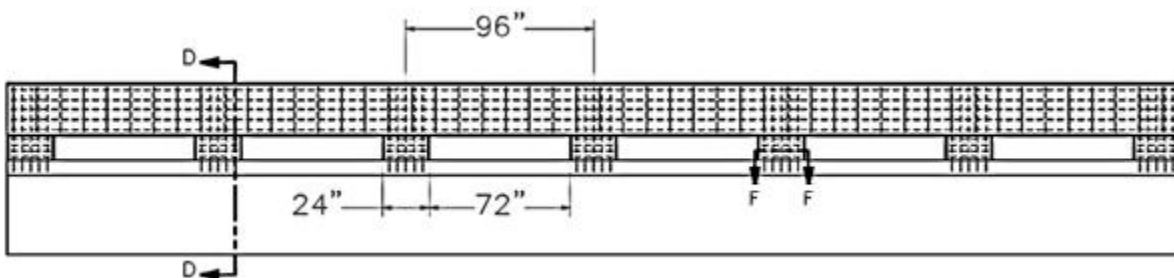


Figure 117. Initial Configuration 1, Elevation View

### 6.2.2 Initial Configuration 2

The second option consisted of a 27-in. tall by 16-in. wide rail atop 12-in. tall by 10-in. wide by 36-in. long posts spaced at 108 in. on center, as shown in Figures 118 and 119. Post reinforcement consisted of 12 No. 5 rebars, six each on the front and back faces, longitudinally spaced at  $6\frac{3}{4}$  in. Rail reinforcement consisted of eight No. 6 rebars, four each on the front and back faces, vertically spaced at  $5\frac{7}{8}$  in. Shear reinforcement consisted of four No. 4 stirrups vertically spaced at 3 in. in the post, and No. 4 stirrups spaced at 12 in. throughout the rail. Shear reinforcement spacings were preliminarily selected to be similar to previous open concrete bridge rail designs. The rail moment capacity was 105.5 kip-ft, and the post moment capacity was 66.0 kip-ft. Rail shear capacity was calculated to be 130.3 kips for a single span length, and post shear capacity was calculated to be 109.2 kips. Utilization of the Modified AASHTO Post and Beam Method determined the total capacity of the bridge rail to be 72.7 kips, with a 3-span failure mechanism, exceeding the design load of 72.3 kips. Full calculations are provided in a thesis written by DeLone [38].

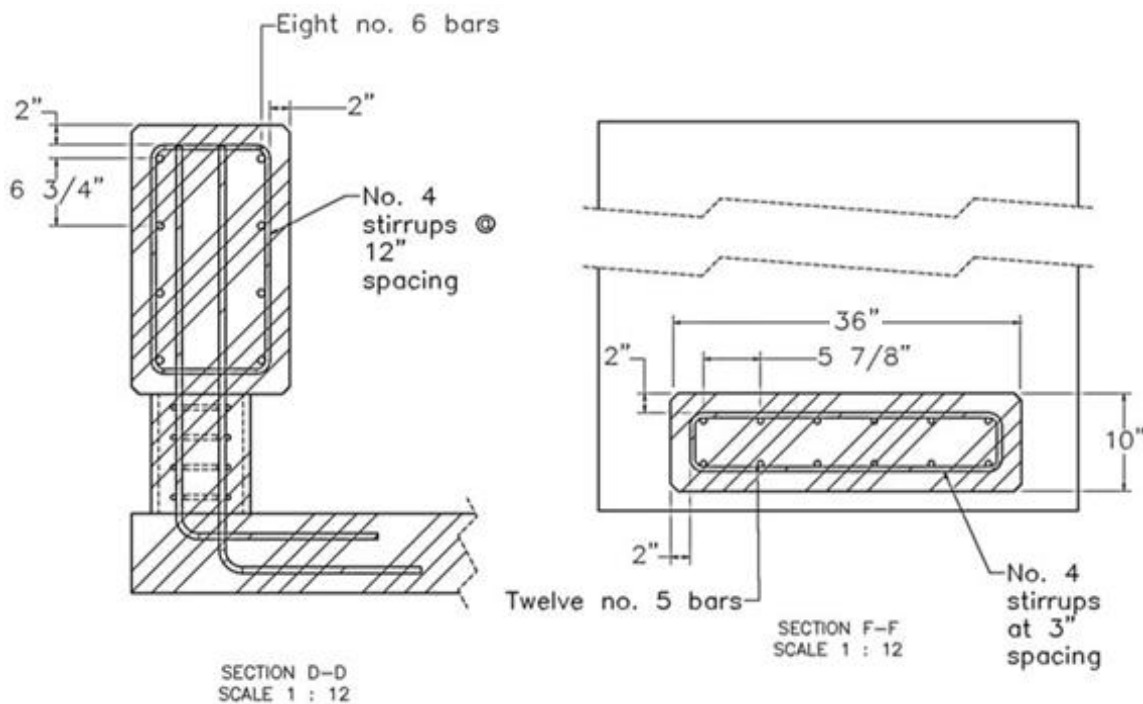


Figure 118. Initial Configuration 2, Reinforcement Details

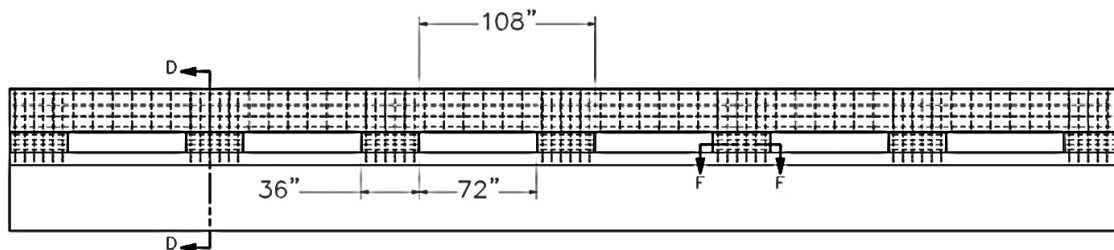


Figure 119. Initial Configuration 2, Elevation View

### 6.3 Final Design

Initial configuration 2 was selected as the basis for the final design. It offered more equalized post and beam moment strengths, with longer posts to provide a longer distribution length to the deck. The geometry and steel reinforcement of this configuration were modified throughout the design process to optimize the final configuration for strength, constructability, weight, footprint, and aesthetics. The final design consisted of a 27-in. tall by 14-in. wide beam supported by 12-in. tall by 10-in. wide by 36-in. long posts, as shown in Figures 120 through 122. The width of the beam was reduced from 16 in. to 14 in. after it was determined that extending the width of the beam past the rear face of the post would align the vertical post reinforcement and beam reinforcement. Post length in the interior section of the bridge rail was 36 in., and posts were separated by 72-in. long gaps. Thirty-six reinforcement configurations for the interior section were analyzed by varying combinations of No. 5 and No. 6 bars. For the interior region, groups of 8, 10, 12, and 14 bars in both the post and beam were considered. Configurations exceeding 7 bars on the front and back faces of the post and beam resulted in bar spacings that were believed to be too close for concrete aggregate to fill in the spaces, thus resulting in the potential for internal voids in the post and beam. Beam longitudinal reinforcement consisted of eight No. 6 rebars, four each on the front and back faces, vertically spaced at 6½ in. Post vertical reinforcement consisted of 12 No. 5 bars, six on each face of the post, spaced laterally at 6 in. Post shear reinforcement consisted of three No. 4 stirrups vertically spaced at 3 in. in the post, and No. 4 stirrups spaced at 12 in. throughout the beam. The beam moment capacity was 86.9 kip-ft, and the post moment capacity was 74.4 kip-ft. The beam shear capacity was calculated to be 110.4 kips for a single span, and post shear capacity was calculated to be 88.1 kips. This configuration was believed to provide sufficient space for concrete aggregate to fill spaces between post and rail reinforcement. Utilization of the Modified AASHTO Post and Beam Method determined the capacity of the interior section of the bridge rail to be 72.6 kips at a load application height of 30 in., with a 3-span failure mechanism, exceeding the design load of 72.3 kips at a load application height of  $\bar{Y} = 25\frac{1}{2}$  in. Full calculations are provided in a thesis written by DeLone [38].

After design of the interior section was finalized, the end section design was completed. Post length in the end section was 72 in. long, and posts were separated by a 72-in. long gap. The length of the end post was selected to be 72 in. to ensure the end section capacity was greater than the interior section capacity and that the entire post capacity could be transferred and distributed to the deck without significant deck damage occurring. End section beam longitudinal reinforcement consisted of 14 No. 6 bars, seven on each face, vertically spaced at 3¼ in. This configuration was created by adding additional longitudinal reinforcement to the beam at the midpoints between the eight longitudinal bars from the interior section configuration. End section post vertical reinforcement consisted of 28 No. 5 bars, 14 on each face, longitudinally spaced at 5 in. The beam moment capacity was 141.5 kip-ft, and the post moment capacity was 162.9 kip-ft. Utilization of the Modified AASHTO Post and Beam Method determined the capacity of the end section of the bridge rail to be 74.4 kips at a load application height of 30 in., with a 1-span failure mechanism, exceeding the design load of 72.3 kips at a load application height of  $\bar{Y} = 25\frac{1}{2}$  in. It is recommended that the final barrier design be full-scale crash tested, and that the failure mechanisms in the test and capacity prediction methods be compared.

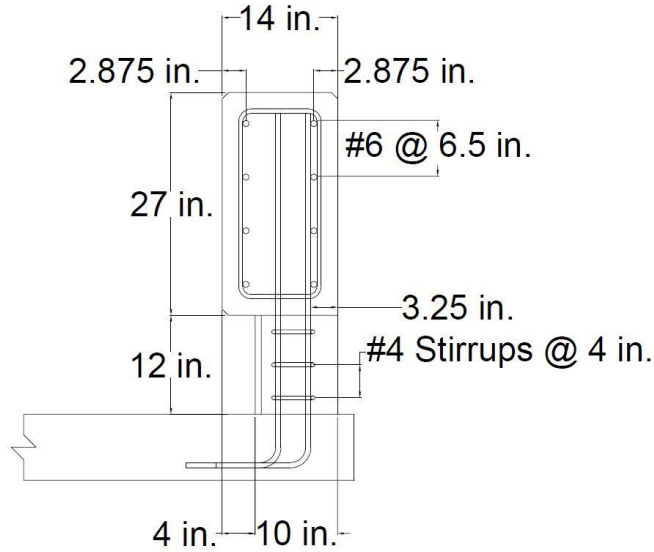


Figure 120. New Open Concrete Bridge Rail Interior Section, Cross Section

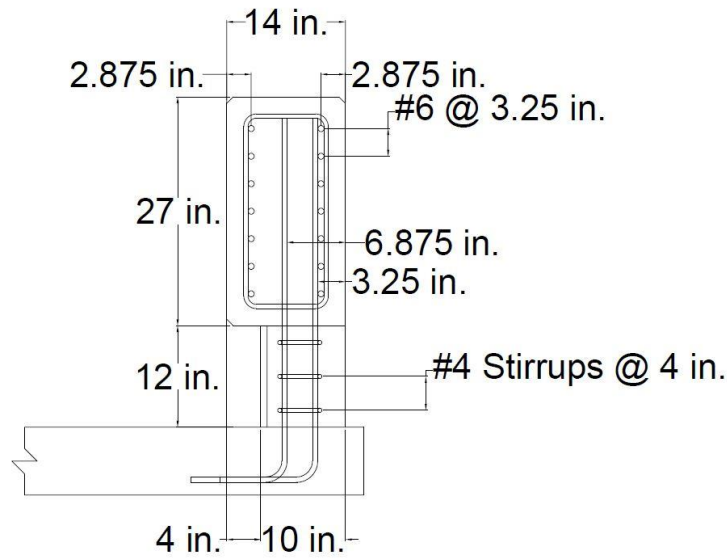


Figure 121. New Open Concrete Bridge Rail End Section, Cross Section

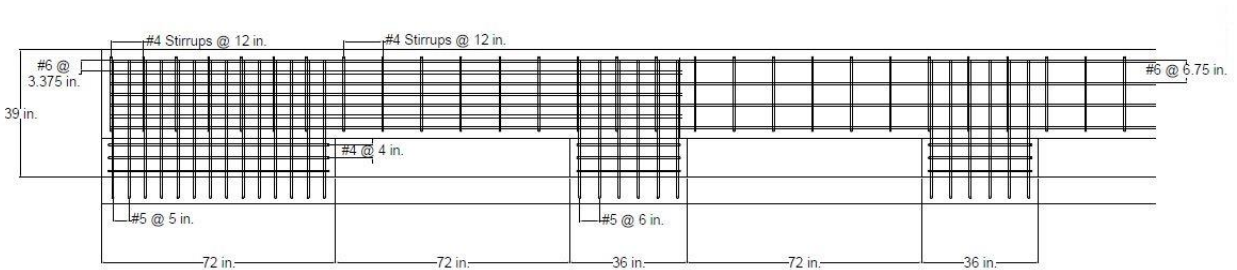


Figure 122. New Open Concrete Bridge Rail End and Interior Section, Elevation View

### 6.4 36-in. Tall Configuration

For transportation agencies that mill the existing wearing surface before applying a new wearing surfacing, the 39-in. configuration would not be necessary to install. Thus, an option for only a 36-in. barrier was configured. There are two possible options: (1) maintaining a 12-in. vertical opening beneath the rail, or (2) maintaining a 9-in. vertical opening beneath the rail, as is the case when a 3-in. overlay is applied to the 39-in. tall barrier. The option with the 12-in. vertical opening is discussed below.

A 36-in. tall configuration of the open concrete bridge rail was developed in addition to the 39-in. tall open concrete bridge rail, as some of the sponsors will utilize the bridge rail without the inclusion of a 3-in. thick asphalt overlay. The 36-in. tall configuration consisted of a 24-in. tall by 14-in. wide rail supported by 12-in. tall by 10-in. wide posts, as shown in Figures 123 through 125. Posts in the interior section of the bridge rail were 36 in. long and posts were separated by 72-in. long gaps. Longitudinal and vertical reinforcement in the rail and posts was not altered, as the 3-in. reduction in height resulted in a higher capacity due to the  $P_p$  value being calculated with a smaller  $\bar{Y}$  value. Interior section capacity was determined to be 82.5 kips at an effective height of 25 in. with a 3-span failure mechanism by use of the Modified AASHTO Post and Beam Method, and the end section capacity was determined to be 85.3 kips at an effective height of 25 in. with a 1-span failure mechanism, both of which exceeded the design load of 70.0 kips.

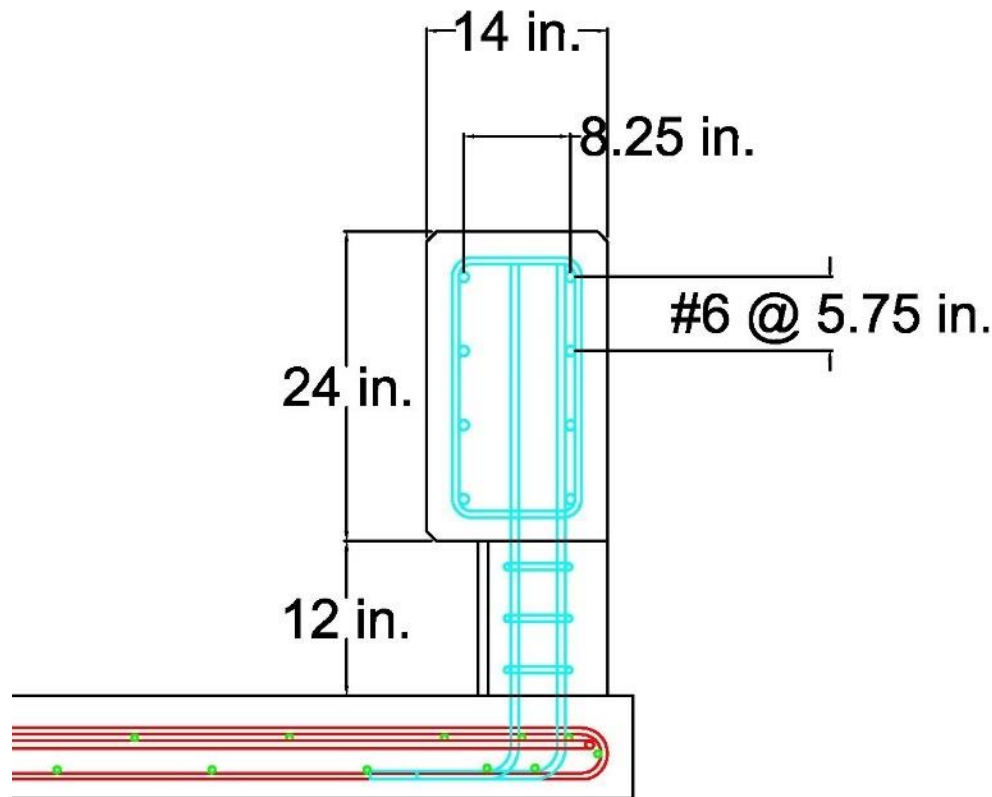


Figure 123. 36-in. Open Concrete Bridge Rail Interior Section, Cross Section

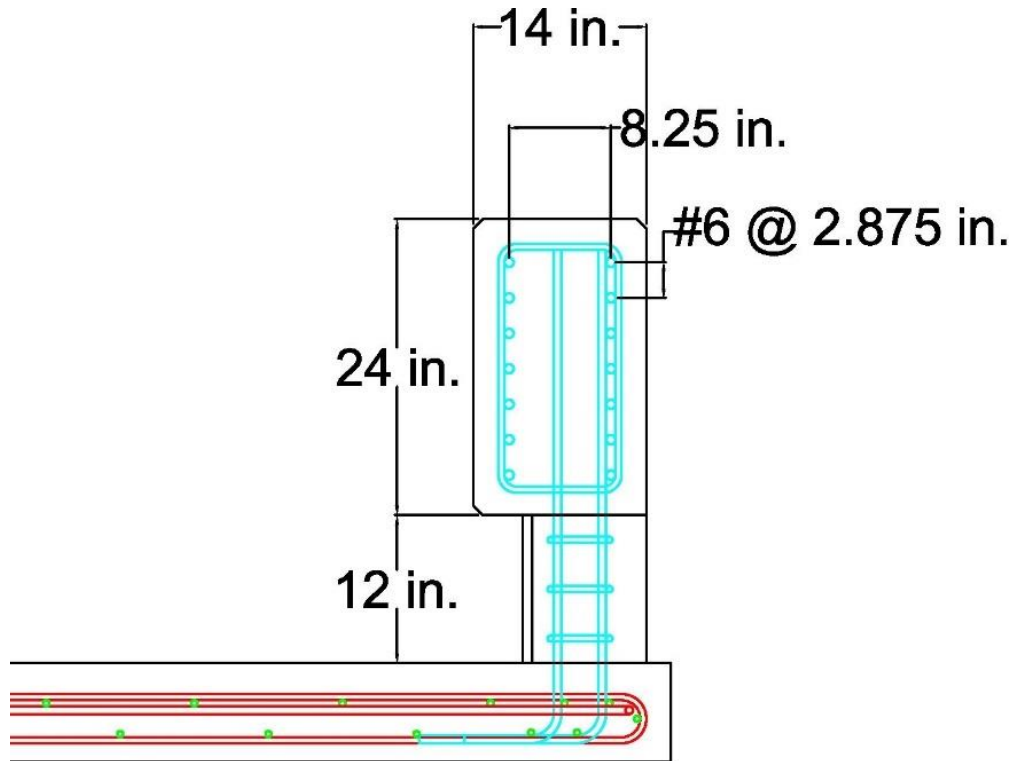


Figure 124. 36-in. Open Concrete Bridge Rail End Section, Cross Section

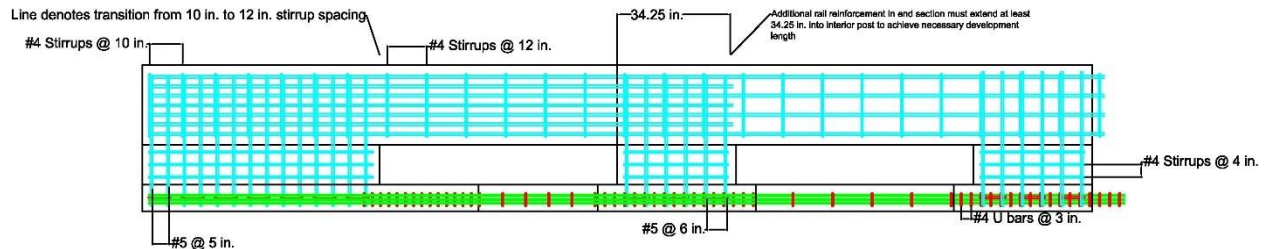


Figure 125. 36-in. Open Concrete Bridge Rail End and Interior Section, Elevation View

## 6.5 Comparison to Similar Systems

The final design of the new MASH TL-4 open concrete bridge rail was compared to similar, previously developed bridge rails, as shown in Table 18. Comparisons were conducted to determine how the strength and weight of the new open concrete bridge rail compared to similar bridge rail systems. The capacities of similar systems were estimated by calculating the rail and post moment strengths and utilizing the Modified AASHTO Post and Beam Method. Additionally, the concrete weight, steel weight, and total system weight were determined and compared to the final design. Note that the MwRSF optimized single-slope bridge rail was a closed, single-slope parapet and was included in comparisons because it is a recently developed MASH TL-4 bridge rail [19-20]. This bridge rail did not incorporate posts like the open concrete bridge rails, so the Modified AASHTO Inelastic Method could not be utilized, and its capacity was determined using Yield-Line Theory.



The new MASH TL-4 open concrete bridge rail was heavier than all but the California Type 85 bridge rail. The large weight of the new bridge rail was attributed to the increased size of the rail over previous systems due to the increased MASH TL-4 strength demands and the increased overall bridge rail height. Although the concrete weight is significant, the steel weight per linear foot of bridge rail is less than all other MASH open concrete bridge rails. The new open concrete bridge rail has the lowest capacity of any of the MASH systems, but still exceeded the selected design load of 72.3 kips determined in NCHRP Report No. 22-20(2) [17]. Although the Modified Post and Beam method provided a more conservative estimate of capacity compared to Yield-Line Theory, it was less conservative than the original Post and Beam method. The capacity and damage to the new bridge rail will be further evaluated through full-scale crash testing.

The 36-in. and 39-in. tall open concrete bridge rails were similar to the 27-in. and 32-in. tall Kansas Corral Rails in that they consisted of 36-in. long posts spaced at 108 in. on center and incorporated a 12-in. tall vertical opening and 4-in. wide post setback. The 27-in. and 32-in. tall Kansas Corral Rails incorporated 36-in. long posts spaced at 120 in. on center, a 13-in. tall vertical opening, and a 2-in. wide post setback. The new open concrete bridge rails had different post, rail, and overall capacities from the original Kansas Corral Rails. The rail moment capacities of the new open concrete bridge rails were less than that of the 27-in. and 32-in. tall Kansas Corral Rails, and the post moment capacity of the new open concrete bridge rail was greater than that of the 27-in. and 32-in. tall Kansas Corral Rails. This resulted in the new 36-in. and 39-in. tall configurations having capacities of 72.6 kips and 81.2 kips respectively, each with a three-span failure mechanism. The 27-in. and 32-in. tall Kansas Corral Rails had capacities of 80 kips and 77.3 kips respectively, each with a single span failure mechanism. The total system weights of the new configurations were much greater than the 27-in. and 32-in. tall Kansas Corral Rails due to the larger rail in the new configurations.

Table 18. Similar Concrete Bridge Rail System Comparisons

System Description	Height in.	Test Criteria	Rail Moment Capacity kip-ft	Post Moment Capacity kip-ft	Failing Spans	System Capacity kips	Concrete Weight lb/ft	Steel Weight lb/ft	Total Weight lb/ft
New Rail: 39-in. Tall Final Design	39	MASH TL-4	86.9	74.4	3	72.6	435.4	13.7	449.1
New Rail: 36-in. Tall Final Design	36	MASH TL-4	86.9	74.4	3	81.2	421.5	13.7	435.2
CA Type 85	42	MASH TL-4	66.3	122.7	1	81.7	477.9	35.8	513.7
MwRSF Optimized Single Slope	39	MASH TL-4	84.8	N/A	N/A	74.3	365.6	13.0	378.6
NDOT Open Rail	29	AASHTO GSR PL-2	52.5	67.2	3	55.7	270.6	7.5	278.1
27-in. Tall KDOT Corral Rail	27	NCHRP 350 TL-4	60.0	137.8	1	80	215.6	12.8	228.4
32-in. Tall KDOT Corral Rail	32	AASHTO GSR PL-2	67.6	137.8	1	77.3	278.1	12.8	291
NDOT Aesthetic Rail	42	NCHRP 350 TL-5	102.4	100.7	3	102.7	412.2	14.8	427.0
TxDOT T203	27	NCHRP 350 TL-3	48.3	155.9	1	85.9	247.7	9.3	257.0
TxDOT T223	32	MASH TL-3	73.6	82.8	3	70.9	358.2	10.4	368.6
TxDOT T224	42	MASH TL-5	126.5	136.5	3	121.3	570.7	16.5	587.2

NA – No post moment capacity as this was a continuous parapet.

## 6.6 Summary

Utilizing the Modified AASHTO Post and Beam Method, two new open concrete bridge rails 36 in. and 39 in. in height were designed to resist MASH TL-4 impact loads. The 36-in. tall bridge rail had a capacity of 81.2 kips and a 3-span failure mechanism at a load application height of 25 in. in the interior section, and end section capacity was determined to be 83.2 kips. with a 1-span failure mechanism, both of which exceeded the design load of 72.3 kips. The 39-in. tall bridge rail had a capacity of 72.6 kips and a 3-span failure mechanism at a load application height of 30 in. in the interior section, and end section capacity was determined to be 74.4 kips at a load application height of 30 in., with a 1-span failure mechanism, both of which exceeded the design load of 72.3 kips. Comparisons of the new configurations to similar concrete bridge rails determined the weight of the new configurations to be greater than older systems, which can be attributed to the required height increase.

## 7 DECK DESIGN

### 7.1 Design Loads and Minimum Steel Required

Bridge deck overhang design was conducted by determining the required area of steel necessary to resist combined tensile and moment loads imparted on the bridge deck for the three design cases (horizontal impact load, vertical impact load, and live load, as shown in Table 13), as well as the dead loads of the barrier, bridge deck, and wearing surface for the interior and end regions of the bridge rail. The bridge deck overhang was 60 in. wide by 8 in. thick. Design section 1 was at the face of the bridge rail post, and design section 2 was located at the beginning of the overhang. Loads were assumed to distribute at a 30-degree angle beginning at the back of the posts, as discussed in Chapter 4, and shown in Figures 126 and 127. *AASHTO LRFD Bridge Design Specifications* specify that load modification factors can be applied to the impact and dead loads for the Strength I and Extreme Event limit states [14], as was summarized in Table 14. Dead load modification factors have a permissible range used to decrease or increase the magnitude of the dead loads. Because the use of this factor is at the discretion of the designer, load modification factors were not utilized for design cases 1 and 2 but were utilized in design case 3, which was anticipated to produce the smallest loads. Multiple presence factors and dynamic load allowance were not considered for any design case.

Strength reduction factors of 0.75 for shear and 0.9 for flexural capacities of the bridge deck configurations were utilized throughout the design process. Although not considered in this design process, the designer may wish to calculate vertical punching shear capacity of the bridge deck at post locations. The calculated design moments and tensile loads acting in the interior and end post regions is shown in Table 19. Details of these calculations can be found in a thesis written by DeLone [38].

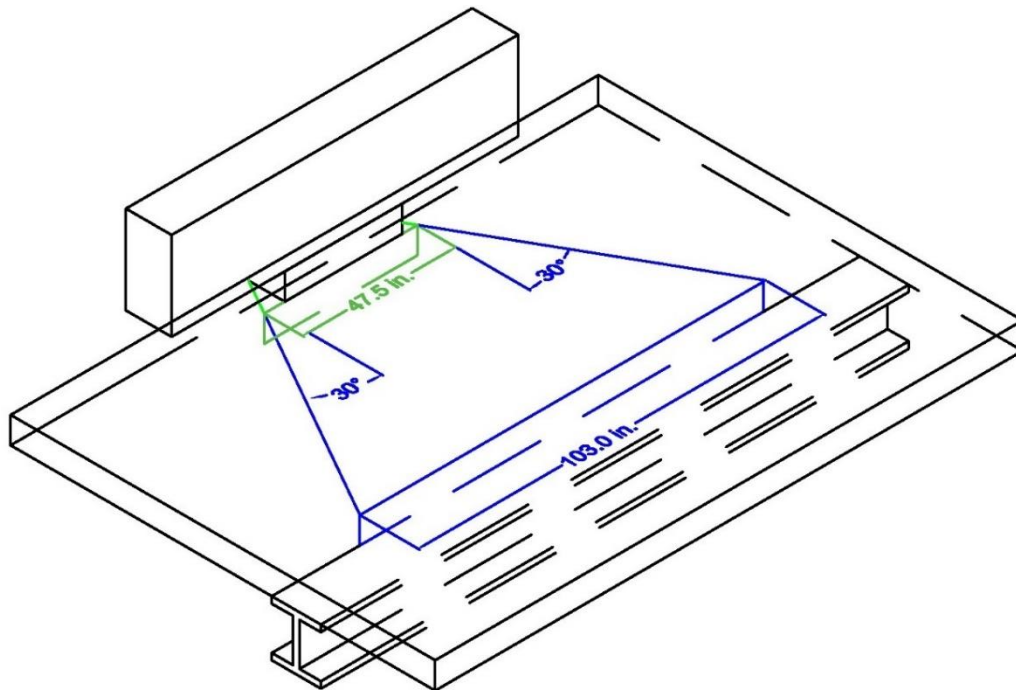


Figure 126. Design Section Lengths at Interior Posts

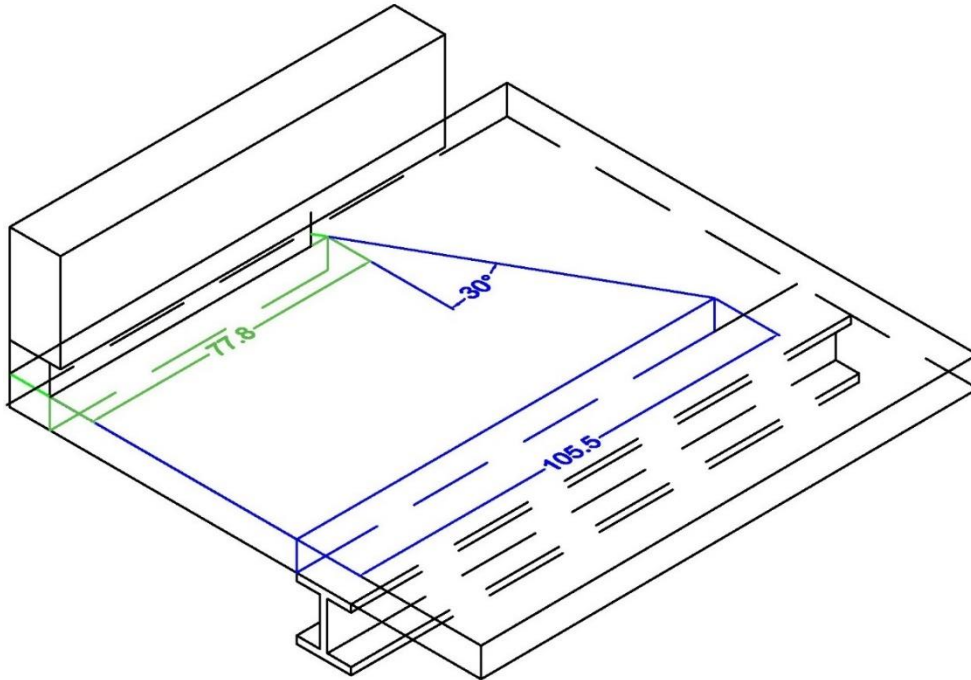


Figure 127. End Post Design Section Lengths

The area of steel required to resist the tensile load acting in the design sections was determined by dividing the kip/ft tensile load by the yield strength of the steel reinforcement, which was 60 ksi. This resulted in the required area of steel reinforcement per length of the design section in units of  $\text{in.}^2/\text{ft}$ . The area of steel required to resist the moment load acting in the design sections was determined by multiplying the kip-ft/ft load by the length of the design section, resulting in the required moment in kip-ft. Depths of steel reinforcement layers were then selected. The minimum area of steel required to resist the moment in the design section could then be determined assuming tension-controlled failure, and balancing the moments produced by the concrete and steel reinforcement about the neutral axis of the bridge deck. The required area of steel was then divided by the length of the design section, resulting in the required area of steel reinforcement per length of the design section in units of  $\text{in.}^2/\text{ft}$ . The required area of steel for the tensile and moment loads was then added together, resulting in the required area of steel for the design section, as summarized in Table 20. Design section 1 for interior and end sections was the controlling case for both sections, requiring  $2.1 \text{ in.}^2/\text{ft}$  and  $2.5 \text{ in.}^2/\text{ft}$  respectively.

Table 19. Interior and End Section Tensile and Moment Loads

Barrier Section	Design Section	Load	Design Case 1	Design Case 2	Design Case 3
Interior Section	Section 1	Moment kip-ft/ft	19.6	2.3	N/A
		Tension kips/ft	7.6	N/A	N/A
	Section 2	Moment kip-ft/ft	12.1	12.3	8.4
		Tension kips/ft	3.5	N/A	N/A
End Section	Section 1	Moment kip-ft/ft	25.4	1.9	N/A
		Tension kips/ft	11.8	N/A	N/A
	Section 2	Moment kip-ft/ft	22.3	11.5	9.3
		Tension kips/ft	8.7	N/A	N/A

NA – Not applicable to the design case

Table 20. Area of Steel Requirements

Barrier Section	Design Section	Required Area of Steel in. <sup>2</sup> /ft
Interior Section	Section 1	2.1
	Section 2	0.8
End Section	Section 1	2.5
	Section 2	2.2

## 7.2 Bridge Deck Overhang Configurations

Three bridge deck overhangs were designed to provide the sponsors with multiple examples of reinforcement configurations that are compatible with the new open concrete bridge rail. Sponsors indicated that the required concrete cover measured from the surface of the bridge deck to the top layer of reinforcement was to be a minimum of 2½ in., and concrete cover measured from the bottom of the bridge deck to the lower layer of reinforcement was to be a minimum of 1½ in. Reinforcement spacings in the interior and end sections were selected such that transverse deck rebar was adjacent to the vertical post reinforcement. Additionally, hooked bars in the bridge deck were preferred due to their reduced development length requirement and reduced deck damage.

### 7.2.1 Option 1

Bridge deck overhang option 1 shown in Figures 128 through 130 consisted of No. 4 vertical U bars, and No. 5 lateral U bars that wrapped around vertical post reinforcement in design section 1 of both the interior and end section posts to satisfy the area of steel requirement in this section. Lateral U bars were included to provide additional flexural reinforcement as well as tension reinforcement. Clear cover from the top of the bridge deck to the top layer of reinforcement was 2½ in., and clear cover from the bottom of the bridge deck to the bottom layer of reinforcement was 1½ in. Lateral and longitudinal clear cover from the edge of the bridge deck to the end of the lateral and longitudinal deck reinforcement was 2 in. In design section 1 of the interior post, No. 4 vertical U bars were spaced at 3 in., as this spacing aligned with the vertical post reinforcement. Design section 1 was 47½ in. long and included 16 total No. 4 vertical U bars. Each No. 5 lateral U bar wrapped around two rows of vertical post reinforcement bars, resulting in three total No. 5 lateral U bars. The total area of steel reinforcement was 8.3 in.<sup>2</sup>, or 2.1 in.<sup>2</sup>/ft, at design section 1. In the remaining distance between design section 1 and 2 the No. 4 vertical U bars were spaced at 12 in., resulting in the inclusion of two additional No. 4 vertical bars in design section 2. This resulted in a total area of steel reinforcement of 10.1 in.<sup>2</sup>, or 1.2 in.<sup>2</sup>/ft, for design section 2. The longitudinal distance between design section 2 of the interior posts was 5 in., leaving little bridge deck area outside of the design sections. Bar spacings in all sections satisfied the ACI 318 minimum spacing requirements.

In design sections 1 and 2 of the end post, the vertical No. 4 U bars were spaced at 2½ in., as this spacing aligned with the vertical post reinforcement. End section geometry did not allow for load transfer across the expansion gap, resulting in tensile and moment loads not distributing as far as they did in the interior post region. Thus, loads remained highly concentrated in design section 2, and maintaining the 2½ in. spacing of the lateral U bars throughout both sections was required to meet moment and tensile load demands in both design sections. A total of 30 No. 4 vertical U bars were included in design section 1, and ten additional No. 4 vertical U bars were included in design section 2. Lateral No. 5 lateral U bars spaced at 10 in. and wrapped around two vertical post bars, resulting in seven total No. 5 lateral U bars in design section 1. This resulted in an area of steel in design section 1 of 16.3 in.<sup>2</sup>, or 2.5 in.<sup>2</sup>/ft, and an area of steel in design section 2 of 20.3 in.<sup>2</sup>, or 2.3 in.<sup>2</sup>/ft. The longitudinal distance between design section 2 of the end post and design section 2 of the interior post was 23 in. Because the No. 4 U bars spaced at 12 in. in design section 2 of the interior post could not be evenly spaced in the transition between the end and the adjacent interior post, No. 4 vertical U bars outside of design section 1 of the interior post were spaced at 9 in. Longitudinal bridge deck reinforcement was placed adjacent to vertical post bars to reduce the possibility of reinforcement pulling out of the concrete, and the remaining bars were spaced at 12 in. across the top and bottom mats, as was previously done in MASH TL-4 crash testing [19-20].

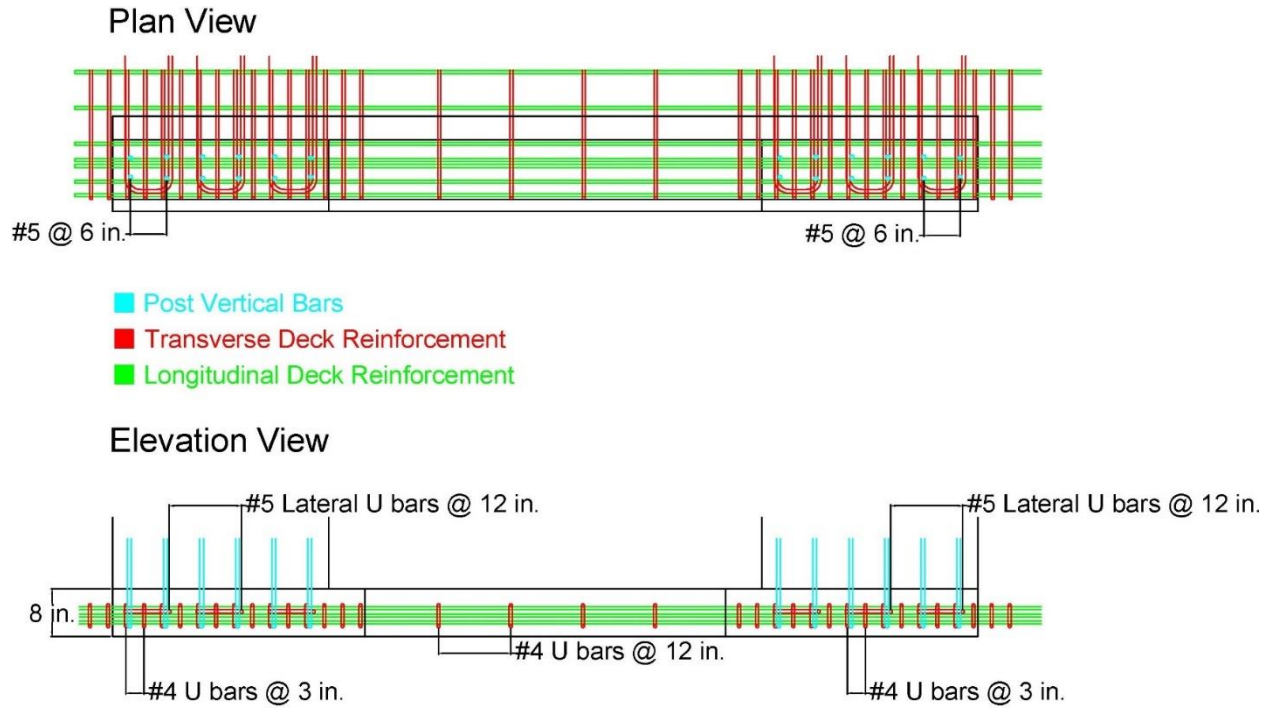


Figure 128. Option 1, Interior Post Deck Reinforcement, Plan and Elevation Views

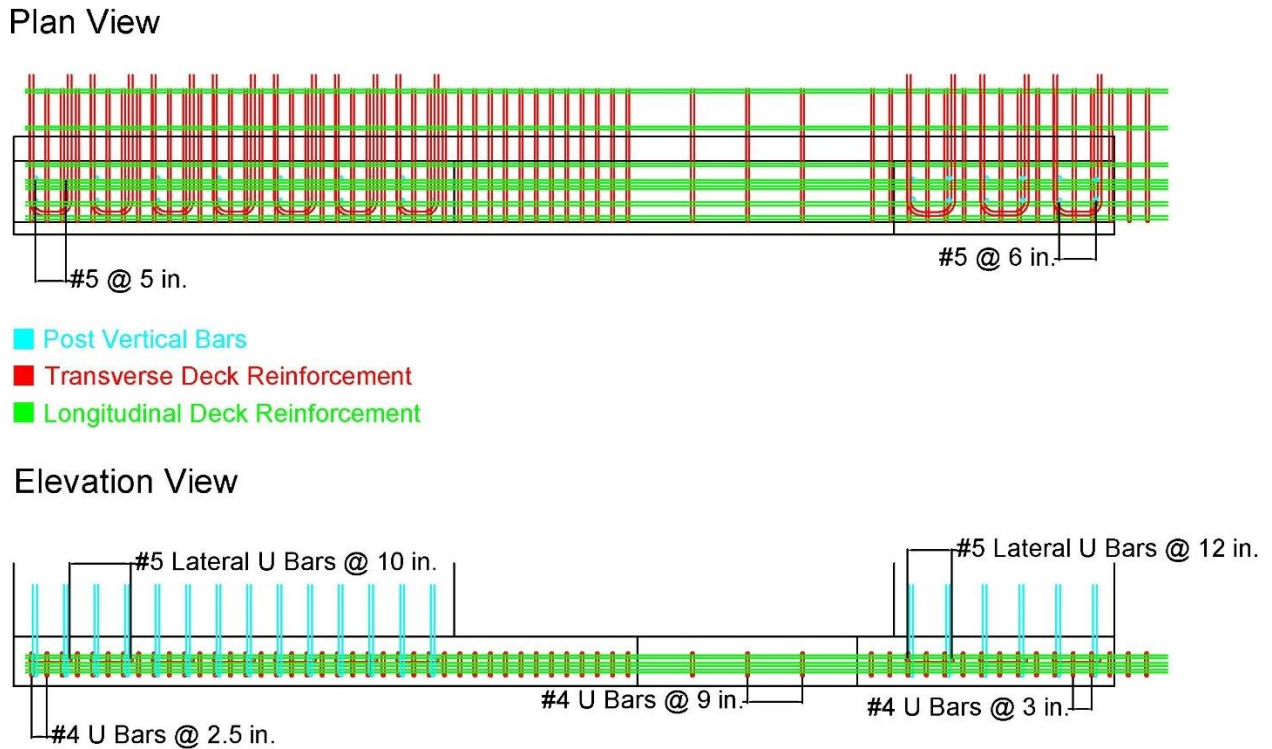


Figure 129. Option 1, End Post to Interior Post Transition Deck Reinforcement, Plan and Elevation Views



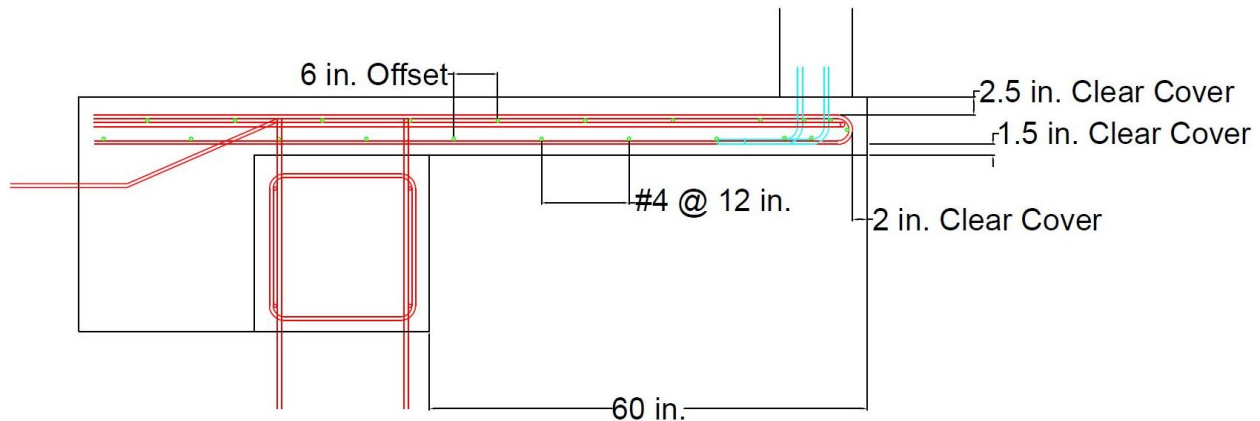


Figure 130. Option 1, Bridge Deck Overhang Cross Section

### 7.2.2 Option 2

Bridge deck overhang option 2 shown in Figures 131 through 133 consisted of a lower layer of straight No. 6 rebar and two upper layers of No. 6 horizontal U bars that wrapped around vertical post reinforcement bars. Clear cover from the top of the bridge deck to the top layer of reinforcement was 2½ in., and clear cover from the bottom of the bridge deck to the bottom layer of reinforcement was 1½ in. Lateral and longitudinal clear cover from the edge of the bridge deck to the end of the lateral and longitudinal deck reinforcement was 2 in. In design section 1 of the interior post, straight No. 6 bars in the lower layer were spaced at 6 in., which aligned with post reinforcement spacing. Design section 1 was 47.5 in. long, resulting in eight total straight No. 6 bars. Horizontal No. 6 U bars were spaced at 12 in., for a total of six U bars at each post. This resulted in a total area of steel reinforcement of 8.8 in.<sup>2</sup>, or 2.2 in.<sup>2</sup>/ft, in design section 1. In the remaining distance between design section 1 and 2 the No. 6 straight bars were spaced at 12 in., resulting in the inclusion of two additional No. 6 straight bars in design section 2. This resulted in a total area of steel reinforcement of 9.7 in.<sup>2</sup>, or 1.2 in.<sup>2</sup>/ft, in design section 2. The longitudinal distance between design section 2 of the interior posts was 5 in. Bar spacings in all sections satisfied the ACI minimum spacing requirements.

In design sections 1 and 2 of the end post, lateral No. 6 straight bars were laterally spaced at 6 in., as this spacing aligned with the vertical post reinforcement. End section geometry did not allow for load transfer across the expansion gap, resulting in tensile and moment loads not distributing as far as they did in the interior post region, thus, loads remained highly concentrated in design section 2 and maintaining the 6 in. spacing of the No. 6 straight bars throughout both sections was required to meet moment and tensile load demands. A total of 15 No. 6 straight bars were included in design section 1, and four additional straight No. 6 straight bars were included in design section 2. Lateral No. 6 U bars each wrapped around two vertical post bars and were spaced at 10 in., resulting in 14 total No. 6 lateral U bars in design section 1. This resulted in an area of steel in design section 1 of 18.9 in.<sup>2</sup>, or 2.5 in.<sup>2</sup>/ft, and an area of steel in design section 2 of 20.7 in.<sup>2</sup>, or 2.4 in.<sup>2</sup>/ft. The longitudinal distance between design section 2 of the end post and design section 2 of the interior post was 23 in. Because the No. 6 straight bars spaced at 12 in. in design section 2 of the interior post could not be evenly spaced in the transition between the end and the interior post, No. 6 straight bars outside of design section 1 of the interior post were laterally spaced at 9 in. Longitudinal bridge deck reinforcement was placed adjacent to vertical post bars to reduce

the possibility of reinforcement pulling out of the concrete, and the remaining bars were spaced at 12 in. across the top and bottom reinforcement layers, as was previously done in MASH TL-4 crash testing [19-20].

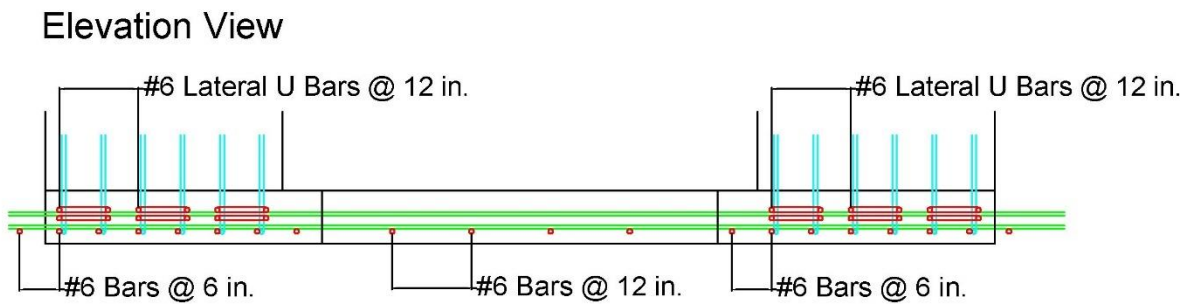
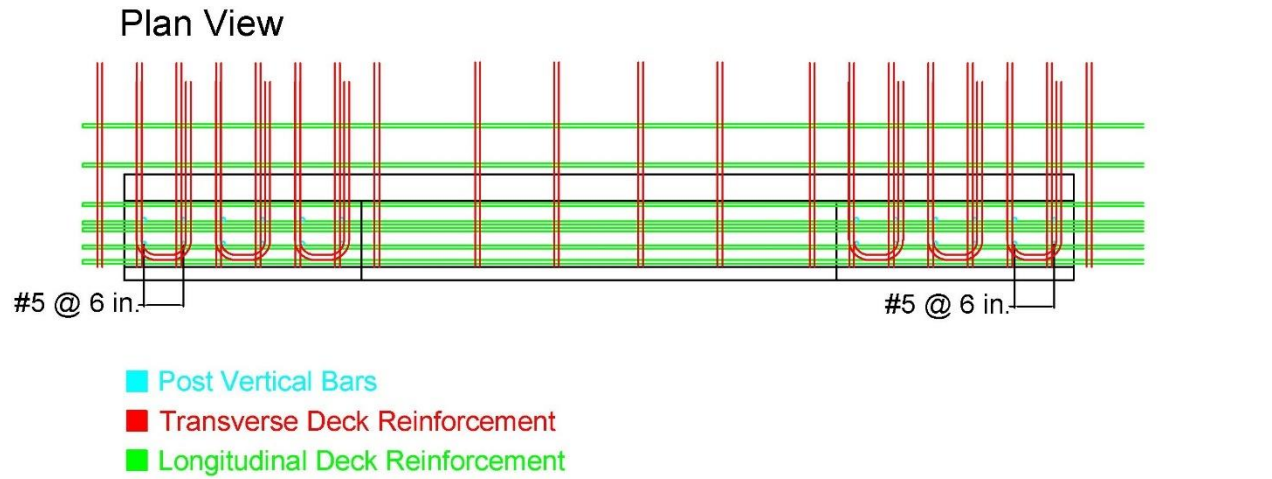
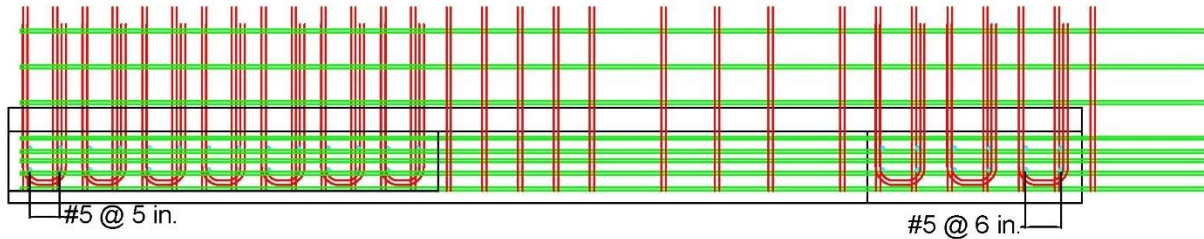


Figure 131. Option 2, Interior Post Deck Reinforcement, Plan and Elevation Views

Plan View



- Post Vertical Bars
- Transverse Deck Reinforcement
- Longitudinal Deck Reinforcement

Elevation View

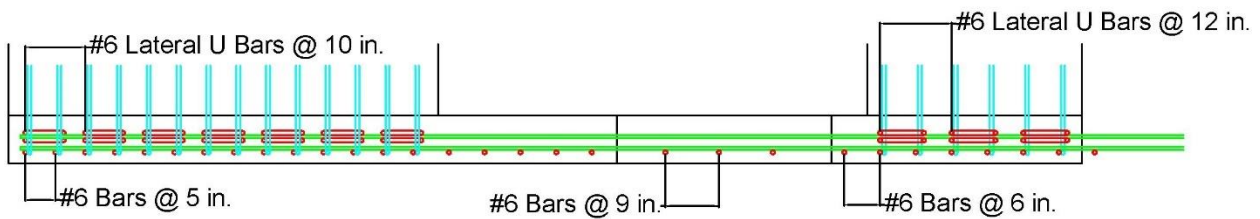


Figure 132. Option 2, End Post to Interior Post Transition Deck Reinforcement, Plan and Elevation Views

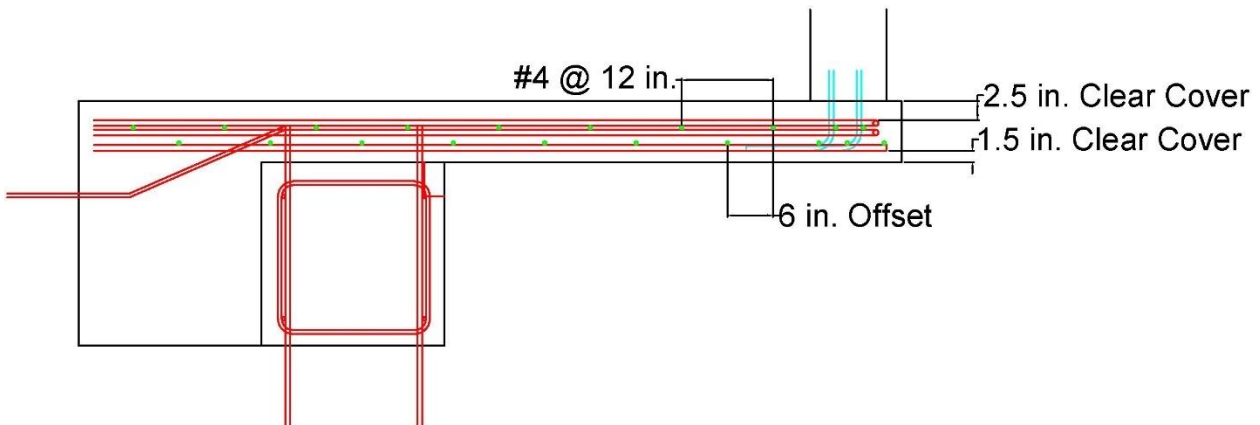


Figure 133. Option 2, Bridge Deck Overhang Cross Section

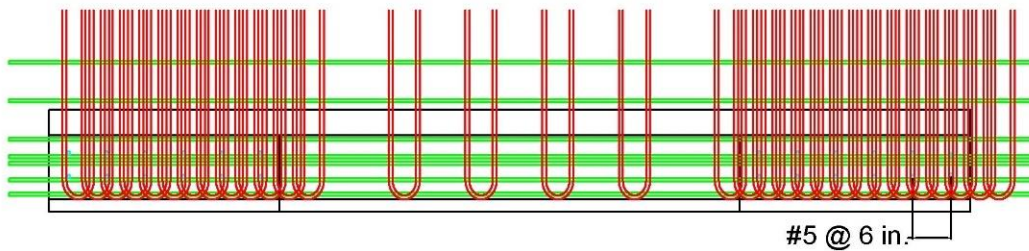
**7.2.3 Option 3**

Bridge deck overhang option 3, shown in Figures 134 through 136, consisted of angled No. 5 U bars in design sections 1 and 2 of the interior and end posts. In design section 1 of the interior post, angled No. 5 U bars were spaced at 3 in., which aligned with post reinforcement spacing. Clear cover from the top of the bridge deck to the top layer of reinforcement was 2½ in., and clear cover from the bottom of the bridge deck to the bottom layer of reinforcement was 1½ in. Lateral and longitudinal clear cover from the edge of the bridge deck to the end of the lateral and

longitudinal deck reinforcement was 2 in. Design section 1 was 47.5 in. long, resulting in 17 total angled No. 5 U bars and a total area of steel reinforcement of 9.9 in.<sup>2</sup>, or 2.5 in.<sup>2</sup>/ft, at design section 1. In the remaining distance between design section 1 and 2, the angled No. 5 U bars were spaced at 12 in., resulting in the inclusion of two angled No. 5 U bars. This resulted in a total area of steel reinforcement of 11.2 in.<sup>2</sup>, or 1.3 in.<sup>2</sup>/ft, in design section 2. The longitudinal distance between design section 2 of the interior posts was 5 in. Bar spacings in all sections satisfied the ACI minimum spacing requirements.

In design sections 1 and 2 of the end post, angled No. 5 U bars were spaced at 2.5 in. and 5 in. respectively. A total of 30 angled No. 5 U bars were included in design section 1, and four additional angled No. 5 U bars were included in design section 2. This resulted in an area of steel in design section 1 of 18.6 in.<sup>2</sup>, or 2.9 in.<sup>2</sup>/ft, and an area of steel in design section 2 of 21.1 in.<sup>2</sup>, or 2.4 in.<sup>2</sup>/ft. The longitudinal distance between design section 2 of the end post and design section 2 of the interior post was 23 in. Because the angled No. 5 U bars spaced at 12 in. in design section 2 of the interior post could not be evenly spaced in the transition between the end and the interior post, angled No. 5 U bars outside of design section 1 of the interior post were laterally spaced at 9 in. Longitudinal bridge deck reinforcement was placed adjacent to vertical post bars to reduce the possibility of reinforcement pulling out of the concrete, and the remaining bars were spaced at 12 in. across the top and bottom reinforcement layers, as was previously done in MASH TL-4 crash testing [19-20].

### Plan View



- Post Vertical Bars
- Transverse Deck Reinforcement
- Longitudinal Deck Reinforcement

### Elevation View

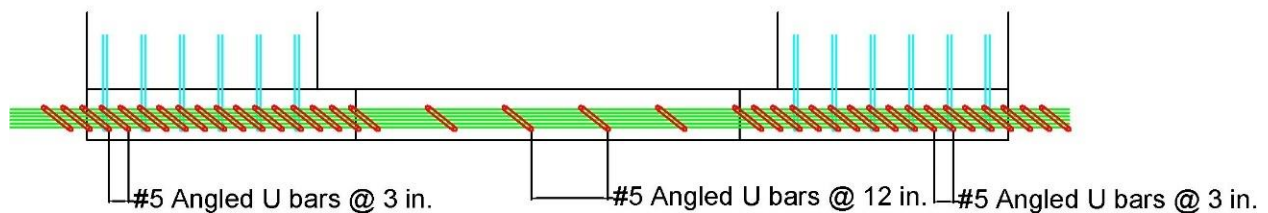
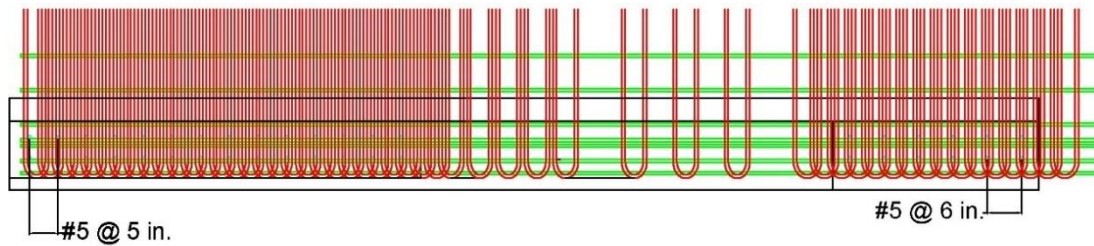


Figure 134. Option 3, Interior Post Deck Reinforcement, Plan and Elevation Views

Plan View



- Post Vertical Bars
- Transverse Deck Reinforcement
- Longitudinal Deck Reinforcement

Elevation View

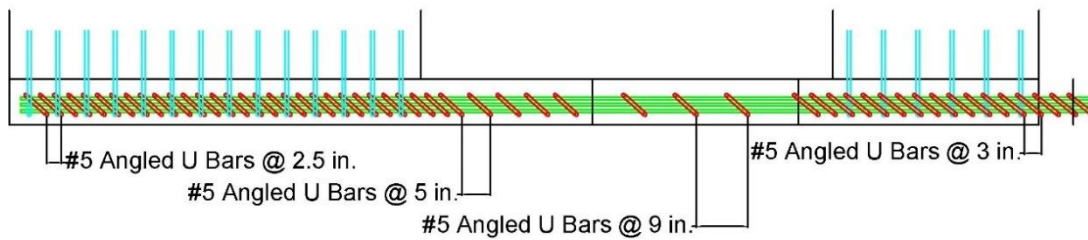


Figure 135. Option 3, End Post to Interior Post Transition Deck Reinforcement, Plan and Elevation Views

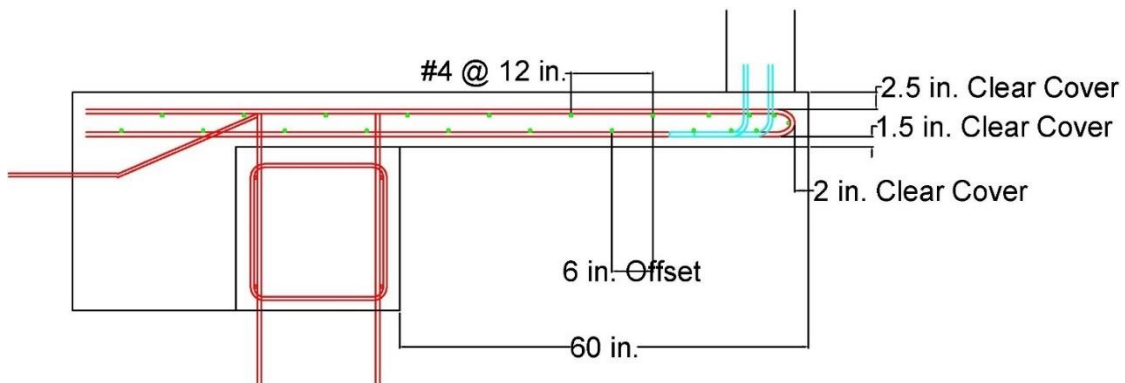


Figure 136. Option 3, Bridge Deck Overhang Cross Section

### 7.3 Summary

All three deck reinforcement configurations provide the required area of steel in the design sections for the interior and end posts. Although all three options had enough strength to support the new bridge rail, Option 1 had the lowest estimated strength. Thus, Option 1 was identified as the critical deck reinforcement configuration and was recommended for full-scale crash testing. A successful crash test on Option 1 could be used to justify the use of either of the other two deck design options.

## 8 SUMMARY, CONCLUSIONS, AND RECOMMENDATIONS

### 8.1 Summary and Conclusions

A new MASH TL-4 open concrete bridge rail was developed. Geometry of the Kansas Corral Rail was utilized as a starting point but was modified throughout the design process. A literature review was conducted on the geometry of similar bridge rail systems and its effect on bridge rail performance. Post setbacks and bridge rail vertical openings were the focus of the review. It was determined that as vertical openings increase in height the potential for snagging increases, and therefore, post setback distances must also increase. Ultimately, a 12-in. tall vertical opening and a post setback of 4 in. were selected for the new open concrete bridge railing.

The project sponsors indicated a desire for rectangular posts instead of incorporating tapered post edges. The rear side of the bridge rail was offset 2 in. from the edge of the deck, and the overall footprint of the bridge rail was limited to 16 in. Larger and stronger end posts would be used at the railing ends and adjacent to any expansion joints. The deck overhang width and thickness selected for full-scale crash testing were 60 in. and 8 in. respectively, which ensured that sponsors wishing to construct the new open concrete bridge rail on shorter and/or thicker bridge decks would be able to do so.

Three design methodologies were investigated for designing the new open concrete bridge rail: Yield-Line Theory, the AASHTO Post and Beam Method, and a Modified AASHTO Post and Beam Method. Yield-Line Theory was limited in its applicability to open concrete bridge rails as it only considered single span failure mechanisms. Additionally, Yield-Line Theory assumed load application height to be fixed at the top of the barrier and did not account for variable load application heights. The AASHTO Post and Beam Method was limited in its applicability to open concrete bridge rails as the failure mechanism for the beam was assumed to develop at post centers, and it was believed that geometry of open concrete bridge rails would result in the failure mechanism developing adjacent to post edges. The AASHTO Post and Beam Method assumed load application height to be fixed at the geometric center of the rail  $\bar{Y}$ , and did not account for variable load application heights. Because the AASHTO Post and Beam Method did consider multiple span failure mechanisms, it was selected as the equation to be modified for designing the new open concrete bridge rail.

The assumed failure mechanism of the Modified AASHTO Post and Beam Method shifted the plastic hinges in the rail from the center of the posts to be adjacent to posts. A load application height factor was also incorporated, which allowed for the capacity of the bridge rail to be calculated at the same height as the applied design load.

The selected bridge rail configuration consisted of 36-in. long by 10-in. wide by 12 in. tall posts in the interior section. End section posts were doubled in length to 72-in. All posts were by separated by 72-in. long gaps. Vertical reinforcement in the interior posts consisted of 12 No. 5 rebars, six on each face of the post, spaced at 6 in., resulting in a moment capacity of 74.4 kip-ft. Vertical reinforcement in the end posts consisted of 28 No. 5 rebars, 14 on each face of the post, longitudinally spaced at 5 in., resulting in a moment capacity of 162.9 kip-ft. A 27-in. tall by 14-in. wide rail was supported by the posts, producing a 4-in. post setback measured from the face of the rail to the face of the posts. Longitudinal rail reinforcement in the interior section rail consisted of eight No. 6 rebars, four on the front and back faces, vertically spaced at 6½ in., resulting in a

moment capacity of 86.9 kip-ft. Longitudinal rail reinforcement in the end section consisted of 14 No. 6 rebars, seven on the front and back faces, vertically spaced at 3¼ in., resulting in a moment capacity of 141.5 kip-ft.

The new bridge rail was developed with a 39-in. top height to satisfy the MASH TL-4 minimum height of 36 in. even after a 3-in. thick roadway overlay. However, a 36-in. tall version could be installed on bridges that would never incorporate overlays. For a 36-in. tall version of the railing, the posts should remain 12 in. tall, but the height of the rail/beam should be reduced by 3 in. to 24 in. General reinforcement patterns should remain the same. Capacities and failure mechanisms of the interior and end sections of the 36-in. and 39-in. tall open concrete bridge rails as determined by the Modified AASHTO Post and Beam Method are summarized in Table 21.

Table 21. New Open Concrete Bridge Rail Capacities and Failure Mechanisms

System Name	Interior Section		End Section	
	Capacity, kips	Failing spans, N	Capacity, kips	Failing spans, N
36-in. Tall Open Concrete Bridge Rail	81.3	3	83.2	1
39-in. Tall Open Concrete Bridge Rail	72.6	3	74.4	1

Three bridge deck reinforcement configurations were developed that had a capacity greater than the bridge rail posts to minimize the potential for deck damage. The minimum area of steel was determined by calculating the combined tensile and moment loads according to three design cases defined within *AASHTO LFRD BDS*. The three design cases corresponded to (1) a horizontal impact load or the capacity of the bridge rail posts, (2) a vertical applied load of 33 kips distributed over 18 ft, and (3) a 1-kip/ft strip load applied 1 ft in front of the face of the barrier. For the new open concrete bridge rail, the horizontal impact load of case 1 was the controlling design case. The design loads were evaluated for two design sections: section 1 located at the face of the post and section 2 located adjacent to the exterior girder. Their length was calculated by assuming the load distributed inward from the back of the posts at a 30-degree angle.

## 8.2 Recommendations

The new TL-4 open concrete bridge rail should be evaluated through crash testing to demonstrate its safety performance. MASH recommends three full-scale crash tests for TL-4 conditions to fully evaluate a bridge rail: (1) MASH test designation no. 4-10 with the 1100C small car, (2) MASH test designation no. 4-11 with the 2270P pickup truck, and (3) MASH test designation no. 4-12 with the 10000S single-unit truck. The 1100C and 2270P vehicles pose the greatest potential for vehicle elements to extend underneath the rail and snag on the posts of the bridge rail. Vehicle snag could result in excessive vehicle decelerations or excessive occupant compartment crush. The 10000S vehicle would impart the greatest load to the bridge rail. Thus,

MASH test designation no. 4-12 is necessary to evaluate the bridge railing's strength and potential for damage.

It is recommended that full-scale crash testing be conducted on the 39-in. tall open concrete bridge rail without an overlay in place, as shown in Figures 137 through 155. Multiple previous crash tests have demonstrated that 36-in. tall systems can contain the 10000S vehicle at MASH TL-4 conditions [18]. Recall, NCHRP Project 22-20(2) showed that the magnitude and effective height of impact loads increases with increases in barrier height. Thus, impacting the 39-in. tall configuration would subject the railing to the maximum impact loads. Additionally, without an overlay, a 12-in. tall vertical opening will be present below the rail, which maximizes the potential for snagging to occur with the 1100C and 2270P vehicles.

A 60-in. wide by 8-in. thick bridge deck was recommended for full-scale crash testing, as the 60-in. wide overhang represents the largest cantilever distance used by the project sponsors and 8-in. was determined to be the thinnest bridge deck. Upon successful completion of the MASH TL-4 crash tests on the bridge rail, alternative deck configurations with reduced cantilever length or increased thickness could be utilized.



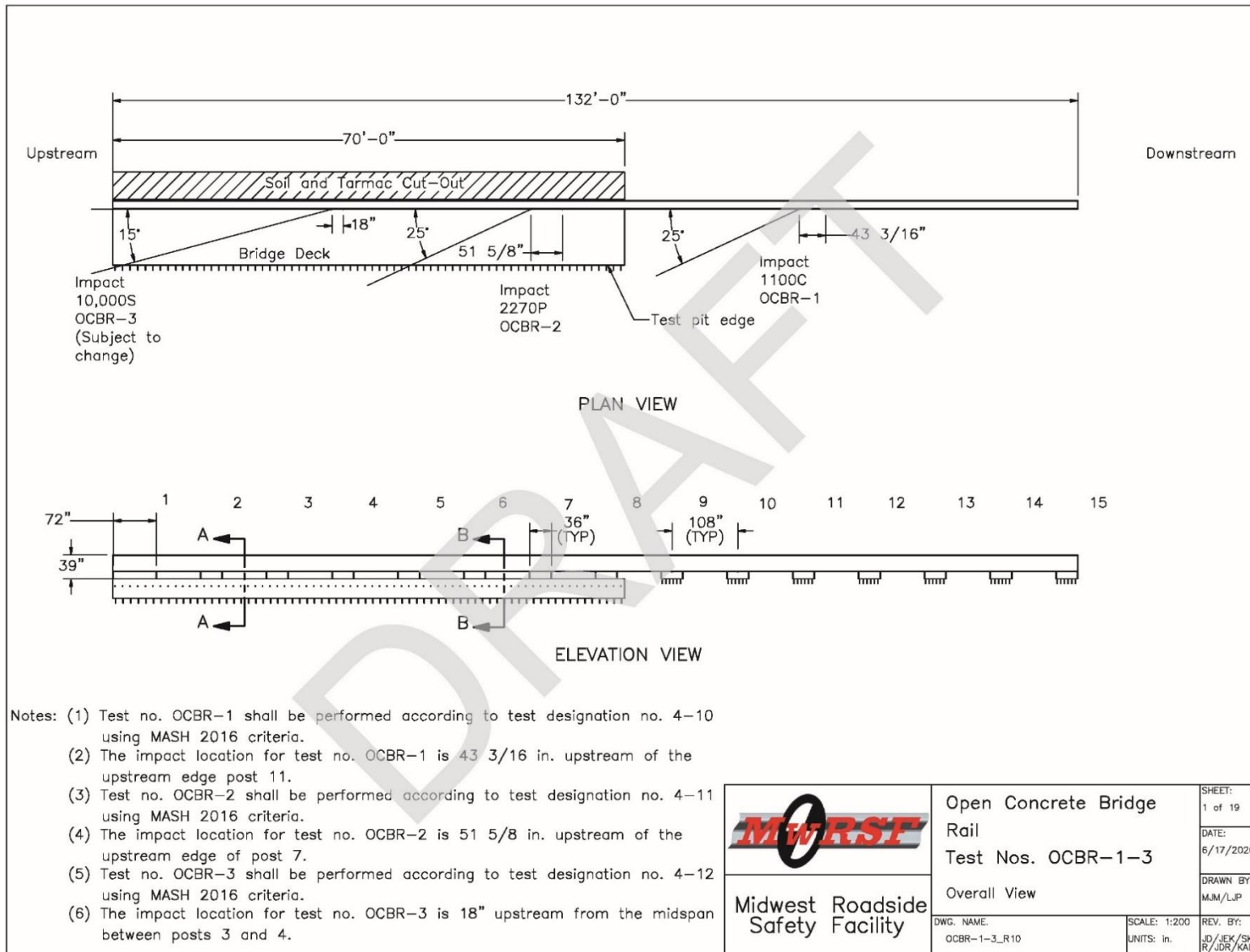
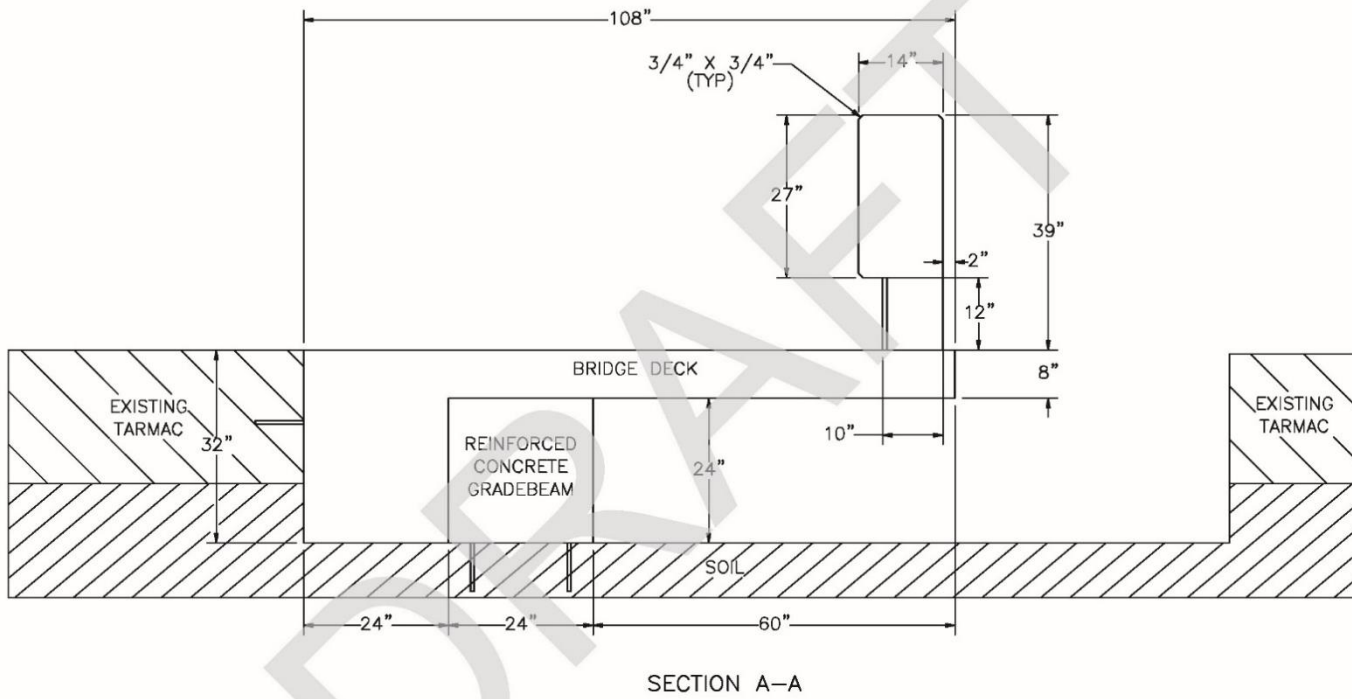


Figure 137. Open Concrete Bridge Rail Overall View



Note: (1) Reinforcement not shown for clarity in section A-A.

 <b>Midwest Roadside Safety Facility</b>	<b>Open Concrete Bridge Rail</b> Test Nos. OCBR-1-3	SHEET: 2 of 19
	System Profile View	DATE: 6/17/2020
DWG. NAME: OCBR-1-3_R10	SCALE: 1:25 UNITS: in.	DRAWN BY: MJM/LJP
		REV. BY: JD/JEK/SK R/JDR/KAL

Figure 138. Open Concrete Bridge Rail System Profile View

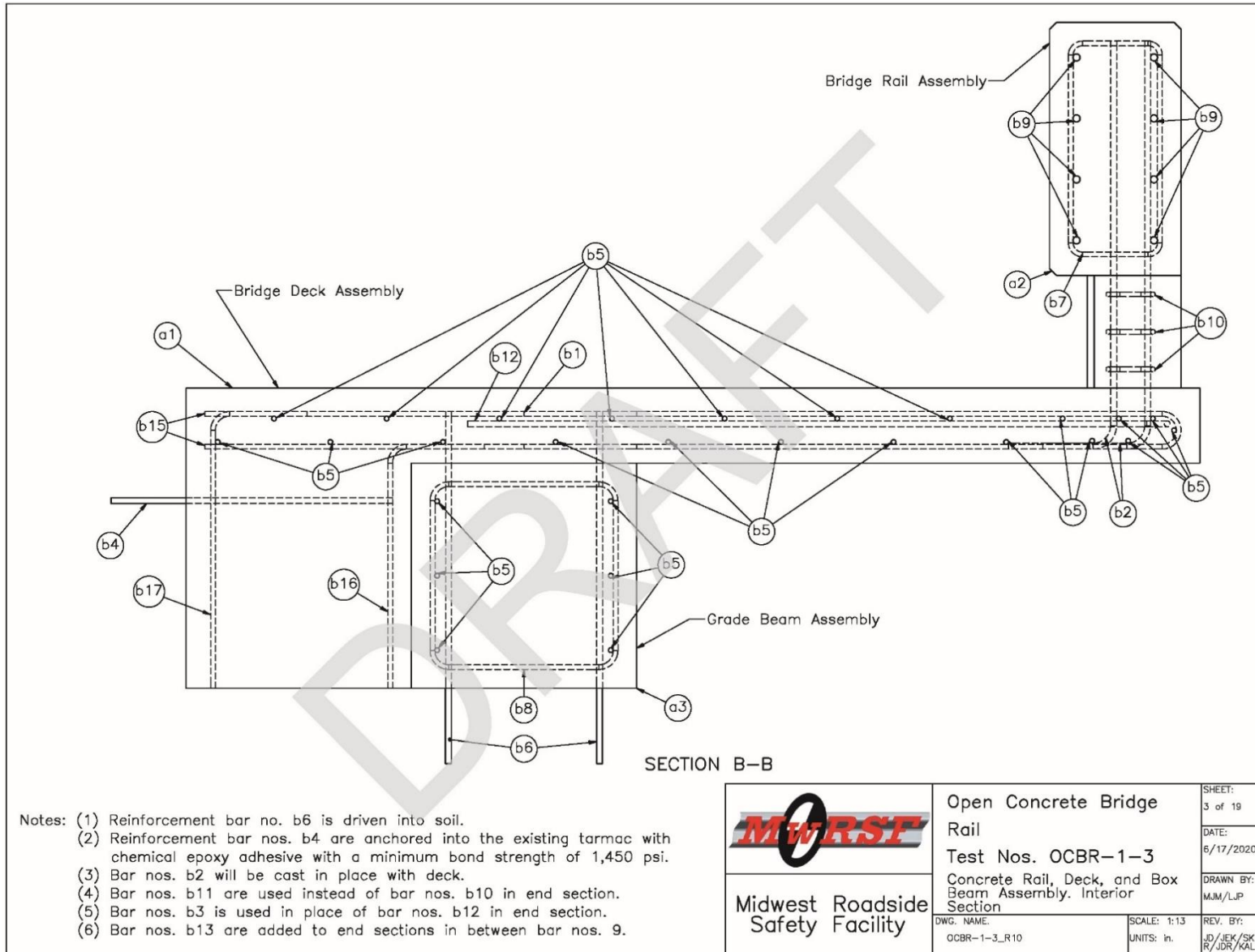
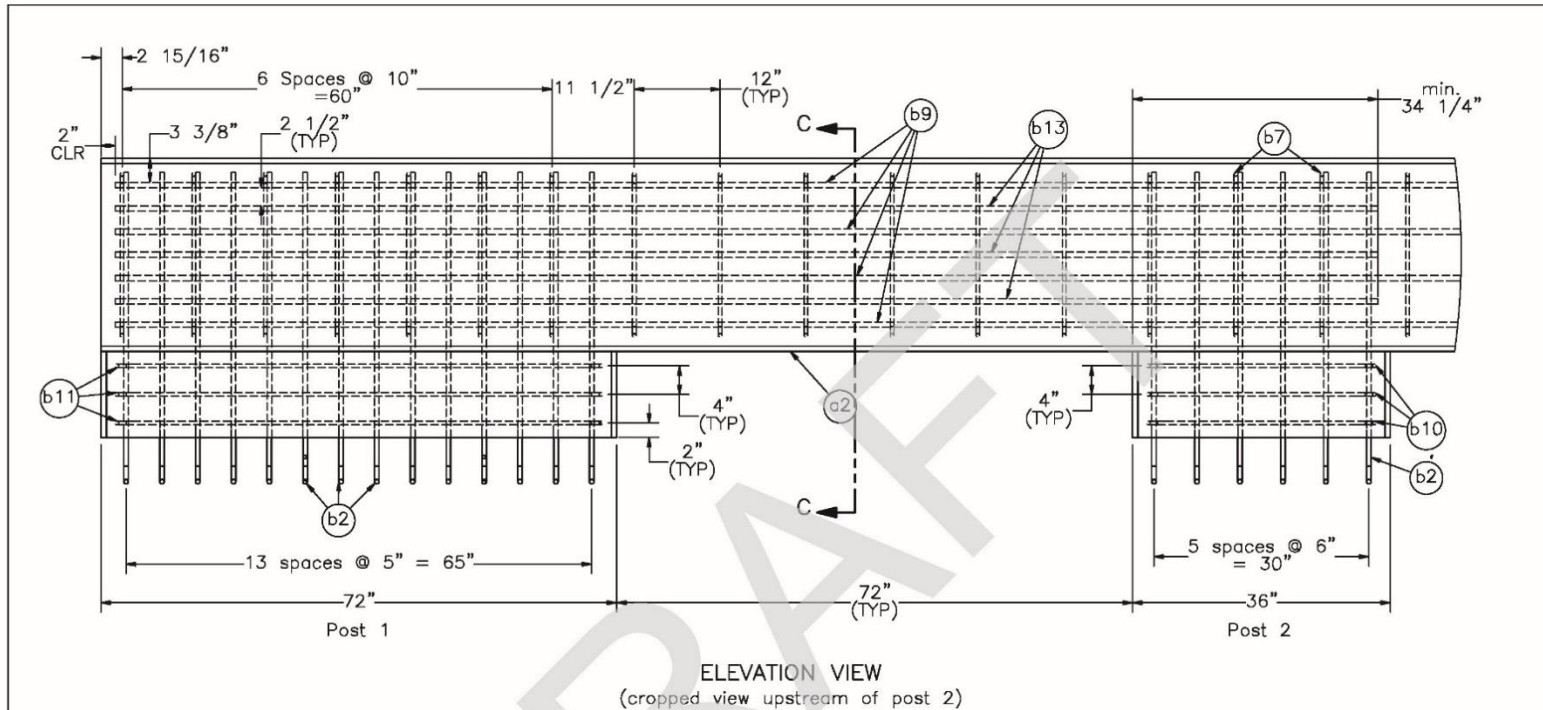


Figure 139. Open Concrete Bridge Rail Deck and Grade Beam Assembly, Interior Section



Item No.	QTY.	Description	Material Specification	Treatment Specification
-	1	Modified Bridge Rail Assembly	-	-
a2	1	Bridge Rail Concrete	Min. f'c = 4,000 psi NE Mix 47BD	-
b2	112	#5 Rebar, 52 5/16" Total Unbent Length	ASTM A615 Gr. 60	Epoxy Coated (ASTM A775 or A934)
b7	133	#4 Bent Rebar, 61 7/8" Total Unbent Length	ASTM A615 Gr. 60	Epoxy Coated (ASTM A775 or A934)
b9	8	#6 Rebar, 1580" Total Length	ASTM A615 Gr. 60	Epoxy Coated (ASTM A775 or A934)
b10	42	#4 Bent Rebar, 70 3/8" Total Unbent Length	ASTM A615 Gr. 60	Epoxy Coated (ASTM A775 or A934)
b11	3	#4 Bent Rebar, 142 3/8" Total Unbent Length	ASTM A615 Gr. 60	Epoxy Coated (ASTM A775 or A934)
b13	6	#6 Rebar, 176 1/4" Total Length	ASTM A615 Gr. 60	Epoxy Coated (ASTM A775 or A934)
b14	84	#5 Rebar, 45" Total Length	ASTM A615 Gr. 60	Epoxy Coated (ASTM A775 or A934)

- Notes: (1) Reinforcement bar nos. b7 have lateral spacings of 12", except at end sections, as detailed above throughout the entire bridge rail.  
 (2) Reinforcement bar nos. b2 have lateral spacings of 6" as detailed above in all interior post sections throughout the bridge deck.  
 (3) Bar nos. b2 will be cast in place with deck.

**Midwest Roadside Safety Facility**

<b>Open Concrete Bridge Rail</b>		SHEET: 4 of 19
Test Nos. OCBR-1-3		DATE: 6/17/2020
Modified Bridge Rail Assembly: Post Nos. 1-2		DRAWN BY: MJM/LJP
DWG. NAME: OCBR-1-3_R10	SCALE: 1:21 UNITS: in.	REV. BY: JD/JEK/SK R/JDR/KAL

Figure 140. Open Concrete Bridge Rail Post Nos. 1 and 2

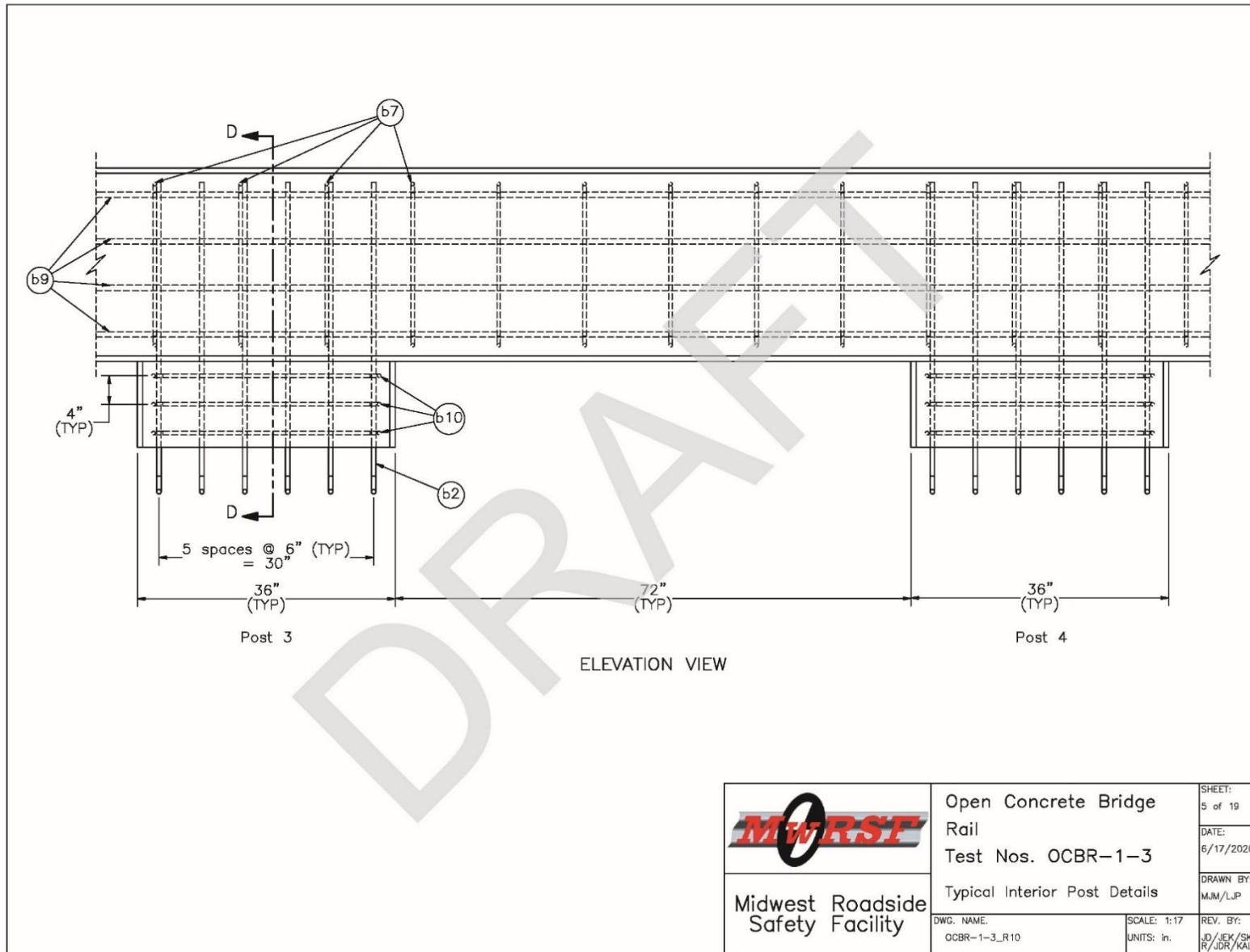


Figure 141. Open Concrete Bridge Rail Interior Post Details

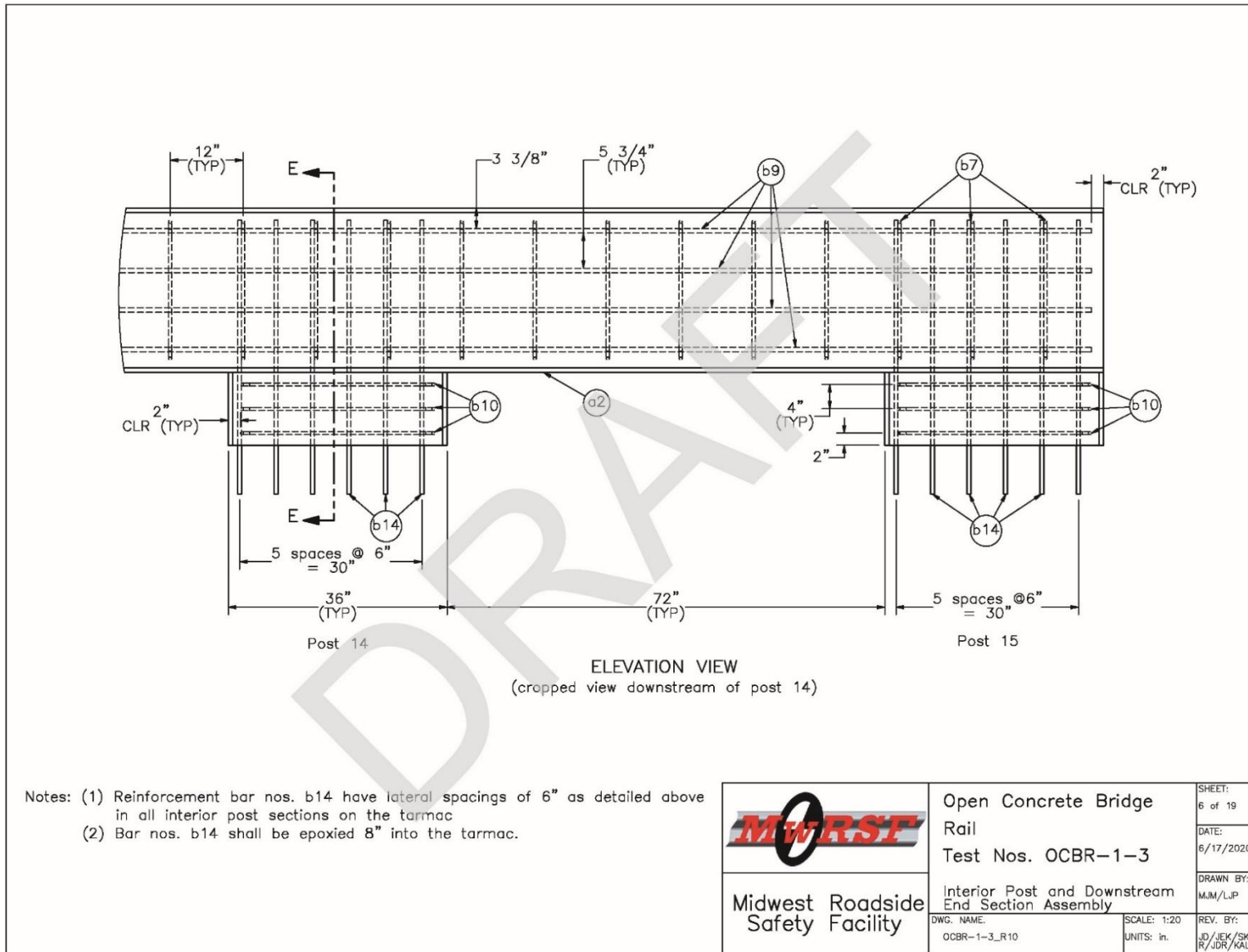


Figure 142. Open Concrete Bridge Rail Interior Post and Downstream End Section Assembly

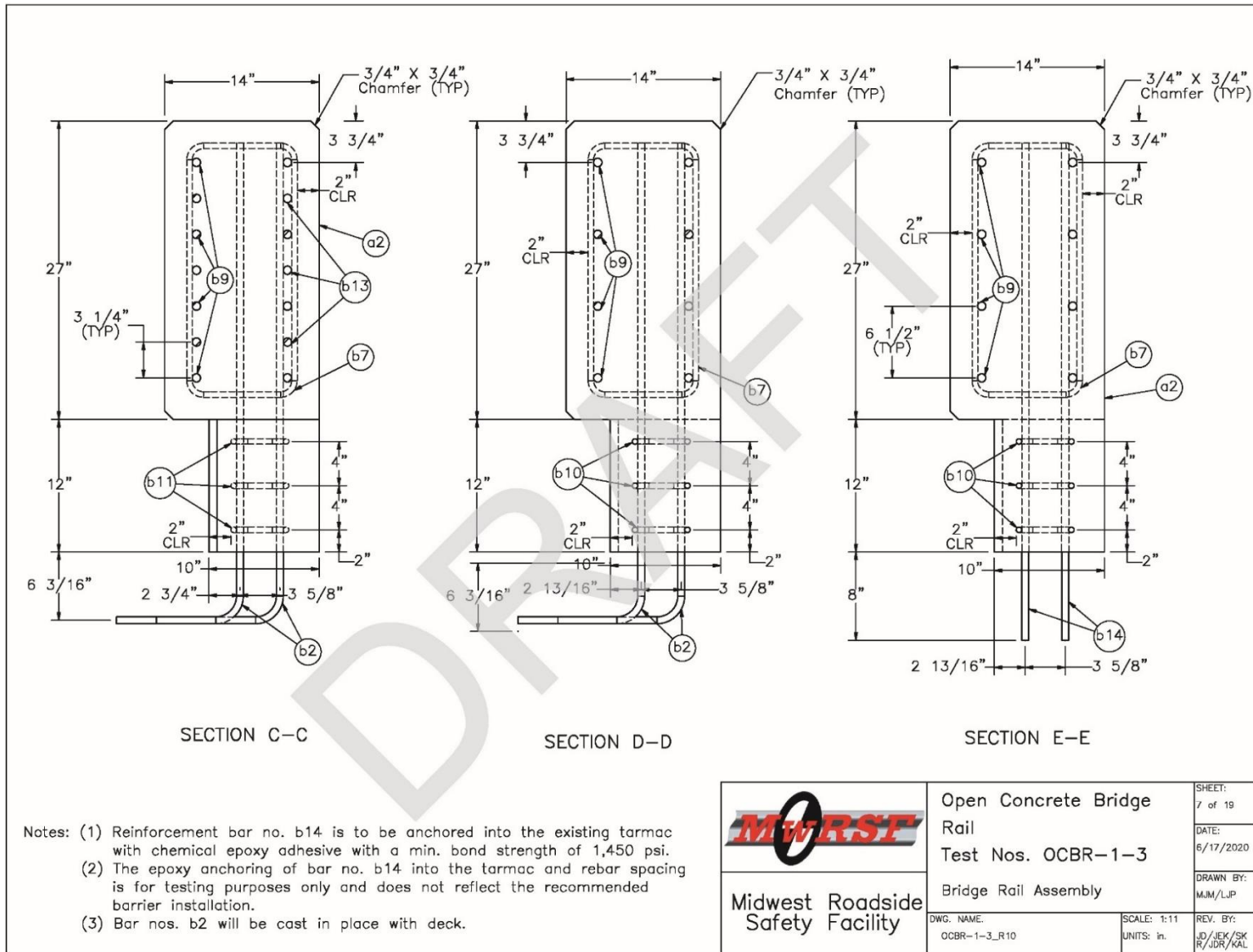


Figure 143. Open Concrete Bridge Rail Assembly

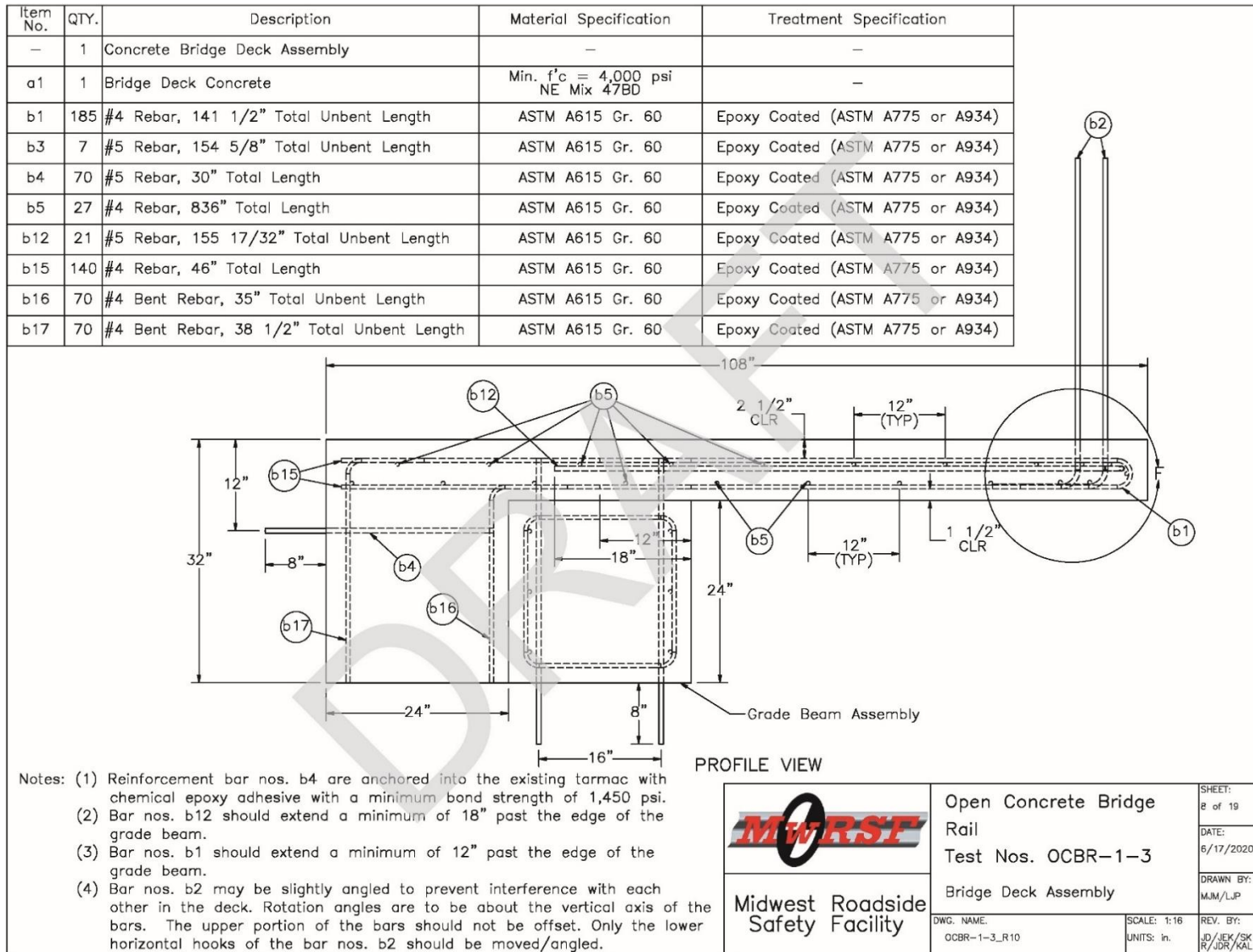


Figure 144. Open Concrete Bridge Rail Bridge Deck Assembly



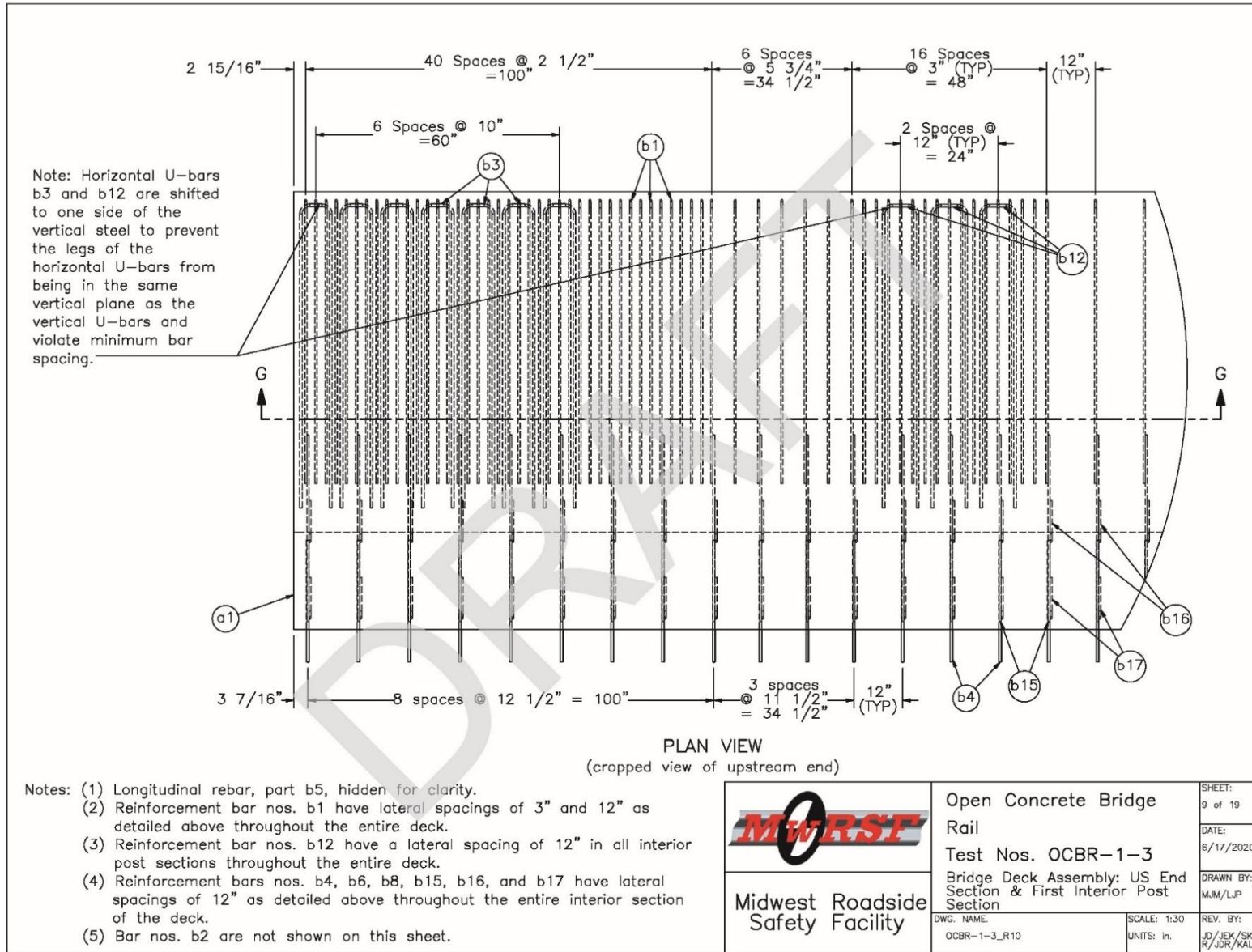


Figure 145. Open Concrete Bridge Rail Upstream End Section and First Interior Post Bridge Deck Assembly

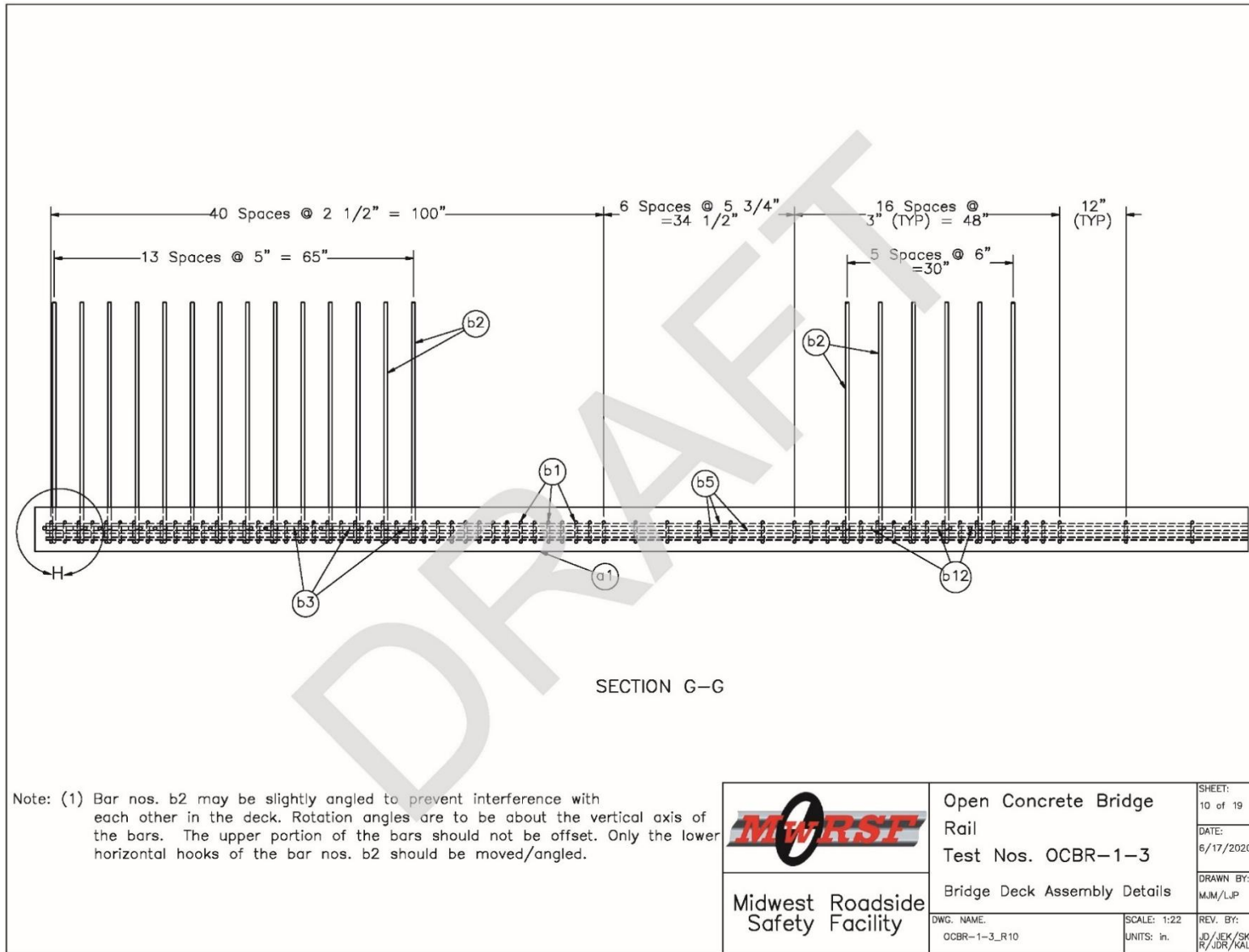


Figure 146. Open Concrete Bridge Rail Upstream End Section and First Interior Post Bridge Deck Assembly

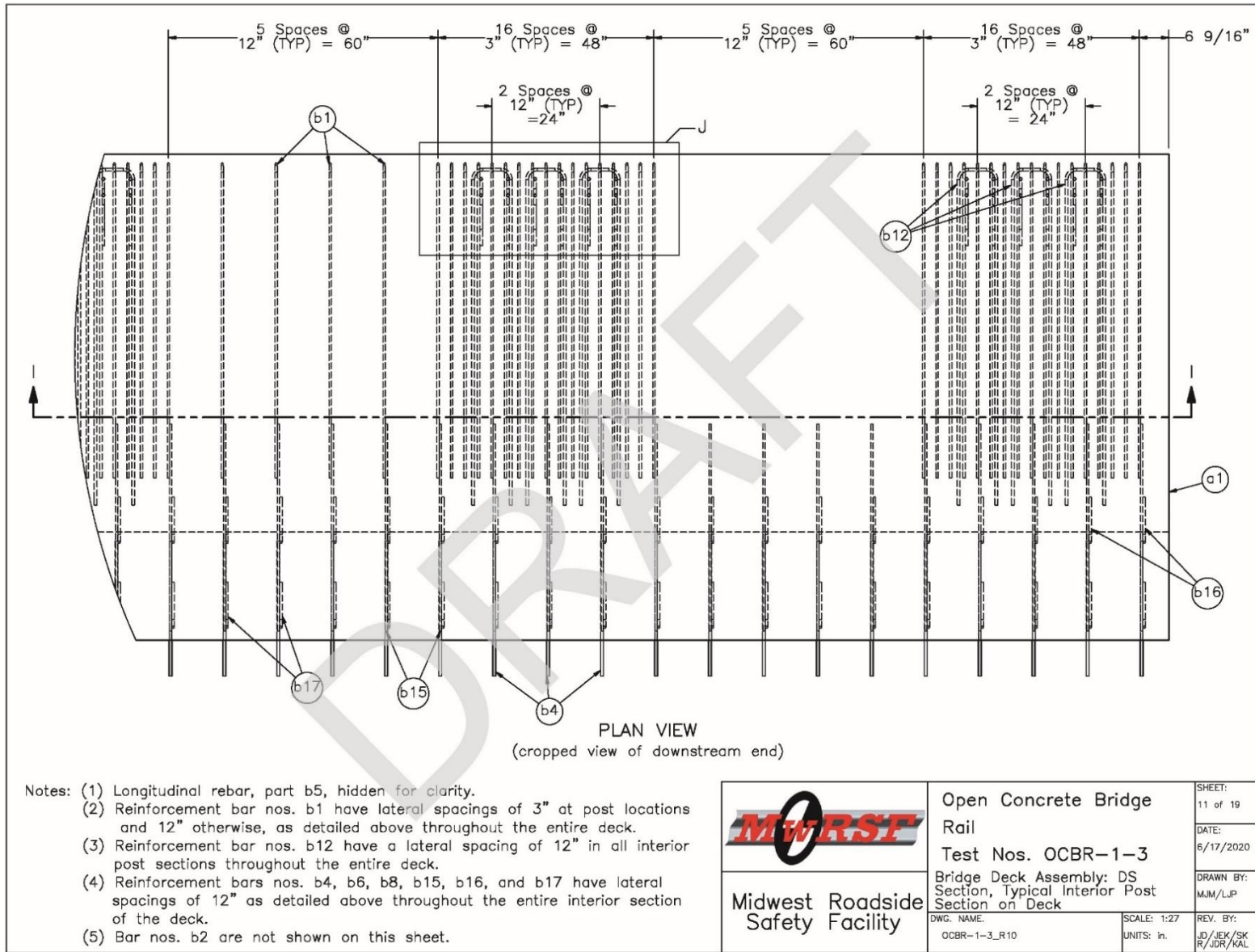


Figure 147. Open Concrete Bridge Interior Post on Bridge Deck and Tarmac Assembly

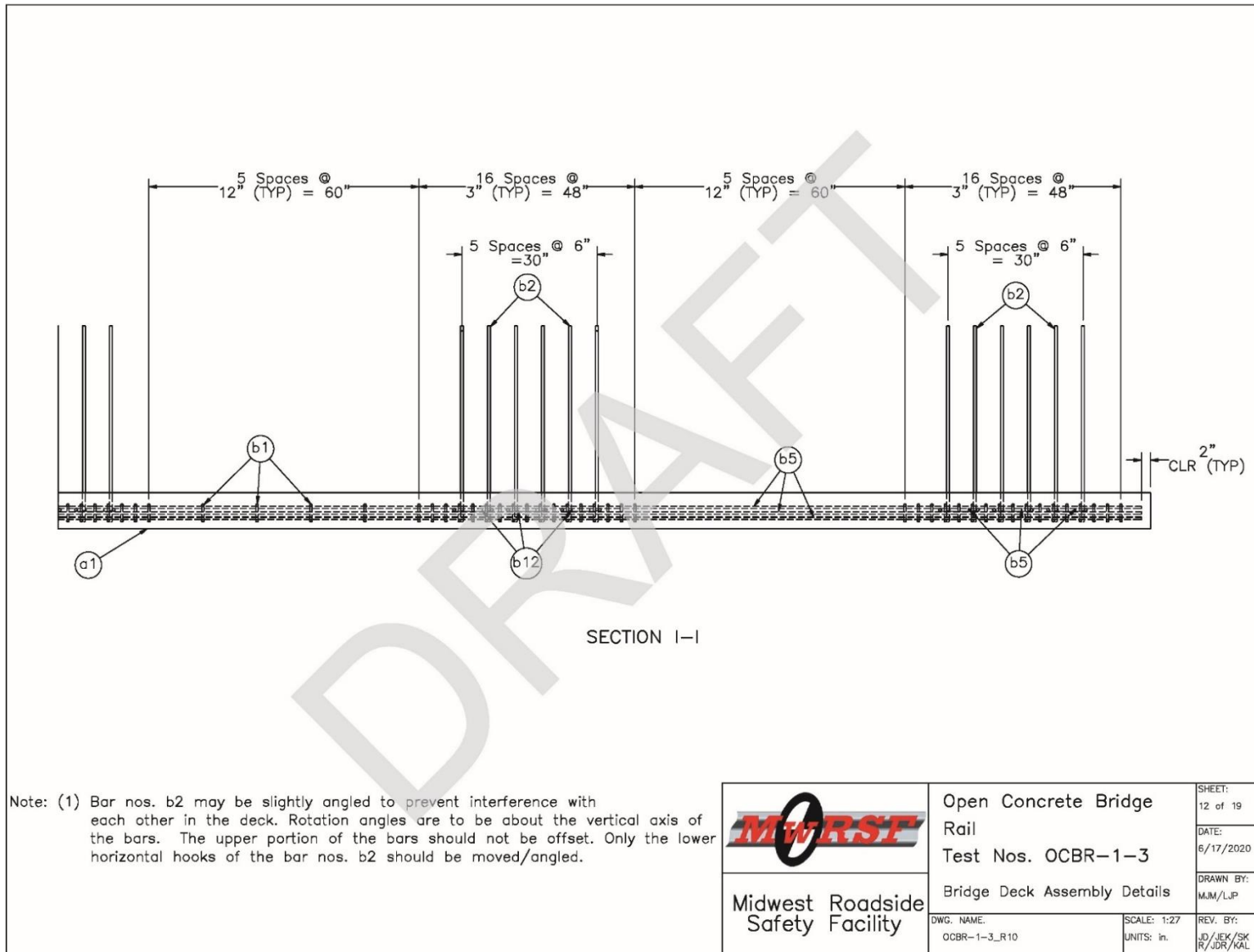


Figure 148. Open Concrete Bridge Rail Bridge Deck Assembly Details

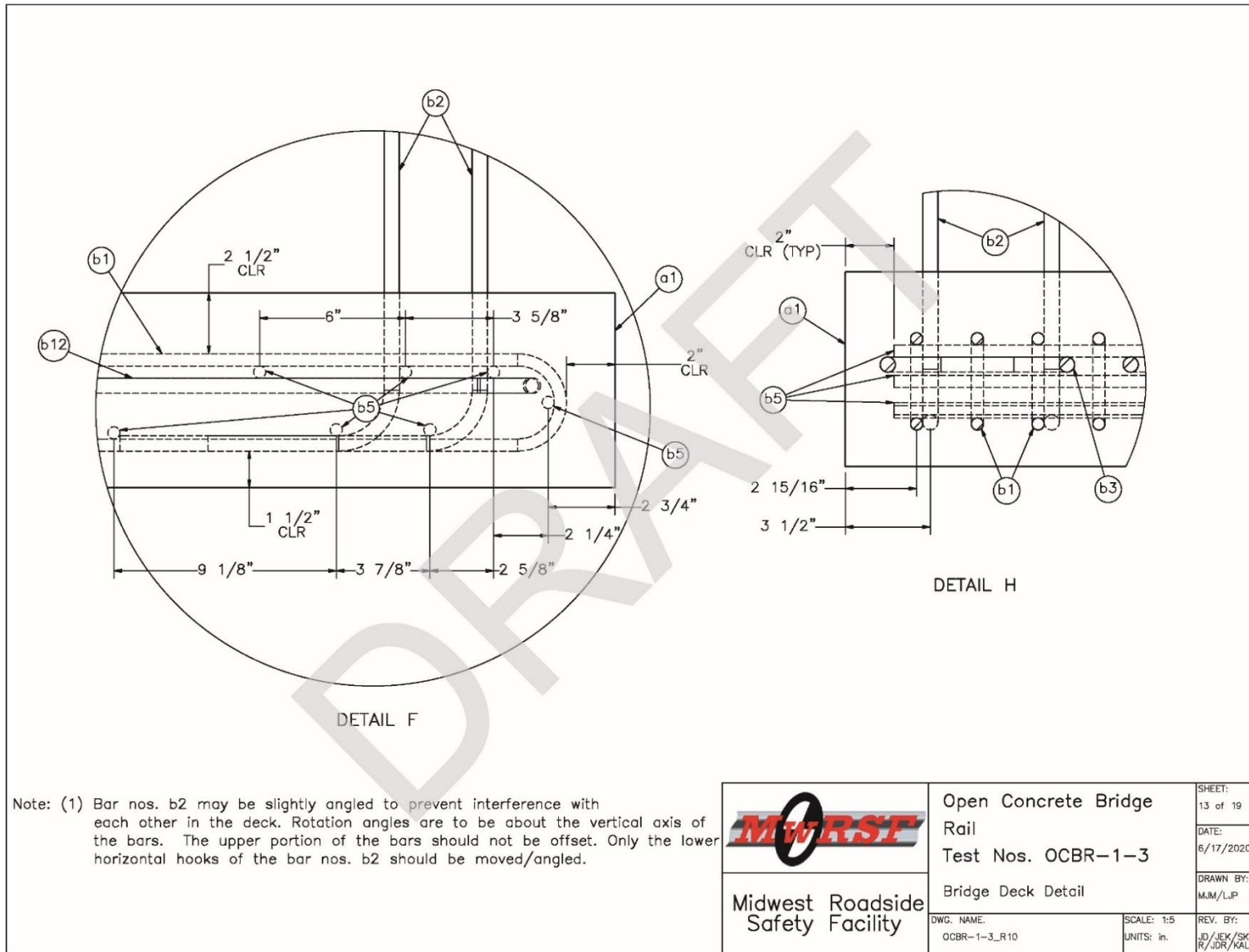


Figure 149. Open Concrete Bridge Rail Deck Detail

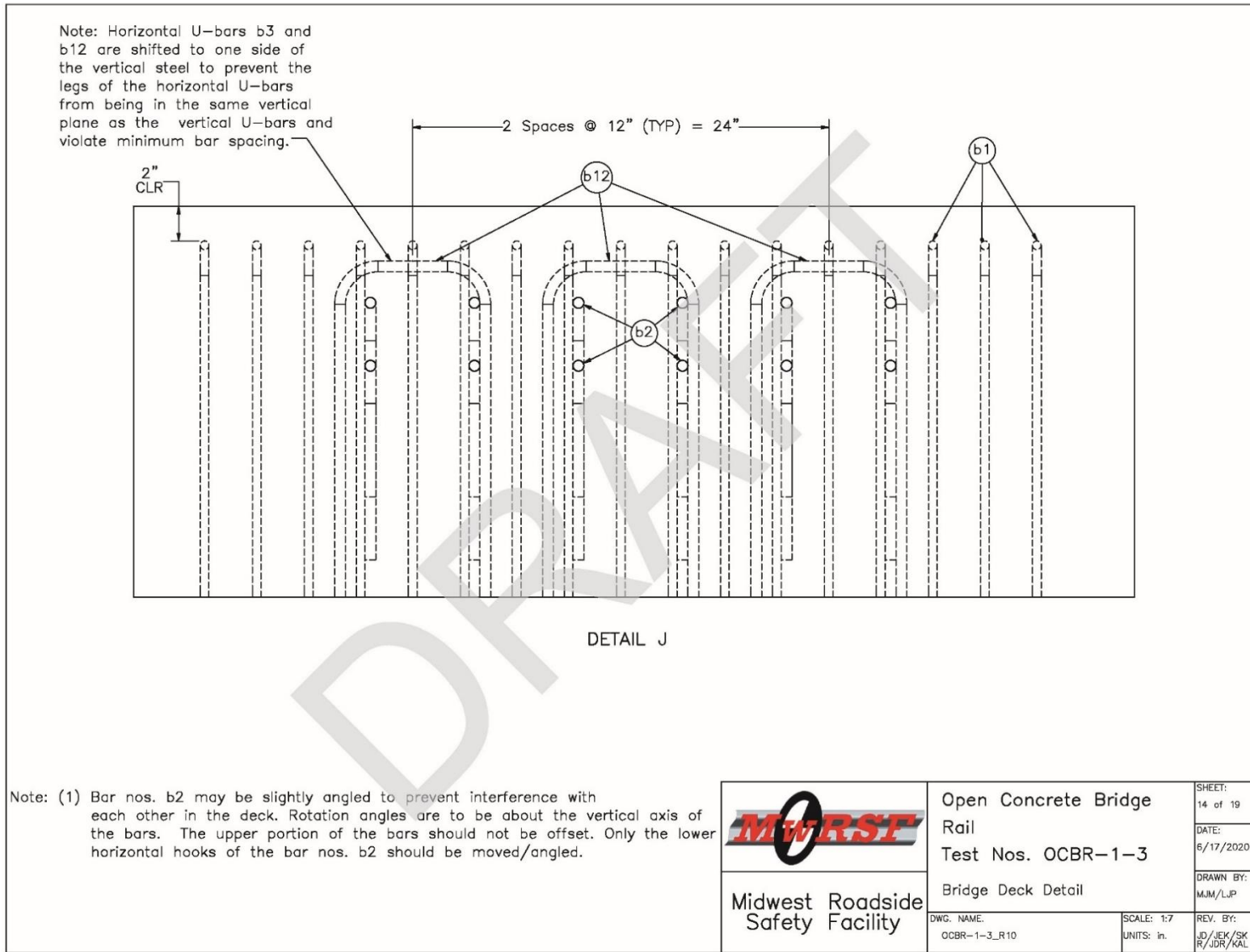


Figure 150. Open Concrete Bridge Rail Deck Detail

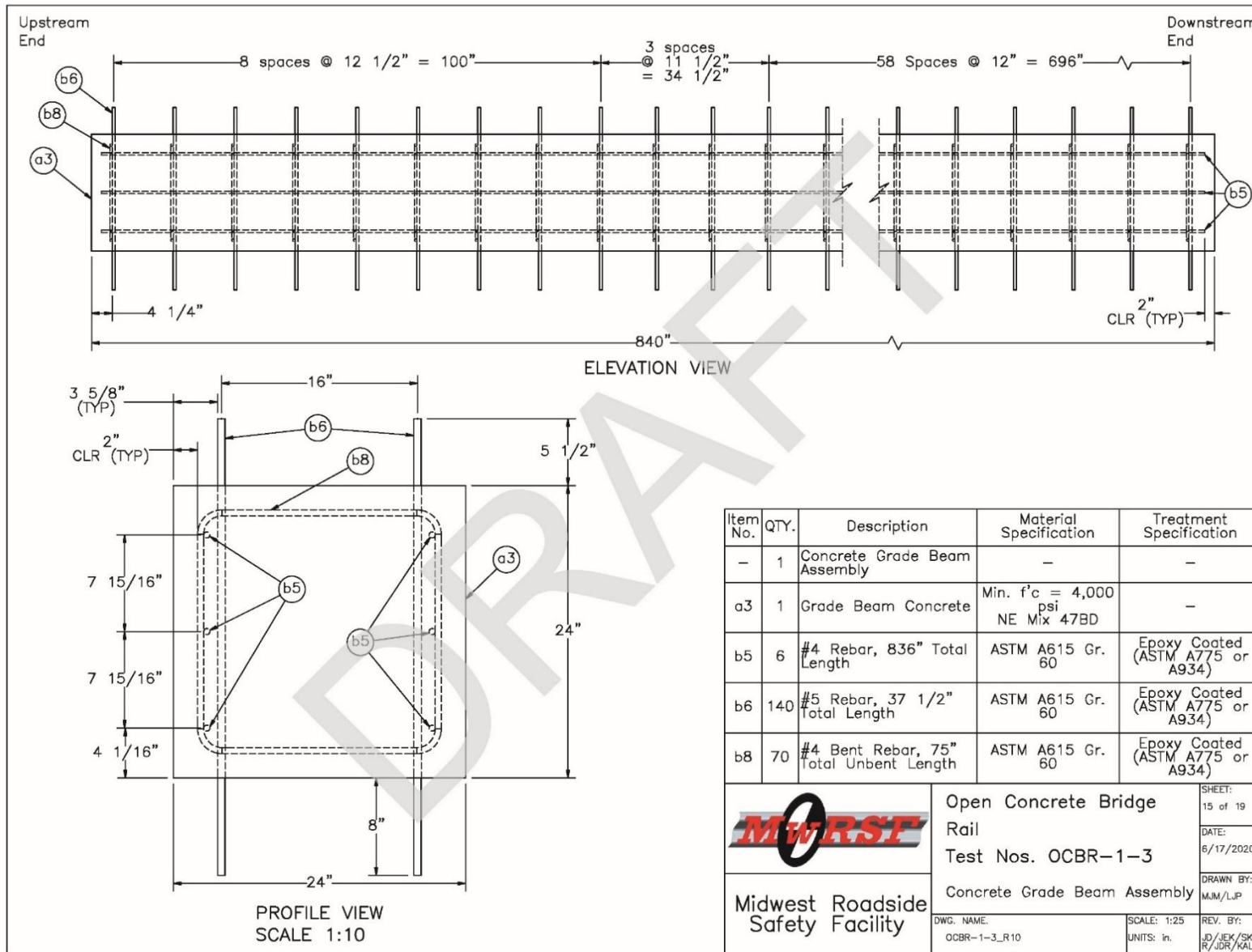


Figure 151. Open Concrete Bridge Rail Grade Beam Detail

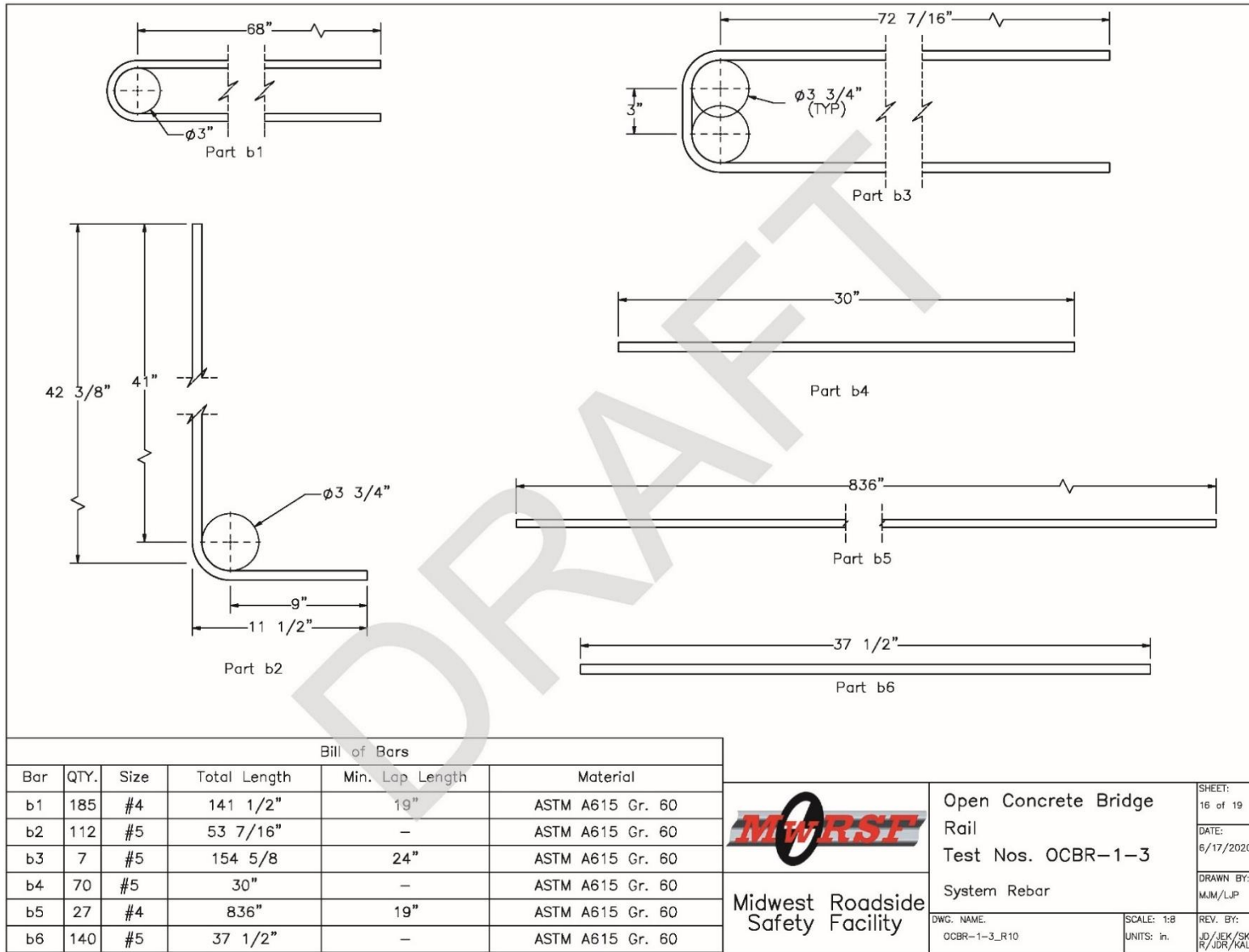


Figure 152. Open Concrete Bridge Rail System Rebar



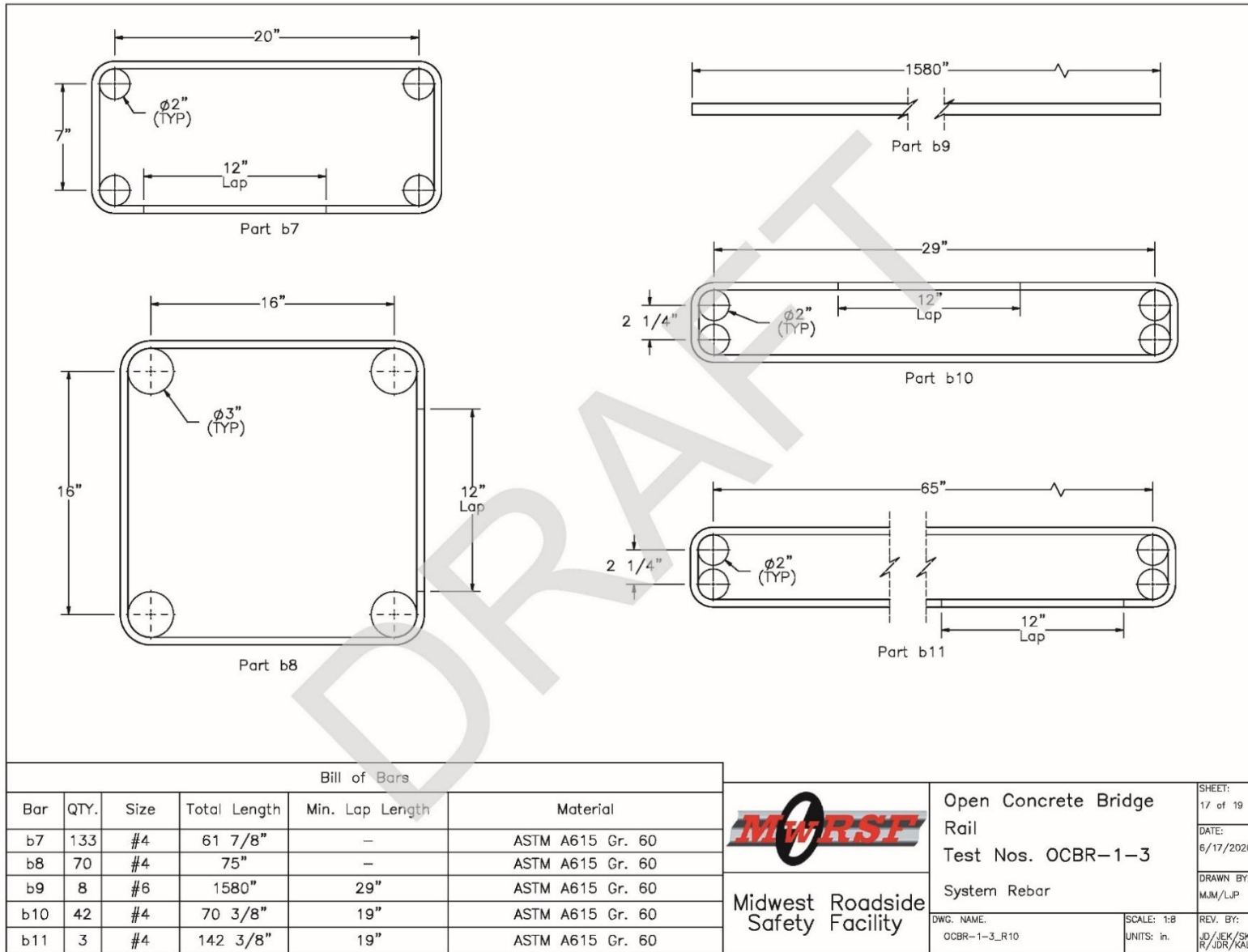


Figure 153. Open Concrete Bridge Rail System Rebar

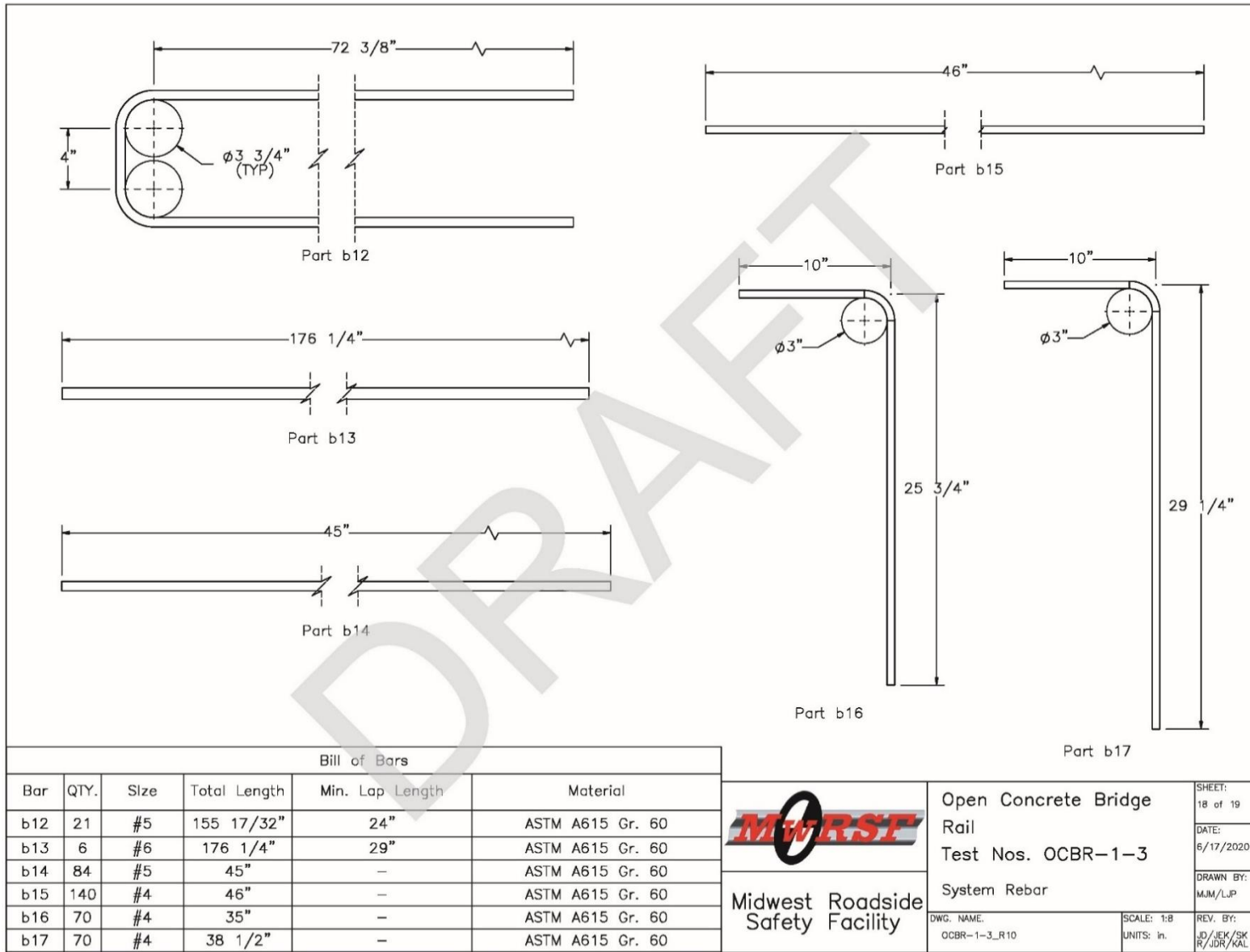


Figure 154. Open Concrete Bridge Rail System Rebar

Item No.	QTY.	Description	Material Specification	Treatment Specification
a1	1	Bridge Deck Concrete	Min. f'c = 4,000 psi NE Mix 47BD	—
a2	1	Bridge Rail Concrete	Min. f'c = 4,000 psi NE Mix 47BD	—
a3	1	Grade Beam Concrete	Min. f'c = 4,000 psi NE Mix 47BD	—
b1	185	#4 Rebar, 141 1/2" Total Unbent Length	ASTM A615 Gr. 60	Epoxy Coated (ASTM A775 or A934)
b2	112	#5 Rebar, 53 7/16" Total Unbent Length	ASTM A615 Gr. 60	Epoxy Coated (ASTM A775 or A934)
b3	7	#5 Rebar, 154 5/8" Total Unbent Length	ASTM A615 Gr. 60	Epoxy Coated (ASTM A775 or A934)
b4	70	#5 Rebar, 30" Total Length	ASTM A615 Gr. 60	Epoxy Coated (ASTM A775 or A934)
b5	27	#4 Rebar, 836" Total Length	ASTM A615 Gr. 60	Epoxy Coated (ASTM A775 or A934)
b6	140	#5 Rebar, 37 1/2" Total Length	ASTM A615 Gr. 60	Epoxy Coated (ASTM A775 or A934)
b7	133	#4 Bent Rebar, 61 7/8" Total Unbent Length	ASTM A615 Gr. 60	Epoxy Coated (ASTM A775 or A934)
b8	70	#4 Bent Rebar, 75" Total Unbent Length	ASTM A615 Gr. 60	Epoxy Coated (ASTM A775 or A934)
b9	8	#6 Rebar, 1580" Total Length	ASTM A615 Gr. 60	Epoxy Coated (ASTM A775 or A934)
b10	42	#4 Bent Rebar, 70 3/8" Total Unbent Length	ASTM A615 Gr. 60	Epoxy Coated (ASTM A775 or A934)
b11	3	#4 Bent Rebar, 142 3/8" Total Unbent Length	ASTM A615 Gr. 60	Epoxy Coated (ASTM A775 or A934)
b12	21	#5 Rebar, 155 17/32" Total Unbent Length	ASTM A615 Gr. 60	Epoxy Coated (ASTM A775 or A934)
b13	6	#6 Rebar, 176 1/4" Total Length	ASTM A615 Gr. 60	Epoxy Coated (ASTM A775 or A934)
b14	84	#5 Rebar, 45" Total Length	ASTM A615 Gr. 60	Epoxy Coated (ASTM A775 or A934)
b15	140	#4 Rebar, 46" Total Length	ASTM A615 Gr. 60	Epoxy Coated (ASTM A775 or A934)
b16	70	#4 Bent Rebar, 35" Total Unbent Length	ASTM A615 Gr. 60	Epoxy Coated (ASTM A775 or A934)
b17	70	#4 Bent Rebar, 38 1/2" Total Unbent Length	ASTM A615 Gr. 60	Epoxy Coated (ASTM A775 or A934)


 Midwest Roadside Safety Facility	Open Concrete Bridge Rail Test Nos. OCBR-1-3	SHEET: 19 of 19 DATE: 6/17/2020
	Bill of Materials	DRAWN BY: MJM/LJP
DWG. NAME: OCBR-1-3_R10	SCALE: None UNITS: in.	REV. BY: JD/JEK/SK R/JDR/KAL

Figure 155. Open Concrete Bridge Rail Bill of Materials

## 9 REFERENCES

1. Polivka, K.A., Faller, R.K., Rohde, J.R., Reid, J.D., Sicking, D.L., and Holloway, J.C., *Safety Performance Evaluation of the Nebraska Open Bridge Rail on an Inverted Tee Bridge Deck*, Report No. TRP-03-133-04, Midwest Roadside Safety Facility, University of Nebraska-Lincoln, Lincoln, Nebraska, January 21, 2004.
2. Williams, W.F., Bligh, R.P., Menges, W.L., and Kuhn, D.L., *Crash Test and Evaluation of the TxDOT T224 Bridge Rail*, Test Report 9-1002-15-5, Texas A&M Transportation Institute, August 2015.
3. Rosenbaugh, S.K., Sicking, D.L., and Faller, R.K., *Development of a TL-5 Vertical Faced Concrete Median Barrier Incorporating Head Ejection Criteria*, Report No. TRP-03-194-07, Midwest Roadside Safety Facility, University of Nebraska-Lincoln, Lincoln, Nebraska, December 10, 2017.
4. Michie, J.D., *Recommended Procedures for the Safety Performance Evaluation of Highway Appurtenances*, National Cooperative Highway Research Program (NCHRP) Report No. 230, Transportation Research Board, Washington, D.C., March 1981.
5. *Guide Specifications for Bridge Railings*, American Association of State Highway Transportation Officials (AASHTO), Washington, D.C., 1987.
6. Bronstad, M.E., Michie, J.D., Calcote, L.R., Hancock, K.L., and Meyer Jr., J.B., *Bridge Rail Design and Performance Standards Volume I: Research Report*, Project No. 06-7908-1, Southwest Research Institute, San Antonio, TX, February, 1987.
7. Holloway, J.C., Pfeifer B.G., Faller, R.K., and Post, E.R., *Full-Scale 18,000 lb Vehicle Crash Test on the Kansas 32 in. Corral Rail*, Report No. TRP-03-26-91, Midwest Roadside Safety Facility, University of Nebraska-Lincoln, Lincoln, Nebraska, July 1991.
8. *Manual for Assessing Safety Hardware (MASH), Second Edition*, American Association of State Highway and Transportation Officials (AASHTO), Washington, D.C., 2016.
9. Ross, H.E., Sicking, D.L., Zimmer, R.A., and Michie, J.D., *Recommended Procedures for the Safety Performance Evaluation of Highway Features*, National Cooperative Highway Research Program (NCHRP) Report 350, Transportation Research Board, Washington, D.C., 1993.
10. Polivka, K.A., Faller, R.K., Sicking, D.L., Rohde, J.R., Bielenberg, R.W., Reid, J.D., and Coon, B.A. *Performance Evaluation of the Permanent New Jersey Safety Shape Barrier - Update to NCHRP 350 Test No. 4-12 (2214NJ-2)*. Report No. TRP-03-178-06, Midwest Roadside Safety Facility, University of Nebraska-Lincoln, Lincoln, Nebraska, October, 2006.

11. Bullard, D.L., Bligh, R.P., Menges, W.L., and Haug, R.R. *Volume I: Evaluation of Existing Roadside Safety Hardware Using Updated Criteria – Technical Report*. NCHRP Project 22-14(03), National Cooperative Highway Research Program (NCHRP) Web-Only Report 157. Transportation Research Board, Washington, D.C., March 2010.
12. Caltrans Roadside Safety Research Group, Type 85 Bridge Rail, Available: <https://dot.ca.gov/programs/research-innovation-system-information/roadside-safety-research-group/california-type-85-concrete-post-and-beam-bridge-rail>, 2020.
13. Arrington, D.R., Bligh, R.P., and Menges, W.L., *MASH Test 3-11 on the 5-Inch Cast in Place Deck Barrier Anchors*, Test Report 9-1002-7, Texas A&M Transportation Institute, October 2011.
14. *AASHTO LRFD Bridge Design Specifications, 8<sup>th</sup> Edition*, American Association of State Highway and Transportation Officials (AASHTO), Washington, D.C., 2017.
15. Silvestri-Dobrovolny, C., Schulz, N., Moran, S., Skinner, S., Bligh, R., and Williams, W., *MASH Equivalency of NCHRP Report 350-Approved Bridge Railings*, Project No. 20-07, Texas A&M Transportation Institute, College Station Texas, November 2017.
16. Buth, C.E., Williams, W.F., Bligh, R.P., and Menges, W.L., *NCHRP Report 350 Testing of the Texas Type T202 Bridge Rail*, Report No. 1904-6, Texas Transportation Institute, College Station, Texas, December 1998.
17. Bligh, R.P., Briaud, J-L., Abu-Odeh, A., Saez B., D.O., Maddah, L.S., and Kim, M.K., *Design Guidelines for Test Level 3 (TL-3) Through Test Level 5 (TL-5) Roadside Barrier Systems Placed on Mechanically Stabilized Earth (MSE) Retaining Wall*, Report No. Research Foundation Project 478130, Texas A&M Transportation Institute, College Station, Texas, June, 2017.
18. Nauman, M.S., Bligh, R.P., Menges, W.L., *Determination of Minimum Height and Lateral Design Load for MASH Test Level 4 Bridge Rails*, Report No. FHWA/TX-12/9-1002-5, Texas Transportation Institute, College Station, Texas, 2011.
19. Rosenbaugh, S.K., Rasmussen, J.D., and Faller, R.K., *Development and Testing of a Test Level 4 Concrete Bridge Rail and Deck Overhang*, Transportation Research Record: Journal of the Transportation Research Board, Midwest Roadside Safety Facility, University of Nebraska-Lincoln, Lincoln, Nebraska, June 23, 2020. DOI: 10.1177/0361198120924406.
20. Rosenbaugh, S.K., Rasmussen, J.D., Dixon, J., Loken, A., Flores, J., and Faller, R.K., *Development and Testing of an Optimized MASH Test Level 4 Bridge Rail*, Report No. TRP-03-415-21, Midwest Roadside Safety Facility, University of Nebraska-Lincoln, Lincoln Nebraska, March 26, 2021.
21. Faller, R.K., Holloway, J.C., Polivka, K.A., Rohde, J.R., and Sicking, D.L., *Development, Testing, and Evaluation of NDOR's TL-5 Aesthetic Open Concrete Bridge Rail*, Report No. TRP-03-148-05, Midwest Roadside Safety Facility, University of Nebraska-Lincoln, Lincoln, Nebraska, December 1, 2005.

22. Holloway, J.C., Faller, R.K., Wolford, D.F., Dye, D.L., and Sicking, D.L., *Performance Level 2 Tests on a 29-in. Open Concrete Bridge Rail*, Report No. TRP-03-51-95, Midwest Roadside Safety Facility, University of Nebraska-Lincoln, Lincoln, Nebraska, June 1996.
23. Buth, E.C., Williams, W.F., Bligh, R.P., Menges, W.L., and Haug, R.R., *Performance of the TxDOT T202 (MOD) Bridge Rail Reinforced with Fiber Reinforced Polymer Bars*, Report No. 0-4138-3, Texas Transportation Institute, College Station, Texas, November 2003.
24. Rosenbaugh, S.K., Faller, R.K., Bielenberg, R.W., Sicking, D.L., Reid, J.D., *Phase I Development of an Aesthetic Precast Concrete Bridge Rail*, Report No. TRP-03-239-12, Midwest Roadside Safety Facility, University of Nebraska-Lincoln, Lincoln, Nebraska, February 13, 2012.
25. Williams, W.F., Bligh, R.P., and Menges, W.L., *Dynamic Testing of the TxDOT T223 Bridge Rail*, Report No. 0-5210-8, Texas A&M Transportation Institute, College Station, Texas, April 2009.
26. Hirsch, T.J., Buth, C.E., Campise, W.L., and Kaderka, D., *Crash Test of the Texas T202 Bridge Rail*, Report No. 1179-2F, Texas Transportation Institute, College Station, Texas, August, 1989.
27. Her, V., Caldwell, C., Jewell, J., and Meline, R. *Compliance Crash Testing of the CA ST-70SM Side Mounted Bridge Rail*, Report No. FHWA/CA17-2557, California Department of Transportation, Sacramento, California, February 2017.
28. Buth, C.E., Menges, W.L., and Williams, W.F., *Testing and Evaluation of the Massachusetts Type S3-TL4 Bridge Railing*, Report No. 404251-F, Texas Transportation Institute, College Station, Texas, December 1999.
29. Pena, O., Faller, R.K., Schmidt, J.D., Steelman, J.S., Rosenbaugh, S.K., Bielenberg, R.W., and Mauricio, P., *Development of a MASH Test Level 4 Steel, Side-Mounted, Beam and-Post, Bridge Rail*, Report No. TRP-03-410-19, Midwest Roadside Safety Facility, University of Nebraska-Lincoln, Nebraska, April 19, 2019.
30. Pena, O., *Development of a MASH TL-4 Steel Side-Mounted, Post and Beam, Bridge Rail*, Thesis toward a Degree of Master of Science in Civil Engineering, Midwest Roadside Safety Facility, University of Nebraska-Lincoln, Nebraska, April 19, 2019.
31. Mauricio, P., Rasmussen, J.D., Faller, R.K., Rosenbaugh S.K., Bielenberg, R.W., Pena, O., Steelman, J.S., and Stolle, C.S., *Development of a Post to Deck Connection for a TL-4 Steel Tube Bridge Rail*, Report No. TRP-03-409-20, Midwest Roadside Safety Facility, University of Nebraska-Lincoln, Nebraska, May 27, 2020.
32. Mauricio, P., *Development of Post-to-Deck Connections for use in a MASH TL-4 Steel-Tube Bridge Rail*, Thesis toward a Degree of Master of Science in Civil Engineering, Midwest Roadside Safety Facility, University of Nebraska-Lincoln, Nebraska, April 19, 2019.

33. Schmidt, J.D., Asselin, N., Faller, R.K., Fallet, W.G., Holloway J.C., and Lechtenberg, K.A., *Evaluation of the Minnesota Noise Wall and Rubrail System*, Report No. TRP-03-396-19, Midwest Roadside Safety Facility, University of Nebraska-Lincoln, Nebraska, January 31, 2019.
34. Schmidt, J.D., Schmidt, T.L., Rosenbaugh, S.K., Faller, R.K., Bielenberg, R.W., Reid, J.D., Holloway, J.C., and Lechtenberg, K.A., *MASH TL-4 Testing and Evaluation of the Restore Barrier*, Report No. TRP-03-318-15, Midwest Roadside Safety Facility, University of Nebraska-Lincoln, Nebraska, November 3, 2015.
35. Rosenbaugh, S.K., Asselin, N., Faller, R.K., and Hartwell, J.A., *Development of a Standardized End Buttress for Approach Guardrail Transitions*, Report No. TRP-03-369-18, Midwest Roadside Safety Facility, University of Nebraska-Lincoln, Nebraska, May 3, 2018.
36. Rosenbaugh, S.K., Fallet, W.G., Faller, R.K., and Bielenberg, R.W., *34-in. Tall Thrie Beam Transition to Concrete End Buttress*, Report No. TRP-03-367-17, Midwest Roadside Safety Facility, University of Nebraska-Lincoln, Nebraska, March 8, 2019.
37. Hirsch, T.J., *Analytical Evaluation of Texas Bridge Rails to Contain Buses and Trucks*, Research Report No. 230-2, Texas Transportation Institute, College Station, Texas, September 1, 1977.
38. Delone, J.A., *Development of a MASH Test Level 4 Open Concrete Bridge Rail*, Thesis toward a Degree of Master of Science in Civil Engineering, University of Nebraska-Lincoln, July 2020.
39. Williams, W.F., Buth, E.C., and Menges, W.L., *Repair/Retrofit Anchorage Designs for Bridge Rails*, Report No. FHWA/TX-06/0-4823-T1-1, Texas Transportation Institute, College Station, Texas, March 2007.
40. Grubb, M.A., Wilson, K.E., White, C.D., and Nicka, W.N., *Load and Resistance Factor Design (LRFD) for Highway Bridge Superstructures – Reference Manual*, Report No. FHWA-NHI-15-047, Federal Highway Administration National Highway Institute, Arlington, VA, July 2015.
41. Wilson, K.E., Bouscher, J.W., Amrhein, W.A., and Modjeski and Masters, Inc., *Load and Resistance Factor Design (LRFD) for Highway Bridge Superstructures – Design Examples*, Report NO. FHWA NHI-15-058, Federal Highway Administration National Highway Institute, Arlington, VA, August 2015.
42. Frosch, R.J., and A.J. Morel. *Guardrails for Use on Historic Bridges: Volume 2 – Bridge Deck Overhang Design*. Report No. FHWA/IN/JTRP-2016/34. Joint Transportation Research Program, West Lafayette, Indiana, Purdue University, 2016.

**END OF DOCUMENT**